

GRAHAM COOP

POPULATION AND QUANTITATIVE GENETICS

Author: Graham Coop

Author address: Department of Evolution and Ecology & Center for Population Biology,
University of California, Davis.

To whom correspondence should be addressed: gmccoop@ucdavis.edu

This work is licensed under a Creative Commons Attribution 3.0 Unported License.

<http://creativecommons.org/licenses/by/3.0/>

i.e. you are free to reuse and remix this work, but please include an attribution to the original.

Typeset using L^AT_EX and the TUFTE-LATEX book style.

The L^AT_EX code and R code for this book are kept here <https://github.com/cooplab/popgen-notes/> and again are
under a Creative Commons Attribution 3.0 Unported License.

Updated on June 2019

This book was developed from my set of notes for the Population Biology graduate group core class (PBG200A) and Undergraduate Population and Quantitative Genetics class (EVE102) at UC Davis. Thanks to the many students who've read these notes and suggested improvements. Thanks to Simon Aeschbacher, Vince Buffalo, and Erin Calfee who read and extensively edited earlier drafts of these notes. To illustrate these notes I've used old scientific and natural history illustrations, in part because they are out of copyright but mainly because they bring me joy. Many of the old images come from Biodiversity Heritage Library a consortium of natural history institutions that are digitizing their collections and make them freely available online. If you enjoy the images consider donating to the BHL. Many of the data and simulation graphics in the book were prepared in R (2018), the code for each is linked to from the caption of each figure. In many cases data were extracted from old figures using the WebPlotDigitizer tool, as such I advise re-extracting the data if you wish to use it for research purposes.

Contents

1	<i>Introduction</i>	7
2	<i>Allele and Genotype Frequencies</i>	11
3	<i>Genetic Drift and Neutral Diversity</i>	45
4	<i>Phenotypic Variation and the Resemblance Between Relatives.</i>	89
5	<i>The Response to Phenotypic Selection</i>	109
6	<i>One-Locus Models of Selection</i>	129
7	<i>The Impact of Genetic Drift on Selected Alleles</i>	167
8	<i>The Effects of Linked Selection.</i>	179
9	<i>Interaction of multiple selected loci.</i>	195
10	<i>Bibliography</i>	207

1

2 Introduction

BIOLOGICAL EVOLUTION IS THE CHANGE OVER TIME IN THE
4 GENETIC COMPOSITION OF A POPULATION.¹ Our population is
made up of a set of interbreeding individuals, the genetic composition
6 of which is made up of the genomes that each individual carries. The
genetic composition of the population alters due to the death of indi-
8 viduals or the migration of individuals in or out of the population. If
our individuals vary in the number of children they have, this also al-
10 ters the genetic composition of the population in the next generation.
Every new individual born into the population subtly changes the
12 genetic composition of the population. Their genome is a unique com-
bination of their parents' genomes, having been shuffled by segregation
14 and recombination during meioses, and possibly changed by mutation.
These individual events seem minor at the level of the population, but
16 it is the accumulation of small changes in aggregate across individuals
and generations that is the stuff of evolution. It is the compounding
18 of these small changes over tens, hundreds, and millions of genera-
tions that drives the amazing diversity of life that has emerged on this
20 earth.

Population genetics is the study of the genetic composition of natu-
22 ral populations and its evolutionary causes and consequences. Quantitative genetics is the study of the genetic basis of phenotypic variation
24 and how phenotypic changes evolve over time. Both fields are closely
conceptually aligned as we'll see throughout these notes. They seek to
26 describe how the genetic and phenotypic composition of populations
can be changed over time by the forces of mutation, recombination,
28 selection, migration, and genetic drift. To understand how these forces
interact, it is helpful to develop simple theoretical models to help our
30 intuition. In these notes we will work through these models and sum-
marize the major areas of population- and quantitative-genetic theory.

32 While the models we will develop will seem naïve, and indeed they
are, they are nonetheless incredibly useful and powerful. Throughout

¹ DOBZHANSKY, T., 1951 *Genetics and the Origin of Species* (3rd Ed. ed.), pp. 16

"All models are wrong but some are useful" - Box (1979).

³⁴ the course we will see that these simple models often yield accurate predictions, such that much of our understanding of the process of evolution is built on these models. We will also see how these models are incredibly useful for understanding real patterns we see in the evolution of phenotypes and genomes, such that much of our analysis of evolution, in a range of areas from human medical genetics to conservation, is based on these models. Therefore, population and quantitative genetics are key to understanding various applied questions, from how medical genetics identifies the genes involved in disease to how we preserve species from extinction.

⁴⁴ Population genetics emerged from early efforts to reconcile Mendelian genetics with Darwinian thought. Part of the power of population genetics comes from the fact that the basic rules of transmission genetics are simple and nearly universal. One of the truly remarkable things about population genetics is that many of the important ideas and mathematical models emerged before the 1940s, long before the mechanistic-basis of inheritance (DNA) was discovered, and yet the usefulness of these models has not diminished. This is a testament to the fact that the models are established on a very solid foundation, building from the basic rules of genetic transmission combined with simple mathematical and statistical models.

⁵⁶ Much of this early work traces to the ideas of R.A. Fisher, Sewall Wright, and J.B.S. Haldane, who, along with many others, described the early principals and mathematical models underlying our understanding of the evolution of populations. Building on this conceptual fusion of genetics and evolution, there followed a flourishing of evolutionary thought, the modern evolutionary synthesis, combining these ideas with those from the study of speciation, biodiversity, and paleontology. In total this work showed that both short-term evolutionary change and the long-term evolution of biodiversity could be well understood through the gradual accumulation of evolutionary change within and among populations. This evolutionary synthesis continues to this day, combining new insights from genomics, phylogenetics, ecology, and developmental biology.

⁶⁸ Population and quantitative genetics are a necessary but not a sufficient description of evolution; it is only by combining the insights of many fields that a rich and comprehensive picture of evolution emerges. We certainly do not need to know the genes underlying the displays of the birds of paradise to study how the divergence of these displays, due to sexual selection, may drive speciation. Indeed, as we'll see in our discussion of quantitative genetics, we can predict how populations respond to selection, including sexual selection and assortative mating, without any knowledge of the loci involved. Nor do we need to know the precise selection pressures and the ordering of genetic

See PROVINE (2001) for a history of early population genetics.

PROVINE, W. B., 2001 *The origins of theoretical population genetics: with a new afterword.* University of Chicago Press

“DOBZHANSKY (1951)
once defined evolution as ‘a
change in the genetic com-
position of the populations’
an epigram that should not
be mistaken for the claim
that everything worth saying
about evolution is contained
in statements about genes”

– LEWONTIN

78 changes to study the emergence of the tetrapod body plan. We do
not necessarily need to know all the genetic details to appreciate the
80 beauty of these, and many other, evolutionary case-studies. However,
every student of biology gains from understanding the basics of pop-
82 ulation and quantitative genetics, allowing them to base their studies
and speculations on a solid bedrock of understanding of the processes
84 that underpin all evolutionary change.

2

⁸⁶ *Allele and Genotype Frequencies*

In this chapter we will work through how the basics of Mendelian
⁸⁸ genetics play out at the population level in sexually reproducing organisms.

⁹⁰ Loci and alleles are the basic currency of population genetics—and indeed of genetics. If all individuals in the population carry the same
⁹² allele, we say that the locus is *monomorphic*; at this locus there is no genetic variability in the population. If there are multiple alleles in
⁹⁴ the population at a locus, we say that this locus is *polymorphic* (this is sometimes referred to as a segregating site).

⁹⁶ Table 2.1 show a small stretch orthologous sequence for the ADH locus from samples from *Drosophila melanogaster*, *D. simulans*, and ⁹⁸ *D. yakuba*. *D. melanogaster* and *D. simulans* are sister species and *D. yakuba* is a close outgroup to the two. Each column represents a ¹⁰⁰ single haplotype from an individual (the individuals are diploid but were inbred so they're homozygous for their haplotype). Only sites that differ among individuals of the three species are shown. Site 834 ¹⁰² is an example of a polymorphism; some *D. simulans* individuals carry a *C* allele while others have a *T*. Fixed differences are sites that differ between the species but are monomorphic within the species. Site 781 ¹⁰⁴ is an example of a fixed difference between *D. melanogaster* and the other two species.

¹⁰⁶ We can also annotate the alleles and loci in various ways. For example, position 781 is a non-synonymous fixed difference. We call the ¹⁰⁸ less common allele at a polymorphism the *minor allele* and the common allele the *major allele*, e.g. at site 1068 the *T* allele is the minor ¹¹⁰ allele in *D. melanogaster*. We call the more evolutionarily recent of the two alleles the *derived allele* and the older of the two the *ancestral allele*. The *T* allele at site 1068 is the derived allele as the *C* is found in ¹¹² both the other species, suggesting that the *T* allele arose via a *C* → *T* mutation.

A *locus* (plural: *loci*) is a specific spot in the genome. A locus may be an entire gene, or a single nucleotide base pair such as A-T. At each locus, there may be multiple genetic variants segregating in the population—these different genetic variants are known as *alleles*.

Question 1. **A)** How many segregating sites does the sample

pos.	con.	a	b	c	d	e	f	g	h	i	j	k	l	a	b	c	d	e	f	g	h	i	j	k	l	NS/S	
781	G	T	T	T	T	T	T	T	T	T	-	-	-	-	-	-	-	-	-	-	-	-	-	-	-	NS	
789	T	-	-	-	-	-	-	-	-	-	-	-	-	C	C	C	C	C	C	C	C	C	C	C	C	C	S
808	A	-	-	-	-	-	-	-	-	-	T	T	T	T	T	T	T	-	-	G	G	G	G	G	G	NS	
816	G	T	T	T	T	-	-	-	-	-	-	-	-	C	C	-	-	-	-	G	G	G	G	G	G	G	S
834	T	-	-	-	-	-	-	-	-	-	-	-	-	C	-	-	-	-	-	-	-	-	-	-	-	S	
859	C	-	-	-	-	-	-	-	-	-	-	-	-	G	G	G	G	G	G	G	G	G	G	G	G	NS	
867	C	-	-	-	-	-	-	-	-	-	-	-	-	G	G	G	G	G	A	G	G	G	G	G	G	S	
870	C	T	T	T	T	T	T	T	T	T	-	-	-	-	-	-	-	-	-	-	-	-	-	-	S		
950	G	-	-	-	-	-	-	-	-	-	-	-	-	A	-	-	-	-	-	-	-	-	-	-	-	S	
974	G	-	-	-	-	-	-	-	-	-	T	-	T	T	T	T	-	-	-	-	-	-	-	-	S		
983	T	-	-	-	-	-	-	-	-	-	-	-	-	C	C	C	C	C	C	C	C	C	C	C	C	S	
1019	C	-	-	-	-	-	-	-	-	-	-	-	-	-	-	-	-	-	-	A	-	-	-	-	S		
1031	C	-	-	-	-	-	-	-	-	-	-	-	-	-	-	-	-	-	-	-	-	-	-	-	S		
1034	T	-	-	-	-	-	-	-	-	-	-	-	-	C	C	C	C	C	-	-	C	-	C	C	S		
1043	C	-	-	-	-	-	-	-	-	-	-	-	-	-	-	-	-	-	-	A	-	-	-	-	S		
1068	C	T	T	-	-	-	-	-	-	-	-	-	-	-	-	-	-	-	-	-	-	-	-	-	S		
1089	C	-	-	-	-	-	-	-	-	-	A	A	A	A	A	A	-	-	-	-	-	-	-	-	NS		
1101	G	-	-	-	-	-	-	-	-	-	-	-	-	A	A	A	A	A	A	A	A	A	A	A	NS		
1127	T	-	-	-	-	-	-	-	-	-	-	-	-	C	C	C	C	C	C	C	C	C	C	C	S		
1131	C	-	-	-	-	-	-	-	-	-	-	-	-	-	-	-	-	-	-	T	-	-	-	-	S		
1160	T	-	-	-	-	-	-	-	-	-	-	-	-	C	C	C	C	C	C	C	C	C	C	C	S		

- from *D. simulans* have in the ADH gene?
B) How many fixed differences are there between *D. melanogaster* and *D. yakuba*?

2.1 Allele frequencies

Allele frequencies are a central unit of population genetics analysis, but from diploid individuals we only get to observe genotype counts. Our first task then is to calculate allele frequencies from genotype counts. Consider a diploid autosomal locus segregating for two alleles (A_1 and A_2). We'll use these arbitrary labels for our alleles, merely to keep this general. Let N_{11} and N_{12} be the number of A_1A_1 homozygotes and A_1A_2 heterozygotes, respectively. Moreover, let N be the total number of diploid individuals in the population. We can then define the relative frequencies of A_1A_1 and A_1A_2 genotypes as $f_{11} = N_{11}/N$ and $f_{12} = N_{12}/N$, respectively. The frequency of allele A_1 in the population is then given by

$$p = \frac{2N_{11} + N_{12}}{2N} = f_{11} + \frac{1}{2}f_{12}. \quad (2.1)$$

Note that this follows directly from how we count alleles given in individuals' genotypes, and holds independently of Hardy–Weinberg proportions and equilibrium (discussed below). The frequency of the alternate allele (A_2) is then just $q = 1 - p$.

2.1.1 Measures of genetic variability

Nucleotide diversity (π) One common measure of genetic diversity is the average number of single nucleotide differences between haplotypes chosen at random from a sample. This is called nucleotide diversity and is often denoted by π . For example, we can calculate π for our ADH locus from Table 2.1 above: we have 6 sequences from *D. simulans* (a-f), there's a total of 15 ways of pairing these sequences, and

Table 2.1: Variable sites in exons 2 and 3 of the ADH gene in *Drosophila* McDONALD and KREITMAN (1991). The first column (pos.) gives the position in the gene; exon 2 begins at position 778 and we've truncated the dataset at site 1175. The second column gives the consensus nucleotide (con.), i.e. the most common base at that position; individuals with nucleotides that match the consensus are marked with a dash. The first columns of sequence (a-l) are from *D. melanogaster*; the next columns (a-f) give sequences from *D. simulans*, and the final set of columns (a-l) from *D. yakuba*. The last column shows whether the difference is a non-synonymous (N) or synonymous (S) change.

144

$$\pi = \frac{1}{15} ((2+1+1+1+0)+(3+3+3+2)+(0+0+1)+(0+1)+(1)) = 1.2\bar{6} \quad (2.2)$$

where the first bracketed term gives the pairwise differences between
 146 a and b-f, the second bracketed term the differences between b and c-f
 and so on.

148 Our π measure will depend on the length of sequence it is calcu-
 lated for. Therefore, π is usually normalized by the length of sequence,
 150 to be a per site (or per base) measure. For example, our ADH se-
 quence covers 397bp of DNA and so $\pi = 1.2\bar{6}/397 = 0.0032$ per site
 152 in *D. simulans* for this region. Note that we could also calculate π
 per synonymous site (or non-synonymous). For synonymous site π , we
 154 would count up number of synonymous differences between our pairs
 of sequences, and then divide by the total number of sites where a
 156 synonymous change could have occurred.¹

Number of segregating sites. Another measure of genetic variability
 158 is the total number of sites that are polymorphic (segregating) in our
 sample. One issue is that the number of segregating sites will grow
 160 as we sequence more individuals (unlike π). Later in the course, we'll
 talk about how to standardize the number of segregating sites for the
 162 number of individuals sequenced (see eqn (3.39)).

The frequency spectrum. We also often want to compile information
 164 about the frequency of alleles across sites. We call alleles that are
 found once in a sample singletons, alleles that are found twice in a
 166 sample doubletons, and so on. We count up the number of loci where
 an allele is found i times out of n , e.g. how many singletons are there
 168 in the sample, and this is called the frequency spectrum. We'll want
 to do this in some consistent manner, so we often calculate the minor
 170 allele frequency spectrum, or the frequency spectrum of derived alleles.

Question 2. How many minor-allele singletons are there in *D.*
 172 *simulans* in the ADH region?

Levels of genetic variability across species. Two observations have
 174 puzzled population geneticists since the inception of molecular popula-
 tion genetics. The first is the relatively high level of genetic variation
 176 observed in most obligately sexual species. This first observation, in
 part, drove the development of the Neutral theory of molecular evolu-
 178 tion, the idea that much of this molecular polymorphism may simply
 reflect a balance between genetic drift and mutation. The second ob-
 180 servation is the relatively narrow range of polymorphism across species

¹ Technically we would need to divide by the total number of possible point mutations that would result in a synonymous change; this is because some mutational changes at a particular nucleotide will result in a non-synonymous or synonymous change depending on the base-pair change.

with vastly different census sizes. This observation represented a puzzle as Neutral theory predicts that levels of genetic diversity should scale population size. Much effort in theoretical and empirical population genetics has been devoted to trying to reconcile models with these various observations. We'll return to discuss these ideas throughout our course.

The first observations of molecular genetic diversity within natural populations were made from surveys of allozyme data, but we can revisit these general patterns with modern data.

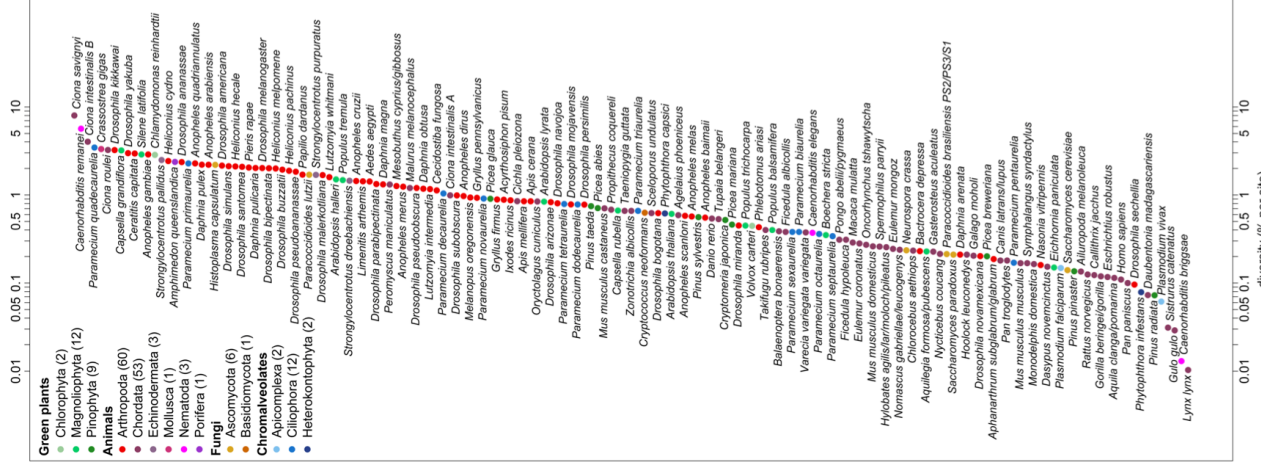
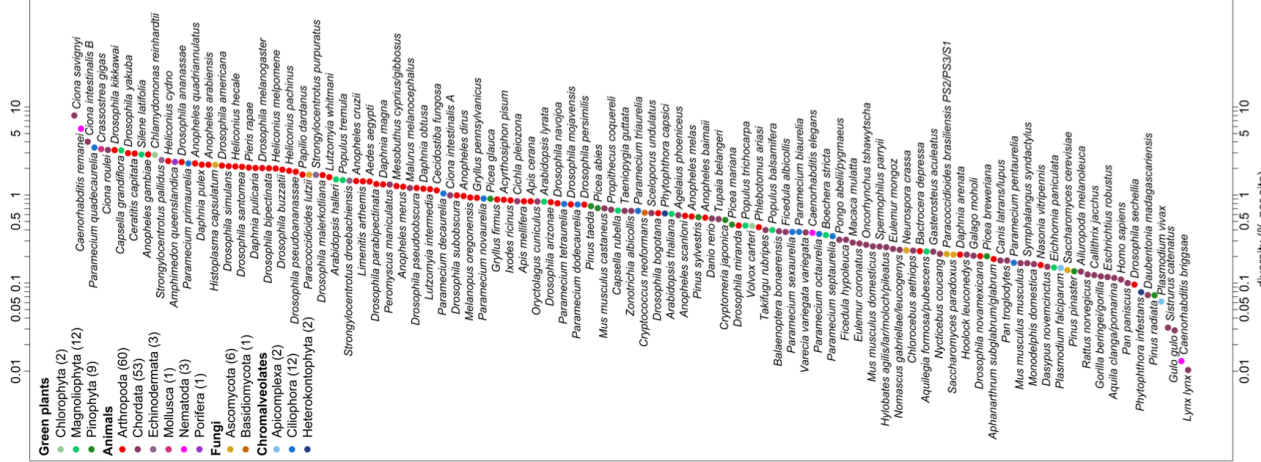


Figure 2.1: Sea Squirt (*Ciona intestinalis*).

Einleitung in die vergleichende gehirnphysiologie und Vergleichende psychologie. Loeb, J. 1899. Image from the Biodiversity Heritage Library. Contributed by MBLWHOI Library. No known copyright restrictions.



For example, LEFFLER *et al.* (2012) compiled data on levels of within-population, autosomal nucleotide diversity (π) for 167 species across 14 phyla from non-coding and synonymous sites (Figure 2.2). The species with the lowest levels of π in their survey was Lynx, with $\pi = 0.01\%$, i.e. only 1/10000 bases differed between two sequences. In contrast, some of the highest levels of diversity were found in *Ciona savignyi*, Sea Squirts, where a remarkable 1/12 bases differ between pairs of sequences. This 800-fold range of diversity seems impressive, but census population sizes have a much larger range.

2.1.2 Hardy–Weinberg proportions

Imagine a population mating at random with respect to genotypes, i.e. no inbreeding, no assortative mating, no population structure, and no sex differences in allele frequencies. The frequency of allele A_1 in the population at the time of reproduction is p . An A_1A_1 genotype is made by reaching out into our population and independently drawing two A_1 allele gametes to form a zygote. Therefore, the probability that an individual is an A_1A_1 homozygote is p^2 . This probability is also the expected frequencies of the A_1A_1 homozygote in the popula-

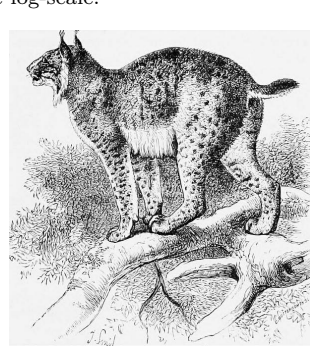


Figure 2.3: Eurasian Lynx (*Lynx lynx*).

An introduction to the study of mammals living and extinct. Flower, W.H. and Lydekker, R. 1891. Image from the Biodiversity Heritage Library. Contributed by Cornell University Library. No known copyright restrictions.

208 tion. The expected frequency of the three possible genotypes are

$$\begin{array}{ccc} f_{11} & f_{12} & f_{22} \\ \hline p^2 & 2pq & q^2 \end{array}$$

210 Note that we only need to assume random mating with respect to
our focal allele in order for these expected frequencies to hold in the
212 zygotes forming the next generation. Evolutionary forces, such as
selection, change allele frequencies within generations, but do not
214 change this expectation for new zygotes, as long as p is the frequency
of the A_1 allele in the population at the time when gametes fuse.

216 **Question 3.** On the coastal islands of British Columbia there is
a subspecies of black bear (*Ursus americanus kermodei*, Kermode's
218 bear). Many members of this black bear subspecies are white; they're
sometimes called spirit bears. These bears aren't hybrids with polar
220 bears, nor are they albinos. They are homozygotes for a recessive
change at the MC1R gene. Individuals who are *GG* at this SNP are
222 white while *AA* and *AG* individuals are black.

Below are the genotype counts for the MC1R polymorphism in
224 a sample of bears from British Columbia's island populations from
RITLAND *et al.*.

	<i>AA</i>	<i>AG</i>	<i>GG</i>
226	42	24	21

What are the expected frequencies of the three genotypes under
228 HWE?

See Figure 2.5 for a nice empirical demonstration of Hardy-Weinberg
230 proportions. The mean frequency of each genotype closely match their
HW expectations, and much of the scatter of the dots around the ex-
232 pected line is due to our small sample size (~ 60 individuals). While
HW often seems like a silly model, it often holds remarkably well
234 within populations. This is because individuals don't mate at random,
but they do mate at random with respect to their genotype at most of
236 the loci in the genome.

238 **Question 4.** You are investigating a locus with three alleles, A,
B, and C, with allele frequencies p_A , p_B , and p_C . What fraction of the
population is expected to be homozygotes under Hardy-Weinberg?

240 Microsatellites are regions of the genome where individuals vary
for the number of copies of some short DNA repeat that they carry.
242 These regions are often highly variable across individuals, making
them a suitable way to identify individuals from a DNA sample. This
244 so-called DNA-fingerprinting has a range of applications from estab-
lishing paternity, identifying human remains, to matching individuals
246 to DNA samples from a crime scene. The FBI make use of the CODIS



Figure 2.4: Kermode's bear.
Extinct and vanishing mammals of the western hemisphere. 1942. Glover A. Image from the Biodiversity Heritage Library. Contributed by Prelinger Library. Not in copyright.



Figure 2.5: Demonstrating Hardy–Weinberg proportions using 10,000 SNPs from the HapMap European (CEU) and African (YRI) populations. Within each of these populations the allele frequency against the frequency of the 3 genotypes; each SNP is represented by 3 different coloured points. The solid lines show the mean genotype frequency. The dashed lines show the predicted genotype frequency from Hardy–Weinberg equilibrium. [Code here](#). [Blog post on figure here](#).

database². The CODIS database contains the genotypes of over 13 million people, most of whom have been convicted of a crime. Most of the profiles record genotypes at 13 microsatellite loci that are tetranucleotide repeats (since 2017, 20 sites have been genotyped).

The allele counts for two loci (D16S539 and TH01) are shown in table 2.2 and 2.3 for a sample of 155 people of European ancestry. You can assume these two loci are on different chromosomes.

allele name	80	90	100	110	120	121	130	140	150
allele count	3	34	13	102	97	1	44	13	3

allele name	60	70	80	90	93	100	110
allele counts	84	42	37	67	77	1	2

Question 5. You extract a DNA sample from a crime scene. The genotype is 100/80 at the D16S539 locus and 70/93 at TH01.

- A) You have a suspect in custody. Assuming this suspect is innocent and of European ancestry, what is the probability that their genotype would match this profile by chance (a false-match probability)?
- B) The FBI uses ≥ 13 markers. Why is this higher number necessary to make the match statement convincing evidence in court?
- C) An early case that triggered debate among forensic geneticists was a crime among the Abenaki, a Native American community in Vermont (see LEWONTIN, 1994, for discussion). There was a DNA sample from the crime scene, and the perpetrator was thought likely

² CODIS: Combined DNA Index System

Table 2.2: Data for 155 Europeans at the D16S539 microsatellite from CODIS from ALGEE-HEWITT *et al.*. The top row gives the number of tetranucleotide repeats for each allele, the bottom row gives the sample counts.

Table 2.3: Same as 2.2 but for the TH01 microsatellite.

- 266 to be a member of the Abenaki community. Given that allele frequencies vary among populations, why would people be concerned about
 268 using data from a non-Abenaki population to compute a false match probability?

270 *2.2 Allele sharing among related individuals and Identity by Descent*

272 All of the individuals in a population are related to each other by a giant pedigree (family tree). For most pairs of individuals in a population these relationships are very distant (e.g. distant cousins),
 274 while some individuals will be more closely related (e.g. sibling/first
 276 cousins). All individuals are related to one another by varying levels
 278 of relatedness, or *kinship*. Related individuals can share alleles that
 have both descended from the shared common ancestor. To be shared,
 280 these alleles must be inherited through all meioses connecting the two
 individuals (e.g. surviving the $1/2$ probability of segregation each meiosis). As closer relatives are separated by fewer meioses, closer relatives
 282 share more alleles. In Figure 2.6 we show the sharing of chromosomal
 284 regions between two cousins. As we'll see, many population and quantitative genetic concepts rely on how closely related individuals are, and thus we need some way to quantify the degree of kinship among
 286 individuals.



Figure 2.6: First cousins sharing a stretch of chromosome identical by descent. The different grandparental diploid chromosomes are coloured so we can track them and recombinations between them across the generations. Notice that the identity by descent between the cousins persists for a long stretch of chromosome due to the limited number of generations for recombination.

We will define two alleles to be identical by descent (IBD) if they
 288 are identical due to transmission from a common ancestor in the past few generations³. For the moment, we ignore mutation, and we will
 290 be more precise about what we mean by 'past few generations' later on. For example, parent and child share exactly one allele identical
 292 by descent at a locus, assuming that the two parents of the child are randomly mated individuals from the population. In Figure 2.12, I
 294 show a pedigree demonstrating some configurations of IBD.

³ COTTERMAN, C. W., 1940 A calculus for statistico-genetics. Ph. D. thesis, The Ohio State University; and MALÉCOT, G., 1948 Les mathématiques de l'hérédité

One summary of how related two individuals are is the probability
 296 that our pair of individuals share 0, 1, or 2 alleles identical by descent
 (see Figure 2.7). We denote these probabilities by r_0 , r_1 , and r_2 re-
 298 spectively. See Table 2.4 for some examples. We can also interpret
 300 these probabilities as genome-wide averages. For example, on aver-
 age, at a quarter of all their autosomal loci full-sibs share zero alleles
 identical by descent.

302 One summary of relatedness that will be important is the prob-
 ability that two alleles picked at random, one from each of the two
 304 different individuals i and j , are identical by descent. We call this
 quantity the *coefficient of kinship* of individuals i and j , and denote it
 306 by F_{ij} . It is calculated as

$$F_{ij} = 0 \times r_0 + \frac{1}{4}r_1 + \frac{1}{2}r_2. \quad (2.3)$$

The coefficient of kinship will appear multiple times, in both our dis-
 308 cussion of inbreeding and in the context of phenotypic resemblance
 between relatives.

Relationship (i,j)*	r_0	r_1	r_2	F_{ij}
parent-child	0	1	0	$1/4$
full siblings	$1/4$	$1/2$	$1/4$	$1/4$
Monzygotic twins	0	0	1	$1/2$
1 st cousins	$3/4$	$1/4$	0	$1/16$

310 **Question 6.** What are r_0 , r_1 , and r_2 for $1/2$ sibs? ($1/2$ sibs share
 one parent but not the other).

Our r coefficients are going to have various uses. For example,
 they allow us to calculate the probability of the genotypes of a pair
 of relatives. Consider a biallelic locus where allele 1 is at frequency p ,
 and two individuals who have IBD allele sharing probabilities r_0 , r_1 ,
 r_2 . What is the overall probability that these two individuals are both
 homozygous for allele 1? Well that's

$$\begin{aligned} P(A_1A_1) &= P(A_1A_1|0 \text{ alleles IBD})P(0 \text{ alleles IBD}) \\ &\quad + P(A_1A_1|1 \text{ allele IBD})P(1 \text{ allele IBD}) \\ &\quad + P(A_1A_1|2 \text{ alleles IBD})P(2 \text{ alleles IBD}) \end{aligned} \quad (2.4)$$

Or, in our r_0 , r_1 , r_2 notation:

$$\begin{aligned} P(A_1A_1) &= P(A_1A_1|0 \text{ alleles IBD})r_0 \\ &\quad + P(A_1A_1|1 \text{ allele IBD})r_1 \\ &\quad + P(A_1A_1|2 \text{ alleles IBD})r_2 \end{aligned} \quad (2.5)$$



Figure 2.7: A pair of diploid individu-
 als (X and Y) sharing 0, 1, or 2 alleles
 IBD where lines show the sharing of
 alleles by descent (e.g. from a shared
 ancestor).

Table 2.4: Probability that two
 individuals of a given relationship
 share 0, 1, or 2 alleles identical by
 descent on the autosomes. *Assuming
 this is the only close relationship the
 pair shares.

312 If our pair of relatives share 0 alleles IBD, then the probability that
 they are both homozygous is $P(A_1A_1|0 \text{ alleles IBD}) = p^2 \times p^2$, as all
 314 four alleles represent independent draws from the population. If they
 share 1 allele IBD, then the shared allele is of type A_1 with probability
 316 p , and then the other non-IBD allele, in both relatives, also needs to
 be A_1 which happens with probability p^2 , so $P(A_1A_1|1 \text{ alleles IBD}) =$
 318 $p \times p^2$. Finally, our pair of relatives can share two alleles IBD, in which
 case $P(A_1A_1|2 \text{ alleles IBD}) = p^2$, because if one of our individuals is
 320 homozygous for the A_1 allele, both individuals will be. Putting this all
 together our equation (2.5) becomes

$$P(A_1A_2) = p^4r_0 + p^3r_1 + p^2r_2 \quad (2.6)$$

322 Note that for specific cases we could also calculate this by summing
 over all the possible genotypes their shared ancestor(s) had; however,
 324 that would be much more involved and not as general as the form we
 have derived here.

326 We can write out terms like eq (2.6) for all of the possible configura-
 tions of genotype sharing/non-sharing between a pair of individuals.
 328 Based on this we can write down the expected number of polymorphic
 sites where our individuals are observed to share 0, 1, or 2 alleles.

330 **Question 7.** The genotype of our suspect in Question 5 turns
 out to be 100/80 for D16S539 and 70/80 at TH01. The suspect is not
 332 a match to the DNA from the crime scene; however, they could be a
 sibling.

334 Calculate the joint probability of observing the genotype from the
 crime and our suspect:

- 336 A) Assuming that they share no close relationship.
- B) Assuming that they are full sibs.
- 338 C) Briefly explain your findings.

340 There's a variety of ways to estimate the relationships among in-
 dividuals using genetic data. An example of using allele sharing to
 identify relatives is offered by the work of Nancy Chen (in collabo-
 342 ration with Stepfanie Aguillon, see CHEN *et al.*, 2016; AGUILLO
et al., 2017). CHEN *et al.* has collected genotyping data from thou-
 344 sandes of Florida Scrub Jays at over ten thousand loci. These Jays
 live at the Archbold field site, and have been carefully monitored for
 346 many decades allowing the pedigree of many of the birds to be known.
 Using these data she estimates allele frequencies at each locus. Then
 348 by equating the observed number of times that a pair of individuals
 share 0, 1, or 2 alleles to the theoretical expectation, she estimates
 350 the probability of r_0 , r_1 , and r_2 for each pair of birds. A plot of these
 are shown in Figure 2.9, showing how well the estimates match those
 352 known from the pedigree.



Figure 2.8: Florida Scrub-Jays (*Aphelocoma coerulescens*).
 The birds of America : from drawings made in
 the United States and their territories. 1880.
 Audubon J.J. Image from the Biodiversity
 Heritage Library. Contributed by Smithsonian
 Libraries. Licensed under CC BY-2.0.



Figure 2.9: Estimated coefficient of kinship from Florida Scrub Jays. Each point is a pair of individuals, plotted by their estimated IBD (r_1 and r_2) from their genetic data. The points are coloured by their known pedigree relationships. Note that most pairs have low kinship, and no recent genealogical relationship, and so appear as black points in the lower left corner. Thanks to Nancy Chen for supplying the data. Code here.



Figure 2.10: A simulation of sharing between first cousins. The regions of your grandmother's 22 autosomes that you inherited are coloured red, those that your cousins inherited are coloured blue. In the third panel we show the overlapping genomic regions in purple, these regions will be IBD in you and your cousin. If you are full first cousins, you will also have shared genomic regions from your shared grandfather, not shown here. Details about how we made these simulations here.

Sharing of genomic blocks among relatives. We can more directly see the sharing of the genome among close relatives using high-density SNP genotyping arrays. Below we show a simulation of you and your first cousin's genomic material that you both inherited from your shared grandmother. Colored purple are regions where you and your cousin will have matching genomic material, due to having inherited it IBD from your shared grandmother.

You and your first cousin will share at least one allele of your genotype at all of the polymorphic loci in these purple regions. There's a

range of methods to detect such sharing. One way is to look for unusually long stretches of the genome where two individuals are never homozygous for different alleles. By identifying pairs of individuals who share an unusually large number of such putative IBD blocks, we can hope to identify unknown relatives in genotyping datasets. In fact, companies like 23&me and Ancestry.com use signals of IBD to help identify family ties.

As another example, consider the case of third cousins. You share one of eight sets of great-great grandparents with each of your (likely many) third cousins. On average, you and each of your third cousins each inherit one-sixteenth of your genome from each of those two great-great grandparents. This turns out to imply that on average, a little less than one percent of your and your third cousin's genomes ($2 \times (1/16)^2 = 0.78\%$) will be identical by virtue of descent from those shared ancestors. A simulated example where third cousins share blocks of their genome (on chromosome 16 and 2) due to their great, great grandmother is shown in Figure 2.11.

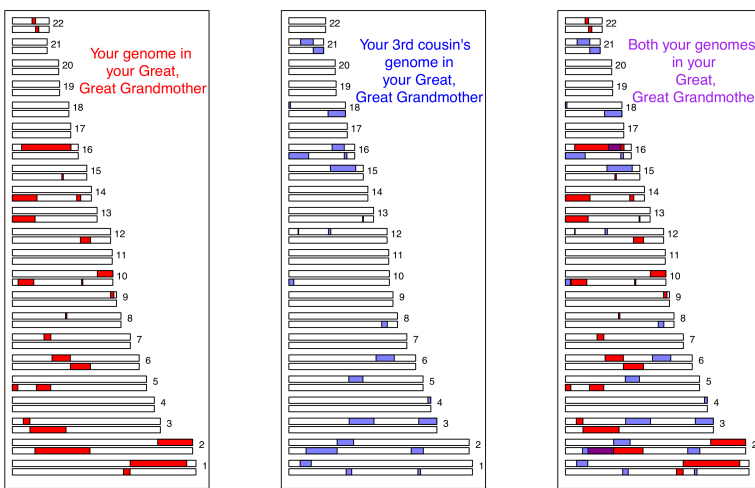


Figure 2.11: A simulation of sharing between third cousins, the details are the same as in Figure 2.10.

Note how if you compare Figure 2.11 and Figure 2.10, individuals inherit less IBD from a shared great, great grandmother than from a shared grandmother, as they inherit from more total ancestors further back. Also notice how the sharing occurs in shorter genomic blocks, as it has passed through more generations of recombination during meiosis. These blocks are still detectable, and so third cousins can be detected using high-density genotyping chips, allowing more distant relatives to be identified than single marker methods alone.⁴ More distant relations than third cousins, e.g. fourth cousins, start to have

⁴ Indeed the suspect in case of the Golden State Killer was identified through identifying third cousins that genetically matched a DNA sample from an old crime scene (see a [here](#) for more details).

- 388 a significant probability of sharing none of their genome IBD. But you
 have many fourth cousins, so you will share some of your genome IBD
 390 with some of them; however, it gets increasingly hard to identify the
 degree of relatedness from genetic data the deeper in the family tree
 392 this sharing goes.

2.2.1 Inbreeding

- 394 We can define an inbred individual as an individual whose parents are
 more closely related to each other than two random individuals drawn
 396 from some reference population.

When two related individuals produce an offspring, that individual can receive two alleles that are identical by descent, i.e. they can be homozygous by descent (sometimes termed autozygous), due to the fact that they have two copies of an allele through different paths through the pedigree. This increased likelihood of being homozygous relative to an outbred individual is the most obvious effect of inbreeding. It is also the one that will be of most interest to us, as it underlies a lot of our ideas about inbreeding depression and population structure. For example, in Figure 2.12 our offspring of first cousins is homozygous by descent having received the same IBD allele via two different routes around an inbreeding loop.

As the offspring receives a random allele from each parent (i and j), the probability that those two alleles are identical by descent is equal to the kinship coefficient F_{ij} of the two parents (Eqn. 2.3). This follows from the fact that the genotype of the offspring is made by sampling an allele at random from each of our parents.

f_{11}	f_{12}	f_{22}
$(1 - F)p^2 + Fp$	$(1 - F)2pq$	$(1 - F)q^2 + Fq$

The only way the offspring can be heterozygous (A_1A_2) is if their
 414 two alleles at a locus are not IBD (otherwise they would necessarily be
 homozygous). Therefore, the probability that they are heterozygous is

$$(1 - F)2pq, \quad (2.7)$$

416 where we have dropped the indices i and j for simplicity. The offspring can be homozygous for the A_1 allele in two different ways.
 418 They can have two non-IBD alleles that are not IBD but happen to be of the allelic type A_1 , or their two alleles can be IBD, such that they
 420 inherited allele A_1 by two different routes from the same ancestor.
 Thus, the probability that an offspring is homozygous for A_1 is

$$(1 - F)p^2 + Fp. \quad (2.8)$$



Figure 2.12: Alleles being transmitted through an inbred pedigree. The two sisters (mum and aunt) share two alleles identical by descent (IBD). The cousins share one allele IBD. The offspring of first cousins is homozygous by descent at this locus.

Table 2.5: Generalized Hardy–Weinberg

422 Therefore, the frequencies of the three possible genotypes can be
written as given in Table 2.5, which provides a generalization of the
424 Hardy–Weinberg proportions.

Note that the generalized Hardy–Weinberg proportions completely
426 specify the genotype probabilities, as there are two parameters (p
and F) and two degrees of freedom (as p and q have to sum to one).
428 Therefore, any combination of genotype frequencies at a biallelic site
can be specified by a combination of p and F .

430 **Question 8.** The frequency of the A_1 allele is p at a biallelic
locus. Assume that our population is randomly mating and that the
432 genotype frequencies in the population follow from HW. We select two
individuals at random to mate from this population. We then mate
434 the children from this cross. What is the probability that the child
from this full sib-mating is homozygous?

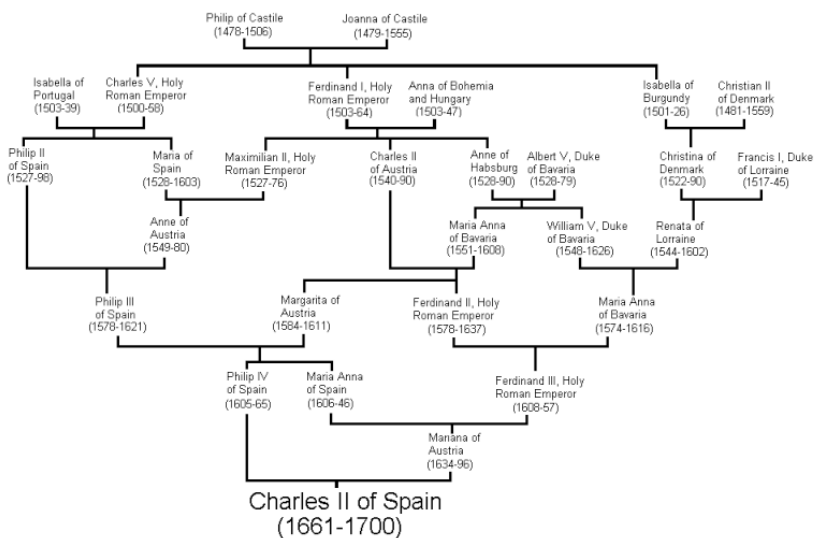
436 *Multiple inbreeding loops in a pedigree.* Up to this point we have as-
sumed that there is at most one inbreeding loop in the recent family
438 history of our individuals, i.e. the parents of our inbred individual
have at most one recent genealogical connection. However, an indi-
440 vidual who has multiple inbreeding loops in their pedigree can be
homozygous by descent thanks to receiving IBD alleles via multiple
442 different different loops. To calculate inbreeding in pedigrees of ar-
bitrary complexity, we can extend beyond our original relatedness
444 coefficients r_0 , r_1 , and r_2 to account for higher order sharing of alleles
IBD among relatives. For example, we can ask, what is the probability
446 that *both* of the alleles in the first individual are shared IBD with one
allele in the second individual? There are nine possible relatedness
448 coefficients in total to completely describe kinship between two diploid
individuals, and we won't go in to them here as it's a lot to keep track
450 of. However, we will show how we can calculate the inbreeding coeffi-
cient of an individual with multiple inbreeding loops more directly.

452 Let's say the parents of our inbred individual (B and C) have K
shared ancestors, i.e. individuals who appear in both B and C's recent
454 family trees. We denote these shared ancestors by A_1, \dots, A_K , and
we denote by n the total number of individuals in the chain from B
456 to C via ancestor A_i , including B, C, and A_i . For example, if B is C's
aunt, then B and C share two ancestors, which are B's parents and,
458 equivalently, C's grandparents. In this case, there are n=4 individuals
from B to C through each of these two shared ancestor. In the general
460 case, the kinship coefficient of B and C, i.e. the inbreeding coefficient
of their child, is

$$F = \sum_{i=1}^K \frac{1}{2^{n_i}} (1 + f_{A_i}) \quad (2.9)$$

where f_{A_i} is the inbreeding coefficient of the ancestor A_i . What's happening here is that we sum over all the mutually-exclusive paths in the pedigree through which B and C can share an allele IBD. With probability $1/2^{n_i}$, a pair of alleles picked at random from B and C is descended from the same ancestral allele in individual A_i , in which case the alleles are IBD.⁵ However, even if B inherits the maternal allele and C inherits the paternal allele of shared ancestor A_i , if A_i was themselves inbred, with probability f_{A_i} those two alleles are themselves IBD. Thus a shared *inbred* ancestor further increases the kinship of B and C.

⁵ For example, in the case of our aunt-nephew case, assuming that the aunt's two parents are their only recent shared ancestors, then $F = 1/2^4 + 1/2^4 = 1/8$, in agreement with the answer we would obtain from eqn (2.3).



486 a child of an uncle-niece marriage.

488 ALVAREZ *et al.* (2009) calculated that Charles II had an inbreeding coefficient of 0.254, equivalent to a full-sib mating, thanks to all of the inbreeding loops in his pedigree. Therefore, he is expected to have 490 been homozygous by descent for a full quarter of his genome. As we'll talk about later in these notes, this means that Charles may have been 492 homozygous for a number of recessive disease alleles, and indeed he was a very sickly man who left no descendants due to his infertility.⁶ 494 Thus plausibly the end of one of the great European dynasties came about through inbreeding.

496 *2.2.2 Calculating inbreeding coefficients from genetic data*

If the observed heterozygosity in a population is H_O , and we assume 498 that the generalized Hardy–Weinberg proportions hold, we can set H_O equal to f_{12} , and solve Eq. (2.7) for F to obtain an estimate of the 500 inbreeding coefficient as

$$\hat{F} = 1 - \frac{f_{12}}{2pq} = \frac{2pq - f_{12}}{2pq}. \quad (2.10)$$

As before, p is the frequency of allele A_1 in the population. This 502 can be rewritten in terms of the observed heterozygosity (H_O) and the heterozygosity expected in the absence of inbreeding, $H_E = 2pq$, as

$$\hat{F} = \frac{H_E - H_O}{H_E} = 1 - \frac{H_O}{H_E}. \quad (2.11)$$

504 Hence, \hat{F} quantifies the deviation due to inbreeding of the observed heterozygosity from the one expected under random mating, relative 506 to the latter.

Question 9. Suppose the following genotype frequencies were observed 508 for an esterase locus in a population of *Drosophila* (A denotes the “fast” allele and B denotes the “slow” allele):

	AA	AB	BB
510	0.6	0.2	0.2

What is the estimate of the inbreeding coefficient at the esterase locus? 512

If we have multiple loci, we can replace H_O and H_E by their means 514 over loci, \bar{H}_O and \bar{H}_E , respectively. Note that, in principle, we could also calculate F for each individual locus first, and then take the average 516 across loci. However, this procedure is more prone to introducing a bias if sample sizes vary across loci, which is not unlikely when we 518 are dealing with real data.

Genetic markers are commonly used to estimate inbreeding for wild 520 and/or captive populations of conservation concern. As an example of

⁶ Pedro Gargantilla, who performed Charles' autopsy, stated that his body "did not contain a single drop of blood; his heart was the size of a peppercorn; his lungs corroded; his intestines rotten and gangrenous; he had a single testicle, black as coal, and his head was full of water." While some of this description may refer to actual medical conditions, some of these details seem a little unlikely. See here.

this, consider the case of the Mexican wolf (*Canis lupus baileyi*), also known as the lobo, a sub-species of gray wolf.

They were extirpated in the wild during the mid-1900s due to hunting, and the remaining five lobos in the wild were captured to start a breeding program. vonHOLDT *et al.* (2011) estimated the current-day, average expected heterozygosity to be 0.18, based on allele frequencies at over forty thousand SNPs. However, the average lobo individual was only observed to be heterozygous at 12% of these SNPs. Therefore, the average inbreeding coefficient for the lobo is $F = 1 - 0.12/0.18$, i.e. $\sim 33\%$ of a lobo's genome is homozygous due to recent inbreeding in their pedigree.

Genomic blocks of homozygosity due to inbreeding. As we saw above, close relatives are expected to share alleles IBD in large genomic blocks. Thus, when related individuals mate and transmit alleles to an inbred offspring, they transmit these alleles in big blocks through meiosis. An example, lets return to the case of our hypothetical first cousins from Figure 2.6. If this pair of individuals had a child, one possible pattern of genetic transmission is shown in Figure 2.16. The child has inherited the red stretch of chromosome via two different routes through their pedigree from the grandparents. This is an example of an autozygous segment, where the child is homozygous by descent at all of the loci in this red region. The inbreeding coefficient



of the child sets the proportion of their genome that will be in these autozygous segments. For example, a child of first full cousins is expected to have $1/16$ of their genome in these segments. The more distant the loop in the pedigree, the more meioses that chromosomes have been through and the shorter individual blocks will be. A child of first cousins will have longer blocks than a child of second cousins, for example.

Individuals with multiple inbreeding loops in their family tree can have a high inbreeding coefficient due to the combined effect of many



Figure 2.15: Grey wolf (*Canis lupus*). Dogs, jackals, wolves, and foxes: a monograph of the Canidae. 1890. y J.G. Keulemans. Image from the Biodiversity Heritage Library. Contributed by University of Toronto - Gerstein Science Information Centre. Not in copyright.

Figure 2.16: .

552 small blocks of autozygosity. For example, Carlos the second had an
553 inbreeding coefficient that is equivalent to that of the child of full-sibs,
554 with a quarter of his genome expected to homozygous by descent, but
555 this would be made up of many shorter blocks.

556 We can hope to detect these blocks by looking for unusually long
557 genomic runs of homozygosity (ROH) sites in an individual's genome.
558 One way to estimate an individual's inbreeding coefficient is then to
559 total up the proportion of an individual's genome that falls in such
560 ROH regions. This estimate is called F_{ROH} .

561 An example of using F_{ROH} to study inbreeding comes from the
562 work of SAMS and BOYKO (2018b), who identified runs of homozy-
563 gosity in 2,500 dogs, ranging from 500kb up to many megabases. Fig-



Figure 2.17: English bulldog. The
dogs of Boytowm. 1918. Dyer, W. A.



Figure 2.18: The distribution of
 F_{ROH} of individuals from various
dog breeds from SAMS and BOYKO
(2018a), licensed under CC BY 4.0.

564 ure 2.18 shows the distribution of F_{ROH} of individuals in each dog
565 breed for the X and autosome. In Figure 2.19 this is broken down by
566 the length of ROH segments.

567 Dog breeds have been subject to intense breeding that has resulted
568 in high levels of inbreeding. Of the population samples examined,
569 Doberman Pinschers have the highest levels of their genome in runs
570 of homozygosity (F_{ROH}), somewhat higher than English bulldogs.
571 In 2.19 we can see that English bulldogs have more short ROH than
572 Doberman Pinschers, but that Doberman Pinschers have more of their
573 genome in very large ROH (> 16Mb). This suggests that English bull-
574 dogs have had long history of inbreeding but that Doberman Pinschers
575 have a lot of recent inbreeding in their history.



Figure 2.19: Cumulative density of length of ROH length, measured in megabases (Mb) from SAMS and BOYKO (2018a) for various dog breeds (licensed under CC BY 4.0). Note that longer lengths of ROH are on the left of the plot.

576 2.3 Summarizing population structure

INDIVIDUALS RARELY MATE COMPLETELY AT RANDOM; your
 578 parents weren't two Bilateria plucked at random from the tree of life.
 Even within species, there's often geographically-restricted mating
 580 among individuals. Individuals tend to mate with individuals from the
 same, or closely related sets of populations. This form of non-random
 582 mating is called population structure and can have profound effects
 on the distribution of genetic variation within and among natural
 584 populations.

2.3.1 Inbreeding as a summary of population structure.

586 It turns out that statements about inbreeding represent one natural
 way way to summarize population structure. We defined inbreeding
 588 as having parents that are more closely related to each other than two
 individuals drawn at random from some reference population. The
 590 question that naturally arises is: Which reference population should
 we use? While I might not look inbred in comparison to allele frequen-
 592 cies in the United Kingdom (UK), where I am from, my parents cer-
 tainly are not two individuals drawn at random from the world-wide
 594 population. If we estimated my inbreeding coefficient F using allele
 frequencies within the UK, it would be close to zero, but would likely
 596 be larger if we used world-wide frequencies. This is because there is a
 somewhat lower level of expected heterozygosity within the UK than
 598 in the human population across the world as a whole.

WRIGHT⁷ developed a set of ‘F-statistics’ (also called ‘fixation indices’) that formalize the idea of inbreeding with respect to different levels of population structure. See Figure 2.20 for a schematic diagram. Wright defined F_{XY} as the correlation between random gametes, drawn from the same level X , relative to level Y . We will return to why F -statistics are statements about correlations between alleles in just a moment. One commonly used F -statistic is F_{IS} , which is the inbreeding coefficient between an individual (I) and the subpopulation (S). Consider a single locus, where in a subpopulation (S) a fraction $H_I = f_{12}$ of individuals are heterozygous. In this subpopulation, let the frequency of allele A_1 be p_S , such that the expected heterozygosity under random mating is $H_S = 2p_S(1 - p_S)$. We will write F_{IS} as

$$F_{IS} = 1 - \frac{H_I}{H_S} = 1 - \frac{f_{12}}{2p_S q_S}, \quad (2.12)$$

a direct analog of eqn. 2.10. Hence, F_{IS} is the relative difference between observed and expected heterozygosity due to a deviation from random mating within the subpopulation. We could also compare the observed heterozygosity in individuals (H_I) to that expected in the total population, H_T . If the frequency of allele A_1 in the total population is p_T , then we can write F_{IT} as

$$F_{IT} = 1 - \frac{H_I}{H_T} = 1 - \frac{f_{12}}{2p_T q_T}, \quad (2.13)$$

which compares heterozygosity in individuals to that expected in the total population. As a simple extension of this, we could imagine comparing the expected heterozygosity in the subpopulation (H_S) to that expected in the total population H_T , via F_{ST} :

$$F_{ST} = 1 - \frac{H_S}{H_T} = 1 - \frac{2p_S q_S}{2p_T q_T}. \quad (2.14)$$

We can relate the three F -statistics to each other as

$$(1 - F_{IT}) = \frac{H_I}{H_S} \frac{H_S}{H_T} = (1 - F_{IS})(1 - F_{ST}). \quad (2.15)$$

Hence, the reduction in heterozygosity within individuals compared to that expected in the total population can be decomposed to the reduction in heterozygosity of individuals compared to the subpopulation, and the reduction in heterozygosity from the total population to that in the subpopulation.

If we want a summary of population structure across multiple subpopulations, we can average H_I and/or H_S across populations, and use a p_T calculated by averaging p_S across subpopulations (or our samples from sub-populations). For example, the average F_{ST} across

⁷ WRIGHT, S., 1943 Isolation by Distance. *Genetics* 28(2): 114–138; and WRIGHT, S., 1949 The Genetical Structure of Populations. *Annals of Eugenics* 15(1): 323–354

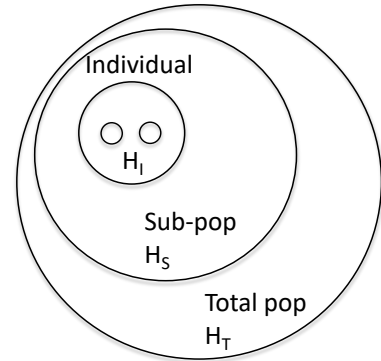


Figure 2.20: The hierarchical nature of F-statistics. The two dots within an individual represent the two alleles at a locus for an individual I . We can compare the heterozygosity on individuals (H_I), to that found by randomly drawing alleles from the sub-population (S), to that found in the total population (T).

632 K subpopulations (sampled with equal effort) is

$$F_{ST} = 1 - \frac{\bar{H}_S}{H_T}, \quad (2.16)$$

where $\bar{H}_S = 1/K \sum_{i=1}^K H_S^{(i)}$, and $H_S^{(i)} = 2p_i q_i$ is the expected heterozygosity in subpopulation i . It follows that the average heterozygosity of the sub-populations $\bar{H}_S \leq H_T$,⁸ and so $F_{ST} \geq 0$ and $F_{IS} \leq F_{IT}$. Furthermore, if we have multiple sites, we can replace H_I , H_S , and H_T with their averages across loci (as above).⁹

638 As an example of comparing a genome-wide estimate of F_{ST} to that at individual loci we can look at some data from blue- and golden-winged warblers (*Vermivora cyanoptera* and *V. chrysoptera* 1-2 & 5-6 o, Figure 2.21).

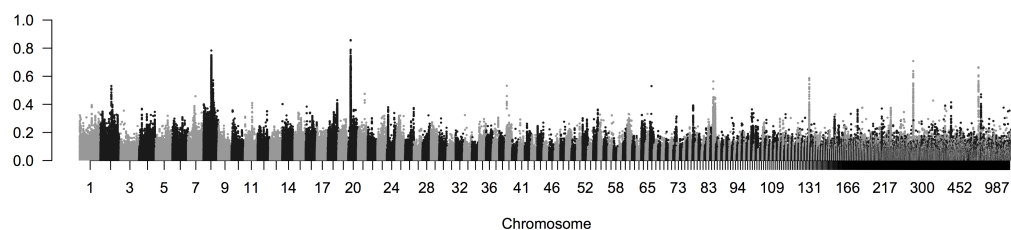
642 These two species are spread across eastern Northern America, with the golden-winged warbler having a smaller, more northerly range. 644 They're quite different in terms of plumage, but have long been known to have similar songs and ecologies. The two species hybridize readily 646 in the wild; in fact two other previously-recognized species, Brewster's and Lawrence's warbler (4 & 3 in 2.21), are actually found to just 648 be hybrids between these two species. The golden-winged warbler is listed as 'threatened' under the Canadian endangered species act. 650 The golden-winged warbler's habitat is under pressure from human activity and increased hybridization with the blue warbler, which is 652 moving north into its range, also poses a significant issue. TOEWS 654 *et al.* investigated the population genomics of these warblers, sequencing ten golden- and ten blue-winged warblers. They found very low divergence among these species, with a genome-wide $F_{ST} = 0.0045$. 656 In Figure 2.22, per SNP F_{ST} is averaged in 2000bp windows moving along the genome. The average is very low, but some regions of very

⁸ This observation that the average heterozygosity of the sub-populations must be less than or equal to that of the total population is called the Wahlund effect.

⁹ Averaging heterozygosity across loci first, then calculating F_{ST} , rather than calculating F_{ST} for each locus individually and then taking the average, has better statistical properties as statistical noise in the denominator is averaged out.



Figure 2.21: Blue-, golden-winged, and Lawrence's warblers (*Vermivora*). The warblers of North America. Chapman, F.M. 1907. Image from the Biodiversity Heritage Library. Contributed by American Museum of Natural History Library. Not in copyright.



658 high F_{ST} stand out. Nearly all of these regions correspond to large 660 allele frequency difference at loci in, or close, to genes known to be 662 involved in plumage colouration difference in other birds. To illustrate these frequency differences TOEWS *et al.* genotyped a SNP in each of these high- F_{ST} regions. Here's their genotyping counts from the SNP, segregating for an allele 1 and 2, in the *Wnt* region, a key regulatory

Figure 2.22: F_{ST} between blue- and golden-winged warbler population samples at SNPs across the genome. Each dot is a SNP, and SNPs are coloured alternating by scaffold. Thanks to David Toews for the figure.

664 gene involved in feather development:

Species	11	12	22
Blue-winged	2	21	31
Golden-winged	48	12	1

666 **Question 10.** With reference to the table of *Wnt*-allele counts:

- A) Calculate F_{IS} in blue-winged warblers.
- B) Calculate F_{ST} for the sub-population of blue-winged warblers compared to the combined sample.
- C) Calculate mean F_{ST} across both sub-populations.

672 *Interpretations of F-statistics* Let us now return to Wright's definition of the F -statistics as correlations between random gametes, drawn from the same level X , relative to level Y . Without loss of generality, 674 we may think about X as individuals and S as the subpopulation. Rewriting F_{IS} in terms of the observed homozygote frequencies (f_{11} , 676 f_{22}) and expected homozygosities (p_S^2, q_S^2) we find

$$F_{IS} = \frac{2psq_S - f_{12}}{2psq_S} = \frac{f_{11} + f_{22} - p_S^2 - q_S^2}{2psq_S}, \quad (2.17)$$

678 using the fact that $p^2 + 2pq + q^2 = 1$, and $f_{12} = 1 - f_{11} - f_{22}$. The form of eqn. (2.17) reveals that F_{IS} is the covariance between pairs of alleles found in an individual, divided by the expected variance 680 under binomial sampling. Thus, F -statistics can be understood as the correlation between alleles drawn from a population (or an individual) above that expected by chance (i.e. drawing alleles sampled at random 682 from some broader population).

684 We can also interpret F -statistics as proportions of variance explained by different levels of population structure. To see this, let 686 us think about F_{ST} averaged over K subpopulations, whose frequencies are p_1, \dots, p_K . The frequency in the total population is 688 $p_T = \bar{p} = \frac{1}{K} \sum_{i=1}^K p_i$. Then, we can write

$$F_{ST} = \frac{2\bar{p}\bar{q} - \frac{1}{K} \sum_{i=1}^K 2p_i q_i}{2\bar{p}\bar{q}} = \frac{\left(\frac{1}{K} \sum_{i=1}^K p_i^2 + \frac{1}{K} \sum_{i=1}^K q_i^2\right) - \bar{p}^2 - \bar{q}^2}{2\bar{p}\bar{q}} = \frac{\text{Var}(p_1, \dots, p_K)}{\text{Var}(\bar{p})}, \quad (2.18)$$

690 which shows that F_{ST} is the proportion of the variance explained by the subpopulation labels.

2.3.2 Other approaches to population structure

692 There is a broad spectrum of methods to describe patterns of population structure in population genetic datasets. We'll briefly discuss two 694 broad-classes of methods that appear often in the literature: assignment methods and principal components analysis.

696 2.3.3 Assignment Methods

Here we'll describe a simple probabilistic assignment to find the probability that an individual of unknown population comes from one of K predefined populations. For example, there are three broad populations of common chimpanzee (*Pan troglodytes*) in Africa: western, central, and eastern. Imagine that we have a chimpanzee, whose population of origin is unknown (e.g. it's from an illegal private collection). If we have genotyped a set of unlinked markers from a panel of individuals representative of these populations, we can calculate the probability that our chimp comes from each of these populations.

We'll then briefly explain how to extend this idea to cluster a set of individuals into K initially unknown populations. This method is a simplified version of what population genetics clustering algorithms such as STRUCTURE and ADMIXTURE do.¹⁰

710 *A simple assignment method* We have genotype data from unlinked S biallelic loci for K populations. The allele frequency of allele A_1 at 712 locus l in population k is denoted by $p_{k,l}$, so that the allele frequencies in population 1 are $p_{1,1}, \dots, p_{1,L}$ and population 2 are $p_{2,1}, \dots, p_{2,L}$ and 714 so on.

You genotype a new individual from an unknown population at 716 these L loci. This individual's genotype at locus l is g_l , where g_l denotes the number of copies of allele A_1 this individual carries at this 718 locus ($g_l = 0, 1, 2$).

The probability of this individual's genotype at locus l conditional 720 on coming from population k , i.e. their alleles being a random HW draw from population k , is

$$P(g_l | \text{pop } k) = \begin{cases} (1 - p_{k,l})^2 & g_l = 0 \\ 2p_{k,l}(1 - p_{k,l}) & g_l = 1 \\ p_{k,l}^2 & g_l = 2 \end{cases} \quad (2.19)$$

722 Assuming that the loci are independent, the probability of the individual's genotype across all S loci, conditional on the individual 724 coming from population k , is

$$P(\text{ind.} | \text{pop } k) = \prod_{l=1}^S P(g_l | \text{pop } k) \quad (2.20)$$

We wish to know the probability that this new individual comes 726 from population k , i.e. $P(\text{pop } k | \text{ind.})$. We can obtain this through Bayes' rule

$$P(\text{pop } k | \text{ind.}) = \frac{P(\text{ind.} | \text{pop } k)P(\text{pop } k)}{P(\text{ind.})} \quad (2.21)$$

¹⁰ PRITCHARD, J. K., M. STEPHENS, and P. DONNELLY, 2000 Inference of population structure using multilocus genotype data. *Genetics* 155(2): 945–959; and ALEXANDER, D. H., J. NOVEMBRE, and K. LANGE, 2009 Fast model-based estimation of ancestry in unrelated individuals. *Genome research* 19(9): 1655–1664

728 where

$$P(\text{ind.}) = \sum_{k=1}^K P(\text{ind.}|\text{pop } k)P(\text{pop } k) \quad (2.22)$$

is the normalizing constant. We interpret $P(\text{pop } k)$ as the prior probability of the individual coming from population k , and unless we have some other prior knowledge we will assume that the new individual has an equal probability of coming from each population $P(\text{pop } k) = 1/K$.

734 We interpret

$$P(\text{pop } k|\text{ind.}) \quad (2.23)$$

as the posterior probability that our new individual comes from each of our $1, \dots, K$ populations.

More sophisticated versions of this are now used to allow for hybrids, e.g., we can have a proportion q_k of our individual's genome come from population k and estimate the set of q_k 's.

740 Question 11.

Returning to our chimp example, imagine that we have genotyped a set of individuals from the Western and Eastern populations at two SNPs (we'll ignore the central population to keep things simpler). The frequency of the capital allele at two SNPs (A/a and B/b) is given by

Population	locus A	locus B
Western	0.1	0.85
Eastern	0.95	0.2

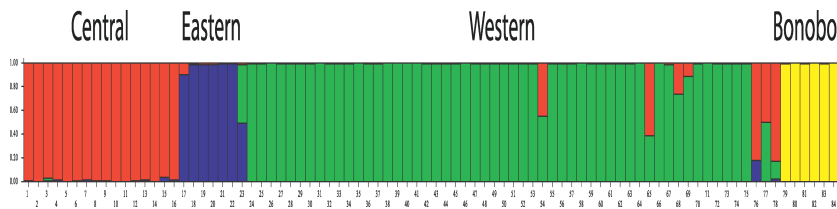
746 **A)** Our individual, whose origin is unknown, has the genotype AA at the first locus and bb at the second. What is the posterior probability 748 that our individual comes from the Western population versus Eastern chimp population?

750 **B)** Let's assume that our individual is a hybrid. At each locus, with probability q_W our individual draws an allele from the Western 752 population and with probability $q_C = 1 - q_W$ they draw an allele from the Eastern population. What is the probability of our individual's 754 genotype given q_C ?

756 **Optional** You could plot this probability as a function of q_W . How does your plot change if our individual is heterozygous at both loci?

Clustering based on assignment methods While it is great to be able 758 to assign our individuals to a particular population, these ideas can be pushed to learn about how best to describe our genotype data in 760 terms of discrete populations without assigning any of our individuals to populations *a priori*. We wish to cluster our individuals into K 762 unknown populations. We begin by assigning our individuals at random to these K populations.

- 764 1. Given these assignments we estimate the allele frequencies at all of
our loci in each population.
- 766 2. Given these allele frequencies we chose to reassign each individual
to a population k with a probability given by eqn. (2.20).
- 768 We iterate steps 1 and 2 for many iterations (technically, this ap-
proach is known as *Gibbs Sampling*). If the data is sufficiently infor-
770 mative, the assignments and allele frequencies will quickly converge on
a set of likely population assignments and allele frequencies for these
populations.



772 To do this in a full Bayesian scheme we need to place priors on
774 the allele frequencies (for example, one could use a beta distribution
prior). Technically we are using the joint posterior of our allele fre-
776 quencies and assignments. Programs like STRUCTURE, use this type
of algorithm to cluster the individuals in an “unsupervised” manner
778 (i.e. they work out how to assign individuals to an unknown set of
populations). See Figure 2.23 for an example of Becquet *et al* using
780 STRUCTURE to determine the population structure of chimpanzees.

STRUCTURE-like methods have proven incredible popular and
782 useful in examining population structure within species. However, the
results of these methods are open to misinterpretation, see LAW-
784 SON *et al.* (2018) for a recent discussion. Two common mistakes
are 1) taking the results of STRUCTURE-like approaches for some
786 particular value of K and taking this to represent the best way to
describe population-genetic variation. 2) Thinking that these clusters
788 represent ‘pure’ ancestral populations.

There is no right choice of K, the number of clusters to partition
790 into. There are methods of judging the ‘best’ K by some statistical
measure given some particular dataset, but that is not the same as
792 saying this is the most meaningful level on which to summarize pop-
ulation structure in data. For example, running STRUCTURE on
794 world-wide human populations for low value of K will result in popula-
tion clusters that roughly align with continental populations (ROSEN-
796 BERG *et al.*, 2002). However, that does not tell us that assigning
ancestral at the level of continents is a particularly meaningful way of
798 partitioning individuals. Running the same data for higher value of K,

Figure 2.23: BECQUET *et al.* (2007) genotyped 78 common chimpanzee and 6 bonobo at over 300 polymorphic markers (in this case microsatellites). They ran STRUCTURE to cluster the individuals using these data into $K = 4$ populations. In BECQUET *et al.* (2007) above figure they show each individual as a vertical bar divided into four colours depicting the estimate of the fraction of ancestry that each individual draws from each of the four estimated populations (licensed under CC BY 4.0). We can see that these four colours/populations correspond to: Red, central; blue, eastern; green, western; yellow, bonobo.

or within continental regions, will result in much finer-scale partitioning of continental groups (ROSENBERG *et al.*, 2002; LI *et al.*, 2008).
 800 No one of these layers of population structure identified is privileged
 802 as being more meaningful than another.

It is tempting to think of these clusters as representing ancestral
 804 populations, which themselves are not the result of admixture. However, that is not the case, for example, running STRUCTURE on
 806 world-wide human data identifies a cluster that contains many European individuals, however, on the basis of ancient DNA we know that
 808 modern Europeans are a mixture of distinct ancestral groups.

2.3.4 Principal components analysis

810 Principal component analysis (PCA) is a common statistical approach
 812 to visualize high dimensional data, and used by many fields. The idea
 814 of PCA is to give a location to each individual data-point on each of
 816 a small number principal component axes. These PC axes are chosen
 818 to reflect major axes of variation in the data, with the first PC being
 that which explains largest variance, the second the second most,
 and so on. The use of PCA in population genetics was pioneered by
 Cavalli-Sforza and colleagues and now with large genotyping datasets,
 818 PCA has made come back.¹¹

Consider a dataset consisting of N individuals at S biallelic SNPs.
 820 The i^{th} individual's genotype data at locus ℓ takes a value $g_{i,\ell} =$
 822 0, 1, or 2 (corresponding to the number of copies of allele A_1 an
 individual carries at this SNP). We can think of this as a $N \times S$ matrix
 (where usually $N \ll S$).

Denoting the sample mean allele frequency at SNP ℓ by p_ℓ , it's
 824 common to standardize the genotype in the following way

$$\frac{g_{i,\ell} - 2p_\ell}{\sqrt{2p_\ell(1 - p_\ell)}} \quad (2.24)$$

826 i.e. at each SNP we center the genotypes by subtracting the mean
 828 genotype ($2p_\ell$) and divide through by the square root of the expected
 variance assuming that alleles are sampled binomially from the mean
 830 frequency ($\sqrt{2p_\ell(1 - p_\ell)}$). Doing this to all of our genotypes, we form
 a data matrix (of dimension $N \times S$). We can then perform principal
 832 components analysis of this data matrix to uncover the major axes
 of genotype variance in our sample. Figure 2.24 shows a PCA from
 BECQUET *et al.* (2007) using the same chimpanzee data as in Figure
 834 2.23.

It is worth taking a moment to delve further into what we are doing
 836 here. There's a number of equivalent ways of thinking about what
 PCA is doing. One of these ways is to think that when we do PCA we
 838 are building the individual by individual covariance matrix and per-

¹¹ MENOZZI, P., A. PIAZZA, and L. CAVALLI-SFORZA, 1978 Synthetic maps of human gene frequencies in Europeans. *Science* 201(4358): 786–792; and PATTERSON, N., A. L. PRICE, and D. REICH, 2006 Population structure and eigenanalysis. *PLoS genetics* 2(12): e190

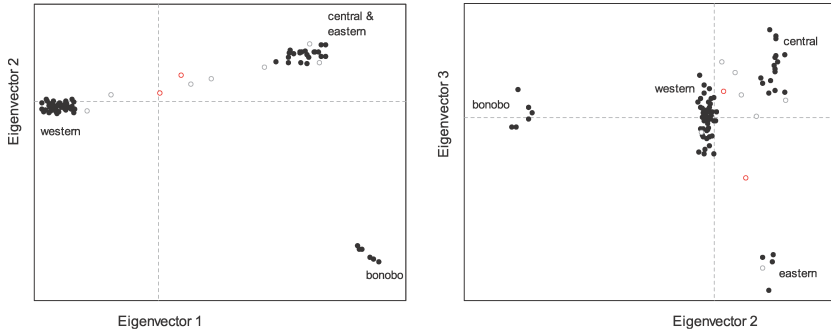


Figure 2.24: Principal Component Analysis by BECQUET *et al.* (2007) using the same chimpanzee data as in Figure 2.23. Here BECQUET *et al.* (2007) plot the location of each individual on the first two principal components (called eigenvectors) in the left panel, and on the second and third principal components (eigenvectors) in the right panel (licensed under CC BY 4.0). PCA, The individuals identified as all of one ancestry by STRUCTURE cluster together by population (solid circles). While the nine individuals identified by STRUCTURE as hybrids (open circles) are for the most part fall at intermediate locations in the PCA. There are two individuals (red open circles) reported as being of a particular population but that but appear to be hybrids.

forming an eigenvalue decomposition of this matrix (with the eigenvectors being the PCs). This individual by individual covariance matrix has entries the $[i, j]$ given by

$$\frac{1}{S-1} \sum_{\ell=1}^S \frac{(g_{i,\ell} - 2p_\ell)(g_{j,\ell} - 2p_\ell)}{2p_\ell(1-p_\ell)} \quad (2.25)$$

Note that this is the covariance, and is very similar to those we encountered in discussing F -statistics as correlations (equation (2.17)), except now we are asking about the covariance between two individuals above that expected if they were both drawn from the total sample at random (rather than the covariance of alleles within a single individual). So by performing PCA on the data we are learning about the major (orthogonal) axes of the kinship matrix.

As an example of the application of PCA, let's consider the case of the putative ring species in the Greenish warbler (*Phylloscopus trochiloides*) species complex. This set of subspecies exists in a ring around the edge of the Himalayan plateau. ALCAIDE *et al.* (2014) collected 95 greenish warbler samples from 22 sites around the ring, and the sampling locations are shown in figure 2.25.



Figure 2.25: The sampling locations of 22 populations of Greenish warblers from ALCAIDE *et al.* (2014). The samples are coloured by the subspecies. Code here.

It is thought that these warblers spread from the south, northward
 856 in two different directions around the inhospitable Himalayan plateau,
 establishing populations along the western edge (green and blue pop-
 858 ulations) and the eastern edge (yellow and red populations). When
 they came into secondary contact in Siberia, they were reproductive
 860 isolated from one another, having evolved different songs and accu-
 mulated other reproductive barriers from each other as they spread
 862 independently north around the plateau, such that *P. t. viridanus*
 (blue) and *P. t. plumbeitarsus* (red) populations presently form a
 864 stable hybrid zone.

ALCAIDE *et al.* (2014) obtained sequence data for their samples
 866 at 2,334 snps. In Figure 2.27 you can see the matrix of kinship coeffi-
 cients, using (2.25), between all pairs of samples. You can already see
 868 a lot about population structure in this matrix. Note how the red and
 yellow samples, thought to be derived from the Eastern route around
 870 the Himalayas, have higher kinship with each other, and blue and
 the (majority) of the green samples, from the Western route, form a
 872 similarly close group in terms of their higher kinship.

We can then perform PCA on this kinship matrix to identify the
 874 major axes of variation in the dataset. Figure 2.28 shows the sam-
 ples plotted on the first two PCs. The two major routes of expansion
 876 clearly occupy different parts of PC space. The first principal com-
 ponent distinguishes populations running North to South along the
 878 western route of expansion, while the second principal component
 distinguishes among populations running North to South along the
 880 Eastern route of expansion. Thus genetic data supports the hypoth-
 esis that the Greenish warblers speciated as they moved around the
 882 Himalayan plateau. However, as noted by ALCAIDE *et al.* (2014), it
 also suggests additional complications to the traditional view of these



Figure 2.26: Greenish warbler,
 subsp. *viridanus* (*Phylloscopus*
trochiloides viridanus).
 Coloured figures of the birds of the British
 Islands. 1885. Lilford T. L. P.. Image from the
 Biodiversity Heritage Library. Contributed by
 American Museum of Natural History Library.
 Not in copyright. (Greenish warblers are rare
 visitors to the UK.)



Figure 2.27: The matrix of kinship coefficients calculated for the 95 samples of Greenish warblers. Each cell in the matrix gives the pairwise kinship coefficient calculated for a particular pair. Hotter colours indicating higher kinship. The x and y labels of individuals are the population labels from Figure 2.25, and coloured by subspecies label as in that figure. The rows and columns have been organized to cluster individuals with high kinship. [Code here.](#)

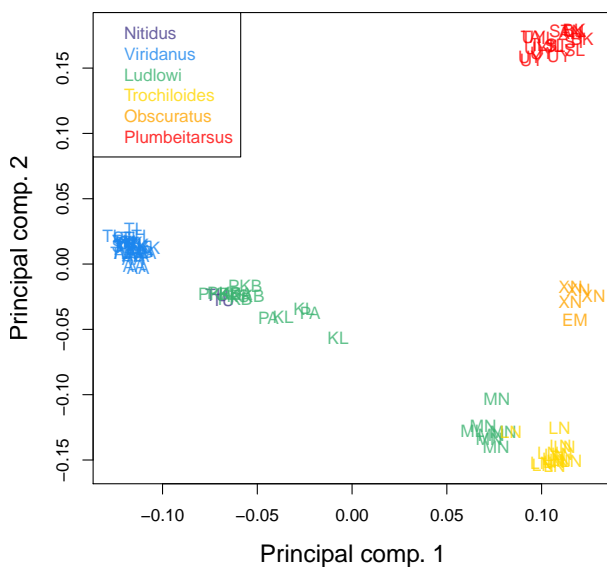


Figure 2.28: The 95 greenish warbler samples plotted on their locations on the first two principal components. The labels of individuals are the population labels from Figure 2.25, and coloured by subspecies label as in that figure. [Code here.](#)

884 warblers as an unbroken ring species, a case of speciation by continuous
885 geographic isolation. The *Ludlowi* subspecies shows a significant
886 genetic break, with the southern most MN samples clustering with the
887 *Trochiloides* subspecies, in both the PCA and kinship matrix (Figures
888 2.28 and 2.27), despite being much more geographically close to the
889 other *Ludlowi* samples. This suggests that genetic isolation is not just
890 a result of geographic distance, and other biogeographic barriers must
891 be considered in the case of this broken ring species.

892 Finally, while PCA is a wonderful tool for visualizing genetic data,
893 care must be taken in its interpretation. The U-like shape in the case
894 of the Greenish warbler PC might be consistent with some low level
895 of gene flow between the red and the blue populations, pulling them
896 genetically closer together and helping to form a genetic ring as well
897 as a geographic ring. However, U-like shapes are expected to appear in
898 PCAs even if our populations are just arrayed along a line, and more
899 complex geometric arrangements of populations in PC space can result
900 under simple geographic models (NOVEMBRE and STEPHENS,
901 2008). Inferring the geographical and population-genetic history of
902 species requires the application of a range of tools; see ALCAIDE
903 *et al.* (2014) and BRADBURD *et al.* (2016) for more discussion of the
904 Greenish warblers.

906 *2.3.5 Correlations between loci, linkage disequilibrium, and recombination*

908 Up to now we have been interested in correlations between alleles
 at the same locus, e.g. correlations within individuals (inbreeding)
 or between individuals (relatedness). We have seen how relatedness
 910 between parents affects the extent to which their offspring is inbred.
 We now turn to correlations between alleles at different loci.

912 *Recombination* To understand correlations between loci we need
 to understand recombination a bit more carefully. Let us consider
 914 a heterozygous individual, containing AB and ab haplotypes. If no
 recombination occurs between our two loci in this individual, then
 916 these two haplotypes will be transmitted intact to the next genera-
 tion. While if a recombination (i.e. an odd number of crossing over
 918 events) occurs between the two parental haplotypes, then $1/2$ the time
 the child receives an Ab haplotype and $1/2$ the time the child receives
 920 an aB haplotype. Effectively, recombination breaks up the association
 between loci. We'll define the recombination fraction (r) to be the
 922 probability of an odd number of crossing over events between our loci
 in a single meiosis. In practice we'll often be interested in relatively
 924 short regions such that recombination is relatively rare, and so we
 might think that $r = r_{BP}L \ll \frac{1}{2}$, where r_{BP} is the average recombi-
 926 nation rate (in Morgans) per base pair (typically $\sim 10^{-8}$) and L is the
 number of base pairs separating our two loci.

928 *Linkage disequilibrium* The (horrible) phrase linkage disequilibrium
 (LD) refers to the statistical non-independence (i.e. a correlation)
 930 of alleles in a population at different loci. It's an awful name for a
 fantastically useful concept; LD is key to our understanding of diverse
 932 topics, from sexual selection and speciation to the limits of genome-
 wide association studies.

934 Our two biallelic loci, which segregate alleles A/a and B/b , have
 allele frequencies of p_A and p_B respectively. The frequency of the two
 936 locus haplotype AB is p_{AB} , and likewise for our other three combi-
 nations. If our loci were statistically independent then $p_{AB} = p_A p_B$,
 938 otherwise $p_{AB} \neq p_A p_B$. We can define a covariance between the A and
 B alleles at our two loci as

$$D_{AB} = p_{AB} - p_A p_B \quad (2.26)$$

940 and likewise for our other combinations at our two loci (D_{Ab} , D_{aB} , D_{ab}).
 Gametes with two similar case alleles (e.g. A and B, or a and b)
 942 are known as *coupling* gametes, and those with different case alleles
 are known as *repulsion* gametes (e.g. a and B, or A and b). Then,

- 944 we can think of D as measuring the *excess* of coupling to repulsion
 gametes. These D statistics are all closely related to each other as
 946 $D_{AB} = -D_{Ab}$ and so on. Thus we only need to specify one D_{AB} to
 know them all, so we'll drop the subscript and just refer to D . Also a
 948 handy result is that we can rewrite our haplotype frequency p_{AB} as

$$p_{AB} = p_A p_B + D. \quad (2.27)$$

If $D = 0$ we'll say the two loci are in linkage equilibrium, while if
 950 $D > 0$ or $D < 0$ we'll say that the loci are in linkage disequilibrium
 (we'll perhaps want to test whether D is statistically different from 0
 952 before making this choice). You should be careful to keep the concepts
 954 of linkage and linkage disequilibrium separate in your mind. Genetic
 linkage refers to the linkage of multiple loci due to the fact that they
 are transmitted through meiosis together (most often because the loci
 956 are on the same chromosome). Linkage disequilibrium merely refers to
 the covariance between the alleles at different loci; this may in part be
 958 due to the genetic linkage of these loci but does not necessarily imply
 this (e.g. genetically unlinked loci can be in LD due to population
 960 structure).

Question 12. You genotype 2 bi-allelic loci (A & B) segregating
 962 in two mouse subspecies (1 & 2) which mate randomly among them-
 selves, but have not historically interbreed since they speciated. On
 964 the basis of previous work you estimate that the two loci are separated
 by a recombination fraction of 0.1. The frequencies of haplotypes in
 966 each population are:

Pop	p_{AB}	p_{Ab}	p_{aB}	p_{ab}
1	.02	.18	.08	.72
2	.72	.18	.08	.02

- 968 **A)** How much LD is there within species? (i.e. estimate D)
B) If we mixed individuals from the two species together in equal
 970 proportions, we could form a new population with p_{AB} equal to the
 average frequency of p_{AB} across species 1 and 2. What value would D
 972 take in this new population before any mating has had the chance to
 occur?

974 Our linkage disequilibrium statistic D depends strongly on the al-
 lele frequencies of the two loci involved. One common way to partially
 976 remove this dependence, and make it more comparable across loci, is
 to divide D through by its the maximum possible value given the fre-
 978 quency of the loci. This normalized statistic is called D' and varies be-
 tween +1 and -1. In Figure 2.29 there's an example of LD across the
 980 TAP2 region in human and chimp. Notice how physically close SNPs,
 i.e. those close to the diagonal, have higher absolute values of D' as



Figure 2.29: LD across the TAP2 gene region in a sample of Humans and Chimps, from PTAK *et al.* (2004), licensed under CC BY 4.0. The rows and columns are consecutive SNPs, with each cell giving the absolute D' value between a pair of SNPs. Note that these are different sets of SNPs in the two species, as shared polymorphisms are very rare.

982 closely linked alleles are separated by recombination less often allowing
983 high levels of LD to accumulate. Over large physical distances, away
from the diagonal, there is lower D' . This is especially notable in
985 humans as there is an intense, human-specific recombination hotspot in
986 this region, which is breaking down LD between opposite sides of this
region.

988 Another common statistic for summarizing LD is r^2 which we write
as

$$r^2 = \frac{D^2}{p_A(1-p_A)p_B(1-p_B)} \quad (2.28)$$

990 As D is a covariance, and $p_A(1-p_A)$ is the variance of an allele drawn
at random from locus A , r^2 is the squared correlation coefficient. Note
992 that this r in r^2 is NOT the recombination fraction.

994 Figure 2.31 shows r^2 for pairs of SNPs at various physical distances
in two population samples of *Mus musculus domesticus*. Again LD
is highest between physically close markers as LD is being generated
996 faster than it can decay via recombination; more distant markers have
much lower LD as here recombination is winning out. Note the decay
998 of LD is much slower in the advanced-generation cross population than
in the natural wild-caught population. This persistence of LD across
1000 megabases is due to the limited number of generations for recombination
since the cross was created.

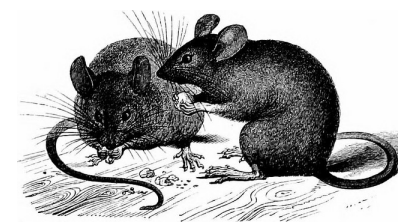
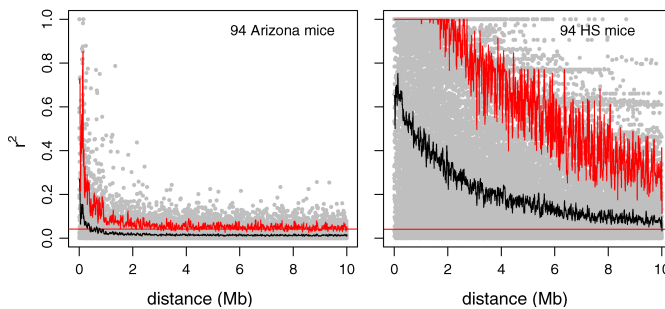


Figure 2.30: *Mus musculus*.
A history of British quadrupeds, including the Cetacea. 1874. Bell T., Tomes, R. F. m Alston E. R. Image from the Biodiversity Heritage Library. Contributed by Cornell University Library. No known copyright restrictions.

Figure 2.31: The decay of LD for autosomal SNP in *Mus musculus domesticus*, as measured by r^2 , in a wild-caught mouse population from Arizona and a set of advanced-generation crosses between inbred lines of lab mice. Each dot gives the r^2 for a pair of SNPs a given physical distance apart, for a total of ~ 3000 SNPs. The solid black line gives the mean, the jagged the 95th percentile, and the flat red line a cutoff for significant LD. From LAURIE *et al.* (2007), licensed under CC BY 4.0.

1002 *The generation of LD.* Various population genetic forces can generate LD. Selection can generate LD by favouring particular combinations
 1004 of alleles. Genetic drift will also generate LD, not because particular combinations of alleles are favoured, but simply because at random
 1006 particular haplotypes can by chance drift up in frequency. Mixing between divergent populations can also generate LD, as we saw in the
 1008 mouse question above.

1010 *The decay of LD due to recombination* We will now examine what happens to LD over the generations if we only allow recombination to occur in a very large population (i.e. no genetic drift, i.e. the frequencies of our loci follow their expectations). To do so, consider the frequency of our AB haplotype in the next generation, p'_{AB} . We lose
 1012 a fraction r of our AB haplotypes to recombination ripping our alleles apart but gain a fraction rp_{APB} per generation from other haplotypes
 1014 recombining together to form AB haplotypes. Thus in the next generation
 1016

$$p'_{AB} = (1 - r)p_{AB} + rp_{APB} \quad (2.29)$$

1018 The last term above, in eqn 2.29, is $r(p_{AB} + p_{Ab})(p_{AB} + p_{aB})$ simplified, which is the probability of recombination in the different diploid
 1020 genotypes that could generate a p_{AB} haplotype.

We can then write the change in the frequency of the p_{AB} haplotype as

$$\Delta p_{AB} = p'_{AB} - p_{AB} = -rp_{AB} + rp_{APB} = -rD \quad (2.30)$$

So recombination will cause a decrease in the frequency of p_{AB} if there is an excess of AB haplotypes within the population ($D > 0$), and an increase if there is a deficit of AB haplotypes within the population ($D < 0$). Our LD in the next generation is

$$\begin{aligned} D' &= p'_{AB} - p'_{APB} \\ &= (p_{AB} + \Delta p_{AB}) - (p_A + \Delta p_A)(p_B + \Delta p_B) \\ &= p_{AB} + \Delta p_{AB} - p_{APB} \\ &= (1 - r)D \end{aligned} \quad (2.31)$$

where we can cancel out Δp_A and Δp_B above because recombination only changes haplotype, not allele, frequencies. So if the level of LD in generation 0 is D_0 , the level t generations later (D_t) is

$$D_t = (1 - r)^t D_0 \quad (2.32)$$

1026 Recombination is acting to decrease LD, and it does so geometrically at a rate given by $(1 - r)$. If $r \ll 1$ then we can approximate this by
 1028 an exponential and say that

$$D_t \approx D_0 e^{-rt} \quad (2.33)$$



Figure 2.32: The decay of LD from an initial value of $D_0 = 0.25$ over time (Generations) for a pair of loci a recombination fraction r apart. Code here.



Figure 2.33: The decay of LD from an initial value of $D_0 = 0.25$ due to recombination over t generations, plotted across possible recombination fractions (r) between our pair of loci. Code here.

- Question 13.** You find a hybrid population between the two mouse subspecies described in the question above, which appears to be comprised of equal proportions of ancestry from the two subspecies.
- 1030
- You estimate LD between the two markers to be 0.0723. Assuming that this hybrid population is large and was formed by a single mixture event, can you estimate how long ago this population formed?
- 1032
- 1034

A particularly striking example of the decay of LD generated by the mixing of populations is offered by the LD created by the interbreeding between humans and Neanderthals. Neanderthals and modern Humans diverged from each other likely over half a million years ago, allowing time for allele frequency differences to accumulate between the Neanderthal and modern human populations. The two populations spread back into secondary contact when humans moved out of Africa over the past hundred thousand years or so. One of the most exciting findings from the sequencing of the Neanderthal genome was that modern-day people with Eurasian ancestry carry a few percent of their genome derived from the Neanderthal genome, via interbreeding during this secondary contact. To date the timing of this interbreeding, SANKARARAMAN *et al.* (2012) looked at the LD in modern humans between pairs of alleles found to be derived from the Neanderthal genome (and nearly absent from African populations). In Figure 2.35 we show the average LD between these loci as a function of the genetic distance (r) between them, from the work of SANKARARAMAN *et al.*

1036

1040

1042

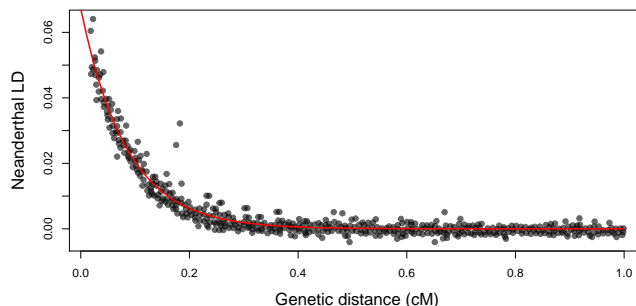
1044

1046

1048

1050

1052



- Assuming a recombination rate r , we can fit the exponential decay of LD predicted by eqn. (2.33) to the data points in this figure; the fit is shown as a red line. Doing this we estimate $t = 1200$ generations, or about 35 thousand years (using a human generation time of 29 years). Thus the LD in modern Eurasians, between alleles derived from the interbreeding with Neanderthals, represents over thirty thousand years of recombination slowly breaking down these old associations.
- 1054
- 1056
- 1058

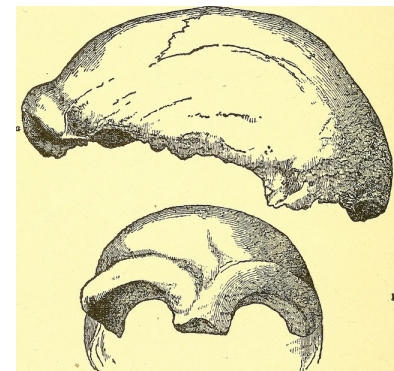


Figure 2.34: The earliest discovered fossil of a Neanderthal, fragments of skull found in a cave in the Neander Valley in Germany.
Man's place in nature. 1890. Huxley, T. H.
Image from the Internet Archive. Contributed by The Library of Congress. No known copyright restrictions.

Figure 2.35: The LD between putative-Neanderthal alleles in a modern European population (the CEU sample from the 1000 Genomes Project). Each point represents the average D statistic between a pair of alleles at loci at a given genetic distance apart (as given on the x-axis and measured in centiMorgans (cM)). The putative Neanderthal alleles are alleles where the Neanderthal genome has a derived allele that is at very low frequency in a modern-human West African population sample (thought to have little admixture from Neanderthals). The red line is the fit of an exponential decay of LD, using non-linear least squared (nls in R).

The calculation done by SANKARARAMAN *et al.* (2012) is actually a bit more involved as they account for inhomogeneity in recombination rates and arrive at a date of 47,334 – 63,146 years.

Genetic Drift and Neutral Diversity

1062 RANDOMNESS IS INHERENT TO EVOLUTION, from the lucky
 birds blown of course to colonize some new oceanic island, to which
 1064 mutations arise first in the HIV strain infecting an individual taking
 anti-retroviral drugs. One major source of stochasticity in evolution-
 1066 ary biology is genetic drift. Genetic drift occurs because more or less
 copies of an allele by chance can be transmitted to the next genera-
 1068 tion. This can occur because, by chance, the individuals carrying a
 particular allele can leave more or less offspring in the next generation.
 1070 In a sexual population, genetic drift also occurs because Mendelian
 transmission means that only one of the two alleles in an individual,
 1072 chosen at random at a locus, is transmitted to the offspring.

Genetic drift can play a role in the dynamics of all alleles in all
 1074 populations, but it will play the biggest role for neutral alleles. A
 neutral polymorphism occurs when the segregating alleles at a poly-
 1076 morphic site have no discernible differences in their effect on fitness.
 We'll make clear what we mean by "discernible" later, but for the
 1078 moment think of this as "no effect" on fitness.

1080 *The neutral theory of molecular evolution.* The role of genetic drift
 in molecular evolution has been hotly debated since the 60s when
 he Neutral theory of molecular evolution was proposed (see OHTA
 1082 and GILLESPIE, 1996, for a history).¹ The central premise of Neu-
 tral theory theory is that patterns of molecular polymorphism within
 1084 species and substitution between species can be well understood by
 supposing that the vast majority of these molecular polymorphisms
 1086 and substitutions were neutral alleles, whose dynamics were just sub-
 ject to the vagaries of genetic drift and mutation. Early proponents of
 1088 this view suggested that the vast majority of new mutations are either
 neutral or highly deleterious (e.g. mutations that disrupt important
 1090 protein functions). This latter class of mutations are too deleterious
 to contribute much to common polymorphisms or substitutions be-

¹ KIMURA, M., 1968 Evolutionary rate at the molecular level. *Nature* *217*(5129): 624–626; KING, J. L. and T. H. JUKES, 1969 Non-darwinian evolution. *Science* *164*(3881): 788–798; and KIMURA, M., 1983 *The neutral theory of molecular evolution*. Cambridge University Press

¹⁰⁹² tween species, because they are quickly weeded out of the population by selection.

¹⁰⁹⁴ Neutral theory can sound strange given that much of the time our first brush with evolution often focuses of adaptation and phenotypic evolution. However, proponents of this world-view didn't deny the existence of advantageous mutations, they simply thought that beneficial mutations are rare enough that their contribution to the bulk of polymorphism or divergence can be largely ignored. They also often thought that much of phenotypic evolution may well be adaptive, but again the loci responsible for these phenotypes are a small fraction of all the molecular change that occur. The original neutral theory of molecular evolution was original proposed to explain protein polymorphism. However, we can apply it more broadly to think about neutral evolution genome-wide. With that in mind, what types of molecular changes could be neutral? Perhaps:

- ¹¹⁰⁸ 1. Changes in non-coding DNA that don't disrupt regulatory sequences. For example, in the human genome only about 2% of the genome codes for proteins. The rest is mostly made up of old transposable element and retrovirus insertions, repeats, pseudo-genes, and general genomic clutter. Current estimates suggesting that, even counting conserved, functional, non-coding regions that < 10% of our genome is subject to evolutionary constraint (RANDS *et al.*, 2014).
 - ¹¹¹⁶ 2. Synonymous changes in coding regions, i.e. those that don't change the amino-acid encoded by a codon.
 - ¹¹¹⁸ 3. Non-synonymous changes that don't have a strong effect on the functional properties of the amino acid encoded, e.g. changes that don't change the size, charge, or hydrophobic properties of the amino acid too much.
 - ¹¹²² 4. An amino-acid change with phenotypic consequences, but little relevance to fitness, e.g. a mutation that causes your ears to be a slightly different shape, or that prevents an organism from living past 50 in a species where most individuals reproduce and die by their 20s.
- ¹¹²⁶ There are counter examples to all of these ideas, e.g. synonymous changes can affect the translation speed and accuracy of proteins and so are subject to selection. However, the list above hopefully convinces you that the general thinking that some portion of molecular change may not be subject to selection isn't as daft as it may have initially sounded.
- ¹¹³² Various features of molecular polymorphism and divergence have been viewed as consistent with the neutral theory of molecular evo-

lution. The two we'll focus on in this chapter are the high level of molecular polymorphism in many species, see for example Figure 2.2, and the molecular clock. We'll see that various aspects of the original neutral theory have merit in describing some features and types of molecular change, but we'll also see that it is demonstrably wrong in some cases. We'll also see the primary utility of the neutral theory isn't whether it is right or wrong, but that it serves as a simple null model that can be tested and in some cases rejected, and subsequently built on. The broader debate currently in the field of molecular evolution is the balance of neutral, adaptive, and deleterious changes that drive different types of evolutionary change.

3.1 Loss of heterozygosity due to drift.

Genetic drift will, in the absence of new mutations, slowly purge our population of neutral genetic diversity, as alleles slowly drift to high or low frequencies and are lost or fixed over time.

Imagine a randomly mating population of a constant size N diploid individuals, and that we are examining a locus segregating for two alleles that are neutral with respect to each other. This population is randomly mating with respect to the alleles at this locus. See Figures 3.1 and 3.2 to see how genetic drift proceeds, by tracking alleles within a small population.

In generation t our current level of heterozygosity is H_t , i.e. the probability that two randomly sampled alleles in generation t are non-identical is H_t . Assuming that the mutation rate is zero (or vanishing small), what is our level of heterozygosity in generation $t + 1$?

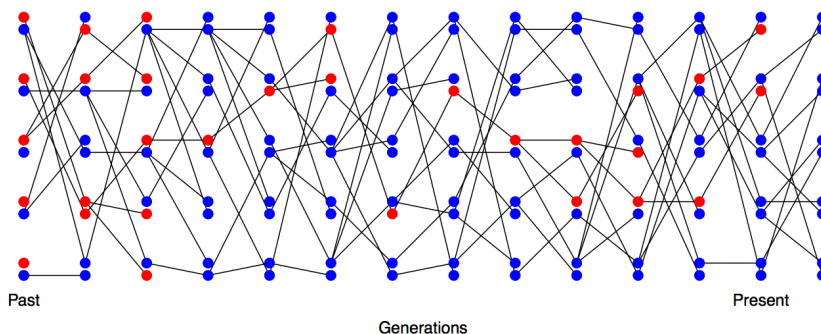


Figure 3.1: Loss of heterozygosity over time, in the absence of new mutations. A diploid population of 5 individuals over the generations, with lines showing transmission. In the first generation every individual is a heterozygote. Code here.

In the next generation ($t + 1$) we are looking at the alleles in the offspring of generation t . If we randomly sample two alleles in generation $t + 1$ which had different parental alleles in generation t , that is just like drawing two random alleles from generation t . So the probability that these two alleles in generation $t + 1$, that have different parental



Figure 3.2: Loss of heterozygosity over time, in the absence of new mutations. A diploid population of 5 individuals. In the first generation I colour every allele a different colour so we can track their descendants. Code here.

¹¹⁶⁴ alleles in generation t , are non-identical is H_t .

Conversely, if the two alleles in our pair had the same parental
¹¹⁶⁶ allele in the proceeding generation (i.e. the alleles are identical by descent one generation back) then these two alleles must be identical
¹¹⁶⁸ (as we are not allowing for any mutation).

In a diploid population of size N individuals there are $2N$ alleles.
¹¹⁷⁰ The probability that our two alleles have the same parental allele in the proceeding generation is $1/(2N)$ and the probability that they have
¹¹⁷² different parental alleles is $1 - 1/(2N)$. So by the above argument, the expected heterozygosity in generation $t + 1$ is

$$H_{t+1} = \frac{1}{2N} \times 0 + \left(1 - \frac{1}{2N}\right) H_t \quad (3.1)$$

¹¹⁷⁴ Thus, if the heterozygosity in generation 0 is H_0 , our expected heterozygosity in generation t is

$$H_t = \left(1 - \frac{1}{2N}\right)^t H_0 \quad (3.2)$$

¹¹⁷⁶ i.e. the expected heterozygosity within our population is decaying geometrically with each passing generation. If we assume that $1/(2N) \ll 1$
¹¹⁷⁸ then we can approximate this geometric decay by an exponential decay (see Question 2 below), such that

$$H_t = H_0 e^{-t/(2N)} \quad (3.3)$$

¹¹⁸⁰ i.e. heterozygosity decays exponentially at a rate $1/(2N)$.

In Figure 3.3 we show trajectories through time for 40 independently simulated loci drifting in a population of 50 individuals. Each population was started from a frequency of 30% some drift up and some drift down eventually being lost or fixed from the population, but on average, across simulations, the allele frequency doesn't change.
¹¹⁸⁴ We also track heterozygosity, you can see that heterozygosity sometimes goes up, and sometimes goes down, but on average we are losing heterozygosity, and this rate of loss is well predicted by eqn. (3.2).
¹¹⁸⁸



Figure 3.3: Change in allele frequency and loss of heterozygosity over time for 40 replicates. Simulations of genetic drift in a diploid population of 50 individuals, in the absence of new mutations. We start 40 independent, biallelic loci each with an initial allele at 30% frequency. The left panel shows the allele frequency over time and the right panel shows the heterozygosity over time, with the mean decay matching eqn. (3.2). Code here.

Question 1. You are in charge of maintaining a population of

delta smelt in the Sacramento river delta. Using a large set of microsatellites you estimate that the mean level of heterozygosity in this population is 0.005. You set yourself a goal of maintaining a level of heterozygosity of at least 0.0049 for the next two hundred years. Assuming that the smelt have a generation time of 3 years, and that only genetic drift affects these loci, what is the smallest fully outbreeding population that you would need to maintain to meet this goal?

Note how this picture of decreasing heterozygosity stands in contrast to the consistency of Hardy-Weinberg equilibrium from the previous chapter. However, our Hardy-Weinberg *proportions* still hold

in forming each new generation. As the offsprings' genotypes in the next generation ($t + 1$) represent a random draw from the previous generation (t), if the parental frequency is p_t , we *expect* a proportion $2p_t(1 - p_t)$ of our offspring to be heterozygotes (and HW proportions for our homozygotes). However, because population size is finite, the observed genotype frequencies in the offspring will (likely) not match exactly with our expectations. As our genotype frequencies likely change slightly due to sampling, biologically this reflects random variation in family size and Mendelian segregation, the allele frequency will change. Therefore, while each generation represents a sample from Hardy-Weinberg proportions based on the generation before, our genotype proportions are not at an equilibrium (an unchanging state) as the underlying allele frequency changes over the generations. We'll develop some mathematical models for these allele frequency changes later on. For now, we'll simply note that under our simple model of drift (formally the Wright Fisher model), our allele count in the $t + 1^{th}$ generation represents a binomial sample (of size $2N$) from the popu-

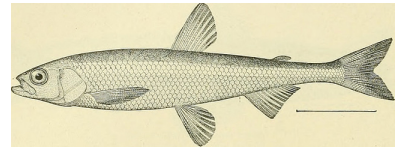


Figure 3.4: Pond smelt (*Hypomesus olidus*), a close relative of delta smelt. Bulletin of the United States Fish Commission, 1906. Image from the Biodiversity Heritage Library. Contributed by Smithsonian Libraries. Not in copyright.

lation frequency p_t in the previous generation. If you've read to here,
 1218 please email Prof Coop a picture of JBS Haldane in a striped suit with
 the title "I'm reading the chapter 3 notes". (It's well worth googling
 1220 JBS Haldane and to read more about his life; he's a true character and
 one of the last great polymaths.)

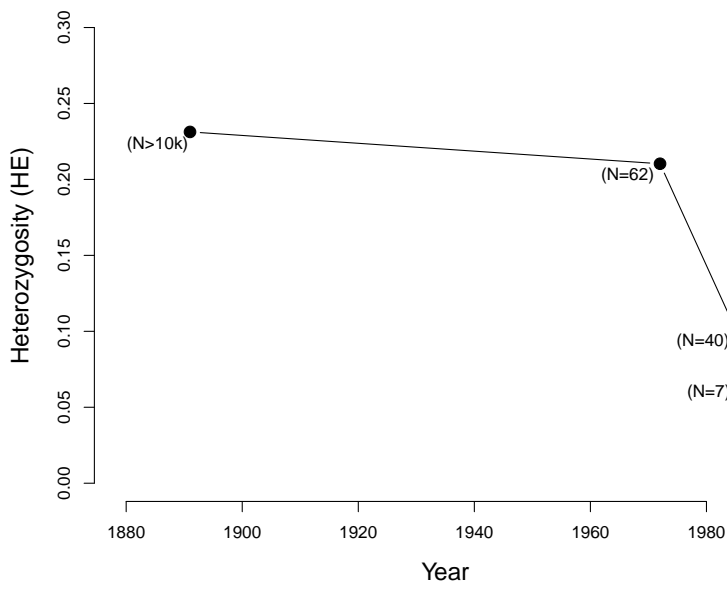


Figure 3.6: Loss of heterozygosity in the Black-footed Ferrets in their declining population. Numbers in brackets give estimated number of individuals alive at that time. Data from WISELY *et al.* (2002). Code here.



Figure 3.5: The black-footed ferret (*M. nigripes*).
 Wild animals of North America. The National geographical society, 1918. Image from the Biodiversity Heritage Library. Contributed by American Museum of Natural History Library. Not in copyright.

1222 To see how a decline in population size can affect levels of heterozygosity, let's consider the case of black-footed ferrets (*Mustela*
 1224 *nigripes*). The black-footed ferret population has declined dramatically through the twentieth century due to destruction of their habitat. In
 1226 1979, when the last known black-footed ferret died in captivity, they were thought to be extinct. In 1981, a very small wild population was
 1228 rediscovered (40 individuals), but in 1985 this population suffered a number of disease outbreaks. All of the 18 remaining wild individuals
 1230 were brought into captivity, 7 of which reproduced. Thanks to intense captive breeding efforts and conservation work, a wild population of
 1232 over 300 individuals has been established since. However, because all of these individuals are descended from those 7 individuals who
 1234 survived the bottleneck, diversity levels remain low. WISELY *et al.* measured heterozygosity at a number of microsatellites in individuals
 1236 from museum collections, showing the sharp drop in diversity as population sizes crashed (see Figure 3.6).

1238 **Question 2.** In mathematical population genetics, a commonly used approximation is $(1 - x) \approx e^{-x}$ for $x \ll 1$ (formally, this

1240 follows from the Taylor series expansion of $\exp(-x)$, ignoring second
 1242 order and higher terms of x). This approximation is especially useful
 1244 for approximating a geometric decay process by an exponential decay
 1246 process, e.g. $(1 - x)^t \approx e^{-xt}$. Using your calculator, or R, check how
 good of an approximation this is compared to the exact expression for
 two values of x , $x = 0.1$, and 0.01 , across two different values of t ,
 $t = 5$ and $t = 50$. I.e. calculate both expressions for these values, hand
 in your answers and briefly comment on your results.

1248 *3.1.1 Levels of diversity maintained by a balance between mutation
 and drift*

1250 Next we're going to consider the amount of neutral polymorphism that
 can be maintained in a population as a balance between genetic drift
 1252 removing variation and mutation introducing new neutral variation,
 see Figure 3.7 for an example. Note in our example, how no-one allele
 1254 is maintained at a stable equilibrium, rather an equilibrium level of
 polymorphism is maintained by a constantly shifting case of alleles.

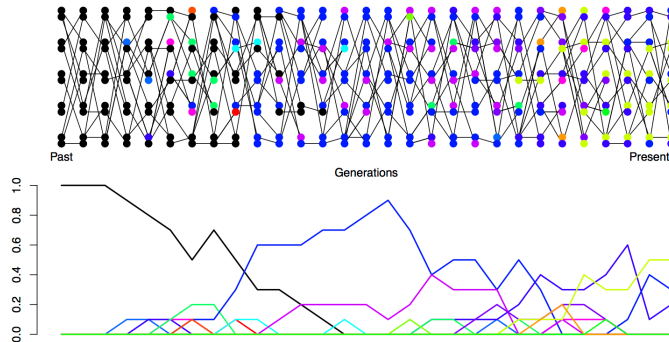


Figure 3.7: Mutation-drift balance. A diploid population of 5 individuals. In the first generation everyone has the same allele (black). Each generation the transmitted allele can mutate and we generate a new colour. In the bottom plot, I trace the frequency of alleles in our population over time. The mutation rate we use is very high, simply to maintain diversity in this small population. Code here.

1256 *The neutral mutation rate.* We'll first want to consider the rate at
 which neutral mutations arise in the population. Thinking back to our
 1258 discussion of the neutral theory of molecular evolution, let's suppose
 that there are only two classes of mutation that can arise in our ge-
 1260 nomic region of interest: neutral mutations and highly deleterious
 1262 mutations. The total mutation rate at our locus is μ_T per genera-
 tion, i.e. per transmission from parent to child. A fraction C of our
 1264 mutations are new alleles that are highly deleterious and so quickly
 removed from the population. We'll call this C parameter the con-
 straint, and it will differ according to the genomic region we consider.
 1266 The remaining fraction $(1 - C)$ are our neutral mutations, such that
 our neutral mutation rate is

$$\mu = (1 - C)\mu_T \quad (3.4)$$

₁₂₆₈ This is the per generation rate.

Question 3. It's worth taking a minute to get familiar with both
₁₂₇₀ how rare, and how common, mutation is. The per base pair mutation
₁₂₇₂ rate in humans is around 1.5×10^{-8} per generation. That means, on
₁₂₇₄ average, we have to monitor a site for ~ 66.6 million transmissions
₁₂₇₆ from parent to child to see a mutation. Yet populations and genomes
₁₂₇₈ are big places, so mutations are common at these levels.

A) Your autosomal genome is ~ 3 billion base pairs long (3×10^9).

₁₂₇₆ You have two copies, the one you received from your mum and one
₁₂₇₈ from your dad. What is the average (i.e. the expected) number of
₁₂₈₀ mutations that occurred in the transmission from your mum and your
₁₂₈₂ dad to you?

B) The current human population size is ~ 7 billion individuals.

₁₂₈₀ How many times, at the level of the entire human population, is a
₁₂₈₂ single base-pair mutated in the transmission from one generation to
₁₂₈₄ the next?

₁₂₈₄ *Levels of heterozygosity maintained as a balance between mutation
₁₂₈₆ and selection.* Looking backwards in time from one generation to
₁₂₈₈ the previous generation, we are going to say that two alleles which
₁₂₉₀ have the same parental allele (i.e. find their common ancestor) in
₁₂₉₂ the preceding generation have *coalesced*, and refer to this event as a
₁₂₉₄ *coalescent event*.

₁₂₉₀ The probability that our pair of randomly sampled alleles have
₁₂₉₂ coalesced in the preceding generation is $1/(2N)$, the probability that our
₁₂₉₄ pair of alleles fail to coalesce is $1 - 1/(2N)$.

₁₂₉₄ The probability that a mutation changes the identity of the trans-
₁₂₉₆ mitted allele is μ per generation. So the probability of no mutation
₁₂₉₈ occurring is $(1 - \mu)$. We'll assume that when a mutation occurs it cre-
₁₃₀₀ ates some new allelic type which is not present in the population. This
₁₃₀₂ assumption (commonly called the infinitely-many-alleles model) makes
₁₃₀₄ the math slightly cleaner, and also is not too bad an assumption bi-
₁₃₀₆ logically. See Figure 3.7 for a depiction of mutation-drift balance in
₁₃₀₈ this model over the generations.

₁₃₀₂ This model lets us calculate when our two alleles last shared a
₁₃₀₄ common ancestor and whether these alleles are identical as a result of
₁₃₀₆ failing to mutate since this shared ancestor. For example, we can work
₁₃₀₈ out the probability that our two randomly sampled alleles coalesce 2
₁₃₁₀ generations in the past (i.e. they fail to coalesce in generation 1 and
₁₃₁₂ then coalesce in generation 2), and that they are identical as

$$\left(1 - \frac{1}{2N}\right) \frac{1}{2N} (1 - \mu)^4 \quad (3.5)$$

Note the power of 4 is because our two alleles have to have failed to

¹³⁰⁸ mutate through 2 meioses each.

More generally, the probability that our alleles coalesce in generation $t + 1$ (counting backwards in time) and are identical due to no mutation to either allele in the subsequent generations is

$$P(\text{coal. in } t+1 \& \text{ no mutations}) = \frac{1}{2N} \left(1 - \frac{1}{2N}\right)^t (1 - \mu)^{2(t+1)} \quad (3.6)$$

¹³¹² To make this slightly easier on ourselves let's further assume that $t \approx t + 1$ and so rewrite this as:

$$P(\text{coal. in } t+1 \& \text{ no mutations}) \approx \frac{1}{2N} \left(1 - \frac{1}{2N}\right)^t (1 - \mu)^{2t} \quad (3.7)$$

¹³¹⁴ This gives us the approximate probability that two alleles will coalesce in the $(t + 1)^{\text{th}}$ generation. In general, we may not know ¹³¹⁶ when two alleles may coalesce: they could coalesce in generation $t = 1, t = 2, \dots$, and so on. Thus, to calculate the probability that ¹³¹⁸ two alleles coalesce in *any* generation before mutating, we can write:

$$\begin{aligned} P(\text{coal. in any generation \& no mutations}) &\approx P(\text{coal. in } t = 1 \& \text{ no mutations}) + \\ &\quad P(\text{coal. in } t = 2 \& \text{ no mutations}) + \dots \\ &= \sum_{t=1}^{\infty} P(\text{coal. in } t \text{ generations \& no mutation}) \end{aligned}$$

which follows from basic probability and the fact that coalescing in a ¹³²⁰ particular generation is mutually exclusive with coalescing in a different generation.

While we could calculate a value for this sum given N and μ , it's difficult to get a sense of what's going on with such a complicated expression. Here, we turn to a common approximation in population genetics (and all applied mathematics), where we assume that $1/(2N) \ll 1$ and $\mu \ll 1$. This allows us to approximate the geometric decay as an exponential decay. Then, the probability two alleles coalesce in generation $t + 1$ and don't mutate can be written as:

$$P(\text{coal. in } t+1 \& \text{ no mutations}) \approx \frac{1}{2N} \left(1 - \frac{1}{2N}\right)^t (1 - \mu)^{2t} \quad (3.8)$$

$$\approx \frac{1}{2N} e^{-t/(2N)} e^{-2\mu t} \quad (3.9)$$

$$= \frac{1}{2N} e^{-t(2\mu+1/(2N))} \quad (3.10)$$

¹³²² Then we can approximate the summation by an integral, giving us:

$$\frac{1}{2N} \int_0^{\infty} e^{-t(2\mu+1/(2N))} dt = \frac{1/(2N)}{1/(2N) + 2\mu} = \frac{1}{1 + 4N\mu} \quad (3.11)$$

The equation above gives us the probability that our two alleles coalesce at some point in time, and do not mutate before reaching their common ancestor. Equivalently, this can be thought of as the probability our two alleles coalesce *before* mutating, i.e. that they are homozygous.

Then, the complementary probability that our pair of alleles are non-identical (or heterozygous) is simply one minus this. The following equation gives the equilibrium heterozygosity in a population at equilibrium between mutation and drift:

$$H = \frac{4N\mu}{1 + 4N\mu} \quad (3.12)$$

compound parameter $4N\mu$, the population-scaled mutation rate, will come up a number of times so we'll give it its own name:

$$\theta = 4N\mu \quad (3.13)$$

So all else being equal, species with larger population sizes should have proportionally higher levels of neutral polymorphism.

Question 4. The sequence-level heterozygosity in *Capsella grandiflora* (grand shepherd's purse) is $\sim 2\%$ per base. Assuming a mutation rate of $10^{-9} bp^{-1}$ per generation, what is your estimate of the population size of *C. grandiflora*?

3.1.2 The effective population size

In practice, populations rarely conform to our assumptions of being constant in size with low variance in reproductive success. Real populations experience dramatic fluctuations in size, and there is often high variance in reproductive success. Thus rates of drift in natural populations are often a lot higher than the census population size would imply. See Figure 3.8 for a depiction of a repeatedly bottlenecked population losing diversity at a fast rate.



This result was derived by KIMURA and CROW (1964) and MALÉCOT (1948) (see MALÉCOT, 1969, for an English translation, the lack of earlier translation meant this result was missed). Technically we're assuming that every new mutation creates a new allele, the so-called "infinitely many alleles" model, otherwise our pair of sequences could be identical due to repeat or back mutation. See this GENETICS blog post and EWENS (2016) for a nice discussion of the history.

the effective population size (N_e) is the population size that would result in the same rate of drift in an idealized population of constant size (following our modeling assumptions) as that observed in our true population .

Figure 3.8: Loss of heterozygosity over time in a bottlenecking population. A diploid population of 10 individuals, that bottlenecks down to three individuals repeatedly. In the first generation, I colour every allele a different colour so we can track their descendants. There are no new mutations. Code here.

1348 To cope with this discrepancy, population geneticists often invoke
 the concept of an *effective population size* (N_e). In many situations
 1350 (but not all), departures from model assumptions can be captured by
 substituting N_e for N .

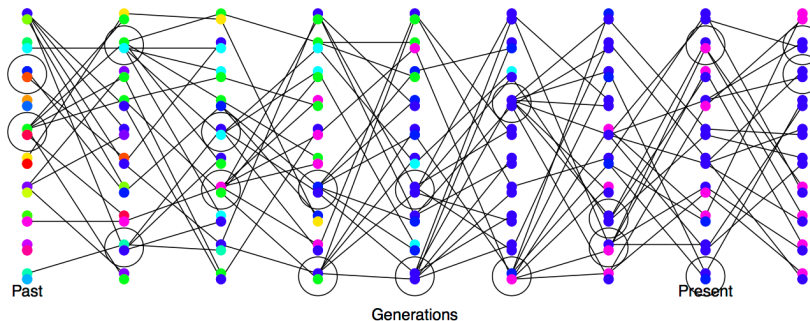
1352 If population sizes vary rapidly in size, we can (if certain conditions
 are met) replace our population size by the harmonic mean population
 1354 size. Consider a diploid population of variable size, whose size is N_t t
 generations into the past. The probability our pairs of alleles have not
 1356 coalesced by generation t is given by

$$\prod_{i=1}^t \left(1 - \frac{1}{2N_i}\right) \quad (3.14)$$

1358 Note that this simply collapses to our original expression $(1 - \frac{1}{2N})^t$ if
 N_i is constant. Under this model, the rate of loss of heterozygosity in
 this population is equivalent to a population of effective size

$$N_e = \frac{1}{\frac{1}{t} \sum_{i=1}^t \frac{1}{N_i}}. \quad (3.15)$$

1360 This is the harmonic mean of the varying population size.²
 Thus our effective population size, the size of an idealized constant
 1362 population which matches the rate of genetic drift, is the harmonic
 mean true population size over time. The harmonic mean is very
 1364 strongly affected by small values, such that if our population size is
 one million 99% of the time but drops to 1000 every hundred or so
 1366 generations, N_e will be much closer to 1000 than a million.



² To see this, note that if $1/(N_i)$ is small, then we can approximate (3.14) using the exponential approximation:

$$\prod_{i=1}^t \exp\left(-\frac{1}{2N_i}\right) = \exp\left(-\sum_{i=1}^t \frac{1}{2N_i}\right). \quad (3.16)$$

When we put the product inside the exponent, it becomes a sum. We can also write the probability of not coalescing by generation t in a population of constant size (N_e) as an exponential, so that it takes the same form as the expression above on the right. Comparing the exponent in the two cases, we see

$$\frac{t}{2N_e} = \sum_{i=1}^t 1/2N_i \quad (3.17)$$

So that if we want a constant effective population size (N_e) that has the same rate of loss of heterozygosity as our variable population, we need to rearrange and solve this equation to give (3.15).

Figure 3.9: High variance on reproductive success increases the rate of genetic drift. A diploid population of 10 individuals, where the circled individuals have much higher reproductive success. In the first generation I colour every allele a different colour so we can track their descendants, there are no new mutations. Code here.

1368 Variance in reproductive success will also affect our effective population size. Even if our population has a large constant size N individuals, if only small proportion of them get to reproduce, then the
 1370 rate of drift will reflect this much smaller number of reproducing individuals. See Figure 3.9 for a depiction of the higher rate of drift in a
 1372 population where there is high variance in reproductive success.

To see one example of this, consider the case where N_F of females
 1374 get to reproduce and N_M males get reproduce. While every individual

has a mother an a father, not every individual gets to be a parent. In
 1376 practice, in many animal species far more females get to reproduce
 than males, i.e. $N_M < N_F$, as a few males get many mating oppor-
 1378 tunities and many males get no/few mating opportunities (see JAN-
 ICKE *et al.*, 2016, for a broad analysis, and note that there are certainly
 1380 many exceptions to this general pattern). When our two alleles pick
 an ancestor, 25% of the time our alleles were both in a female ances-
 1382 tor, in which case they are IBD with probability $1/(2N_F)$, and 25% of
 the time they are both in a male ancestor, in which case they coalesce
 1384 with probability $1/(2N_M)$. The remaining 50% of the time, our alleles
 trace back to two individuals of different sexes in the prior generation
 1386 and so cannot coalesce. Therefore, our probability of coalescence in
 the preceding generation is

$$\frac{1}{4} \left(\frac{1}{2N_M} \right) + \frac{1}{4} \left(\frac{1}{2N_F} \right) \quad (3.18)$$

1388 i.e. the rate of coalescence is the harmonic mean of the two sexes'
 population sizes, equating this to $\frac{1}{2N_e}$ we find

$$N_e = \frac{4N_F N_M}{N_F + N_M} \quad (3.19)$$

1390 Thus if reproductive success is very skewed in one sex (e.g. $N_M \ll N/2$), our effective population size will be much reduced as a re-
 1392 sult. For more on how different evolutionary forces affect the rate
 of genetic drift, and their impact on the effective population size, see
 1394 CHARLESWORTH (2009).

Question 5. You are studying a population of 500 males and 500
 1396 females Hamadryas baboons. Assume that all of the females but only
 1/10 of the males get to mate: **A)** What is the effective population
 1398 size for the autosome?

B) Do you expect the *ratio* of X-chromosome to autosomal diversity
 1400 to be higher or lower in this species compared to a species where the
 sexes have more similar variance in reproductive success? Explain the
 1402 intuition behind your answer.

3.2 The Coalescent and patterns of neutral diversity

1404 "Life can only be understood backwards; but it must be lived for-
 wards." – Kierkegaard

1406 *Pairwise Coalescent time distribution and the number of pairwise
 differences.* Thinking back to our calculations we made about the
 1408 loss of neutral heterozygosity and equilibrium levels of diversity (in
 Sections 3.1 and 3.1.1), you'll note that we could first specify which



Figure 3.10: Male Hamadryas ba-
 boons. Up to ten females live in a
 harem with a single male.
 Brehm's Tierleben (Brehm's animal life).
 Brehm, A.E. 1893. Image from the Biodiversity
 Heritage Library. Contributed by University of
 Illinois Urbana-Champaign. Not in copyright.

¹⁴¹⁰ generation a pair of sequences coalesce in, and then calculate some properties of heterozygosity based on that. That's because neutral
¹⁴¹² mutations do not affect the probability that an individual transmits an allele, and so don't affect the way in which we can trace ancestral
¹⁴¹⁴ lineages back through the generations.

¹⁴¹⁶ As such, it will often be helpful to consider the time to the common ancestor of a pair of sequences, and then think of the impact of that time to coalescence on patterns of diversity. See Figure 3.11 for an
¹⁴¹⁸ example of this.

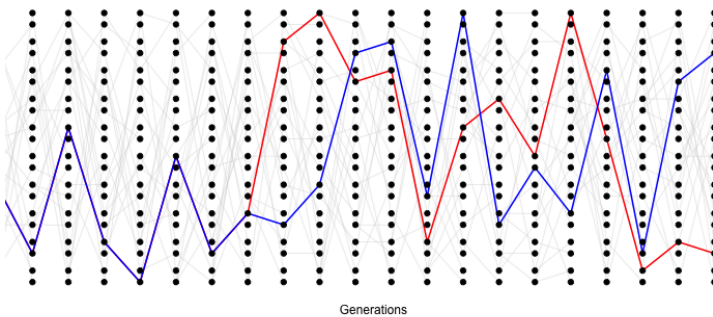


Figure 3.11: A simple simulation of the coalescent process. The simulation consists of a diploid population of 10 individuals (20 alleles). In each generation, each individual is equally likely to be the parent of an offspring (and the allele transmitted is indicated by a light grey line). We track a pair of alleles, chosen in the present day, back 14 generations until they find a common ancestor. [Code here](#).

¹⁴²⁰ The probability that a pair of alleles have failed to coalesce in t generations and then coalesce in the $t + 1$ generation back is

$$P(T_2 = t + 1) = \frac{1}{2N} \left(1 - \frac{1}{2N}\right)^t \quad (3.20)$$

¹⁴²² Thus the coalescent time of our pair of alleles is a Geometrically distributed random variable, where the probability of success is $1/(2N)$; we denote this by $T_2 \sim \text{Geo}(1/(2N))$. The expected (i.e. the mean over many replicates) coalescent time of a pair of alleles is then

$$\mathbb{E}(T_2) = 2N \quad (3.21)$$

generations.

Conditional on a pair of alleles coalescing t generations ago, there are $2t$ generations in which a mutation could occur. If the per generation mutation rate is μ , then the expected number of mutations between a pair of alleles coalescing t generations ago is $2t\mu$ (the alleles have gone through a total of $2t$ meioses since they last shared a common ancestor). So we can write the expected number of mutations

Blurring our eyes a little, we can see that 3.20 is

$$\approx \frac{1}{2N} e^{-t/(2N)} \quad (3.22)$$

and so think of a continuous random variable, i.e. we could say that the coalescent time of a pair of sequences (T_2) is approximately exponentially distributed with a rate $1/(2N)$, i.e. $T_2 \sim \text{Exp}(1/(2N))$. Formally we can do this by taking the limit of the discrete process more carefully.

(S_2) separating two alleles drawn at random from the population as

$$\begin{aligned}\mathbb{E}(S_2) &= \sum_{t=0}^{\infty} \mathbb{E}(S_2|T_2 = t)P(T_2 = t) \\ &= \sum_{t=0}^{\infty} 2\mu t P(T_2 = t) \\ &= 2\mu \mathbb{E}(T_2) \\ &= 4\mu N\end{aligned}\tag{3.23}$$

We'll assume that mutation is rare enough that it never happens at the same basepair twice, i.e. no multiple hits, such that we get to see all of the mutation events that separate our pair of sequences ³ Thus the number of mutations between a pair of sites is the observed number of differences between a pair of sequences. In the previous chapter we denote the observed number of pairwise differences at putatively neutral sites separating a pair of sequences as π (we usually average this over a number of pairs of sequences for a region). Therefore, under our simple, neutral, constant population-size model we expect

$$\mathbb{E}(\pi) = 4N\mu = \theta\tag{3.24}$$

So we can get an empirical estimate of θ from π , let's call this $\hat{\theta}_\pi$, by setting $\hat{\theta}_\pi = \pi$, i.e. our observed level of pairwise genetic diversity. If we have an independent estimate of μ , then from setting $\pi = \hat{\theta}_\pi = 4N\mu$ we can furthermore obtain an estimate of the population size N that is consistent with our levels of neutral polymorphism. If we estimate the population size this way, we should call it the effective coalescent population size (N_e). It's best to think about N_e estimated from neutral diversity as a long-term, effective population size for the species, but there's a boat load of caveats that come along with that assumption. For example, past bottlenecks and population expansions are all subsumed into a single number and so this estimated N_e may not be very representative of the population size at any time. That said, it's not a bad place to start when thinking about the rate of genetic drift for neutral diversity in our population over long time-periods.⁴

Lets take a moment to distinguish our expected heterozygosity (eqn. 3.12) from our expected number of pairwise differences (π). Our expected heterozygosity is the probability that two alleles at a locus, sampled from a population at random, are different from each other. If one or more mutations have occurred since a pair of alleles last shared a common ancestor, then our sequences will be different from each other. On the other hand, our π measure keeps track of the average total number of differences between our loci. As such, π is often a more useful measure, as it records the number of differences between

³ This is called the infinitely-many-sites assumption, which should be fine if $N\mu_{BP} \ll 1$, where μ_{BP} is the mutation rate per base pair).

⁴ Up to this point we've been describing only neutral processes, however, selection can also alter levels of polymorphism. For example, if some synonymous sites directly experience selection, then even if we use π calculated for on synonymous changes we may underestimate the coalescent effective population size. As we'll see later in the notes, selection at linked sites can also impact neutral diversity. As such, if we can, we may want to use genomic sites subject to the weakest selective constraints, and also far from gene-dense or otherwise very constrained regions of the genome, to estimate N_e from π . But even then caution is warranted.

the sequences, not just whether they are different from each other
 1460 (however, for certain types of loci, e.g. microsatellites, heterozygosity
 is often used as we cannot usually count up the minimum number of
 1462 mutations in a sensible way). In the case where our locus is a single
 basepair, the two measures will usually be close to one another, as
 1464 $H \approx \theta$ for small values of θ . For example, comparing two sequences
 at random in humans, $\pi \approx 1/1000$ per basepair, and the probability
 1466 that a specific base pair differs between two sequences is $\approx 1/1000$.
 However, these two quantities start to differ from each other when
 1468 we consider regions with higher mutation rates. For example, if we
 consider a 10kb region, our mutation rate will 10,000 times larger than
 1470 a single base pair. For this length of sequence the probability that two
 randomly chosen haplotypes differ is quite different from the number
 1472 of mutational differences between them. (Try a mutation rate of 10^{-8}
 per base and a population size of 10, 000 in our calculations of $\mathbb{E}[\pi]$
 1474 and H to see this.)

Question 6. ROBINSON *et al.* (2016) found that the endangered
 1476 Californian Channel Island fox on San Nicolas had very low levels
 of diversity ($\pi = 0.000014\text{bp}^{-1}$) compared to its close relative the
 1478 California mainland gray fox (0.0012bp^{-1}).

- A) Assuming a mutation rate of 2×10^{-8} per bp, what effective
 1480 population sizes do you estimate for these two populations?
 B) Why is the effective population size of the Channel Island fox
 1482 so low? [Hint: quickly google Channel island foxes to read up on their
 history, also to see how ridiculously cute they are.]

Question 7. In your own words describe why the coalescent time
 1484 of a pair of lineages scales linearly with the (effective) population size.
 1486



Figure 3.12: Gray Fox, *Urocyon cinereoargenteus*.

Diseases and enemies of poultry. Pearson and Warren. (1897) Image from the Biodiversity Heritage Library. Contributed by University of California Libraries. Not in copyright.

More details on the pairwise coalescent and the randomness of mutation. We've derived the expected number of differences between a
 1488 pair of sequences and talked about how variable the coalescent time
 is for a pair of sequences. The mutation process is also very variable;
 1490 even if two sequences coalesce in the very distant past by chance, they
 may still be identical in the present if there was no mutation during
 1492 that time.

Conditional on the coalescent time t , the probability that our pair
 1494 of alleles are separated by S_2 mutations since they last shared a com-
 mon ancestor is

$$P(S_2|T_2 = t) = \binom{2t}{j} \mu^j (1 - \mu)^{2t-j} \quad (3.25)$$

i.e. mutations happen in j generations and do not happen in $2t - j$
 1498 generations (with $\binom{2t}{j}$ ways this combination of events can possibly

happen). Assuming that $\mu \ll 1$ and that $2t - j \approx 2t$, then we can
 1500 approximate the probability that we have S_2 mutations as a Poisson
 distribution:

$$P(S_2|T_2 = t) = \frac{(2\mu t)^j e^{-2\mu t}}{j!} \quad (3.26)$$

1502 i.e. a Poisson with mean $2\mu t$. We'll not make much use of this result,
 but it is very useful in thinking about how to simulate the process of
 1504 mutation.

3.3 The coalescent process of a sample of alleles.

1506 Usually we are not just interested in pairs of alleles, or the average
 pairwise diversity. Generally we are interested in the properties of di-
 1508 versity in samples of a number of alleles drawn from the population.
 Instead of just following a pair of lineages back until they coalesce, we
 1510 can follow the history of a sample of alleles back through the popula-
 tion.

1512 Consider first sampling three alleles at random from the population.
 The probability that all three alleles choose exactly the same ancestral
 1514 allele one generation back is $1/(2N)^2$. If N is reasonably large, then this
 is a very small probability. As such, it is very unlikely that our three
 1516 alleles coalesce all at once, and in a moment we'll see that it is safe to
 ignore such unlikely events.

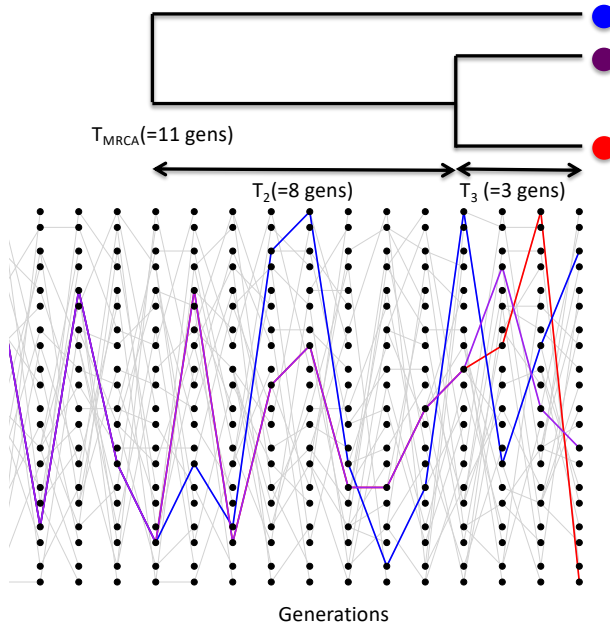


Figure 3.13: A simple simulation of the coalescent process for three lineages. We track the ancestry of three modern-day alleles, the first pair (blue and purple) coalesce four generations back, after which there are only two independent lineages we are tracking. This pair then coalesces twelve generations in the past. Note that different random realizations of this process will differ from each other a lot. The T_{MRCA} is $T_3 + T_2$. The total time in the tree is $T_{tot} = 3T_3 + 2T_2 = 25$ generations. Code here.

1518 The probability that a specific pair of alleles find a common ances-
 tor in the preceding generation is still $1/(2N)$. There are three possible

¹⁵²⁰ pairs of alleles, so the probability that no pair finds a common ancestor in the preceding generation is

$$\left(1 - \frac{1}{2N}\right)^3 \approx \left(1 - \frac{3}{2N}\right) \quad (3.27)$$

¹⁵²² In making this approximation we are multiplying out the right hand-side and ignoring terms of $1/N^2$ and higher. See Figure 3.13 for a ¹⁵²⁴ random realization of this process.

More generally, when we sample i alleles there are $\binom{i}{2}$ pairs,⁵ i.e.

¹⁵²⁶ $i(i - 1)/2$ pairs. Thus, the probability that no pair of alleles in a sample of size i coalesces in the preceding generation is

$$\left(1 - \frac{1}{(2N)}\right)^{\binom{i}{2}} \approx \left(1 - \frac{\binom{i}{2}}{2N}\right) \quad (3.28)$$

¹⁵²⁸ while the probability any pair coalesces is $\approx 2N/\binom{i}{2}$.

We can ignore the possibility that more than pairs of alleles (e.g. ¹⁵³⁰ tripletons) simultaneously coalesce at once as terms of $1/N^2$ and higher can be ignored as they are vanishingly rare. Obviously in reasonable ¹⁵³² sample sizes there are many more triples ($\binom{i}{3}$) and higher order combinations than there are pairs ($\binom{i}{2}$), but if $i \ll N$ then we are safe to ¹⁵³⁴ ignore these terms.

When there are i alleles, the probability that we wait until the $t + 1$ ¹⁵³⁶ generation before any pair of alleles coalesces is

$$P(T_i = t + 1) = \frac{\binom{i}{2}}{2N} \left(1 - \frac{\binom{i}{2}}{2N}\right)^t \quad (3.29)$$

Thus the waiting time to the first coalescent event while there are i ¹⁵³⁸ lineages is a geometrically distributed random variable with probability of success $\binom{i}{2}/2N$, which we denote by

$$T_i \sim \text{Geo}\left(\frac{\binom{i}{2}}{2N}\right). \quad (3.30)$$

¹⁵⁴⁰ The mean waiting time till any of pair within our sample coalesces is

$$\mathbb{E}(T_i) = \frac{2N}{\binom{i}{2}} \quad (3.31)$$

After a pair of alleles first finds a common ancestral allele some number of generations back in the past, we only have to keep track of that common ancestral allele for the pair when looking further into the ¹⁵⁴² past. Thus when a pair of alleles in our sample of i alleles coalesces, we then switch to having to follow $i - 1$ alleles back in time. Then ¹⁵⁴⁴ when a pair of these $i - 1$ alleles coalesce, we then only have to follow $i - 2$ alleles back. This process continues until we coalesce back ¹⁵⁴⁶ to a sample of two, and from there to a single most recent common ancestor (MRCA).

⁵ said as “i choose 2”

To see the continuous time version of this, note that (3.29) is

$$\approx \frac{\binom{i}{2}}{2N} \exp\left(-\frac{\binom{i}{2}}{2N} t\right) \quad (3.32)$$

The waiting time T_i to the first coalescent event in a sample of i alleles is thus exponentially distributed with rate $\binom{i}{2}/2N$, i.e. $T_i \sim \text{Exp}\left(\frac{\binom{i}{2}}{2N}\right)$.

1550 *Simulating a coalescent genealogy* To simulate a coalescent genealogy at a locus for a sample of n alleles we therefore simply follow the
1552 following algorithm:

1. Set $i = n$.
- 1554 2. Simulate a random variable to be the time T_i to the next coalescent event from $T_i \sim \text{Exp}((\frac{i}{2})/2N)$
- 1556 3. Choose a pair of alleles to coalesce at random from all possible pairs.
- 1558 4. Set $i = i - 1$
- 1560 5. Continue looping steps 1-3 until $i = 1$, i.e. the most recent common ancestor of the sample is found.

1562 By following this algorithm we are generating realizations of the genealogy of our sample.

3.3.1 Expected properties of coalescent genealogies and mutations.

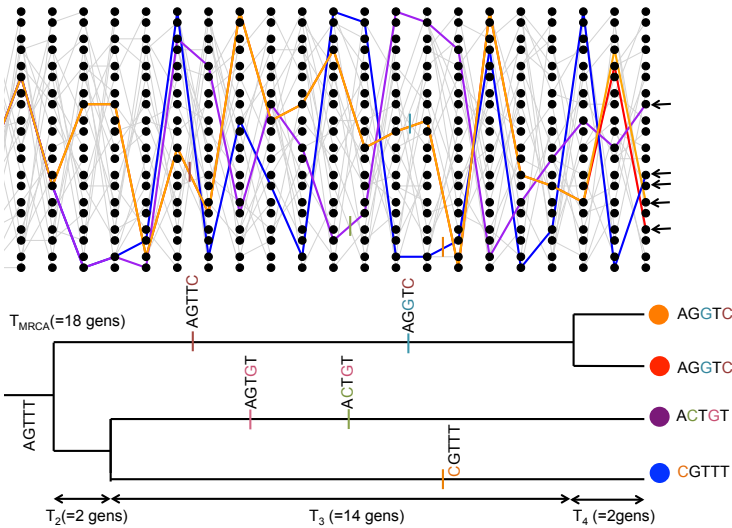


Figure 3.14: A simple coalescent tree from a single coalescent simulation, tracing the genealogy of 4 alleles with mutational changes marked with dashes showing transitions away from the MRCA sequence (AGTTT). The T_{MRCA} is $T_4 + T_3 + T_2$. The total time in the tree is $T_{tot} = 4T_4 + 3T_3 + 2T_2 = 54$ generations. [Code here.](#)

1564 *The expected time to the most recent common ancestor.* We will first consider the time to the most recent common ancestor of the entire
1566 sample (T_{MRCA}). This is

$$T_{MRCA} = \sum_{i=n}^2 T_i \quad (3.33)$$

generations back, where we are summing from $i = n$ alleles counting backwards to $i = 2$ alleles (see Figure 3.14 for example). As our coalescent times for different i are independent, the expected time to the most recent common ancestor is

$$\mathbb{E}(T_{MRCA}) = \sum_{i=n}^2 \mathbb{E}(T_i) = \sum_{i=n}^2 2N / \binom{i}{2} \quad (3.34)$$

Using the fact that $\frac{1}{i(i-1)} = \frac{1}{i-1} - \frac{1}{i}$ and a bit of rearrangement, we can rewrite this as

$$\mathbb{E}(T_{MRCA}) = 4N \left(1 - \frac{1}{n} \right) \quad (3.35)$$

So the average T_{MRCA} scales linearly with population size N . Interestingly, as we move to larger and larger samples (i.e. $n \gg 1$), the average time to the most recent common ancestor converges on $4N$. What's happening here is that in large samples our lineages typically coalesce rapidly at the start and very soon coalesce down to a much smaller number of lineages.

Question 8. Assume an autosomal effective population of 10,000 individuals (roughly the long-term human estimate) and a generation time of 30 years. What is the expected time to the most recent common ancestor of a sample of 20 people? What is this time for a sample of 500 people?

The expected total time in a genealogy and the number of segregating sites. Mutations fall on specific lineages of the coalescent genealogy and are transmitted to all descendants of their lineage. Furthermore, under the infinitely-many-sites assumption, each mutation creates a new segregating site. The mutation process is a *Poisson process*, and the longer a particular lineage, i.e. the more generations of meioses it represents, the more mutations that can accumulate on it. The total number of segregating sites in a sample is thus a function of the *total* amount of time in the genealogy of the sample, or the sum of all the branch lengths on the genealogical tree, T_{tot} . Our total amount of time in the genealogy is

$$T_{tot} = \sum_{i=n}^2 iT_i \quad (3.36)$$

as when there are i lineages, each contributes a time T_i to the total time (see Figure 3.14 for an example). Taking the expectation of the total time in the genealogy,

$$\mathbb{E}(T_{tot}) = \sum_{i=n}^2 i \frac{2N}{\binom{i}{2}} = \sum_{i=n}^2 \frac{4N}{i-1} = \sum_{i=n-1}^1 \frac{4N}{i} \quad (3.37)$$

1598 we see that our expected total amount of time in the genealogy scales
 linearly with our population size N . Our expected total amount of
 1600 time is also increasing with sample size n , but is doing so very slowly.
 This again follows from the fact that in large samples, the initial
 1602 coalescence usually happens very rapidly, so that extra samples add
 little to the total amount of time in the genealogical tree.

1604 We saw above that the number of mutational differences between
 a pair of alleles that coalescence T_2 generations ago was Poisson with
 1606 a mean of $2\mu T_2$, where $2T_2$ is the total branch length in this simple
 2-sample genealogical tree. A mutation that occurs on any branch of
 1608 our genealogy will cause a segregating polymorphism in the sample
 (meeting our infinitely-many-sites assumption). Thus, if the total time
 1610 in the genealogy is T_{tot} , there are T_{tot} generations for mutations. So
 the total number of mutations segregating in our sample (S) is Poisson
 1612 with mean μT_{tot} . Thus the expected number of segregating sites in a
 sample of size n is

$$\mathbb{E}(S) = \mu \mathbb{E}(T_{tot}) = \sum_{i=n-1}^1 \frac{4N\mu}{i} = \theta \sum_{i=n-1}^1 \frac{1}{i} \quad (3.38)$$

1614 Note that this is growing with the sample size n , albeit very slowly
 (roughly at the rate of the log of the sample size). We can use this
 1616 formula to derive another estimate of the population scaled mutation
 rate θ , by setting our observed number of segregating sites in a sample
 1618 (S) equal to this expectation. We'll call this estimator $\hat{\theta}_W$:

$$\hat{\theta}_W = \frac{S}{\sum_{i=n-1}^1 1/i} \quad (3.39)$$

This estimator of θ was devised by WATTERSON (1975), hence the
 1620 W .

The neutral site-frequency spectrum. We can use our coalescent process to find the expected number of derived alleles present i times out of a sample size n , e.g. how many singletons ($i = 1$) do we expect 1622 to find in our sample? For example, in Figure 3.14 in our sample of four sequences, there are 3 singletons and 2 doubletons. The number 1624 of sites with these different allele frequencies depends on the lengths of specific genealogical branches. A mutation that falls on a branch 1626 with i descendants will create a derived allele with frequency i . For example, in our example tree in Figure 3.14, the total number of generations where a mutation could arise and be a doubleton is $T_3 + 2T_2$, 1628 the total length of the branch ancestral to just the orange and red 1630 allele ($T_3 + T_2$) plus the branch ancestral to just the blue and purple 1632 allele (T_2).

To get a better sense of how T_{tot} grows with the sample size, we can approximate the sum 3.37 by an integral, which will work for large n . The result is $\int_1^{n-1} \frac{4N}{i} di = 4N \log(n - 1)$.

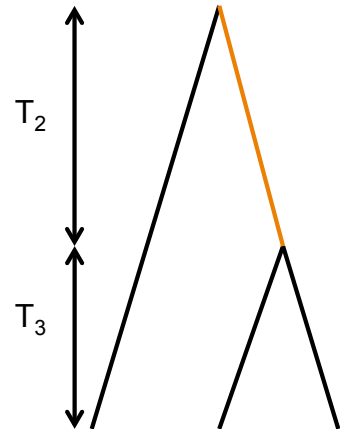


Figure 3.15: A tree for three samples; note that this is the only possible tree shape (treating the tips as unlabeled, i.e. I don't care which pair of sequences carry a doubleton, just that any two sequences carry a derived allele).

¹⁶³⁴ To see how we could go about working this out, lets start by considering the simple coalescent tree, shown in Figure 3.15, for sample of 3
¹⁶³⁶ alleles drawn from a population. Mutations that fall on the branches coloured in black will be derived singletons, while mutations that
¹⁶³⁸ fall along the orange branch will be doubletons in the sample. The total number of generations where a singleton mutation could arise
¹⁶⁴⁰ is $3T_3 + T_2$. Note that we only count the time where there are two lineages (T_2) once. So our expected number of singletons, using eqn
¹⁶⁴² (3.31), is

$$\mathbb{E}(S_i) = \mu (3\mathbb{E}(T_3) + \mathbb{E}(T_2)) = \mu \left(3 \frac{2N}{3} + 2N \right) = \theta \quad (3.40)$$

¹⁶⁴⁴ By similar logic, the time where doubletons could arise is T_2 and our expected number of doubletons is $\mathbb{E}(S_i) = \theta/2$. Thus, there are on average half as many doubletons as singletons.

¹⁶⁴⁶ Extending this logic to larger samples might be doable, but is tedious (I mean really tedious: for 10 alleles there are thousands of
¹⁶⁴⁸ possible tree shapes and the task quickly gets impossible even computationally). A nice, relatively simple proof of the neutral site frequency
¹⁶⁵⁰ spectrum is given by HUDSON, but we won't give this here. The general form is:

$$\mathbb{E}(S_i) = \frac{\theta}{i} \quad (3.41)$$

¹⁶⁵² i.e. there are twice as many singletons as doubletons, three times as many singletons as tripletons, and so on. The other thing that
¹⁶⁵⁴ will be helpful for us to know is that neutral alleles at intermediate frequency tend to be old, and those that are rare in the sample are
¹⁶⁵⁶ young. We expect to see a lot more rare alleles in our sample than common alleles.

¹⁶⁵⁸ **Question 9.** There are two possible tree shapes that could relate four samples. Draw both of them and separately colour (or otherwise
¹⁶⁶⁰ mark) the branches by where singletons, doubletons, and tripleton derived alleles could arise.

¹⁶⁶² We can also ask the probability of observing a derived allele segregating at frequency i/n given that the site is polymorphic in our
¹⁶⁶⁴ sample of size n (i.e. given that $0 < i < n$). We can obtain this probability by dividing the expected number of sites segregating for an
¹⁶⁶⁶ allele at frequency i by the expected number segregating at all of the possible allele frequencies for polymorphisms in our sample

$$P(i|0 < i < n) = \frac{\mathbb{E}(S_i)}{\sum_{j=1}^{n-1} \mathbb{E}(S_j)} = \frac{1/i}{\sum_{j=1}^{n-1} 1/j}. \quad (3.42)$$

¹⁶⁶⁸ We can interpret this probability as the fraction of polymorphic sites we expect to find at a frequency i/n .

1670 *tests based on the site frequency spectrum* Population geneticists have
1672 proposed a variety of ways to test whether an observed site frequency
1674 spectrum conforms to its neutral, constant-population expectations.
1676 These tests are useful for detecting population size changes using data
1678 across many loci, or for detecting the signal of selection at individual
1680 loci. One of the first tests was proposed by TAJIMA, and is called
1682 Tajima's D . Tajima's D is

$$D = \frac{\theta_\pi - \theta_W}{C} \quad (3.43)$$

1684 where the numerator is the difference between the estimate of θ based
1686 on pairwise differences and that based on segregating sites. As these
1688 two estimators both have expectation θ under the neutral, constant-
1690 population model, the expectation of D is zero. The denominator C is
1692 a positive constant; it's the square-root of an estimator of the variance
1694 of this difference under the constant population size, neutral model.
1696 This constant was chosen for D to have mean zero and variance 1
1698 under the null model, so we can test for departures from this simple
1700 null model.

1702 An excess of rare alleles compared to the constant-population,
1704 neutral model will result in a negative Tajima's D , because each ad-
1706ditional rare allele increases the number of segregating sites by 1, but
1708 only has a small effect on the number of pairwise differences between
1710 samples. In contrast, a positive Tajima's D reflects an excess of inter-
1712mediate frequency alleles relative to the constant-population, neutral
1714 expectation. Alleles at intermediate-frequency increase pairwise diver-
1716 sity more per segregating site than typical, thus increasing θ_π more
1718 than θ_W .

3.3.2 Demography and the coalescent

1718 We've already seen how changes in population size can change the rate
1720 at which heterozygosity is lost from the population (see the discussion
1722 around eqn. (3.14)). If the population size in generation i is N_i , the
1724 probability that a pair of lineages coalesce is $1/2N_i$; this conforms to
1726 our intuition that if the population size is small, the rate at which
1728 pairs of lineages find their common ancestor is faster. We can poten-
1730tially accommodate rapid random fluctuations in population size by
1732 simply using the effective population size N_e in place of N . However,
1734 longer term more systematic changes in population size will distort
1736 the coalescent genealogies, and hence patterns of diversity, in more
1738 systematic ways.

1740 We can see how demography potentially distorts the observed fre-
1742quency spectrum away from the neutral expectation in a very large
1744 sample of humans shown in Figure 3.20. For comparison, the neu-

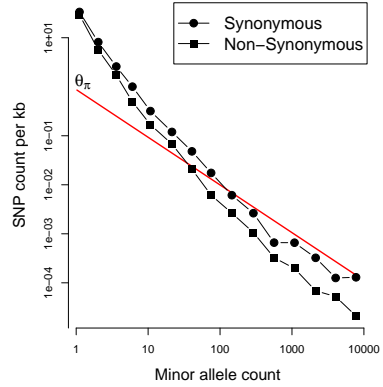
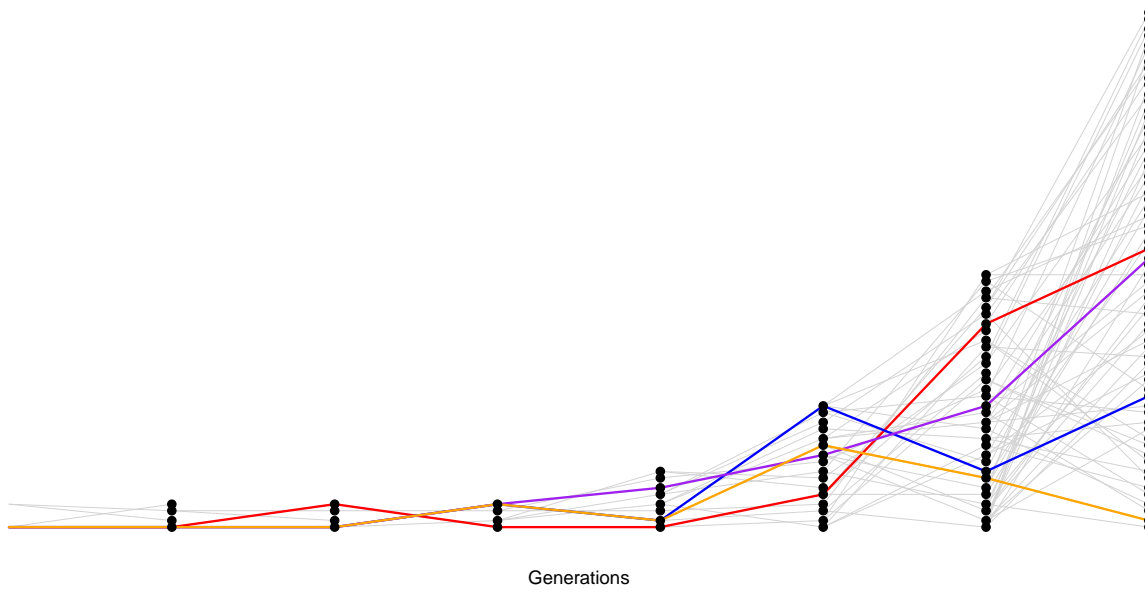


Figure 3.16: Data from 202 genes from 14002 people of European ancestry (28004 alleles). Note the double log-scale. The red line gives the neutral, constant population size estimate of the site frequency spectrum, our equation (3.41), using a θ estimated from π . Note how the non-synonymous changes are even more skewed towards rare alleles, that's likely due to selection against non-synonymous alleles acting to push them towards rare frequency. Data from NELSON *et al.* (2012). Code here.

¹⁷¹⁰ tral frequency spectrum, eqn (3.41), is shown as a red line. There are vastly more rare alleles than expected under our neutral, constant-
¹⁷¹² population-size model, but the neutral prediction and reality agree somewhat more for alleles that are more common.



¹⁷¹⁴ Why is this? Well, these patterns are likely the result of the very recent explosive growth in human populations. If the population has grown rapidly, then the pairwise-coalescent rate in the past may be much higher than the coalescent rate closer to the present. (see Figure 3.17).

¹⁷²⁰ One consequence of a recent population expansion is that there is much less genetic diversity in the population than you'd predict using the census population size. Humans are one example of this effect; ¹⁷²² there are 7 billion of us alive today, but this is due to very rapid population growth over the past thousand to tens of thousands of years. ¹⁷²⁴ Our level of genetic diversity is very much lower than you'd predict given our census size, reflecting our much smaller ancestral population. A second consequence of recent population expansion is that the ¹⁷²⁶ deeper coalescent branches are much more squished together in time, compared to those in a constant population. Mutations on deeper ¹⁷²⁸ branches are the source of alleles at more intermediate frequencies, and so there are even fewer intermediate-frequency alleles in growing ¹⁷³⁰ populations. That's why there are so many rare alleles, especially ¹⁷³² singletons, in this large sample of Europeans.

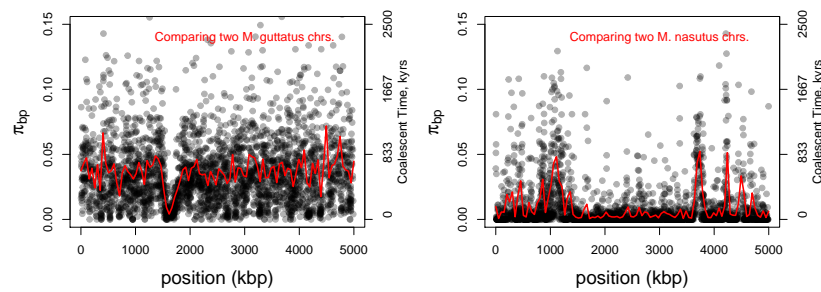
¹⁷³⁴ Another common demographic scenario is a population bottleneck. In a bottleneck, the population size crashes dramatically, and sub-

Figure 3.17: A realization of the coalescent process in a growing population. The population underwent a period of doubling every generation. The initial population size of just two individuals, maintained for a number of generations, is obviously highly unrealistic but serves our purpose. [Code here.](#)

sequently recovers. For example, our population may have had size
 1736 N_{Big} and crashed down to N_{Small} . One example of a bottleneck is
 shown in Figure 3.18. Looking at a sample of lineages drawn from the



1738 population today, if the bottleneck was somewhat recent ($\ll N_{\text{Big}}$
 generations in the past) many of our lineages will not have coalesced
 1740 before reaching the bottleneck, moving backward in time. But during
 the bottleneck our lineages coalesce at a much higher rate, such that
 1742 many of our lineages will coalesce if the bottleneck lasts long enough
 ($\sim N_{\text{Small}}$ generations). If the bottleneck is very strong, then all of
 1744 our lineages will coalesce during the bottleneck, and the resulting site
 frequency spectrum may look very much like our population growth
 1746 model (i.e. an excess of rare alleles). However, if some pairs of lineages
 escape coalescing during the bottleneck, they will coalesce much more
 deeply in time (e.g. the blue and orange ancestral lineages in 3.18).



1748 An example of this is shown Figure 3.19, data from BRANDVAIN
 1750 et al.. *Mimulus nasutus* is a selfing species that arose recently from an
 out-crossing progenitor *M. guttatus*, and experienced a strong bottle-
 1752 neck. *M. guttatus* has a very high levels of genetic diversity ($\pi = 4\%$
 at synonymous sites), but *M. nasutus* has lost much of this diversity

Figure 3.18: A realization of the coalescent process in a bottlenecked population. Our population underwent a bottleneck eight generations in the past. Code here.

Figure 3.19: Diversity along the *Mimulus* genome. Black dots give π in 1kb windows between chromosomes sampled from two individuals, the red line is a moving average (data from BRANDVAIN et al.). Pairwise coalescent times (t) estimated assuming $t = \pi/2\mu$ using $\mu_{BP} = 10^{-9}$. Code here.



Figure 3.20: Yellow Monkeyflower *M. guttatus*.

Choix des plus belles fleurs et des plus beaux fruits. Pierre-Joseph Redouté. (1833). Contributed to Flickr by Swallowtail Garden Seeds. Public Domain.

1754 ($\pi = 1\%$). Looking along the genome, between a pair of *M. guttatus* chromosomes, levels of diversity are fairly uniformly high.

1756 But in comparing two *M. nasutus* chromosomes, diversity is low because the pair of lineages generally coalesce recently. Yet in a few 1758 places we see levels of diversity comparable to *M. guttatus*; these regions correspond to genomic sites where our pair of lineages fail to 1760 coalesce during the bottleneck and subsequently coalesce much more deeply in the ancestral *M. guttatus* population.



Figure 3.21: Data for polymorphism from Maize and Teosinte: 774 genes from WRIGHT *et al.* (2005). **Left)** Genetic diversity levels in maize and Teosinte samples at each of these genes. Note how diversity levels are lower in maize than teosinte, i.e. most points are below the red $x = y$ line. **Right)** The distribution of Tajima's D in maize and teosinte, see how the maize distribution is shifted towards positive values. Code here.

1762 Mutations that arise on deeper lineages will be at intermediate frequency in our sample, and so mild bottlenecks can lead to an excess 1764 of intermediate frequency alleles compared to the standard constant-population model. This can skew Tajima's D, see eqn 3.43, towards 1766 positive values and away from its expectation of zero. One example 1768 of this skew is shown in Figure 3.21. Maize ((*Zea mays* subsp.*mays*) was domesticated from its wild progenitor teosinte ((*Zea mays* subsp. 1770 *parviglumis*) roughly ten thousand years ago. We can see how the 1772 bottleneck associated with domestication has resulted in a loss of genetic diversity in maize, compared to teosinte, and the polymorphism that remains is somewhat skewed towards intermediate frequencies resulting in more positive values of Tajima's D.

1774 **Question 10.** VOIGHT *et al.* (2005) sequenced 40 autosomal regions from 15 diploid samples of Hausa people from Yaounde, 1776 Cameroon. The average length of locus they sequenced for each region was 2365bp. They found that the average number of segregating 1778 sites per locus was $S = 11.1$ and the average $\pi = 0.0011$ per base over the loci. Is Tajima's D positive or negative? Is a demographic model 1780 with a bottleneck or growth more consistent with this result?

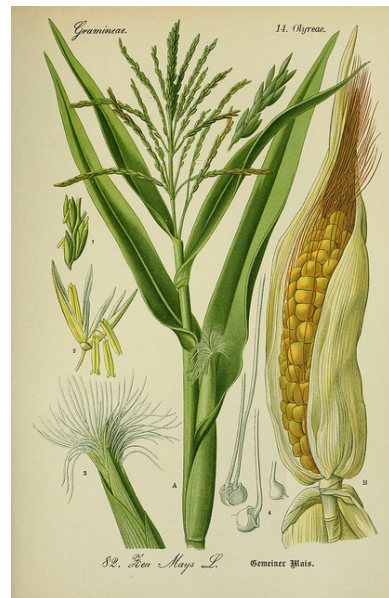


Figure 3.22: Maize (*Zea mays*). Prof. Dr. Thomé's Flora von Deutschland, 1886. Thomé, O. W. Image from the Biodiversity Heritage Library. Contributed by New York Botanical Garden. Not in copyright.

3.4 Molecular Evolution and the fixation of neutral alleles

1782 "history is just one damn thing after another" -Arnold Toynbee

1784 It is very unlikely that a rare neutral allele accidentally drifts up
 1786 to fixation; more likely, such an allele will be eventually lost from the
 population. However, populations experience a large and constant
 1788 influx of rare alleles due to mutation, so even if it is very unlikely that
 an individual allele fixes within the population, some neutral alleles
 will fix by chance.

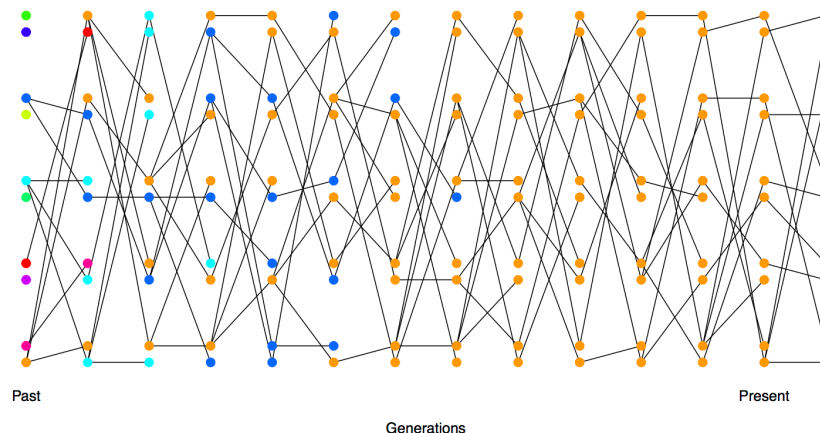


Figure 3.23: Each allele initially present in a small diploid population is given a different colour so we can track their descendants over time. By the 9th generation, all of the alleles present in the population can trace their ancestry back to the orange allele. [Code here.](#)

Probability of the eventual fixation of a neutral allele An allele which reaches fixation within a population is an ancestor to the entire population. In a particular generation there can only be a single allele that all other alleles at the locus in a later generation can claim as an ancestor (See Figure 3.23). At a neutral locus, the actual allele does not affect the number of descendants that the allele has (this follows from the definition of neutrality: neutral alleles don't leave more or less descendants on average than other neutral alleles). An equivalent way to state this is that the allele labels don't affect anything; thus the alleles are *exchangeable*. As a consequence of being exchangeable, any allele is equally likely to be the ancestor of the entire population. In a diploid population of size N , there are $2N$ alleles, all of which are equally likely to be the ancestor of the entire population at some later time point. So if our allele is present in a single copy, the chance that it is the ancestor to the entire population in some future generation is $1/(2N)$, i.e. the chance our neutral allele is eventually fixed is $1/(2N)$. In Figure 3.23, our orange allele in the first generation is one of 10 differently coloured alleles, and so has a $1/10$ chance of being the ancestor of the entire population at some later time point (and

1808 in this simulation it does become the common ancestor, by the 9th generation).

1810 More generally, if our neutral allele is present in i copies in the population, of $2N$ alleles, the probability that this allele becomes fixed 1812 is $i/(2N)$, i.e. the probability that a neutral allele is eventually fixed 1814 is simply given by its frequency (p) in the population. (We can also derive this result by letting $Ns \rightarrow 0$ in eqn. (7.11), a result we'll encounter later.)

1816 A newly arisen mutation only becomes a fixed difference if it is lucky enough to be the ancestor of the entire population. As we saw 1818 above, this occurs with probability $1/(2N)$.

1820 How long does it take on average for such an allele to fix within our population? Well, in developing equation (3.35) we've seen that 1822 it takes $4N$ generations for a large sample of alleles to all trace their ancestry back to a single most recent common ancestral allele. Any 1824 single-base pair change which arose as a single mutation at a locus, and fixed in the population, must have been present in the sequence transmitted by the most recent common ancestor of the population 1826 at that locus. Thus it must take roughly $4N$ generations for a neutral allele present in a single copy within the population to the ancestor 1828 of all alleles within our population. This argument can be made more precise, but in general we would still find that it takes $\approx 4N$ generations 1830 for a neutral allele to go from its introduction to fixation with the population.

1832 *Rate of substitution of neutral alleles* A substitution between populations that do not exchange gene flow is simply a fixation event within 1834 one population. The rate of substitution is therefore the rate at which new alleles fix in the population, so that the long-term substitution 1836 rate is the rate at which mutations arise that will eventually become fixed within our population.

1838 Lets assume, based on our discussion of the neutral theory of molecular evolution, that there are only two classes of mutational changes 1840 that can occur with a region, highly deleterious mutations and neutral mutations. A fraction C of all mutational changes are highly deleterious, 1842 and cannot possibly contribute to substitution nor polymorphism. The other $1 - C$ fraction of mutations are neutral. If our mutation rate 1844 is μ per transmitted allele per generation, then a total of $2N\mu(1 - C)$ neutral mutations enter our population each generation.

1846 Each of these neutral mutations has a $1/(2N)$ probability chance of 1848 eventually becoming fixed in the population. Therefore, the rate at which neutral mutations arise that eventually become fixed within our population is

$$2N\mu(1 - C) \frac{1}{2N} = \mu(1 - C) \quad (3.44)$$

1850 Thus the rate of substitution, under a model where newly arising
1852 alleles are either highly deleterious or neutral, is simply given by the
1854 mutation rate of neutral alleles, i.e. $\mu(1 - C)$.

1856 Consider a pair of species that have diverged for T generations,
1858 i.e. orthologous sequences shared between the species last shared a
1860 common ancestor T generations ago. If these species have maintained
1862 a constant μ over that time, they will have accumulated an average of

$$2\mu(1 - C)T \quad (3.45)$$

1864 neutral substitutions. This assumes that T is a lot longer than the
1866 time it takes to fix a neutral allele, such that the total number of
1868 alleles introduced into the population that will eventually fix is the
1870 total number of substitutions.

1872 This is a really pretty result as the population size has completely
1874 canceled out of the neutral substitution rate. However, there is an-
1876 other way to see this in a more straight forward way. If I look at a
1878 sequence in me compared to, say, a particular chimp, I'm looking at
1880 the mutations that have occurred in both of our germlines since they
1882 parted ways T generations ago. Since neutral alleles do not alter the
1884 probability of their transmission to the next generation, we are simply
1886 looking at the mutations that have occurred in $2T$ generations worth
1888 of transmissions. Thus the average number of neutral mutational dif-
1890 ferences separating our pair of species is simply $2\mu(1 - C)T$.

1892 A number of observations follow under this model, from equation
1894 (3.45), the first is that a primary determinant of patterns of molecu-
1896 lar evolution in a genomic region is the level of constraint (C). This
1898 pattern generally seems to hold empirically: non-coding regions often
1900 evolve more rapidly than coding regions; synonymous substitutions ac-
1902 cumulate faster than nonsynonymous; nonsynonymous changes faster
1904 in less vital proteins than ones that are absolutely necessary for early
1906 development. Note that this is not a unique prediction of the neu-
1908 tral model, e.g. lower pleiotropy means that less constrained regions
1910 may be better able to evolve adaptively. However, it is a fantastically
1912 useful general insight, e.g. it allows us to spot putatively functional
1914 non-coding regions by looking for genomic regions that have very low
1916 levels of divergence among distantly related species.

"functionally less impor-
 tant molecules or parts of a
 molecule evolve faster than
 more important ones."

- KIMURA and OHTA (1974)



Figure 3.24: The numbers of substitutions between various pairs of groups, for three proteins, plotted against the time these groups shared a common ancestor in the fossil record. Data from DICKERSON (1971). The number of observed amino-acid differences is corrected for multiple hits to obtain the corrected number of changes estimated to occur. The lines give the linear regression, constrained to pass through the origin, for each protein. The slope of the regression is given next to the protein name. Code here. See (ROBINSON *et al.*, 2016) who revisited this classic study and confirmed the conclusions.

1884 The second important insight, and critical for the development of
 1886 the neutral theory, is that equation (3.45) is seemingly consistent with
 ZUCKERKANDL and PAULING (1965)'s hypothesis of a surprisingly
 constant, protein molecular clock. The protein molecular clock is the
 1888 observation that for some proteins there's a linear relationship between
 the number of non-synonymous substitutions and the time species last
 1890 shared a common ancestor in the fossil record. DICKERSON (1971)
 provided an early example of this observation (Figure 3.24), by
 1892 comparing various organisms whose molecular sequences were available
 to him. For example, he found that humans and rattlesnakes, who last
 1894 share a common ancestor in the fossil record around 300 million years,
 are separated by roughly 15 NS substitutions per 100 sites in the
 1896 Cytochrome c protein. While, humans and dog fish, which diverged
 around 400 million years, are separated by 19 NS substitutions per 100
 1898 sites in this gene.

In equation (3.45) we double the amount of time separating a pair
 1900 of species T , we double the number of substitutions predicted. Note
 that for this to be true T must be measured in generations. To ex-
 1902 plain a protein molecular clock between species that clearly differed
 dramatically in generation time it was hypothesized that the muta-
 1904 tion rate actually scaled with generation time, i.e. short-lived organ-
 isms introduced less mutations per generation, e.g. as they had fewer
 1906 rounds of mitosis. This generation-time assumption meant that the
 mutation rate per year could be constant, such that μT would be a
 1908 constant for pairs of species that had diverged for similar geological



Figure 3.25: Eastern diamondback rattlesnake (*Crotalus adamanteus*). North American herpetology. Holbrook, J. E. Image from the Biodiversity Heritage Library. Contributed by Smithsonian Libraries. Licensed under CC BY-2.0.

times, which are measured in years, even if the organisms differed in generation time. This assumption would allow neutral theory to be consistent with a protein molecular clock measured in years. We now know that this critical generation time assumption is false, organisms with shorter generation times have somewhat higher mutation rates per year, and so a strict neutral model is inconsistent with the protein molecular clock. We'll return to these ideas when we discuss the fate of very weakly selected mutations in Chapter 7 and OHTA (1973)'s Nearly Neutral theory. If you are still reading this send Graham a picture of Tomoko Ohta receiving the Crafoord Prize, an analog of the Nobel prize for biology, for her contributions to molecular evolution.

The contribution of ancestral polymorphism to divergence. If we are considering T to represent the divergence between long-separated species, then we can think of T as the time that the species split. However, for more recently diverged populations and species, we need to include the fact that the sorting of ancestral polymorphism contributes to divergence among species. In Figure 3.26, we see our two populations split T_s generations ago. However, the coalescence of our A and B lineage is necessarily deeper in time than T_s . The top mutation was polymorphic in the ancestral population but now contributes to the divergence between A and B. Assuming that our ancestral population had effective size N_A individuals, and that our populations split cleanly with no subsequent gene flow, then

$$T = T_s + 2N_A. \quad (3.46)$$

If our species split time is very large compared to $2N$ then we can think of T as the split time.

Question 11. For this, and the next question, assume that humans and chimp diverged around 5.5×10^6 years ago, have a generation time 20 years, that the speciation occurred instantaneously in allopatry with no subsequent gene flow, and the ancestral effective population size of the human and chimp common ancestor population was 10,000 individuals.

Nachman and Crowell sequenced 12 pseudogenes in human and chimp and found substitutions at 1.3% of sites.

A) What is the mutation rate per site per generation at these genes?

B) All of the pseudogenes they sequenced are on the autosomes. What would your prediction be for pseudogenes on the X and Y chromosomes, given that there are fewer rounds of replication in the female germline than in the male germline.

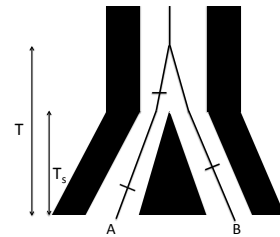


Figure 3.26: The genealogy of two alleles one sampled from population A and B. Mutations on the lineages are shown as dashes. The pair of alleles coalesce in the ancestral population of A and B. The two populations split T_s generations ago, with no subsequent gene flow, but the two lineages must coalesce deeper in time.

¹⁹⁴⁸ 3.5 *Tests of molecular evolution.*

¹⁹⁵⁰ 3.5.1 *Comparing the rates of non-synonymous to synonymous substitutions d_N/d_S*

One common tool in molecular evolution is to compare the estimated number (or rates) of substitutions in different classes of genomic sites, for example the ratio of the number of non-synonymous to synonymous substitutions in a given gene. The simplest way to calculate d_N is to count up the non-synonymous changes and divide by the total number of positions in the gene where a non-synonymous point mutation could occur. We can do likewise for synonymous changes d_S , and then take the ratio d_N/d_S . This is a helpful conceptual way to think about what d_N/d_S represents, however, this ignores the fact that some changes are more likely to occur by mutation than others and also does not account for multiple hits (multiple mutations at the same bp position). Therefore, in practice the ratio d_N/d_S is more typically calculated by model-based likelihood and bayesian methods that can account for these features.

For the vast majority of protein-coding genes in the genome we see that $d_N/d_S < 1$. This observation is consistent with the view that non-synonymous sites are much more constrained than synonymous sites, i.e. that most non-synonymous mutations are deleterious and quickly removed from the population. If we are willing to make the assumption that all synonymous changes are neutral, $d_S = 2T\mu$, then we can estimate the degree of constraint on non-synonymous sites. (Note that synonymous changes can sometimes be subject to both positive and negative selection, but this neutral assumption is a useful starting place.)

Assume that a fraction C of non-synonymous changes are too deleterious to contribute to polymorphism. Then, after T generations of divergence have elapsed between two populations, we'd expect d_N neutral non-synonymous substitutions, where

$$d_N = 2T(1 - C)\mu \quad (3.47)$$

Dividing by d_S , we find

$$d_N/d_S = (1 - C) \quad (3.48)$$

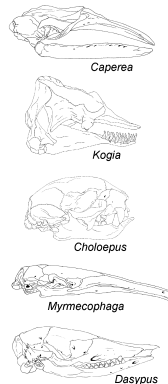
Therefore, if we assume that non-synonymous mutations can only be strongly deleterious or neutral, we estimate the fraction of mutational changes that are constrained by negative selection as $C = 1 - d_N/d_S$. C has the interpretations of being the fraction of non-synonymous mutations that are quickly weeded out of the population by selection, and so do not contribute to divergence among species.

1986 We can test whether our gene is evolving in a constrained way at
 1988 the protein level by estimating d_N/d_S and testing whether this is sig-
 1990 nificantly less than 1. A d_N/d_S test can provide evolutionary evidence
 1992 that a stretch of DNA proposed to be protein-coding is subject to se-
 lective constraint, and so likely does encode for a functional protein.
 We can also perform a d_N/d_S test on specific branches of a phylogeny
 1992 for a gene, to test on which branches the gene is subject to constraint,
 or to test for changes in the level of constraint across the phylogeny.

1994 *Loss of constraint at pseudogenes.* While most protein genes evolve
 under constraint, we can find examples of genes that are evolving
 1996 in a less constrained manner. The simplest example of this is where
 the gene has lost function. Genes can lose function because of inac-
 1998 tivating mutations that stop them being transcribed or translated
 into functional proteins. Such genes are called 'pseudogenes'. When
 2000 a gene completely loses function there is no longer selection against
 non-synonymous changes and so such mutations are just as free to ac-
 2002 cumulate as synonymous changes, and so $d_N/d_S = 1$. Pseudogenes
 are a wonderful example of the extension of Darwin's ideas about
 2004 vestigial traits ('Rudimentary organs') to the DNA level; we can still
 recognize a once useful word (gene) whose spelling is slowly degrading.
 2006 Our genomes are filled with old pseudogenes whose original meanings
 (functional protein coding sequences) are slowly being eroded through
 2008 the accumulation of neutral substitutions. One nice example of a
 gene that has repeatedly lost function, i.e. become repeatedly psue-
 2010 odogenized, is the Enamlin gene from the study of MEREDITH *et al.*
 (2009).

C	818	827	1239	1247	2501	2512	2533	2542	4028	4039
<i>Sus</i>	...AAATCAA	CT	TGTTTACTA	..ACATGCC	ATGCA	..GGGGCACAGTTT				
<i>Hippopotamus</i>	...AAATCAA	CT	TGTTTACTA	..ACATGCC	ATGCA	..GGGGCACAGTTT				
<i>Eubalaena glacialis</i>	...AAATCAA	CT	TGTTTACTA	..ATA	TGCA	..CATC	TTAGATC	..AGGGCACAGTTT		
<i>Eubalaena australis</i>	...AAATCAA	CT	TGTTTACTA	..ATA	TGCA	..CATC	TTAGATC	..AGGGCACAGTTT		
<i>Megaptera</i>	...AAATCAA	CT	TGTTTACTA	..ATA	TGCA	..CATC	TTAGATC	..AGGGCACAGTTT		
<i>Caperea</i>	...AAATCAA	CT	TGTTTACTA	..ATA	TGCA	..CATC	TTAGATC	..AGGGCACAGTTT		
<i>Eschrichtius</i>	...AAATCAA	CT	TGTTTACTA	..ATA	TGCA	..CATC	TTAGATC	..AGGGCACAGTTT		
<i>Kogia sima</i>	...AAATCAA	CT	TGTTTACTA	..ATA	TGCA	..CATC	TTAGATC	..AGGGCA	GTTT	
<i>Kogia breviceps</i>	...AAATCAA	CT	TGTTTACTA	..ATA	TGCA	..CATC	TTAGATC	..AGGGCA	GTTT	

D	918	935	1584	1593	1614	1620	2499	2507	4017	4023
<i>Sus</i>	...GGGA	GTCCAAAAGGCC	..ACCTCCCTA	..CAAAACC	..CAACATGGC	..GCT	AGC			
<i>Bradypterus</i>	...???	???	???	???	???	???	???	???	???	???
<i>Choloepus didactylus</i>	...ACT	TCGC	..CAAAACC	..CAACATGGC	..GTT	AGC				
<i>Choloepus hoffmanni</i>	...???	???	???	???	???	???	???	???	???	???
<i>Myrmecophaga</i>	...GTTG	ATTCAGGAGACTG	..ATT	TCGC	..CAAAACC	..CAACATGGC	..GTT	AGC		
<i>Tamandua</i>	...GAGA	ATTCAGGAGAATC	..ATT	TCGC	..CAAAACC	..CAACATGGC	..GTT	AGC		
<i>Cyclopes</i>	...GAGA	ATTCAGGAGAATC	..ATT	TCGC	..CAAAACC	..CAACATGGC	..GTT	AGC		
<i>Dasypus</i>	...GAGA	ATTCAGGAGAAC	..ATT	TCGC	..CAAAACC	..CAACATGGC	..GTT	AGG		
<i>Tolypeutes</i>	...GAGA	ATTCAGGAGAAC	..ATT	TCGC	..CAAAACC	..CAACATGGC	..GTT	AGG		
<i>Chaetophractus</i>	...GAGA	ATTCAGGAGAAC	..ATT	TCGC	..CAAAACC	..CAACATGGC	..GTT	AGA		
<i>Euphractus</i>	...GAGA	ATTCAGGAGAAC	..ATT	TCGC	..CAAAACC	..CAACATGGC	..GTT	AGG		



"Rudimentary organs may be com-
 pared with the letters in a word,
 still retained in the spelling, but be-
 come useless in the pronunciation,
 but which serve as a clue .. for its
 derivation." – DARWIN (1859) pg. 455

Figure 3.27: Examples of frameshift mutations (insertions blue, deletions red) and premature stop codons in Enamlin in Cetacea and Xenarthra. Figure from MEREDITH *et al.* (2009), licensed under CC BY 4.0.



Figure 3.28: Two-toed sloth (*Choloepus hoffmanni*). An introduction to the study of mammals, living and extinct. 1891. Flower W. H. and Lydekker R. Image from the Biodiversity Heritage Library. Contributed by University of Toronto. Not in copyright.

ample, two-toed sloths (*Choloepus*), Pygmy sperm whales (*Kogia*), and aardvark (*Orycteropus*) all lack enamel on teeth. Other mammals have lost their teeth entirely, e.g. giant anteaters (*Myrmecophaga*) and Baleen whales. Due to this relaxation of constraint on the phenotype, the Enamlin gene has accumulated pseudogenizing substitutions such as premature stop codons and frameshift mutations (see Figure 3.27 for examples). MEREDITH *et al.* sequenced Enamlin across a range of species and found that none of the species with enamel have frameshift mutations in Enamlin, while 17/20 of species that lack enamel or teeth have frameshifts in Enamlin, and all of them carry premature stop codons (Figure 3.29).

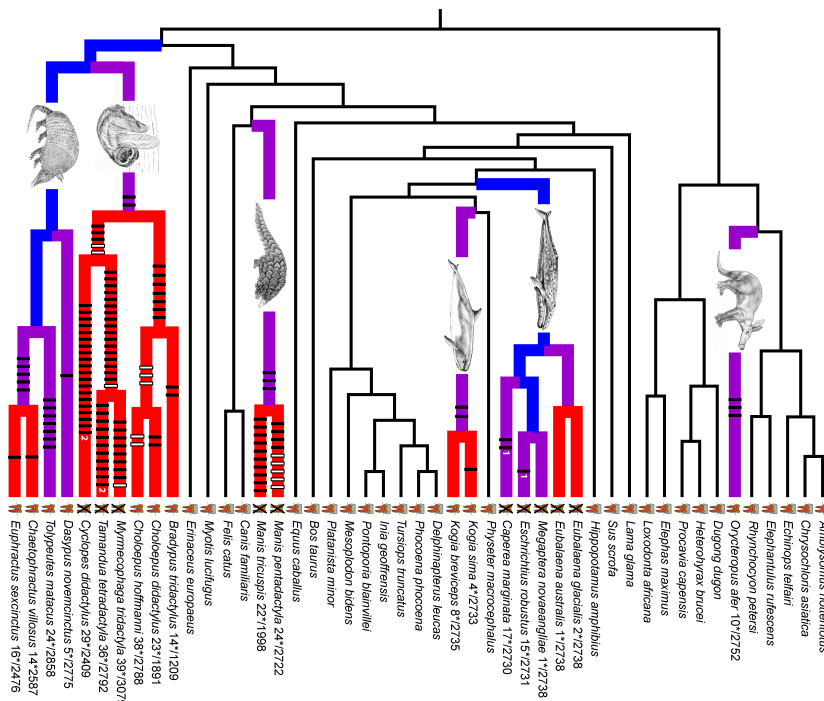


Figure 3.29: The tooth symbol next to each taxon shows whether they have teeth with enamel, lack enamel, or lack teeth. Branches of the phylogeny are coloured by whether their Enamlin is functional (black), pre-mutation (blue), mixed (purple), or pseudogenic (red). The black and white vertical bars on branches show frameshift mutations. The numbers after taxon names indicate minimum number of stop codons in the sequence divided by the length of the sequence. Figure from MEREDITH *et al.* (2009), licensed under CC BY 4.0.

The branches of the Enamlin phylogeny with a functional Enamlin

gene (black) had an estimated $d_N/d_S = 0.51$, consistent with the protein evolving in a constrained manner. In contrast, the branches with a pseudogenized Enamlin (red) had $d_N/d_S = 1.02$, consistent with the gene evolving an unconstrained way. The branches where the gene was likely transitioning from a functional to non-function state, i.e. pre-mutation (blue) and mixed (purple), had intermediate values of $d_N/d_S = 0.83 - 0.98$, consistent with a transition from a constrained to unconstrained mode of protein evolution somewhere along these branches of the phylogeny.

Adaptive evolution and d_N/d_S . Clearly genes are not only subject
 2038 to neutral and deleterious mutations; beneficial mutations must also
 arise and fix from time to time. Let's assume that a fraction B of
 2040 non-synonymous mutations that arise are beneficial such that $2N\mu B$
 beneficial mutations arise per generation. Newly arisen beneficial
 2042 alleles are not destined to fix in the population, as they may be lost to
 genetic drift when they are rare in the population (we'll discuss how
 2044 to calculate the fixation probability for beneficial alleles in Chapter
 7). A newly arisen beneficial allele reaches fixation in the population
 2046 with probability f_B from its initial frequency of $1/2N$. This fixation
 probability may be much higher than that of neutral mutations, but
 2048 still much less than 1. If $2T$ generations of divergence have elapsed
 between the two populations then a total of

$$dN = 2T(1 - C - B)\mu + 2T \times (2N\mu B) \times f_B \quad (3.49)$$

2050 non-synonymous substitutions will have accumulated. Then

$$d_N/d_S = (1 - C - B) + 2NBf_B \quad (3.50)$$

assuming again that all synonymous mutations are neutral. Note that
 2052 this means that our estimates of C using $1 - d_N/d_S$ will be a lower
 bound on the true constraint if even a small fraction of mutations
 2054 are beneficial. Those cases where the gene is evolving more rapidly
 at the protein level than at synonymous sites, i.e. $d_N/d_S > 1$, are
 2056 potentially strong candidates for positive selection rapidly driving
 change at the protein level. We can identify genes that have d_N/d_S
 2058 significantly greater than one, either on the complete gene phylogeny,
 or on particular branches. Note that is a very conservative test that
 2060 few genes in the genome meet, as many genes that are fixing adaptive
 non-synonymous substitutions will have $d_N/d_S < 1$; even if adaptive
 2062 mutations are common, genes may still evolve in a constrained way
 (i.e. $d_N/d_S < 1$) if the rapid fixation of beneficial mutations due to pos-
 2064 itive selection is outweighed by the loss of non-synonymous mutations
 to negative selection.

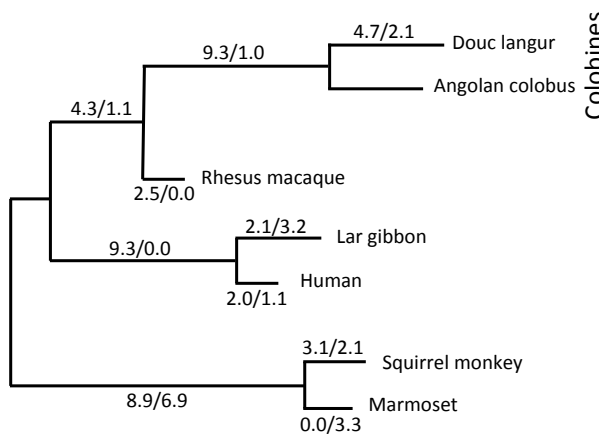


Figure 3.30: A phylogram for the primate lysozyme gene, data from YANG (1998). For each branch, the numbers give the estimated average number of non-synonymous to synonymous changes in the lysozyme protein.

2066 A classic example for looking at adaptive evolution using dN/dS
is the evolution of the lysozyme protein in primates (MESSIER and
2068 STEWART, 1997; YANG, 1998), see the phylogeny in Figure 3.30. The
lysozyme protein is a key component for the breakdown of bacterial
2070 walls. It shows very fast protein evolution, notably on the lineages
leading to apes (e.g. gibbons and humans) and Colobines (e.g. colobus
2072 and langur monkeys). Colobines have leaf-based diets. They digest
these leaves by bacterial fermentation in their foregut, and then use
2074 lysozymes to break down the bacteria to extract energy from the
leaves. In Colobines, the lysozyme protein has evolved to work well
2076 in the high-PH environment of the stomach. Remarkably, the Colobine
lysozyme has convergently evolved this activity via very similar amino-
2078 acid changes at 5 key residuals in cows and Hoatzins (a leaf eating
bird, KORNEGAY *et al.*, 1994)

2080 *The McDonald-Kreitman test* As noted above, a big issue with using
 dN/dS to detect adaptation is that it is very conservative. For a more
2082 powerful test of rapid divergence, what we need to do is adjust for
the level of constraint a gene experiences at non-synonymous sites.
2084 One way to do this is to use polymorphism data as an internal control. If we see little non-synonymous polymorphism at a gene, but a
2086 lot of synonymous polymorphism, we now know that there is likely
strong constraint on the gene (i.e. high C), thus we expect dN/dS to
2088 be low. McDONALD and KREITMAN (1991) devised a simple test
of the neutral theory of molecular evolution at a gene based on this
2090 intuition (building on the conceptually similar HKA test HUDSON
et al., 1987). McDONALD and KREITMAN took the case where we
2092 have polymorphism data at a gene for one species and divergence to

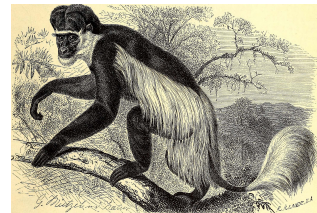


Figure 3.31: Abyssinian black-and-white colobus (*Colobus guereza*). A member of the leaf-eating Colobines. Brehm's Tierleben, Brehm, A.E. 1893. Image from the Biodiversity Heritage Library. Contributed by University of Illinois Urbana-Champaign. Not in copyright.



Figure 3.32: (hoatzin (*Opisthocomus hoazin*)). A leaf-eating bird. A history of birds (1910) Pycraft, W.P. Image from the Biodiversity Heritage Library. Contributed by American Museum of Natural History Library. Not in copyright.

a closely related species. They partitioned polymorphism and fixed differences in their sample into non-synonymous and synonymous changes:

	Poly.	Fixed
Non-Syn.	P_N	D_N
Syn.	P_S	D_S
Ratio	P_N/P_S	D_N/D_S

Under neutral theory, we expect a smaller number of non-synonymous to synonymous fixed differences ($D_N/D_S < 1$) and exactly the same expectation holds for polymorphism (P_N/P_S). Let's consider a gene with L_S and L_N sites where synonymous and non-synonymous mutations could arise respectively. We can think of the underlying gene genealogy at our gene, see Figure 3.33, with the total time on the coalescent genealogy within the species as T_{tot} and the total time for fixed differences between our species as T'_{div} . Then under neutrality we expect $\mu L_N(1 - C)T_{tot}$ non-synonymous polymorphisms (i.e. our number of segregating sites), and $\mu L_N(1 - C)T'_{div}$ non-synonymous fixed differences. We can then fill out the rest of our table as follows:

	Poly.	Fixed
Non-Syn.	$\mu L_N(1 - C)T_{tot}$	$\mu L_N(1 - C)T'_{div}$
Syn.	$\mu L_N T_{tot}$	$\mu L_S T'_{div}$
Ratio	$L_N(1 - C)/(L_S)$	$L_N(1 - C)/(L_S)$

Therefore, we expect the ratio of non-synonymous to synonymous changes to be the same for polymorphism and divergence under a strict neutral model. We can test this expectation of equal ratios via the standard tests of a 2×2 table. If the ratio of N/S is significantly higher for divergence than polymorphism we have evidence that non-synonymous substitutions are accumulating more rapidly than we would predict given levels of constraint alone.

As example of a McDonald-Kreitman table consider the work of FRENTIU *et al.* (2007) on the molecular evolution of L Photopigment opsin in Admiral (*Limenitis*) butterflies, responsible for colour vision in the long-wavelength part of the visual spectrum. FRENTIU *et al.* found that the sensitivity of this opsin had shifted towards blue-shifted in its sensitivity in *L. archippus archippus* (viceroy) compared to *L. arthemis astyanax*. To test whether this molecular evolution reflected positive selection they sequenced 24 *L. arthemis astyanax* individuals and one *L. archippus archippus* sequence. They identified 11 polymorphic sites in *L. arthemis astyanax* and 16 fixed differences, which break down as follows:



Figure 3.33: An example ogene genealogy for a set of alleles sampled within a population and a single allele sampled from a distantly-related species.

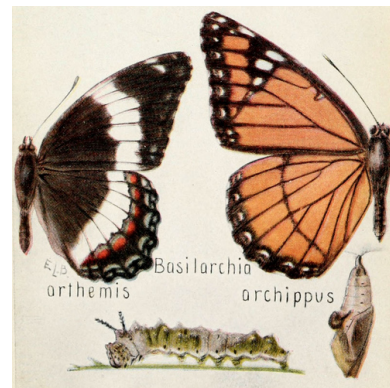


Figure 3.34: White admiral (*Limenitis arthemis*) and Viceroy (*Limenitis archippus*). *Basilarchia* is the old genus that these two species were originally placed in. Viceroy and Monarch butterflies are Müllerian mimics.
Field book of insects (1918). Lutz, F.E. . illustrations by Edna L. Beutenmüller. Image from the Biodiversity Heritage Library. Contributed by MBLWHOI Library. Not in copyright.

	Poly.	Fixed
Non-Syn.	2	12
Syn.	9	4
Ratio	2/9	3/1

2128 Note the strong excess of non-synonymous to synonymous diver-
gence compared to polymorphism (p-value of 0.006, Fisher's exact
2130 test), which is consistent with the gene evolving in an adaptive man-
ner among the two species. We would expect roughly only 3 non-
2132 synonymous substitutions out of 16 substitutions if the gene was
evolving neutrally ($16 \times 2/11$).

2134 *3.6 Neutral diversity and population structure*

We've considered alleles drawn from a randomly-mating population,
2136 and divergence among alleles drawn from two distantly-related pop-
ulations. We'll now turn to consider divergence among more closely
2138 related populations. In thinking about the coalescent within pop-
ulations we made the assumption that any pair of lineages is equally
2140 likely to coalesce with each other. However, when there is population
structure this assumption is violated.

2142 We have previously written the measure of population structure
 F_{ST} as

$$F_{ST} = \frac{H_T - H_S}{H_T} \quad (3.51)$$

2144 where H_S is the probability that two alleles sampled at random from
a subpopulation differ, and H_T is the probability that two alleles
2146 sampled at random from the total population differ.

2148 *A simple population split model* Imagine a population of constant size
of N_e diploid individuals that T generations in the past split into two
daughter populations (sub-populations) each of size N_e individuals,
2150 which do not subsequently exchange migrants. In the current day we
sample an equal number of alleles from both subpopulations.

2152 Consider a pair of alleles sampled within one of our sub-populations
and think about their per site heterozygosity. These alleles have expe-
2154 rienced a population of size N_e and so the probability that they differ
is $H_S \approx 4N_e\mu$ (assuming that $N_e\mu \ll 1$, using our equation 3.12 for
2156 heterozygosity within a population).

The heterozygosity in our total population is a little more tricky
2158 to calculate. Assuming that we equally sample both sub-populations,
when we draw two alleles from our total sample, 50% of the time
2160 they are drawn from the same subpopulation and 50% of the time
they are drawn from different subpopulations. Therefore, our total

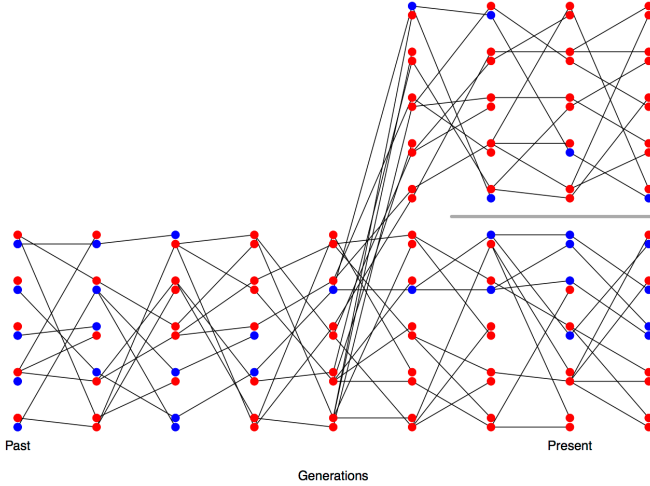


Figure 3.35: Change in allele frequencies following a population split. Code here.

2162 heterozygosity is given by

$$H_T = \frac{1}{2}H_S + \frac{1}{2}H_B \quad (3.52)$$

2164 where H_B is the probability that a pair of alleles drawn from our two different sub-populations differ from each other. A pair of alleles from different sub-populations cannot find a common ancestor with each 2166 other for at least T generations into the past as they are in distinct populations (not connected by migration). Once our alleles find them- 2168 selves back in the combined ancestral population it takes them on average $2N$ generations to coalesce. So the total opportunity for mu- 2170 tation between our pair of alleles sampled from different populations is $2(T + 2N)$ generations of meioses, such that the probability that our 2172 pairs of alleles is different is

$$H_B \approx 2\mu(T + 2N) \quad (3.53)$$

We can plug this into our expression for H_T , and then that in turn 2174 into F_{ST} . Doing so we find that

$$F_{ST} \approx \frac{\mu T}{\mu T + 4N_e \mu} = \frac{T}{T + 4N_e} \quad (3.54)$$

2176 Note that μ cancels out of this equation. In this simple toy model, F_{ST} is increasing because the amount of between-population diversity 2178 increases with the divergence time of the two populations (initially linearly with T). F_{ST} grows at a rate give by $T/(4N_e)$ so that differentiation will be higher between populations separated by long divergence times or with small effective population sizes.

Question 12. The genome-wide F_{ST} between Bornean and Suma- 2182 tran orang-utan species samples (*Pongo pygmaeus* and *Pongo abelii*)

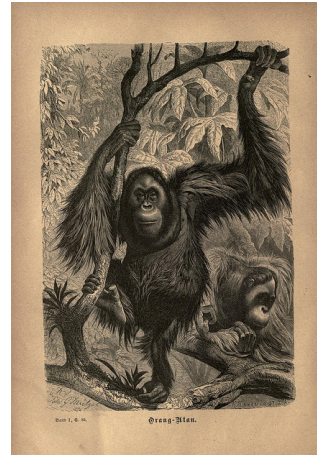


Figure 3.36: Orangutan (*Pongo*). Brehms thierleben, allgemeine kunde des thierreichs. Brehm, A. E. Image from the Biodiversity Heritage Library. Contributed by MBLWHOI Library. Not in copyright.

is ≈ 0.37 (LOCKE *et al.*, 2011), representing a deep population split
 2184 between the species (potentially with little subsequent gene flow).

Within the populations the genome-wide average Watterson's θ is
 2186 $\theta_W = 1.4\text{kb}^{-1}$, estimated from the number of segregating sites. Assume a generation time of 20 years, and a mutation rate of 2×10^{-8}
 2188 per base per generation. How far in the past did the two populations diverge?

2190 *A simple model of migration between an island and the mainland.* We can also use the coalescent to think about patterns of differentiation
 2192 under a simple model of migration-drift equilibrium. Let's consider a small island population that is relatively isolated from a large mainland population, where both of these populations are constant in size.
 2194 We'll assume that the expected heterozygosity for a pair of alleles sampled on the mainland is H_M .

Our island has a population size N_I that is very small compared
 2198 to our mainland population. Each generation some low fraction m of our individuals on the island have migrant parents from the mainland
 2200 the generation before. Our island may also send migrants back to the mainland, but these are a drop in the ocean compared to the large
 2202 population size on the mainland and their effect can be ignored.

If we sample an allele on the island and trace its ancestral lineage backward in time, each generation our ancestral allele has a low probability m of being descended from the mainland in the preceding
 2204 generation (if we go back far enough the allele eventually has to be descended from an allele on the mainland). The probability that a pair
 2206 of alleles sampled on the island are descended from a shared recent common ancestral allele on the island is the probability that our pair
 2208 of alleles coalesces before either lineage migrates. For example, the probability that our pair of alleles coalesces $t + 1$ generations back on
 2210 the island is
 2212

$$\frac{1}{2N_I} (1-m)^{2(t+1)} \left(1 - \frac{1}{2N_I}\right)^t \approx \frac{1}{2N_I} \exp\left(-t\left(\frac{1}{2N_I} + 2m\right)\right), \quad (3.55)$$

with the approximation following from assuming that $m \ll 1$ &
 2214 $\frac{1}{(2N_I)} \ll 1$ (note that this is very similar to our derivation of heterozygosity above). The probability that our alleles coalesce before
 2216 either one of them migrates off the island, irrespective of the time, is

$$\int_0^\infty \frac{1}{2N_I} \exp\left(-t\left(\frac{1}{2N_I} + 2m\right)\right) dt = \frac{1/(2N_I)}{1/(2N_I) + 2m}. \quad (3.56)$$

Let's assume that the mutation rate is very low such that it is very
 2218 unlikely that the pair of alleles mutate before they coalesce on the island. Therefore, the only way that the alleles can be different from

²²²⁰ each other is if one or other of them migrates to the mainland, which happens with probability

$$1 - \frac{1/(2N_I)}{1/(2N_I) + 2m} \quad (3.57)$$

²²²² Conditional on one or other of our alleles migrating to the mainland, both of our alleles represent independent draws from the mainland and ²²²⁴ so differ from each other with probability H_M . Therefore, the level of heterozygosity on the island is given by

$$H_I = \left(1 - \frac{1/(2N_I)}{1/(2N_I) + 2m}\right) H_M \quad (3.58)$$

²²²⁶ So the reduction of heterozygosity on the island compared to the mainland is

$$F_{IM} = 1 - \frac{H_I}{H_M} = \frac{1/(2N_I)}{1/(2N_I) + 2m} = \frac{1}{1 + 4N_I m}. \quad (3.59)$$

²²²⁸ The level of inbreeding on the island compared to the mainland will be high if the migration rate is low and the effective population size ²²³⁰ of the island is low, as allele frequencies on the island are drifting and diversity on the island is not being replenished by migration. The key ²²³² parameter here is the number individuals on the island replaced by immigrants from the mainland each generation ($N_I m$).

²²³⁴ We have framed this problem as being about the reduction in genetic diversity on the island compared to the mainland. However, if we ²²³⁶ consider collecting individuals on the island and mainland in proportion to their population sizes, the total level of heterozygosity would ²²³⁸ be $H_T = H_M$, as samples from our mainland would greatly outnumber those from our island. Therefore, considering the island as our ²²⁴⁰ sub-population, we have derived another simple model of F_{ST} .

Question 13. You are investigating a small river population of ²²⁴² sticklebacks, which receives infrequent migrants from a very large marine population. At a set of putatively neutral biallelic markers the ²²⁴⁴ freshwater population has frequencies:

0.2, 0.7, 0.8

²²⁴⁶ at the same markers the marine population has frequencies:

0.4, 0.5 and 0.7.

²²⁴⁸ From studying patterns of heterozygosity at a large collection of markers, you have estimated the long term effective size of your fresh-²²⁵⁰ water population is 2000 individuals.

²²⁵² What is your estimate of the migration rate from the marine populations into the river?

Incomplete lineage sorting Because it can take a long time for an ²²⁵⁴ polymorphism to drift up or down in frequency, multiple population

splits may occur during the time an allele is still segregating. This
2256 can lead to incongruence between the overall population tree and the
information about relationships present at individual loci. In Figure
2258 3.37 and 3.38 we show simulations of three populations where the
bottom population splits off from the other two first, followed by
2260 the subsequent splitting of the top and the middle populations.
We start both simulations with a newly introduced red allele being
2262 polymorphic in the combined ancestral population. The most likely
fate of this allele is that it is quickly lost from the population, but
2264 sometimes the allele can drift up in frequency and be polymorphic
when the populations split, as the alleles in our two figures have done.
2266 If the allele is lost/fixed in the descendant populations before the next
population split, our allele configuration will agree with the population
2268 tree, as it does in Figure 3.37, and so too the gene tree will agree with
population tree (as shown in the left side of Figure 3.39). However,
2270 if the allele persists as a polymorphism in the ancestral population
till the top and the middle populations split, then the allele can fix in
2272 one of these populations and not the other. Such an event can lead to
a substitution pattern that disagrees with the population tree, as in
2274 Figure 3.38. If we were to construct a phylogeny using the variation
at this site we would see a disagreement between the gene tree and
2276 population tree. In Figure 3.38 an allele drawn from the top and the
bottom populations are necessarily more closely related to each other
2278 than either is to an allele drawn from population 2; tracing our allelic
lineages from the top and bottom populations back through time, they
must coalesce with each other before we reach the point where
2280 the red mutation arose; in contrast, a lineage from the middle population
cannot have coalesced with either other lineage until past the time the
red mutation arose. An example of this 'incomplete lineage sorting' in
2282 terms of the underlying tree is shown on the right side of Figure 3.39 .
2284

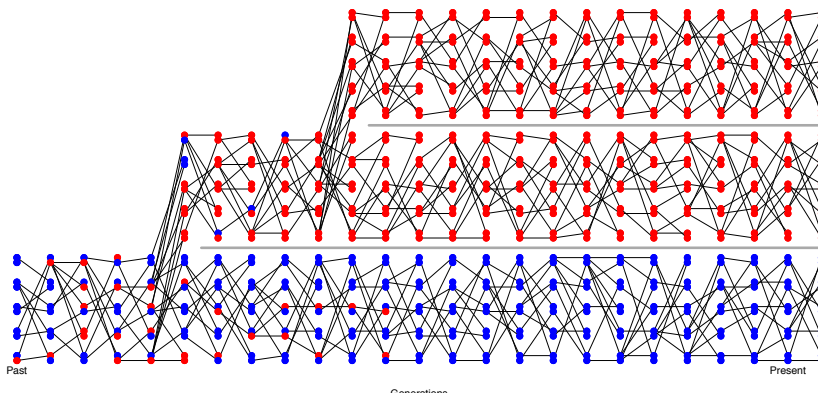


Figure 3.37: An example of alleles assorting among three populations such that there is no incomplete lineage sorting. Code here.

A natural pedigree analogy to incomplete lineage sorting is the fact



Figure 3.38: An example of alleles assorting among three populations leading to incomplete lineage sorting. Code here.



Figure 3.39: The population tree of three populations ((A, B), C) is shown blocked out with black shapes. Two different coalescent trees are relating a single allele drawn from A, B, and C are shown with thinner lines.

2286 that while two biological siblings are more closely related to each other
 2287 genealogically than either is to their cousin, at any given locus one of
 2288 the siblings can share an allele IBD with their cousin that they do not
 2289 share with their own sibling, due to the randomness of Mendelian seg-
 2290 regation down their pedigree. In these cases, the average relatedness of
 2291 the individuals/populations disagrees with the patterns of relatedness
 2292 at a particular locus.

As an empirical example of incomplete lineage sorting, let's consider
 2294 the work of JENNINGS and EDWARDS who sequenced a single allele
 2295 from three different species of Australian grass finches (*Poephila*): two
 2296 sister species of long-tailed finches (*Poephila acuticauda* and *P. hecki*)
 2297 and the black-throated finch (*Poephila cincta*, see Figure 3.40). They
 2298 collected sequence data for 30 genes, and constructed phylogenetic
 2299 gene trees at each of these loci, resulting in 28 well-resolved gene trees.
 2300 16 of the gene trees showed *P. acuticauda* and *P. hecki* as sisters with
P. cincta (the tree ((A,H),C)), while for twelve genes the gene tree
 2301 was discordant with the population tree: for seven of their genes *P.*
hecki fell as an outgroup to the other two and at five *P. acuticauda* fell
 2302 as an outgroup (the trees ((A,C),H) and ((H,C),A) respectively).

Let's use the coalescent to understand this discordance between
 2306 gene trees and species trees. Let's assume that two sister populations
 (A & B) split t_1 generations in the past, with a deeper split from a



Figure 3.40: Banded Grass Finch (*P. cincta*). Illustration by Elizabeth Gould.
Birds of Australia Gould J. 1840. CC BY 4.0 uploaded to Flickr by rawpixel.com.

2308 third outgroup population (C) t_2 generations in the past. We'll assume that there's no gene flow among our populations after each split.
 2310 We can trace back the ancestral lineages of our three alleles. The first opportunity for the A & B lineages to coalesce is t_1 generations ago.
 2312 If they coalesce with each other in their shared ancestral population before t_2 in the past (left side of Figure 3.39) their gene tree will definitely agree with the population tree. So the only way for the gene tree to disagree with the population tree is for the A & B lineages to fail to coalesce in their shared ancestral population between t_1 and t_2 ; this happens with probability $(1 - 1/2N)^{t_2-t_1}$. We'll get a discordant gene tree if A & B make it back to the shared ancestral population with C without coalescing, and then one or the other of them coalesces with the C lineage before they coalesce with each other. This happens with probability 2/3, as at the first pairwise-coalescent event there are 2318 are three possible pairs of lineages that could coalesce, two of which (A & C and B & C) result in a discordant tree. So the probability 2320 that we get a coalescent tree that is discordant with the population tree is

$$\frac{2}{3} (1 - 1/2N)^{t_2-t_1}. \quad (3.60)$$

2326 Thus we should expect gene-tree population-tree discordance when populations split in rapid succession and/or population sizes are large.

2328

Question 14. Let's return to JENNINGS and EDWARDS's Australian grass finches example. They estimated that the ancestral population size of our two long-tailed finches was four hundred thousand. 2330 What is your best estimate of the inter-speciation time, i.e. $t_2 - t_1$?

2334 *Testing for gene flow.* We often want to test whether gene flow has occurred between populations. For example, we might want to establish a case that interbreeding between humans and Neanderthals 2336 occurred or demonstrate that gene flow occurred after two populations began to speciate. A broad range of methods have been designed to 2338 test for gene flow and to estimate gene flow rates, based on neutral expectations. Here we'll briefly just discuss one method based on some 2340 simple coalescent ideas. Above we assumed that gene-tree population-tree discordance was due to incomplete lineage sorting due to populations rapidly splitting. However, gene flow among populations can 2342 also lead to gene-tree discordance. While both ILS and gene flow can lead to discordance, under simplifying assumptions, ILS implies more 2344 symmetry in how these discordances manifest themselves.

2346 Take a look at Figure 3.41. In both cases the lineages from A and B fail to coalesce in their initial shared ancestral population, and one 2348 or the other of them coalesces with the lineage from C before they



Figure 3.41: In both the left and right trees ILS has occurred between our single lineages sampled from populations A, B, and C. Imagine that population D is a somewhat distant outgroup such that the lineages from A through C (nearly) always coalesce with each other before any coalescence with D. The small dash on the branch indicates the mutation A → B occurring, giving rise to the ABBA or BABA mutational pattern shown at the bottom.

coalesce with each other. Each option is equally likely; therefore the
2350 mutational patterns ABBA and BABA are equally likely to occur under ILS.⁶

2352 However, if gene flow occurs from population C into population B,
in addition to ILS the lineage from B can more recently coalesce with
2354 the lineage from C, and so we should see more ABBAs than BABAs.
To test for this effect of gene flow, we can sample a sequence from
2356 each of our 4 populations and count up the number of sites that show
the two mutational patterns consistent with the gene-tree discordance
2358 n_{ABBA} and n_{BABA} and calculate

$$\frac{n_{ABBA} - n_{BABA}}{n_{ABBA} + n_{BABA}} \quad (3.61)$$

This statistic will have expectation zero if the gene-tree discordance is
2360 due to ILS and will be skewed negative if gene flow occurred from C
into B (and skewed positive if gene flow occurred from C into A).

⁶ here we have to assume no structure in the ancestral population.

Phenotypic Variation and the Resemblance Between Relatives.

THE DISTINCTION BETWEEN GENOTYPE AND PHENOTYPE is one of the most useful ideas in Biology.¹ The genotype of an individual (the genome), for most purposes, is decided when the sperm fertilizes egg. The phenotype of an individual represents any measurable aspect of an organism.

Your height, to the amount of RNA transcribed from a given gene, to what you ate last Tuesday: all of these are phenotypes. Nearly any phenotype we can choose to measure about an organism represents the outcome of the information encoded by their genome played out through an incredibly complicated developmental, physiological and/or behavioural processes that in turn interact with a myriad of environmental and stochastic factors. Honestly it boggles the mind how organisms work as well as they do, let alone that I managed to eat lunch last Tuesday.

There are many different ways to think about studying the path from genotype through to phenotype. The one we will take here is to think about how phenotypic variation among individuals in a population arises as a result of genetic variation in the population. One simple way to measure this genotype-phenotype relationship is to calculate the phenotypic mean for each genotype at a locus. For example, WANG *et al.* (2018) explored the genetic basis of budset time in European aspen (*Populus tremula*); the effect of one specific SNP on that phenotype is shown in Figure 4.2. Budset timing is a key trait underlying local adaptation to varying growing season length. The associated SNP falls in a gene (*PtFT2*) that is known to play a strong role in flowering time regulation in other plants.

One way for us to assess the relationship between genotype and phenotype is to find the best fitting linear line through the data, i.e. fit a linear regression of phenotypes for our individuals on their geno-

¹ JOHANNSEN, W., 1911 The Genotype Conception of Heredity. *The American Naturalist* 45(531): 129–159



Figure 4.1: European aspen *P. tremula*. H. Schacht. 1860. BHL Image from the Biodiversity Heritage Library. Contributed by The Library of Congress. Not in copyright.

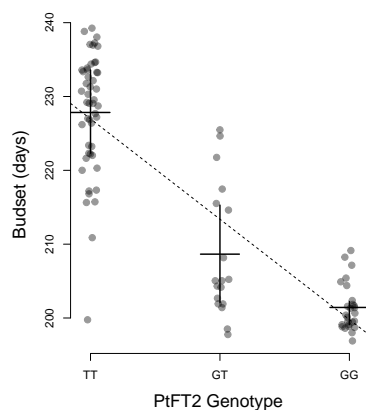


Figure 4.2: The effect of a flowering time gene (*PtFT2*) SNP on budset time in European aspen. Each dot gives the genotype-phenotype combination for an individual. The horizontal lines give the budset mean for each genotype and the vertical lines show the inter-quartile range. The dotted line gives the linear regression of phenotype on genotype. Thanks to Pär Ingvarsson for sharing these data from WANG *et al.* (2018).

²³⁹⁴ types at a particular SNP (l):

$$X \sim \mu + a_l G_l \quad (4.1)$$

In the equation above, X is a vector of the phenotypes of a set of individuals and G_l is our vector of genotypes at locus l , with $G_{i,l}$ taking the value 0, 1, or 2 depending on whether our individual i is homozygote, heterozygote, or the alternate homozygote at our locus of interest. Here μ is our phenotypic mean. The slope of this regression line (a_l) has the interpretation of being the average effect of substituting a copy of allele 2 for a copy of allele 1. In our Aspen example the slope is -13.6 , i.e. swapping a single T for a G allele moves the budset forward by 13.6 days, such that the GG homozygote is predicted to set buds 27.2 days earlier than the TT homozygote.

As a measure of the significance of this genotype-phenotype relationship, we can calculate the p-value of our regression. To try and identify loci that are associated with our trait genome-wide, we can conduct this regression at each SNP we genotype in the genome. One common way to display the results of such an analysis (called a genome-wide association study or GWAS for short) is to plot the logarithm of the p-value for each SNP along genome (a so-called Manhattan plot). Here's one from WANG *et al.* (2018) for their Aspen budset phenotype

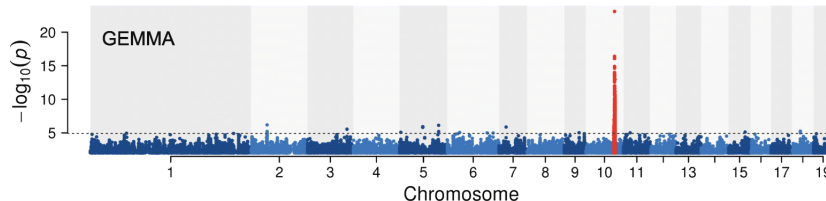


Figure 4.3: Manhattan plot of the p-value of the linear association between genotype and budset in Aspen. Each dot represents the test at a single SNP, plotted at its physical coordinate in the genome. Different chromosomes are plotted in alternating colours. The SNPs surrounding the PtFT2 gene are shown in red. From WANG *et al.* (2018), licensed under CC BY 4.0.

²⁴¹⁴ The SNP with the most significant p-value is the PtFT2 SNP. Note
²⁴¹⁶ that other SNPs in the surrounding region also light up as showing a
²⁴¹⁸ significant association with budset timing. This is because loci that
²⁴²⁰ are in LD with a functional locus may in turn show an association,
²⁴²² not because they directly affect the phenotype, but simply because
²⁴²⁴ the genotypes at the two loci are themselves non-randomly associated.
²⁴²⁶ Below is a zoomed in version (Figure 2 in WANG *et al.* (2018)) with
²⁴²⁸ SNPs coloured by the strength of their LD with the putatively func-
²⁴³⁰ tional SNP. Note how SNPs in strong LD with the functional allele
²⁴³² (redder points) have more significant p-values.

²⁴³⁴ Variation in some traits seems to have a relatively simple genetic
²⁴³⁶ basis. In our Aspen example there is one clear large-effect locus, which
²⁴³⁸ explains 62% of the variation in budset. Note that even in this case,
²⁴⁴⁰ where we have an allele with a very strong effect on a phenotype, this

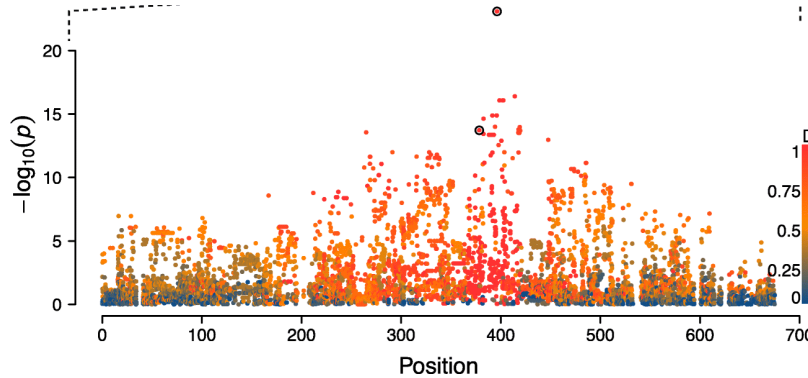


Figure 4.4: The Manhattan plot zoomed in on the top-hit (red SNPs from Figure 4.3). SNPs are now coloured by their D_f value with the most significant SNP. D_f is the LD covariance between a pair of loci (D) normalized by the largest value D can take given the allele frequencies. Figure from WANG *et al.* (2018), licensed under CC BY 4.0.

2428 is not an allele *for* budset, nor is PtFT2 a gene *for* budset. It is an
 2429 allele that is associated with budset in the sampled environments and
 2430 populations. In a different set of environments, this allele's effects
 2431 may be far smaller, and a different set of alleles may contribute to
 2432 phenotype variation. PtFT2, the gene our focal SNP falls close to, is
 2433 just one of many genes and molecular pathways involved in budset.
 2434 A mutant screen for budset may uncover many genes with larger ef-
 2435 fects; this gene is just a locus that happens to be polymorphic in this
 2436 particular set of genotyped individuals.

While phenotypic variation for some phenotypes has a relatively
 2437 simple genetic basis, many phenotypes are likely much more genetically
 2438 complex, involving the functional effect of many alleles at hun-
 2439 dreds or thousands of polymorphic loci. For example hundreds of
 2440 small effect loci affecting human height have been mapped in Euro-
 2441 pean populations to date. Such genetically complex traits are called
 2442 polygenic traits.

2444 In this chapter, we will use our understanding of the sharing of
 2445 alleles between relatives to understand the phenotypic resemblance
 2446 between relatives in quantitative phenotypes. This will allow us to
 2447 understand the contribution of genetic variation to phenotypic varia-
 2448 tion. In the next chapter, we will then use these results to understand
 2449 the evolutionary change in quantitative phenotypes in response to
 2450 selection.

4.0.1 A simple additive model of a trait

2452 Let's imagine that the genetic component of the variation in our trait
 2453 is controlled by L autosomal loci that act in an additive manner. The
 2454 frequency of allele 1 at locus l is p_l , with each copy of allele 1 at this
 2455 locus increasing your trait value by a_l above the population mean.
 2456 The phenotype of an individual, let's call her i , is X_i . Her genotype
 2457 at SNP l is $G_{i,l}$. Here $G_{i,l} = 0, 1$, or 2 , representing the number of

"All that we mean when we speak of a gene [allele] for pink eyes is, a gene which differentiates a pink eyed fly from a normal one —not a gene [allele] which produces pink eyes per se, for the character pink eyes is dependent on the action of many other genes." - STURTEVANT (1915)

²⁴⁵⁸ copies of allele 1 she has at this SNP. Her expected phenotype, given her genotype at all L SNPs, is then

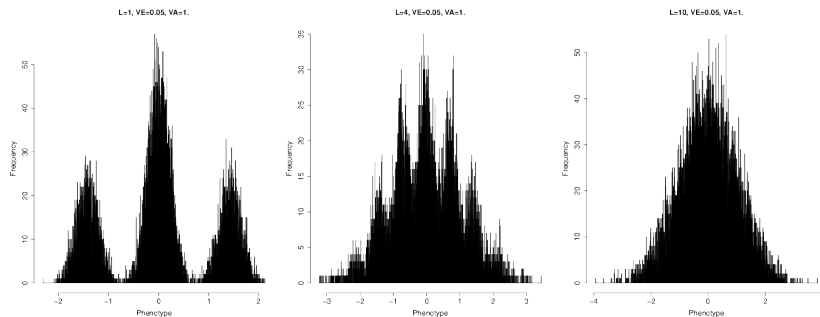
$$\mathbb{E}(X_i|G_{i,1}, \dots, G_{i,L}) = \mu + X_{A,i} = \mu + \sum_{l=1}^L G_{i,l}a_l \quad (4.2)$$

²⁴⁶⁰ where μ is the mean phenotype in our population, and $X_{A,i}$ is the deviation away from the mean phenotype due to her genotype. Now ²⁴⁶² in reality the phenotype is a function of the expression of those alleles in a particular environment. Therefore, we can think of this expected ²⁴⁶⁴ phenotype as being an average across a set of environments that occur in the population.

²⁴⁶⁶ When we measure our individual's observed phenotype we see

$$X_i = \mu + X_{A,i} + X_{E,i} \quad (4.3)$$

²⁴⁶⁸ where X_E is the deviation from the mean phenotype due to the environment. This X_E includes the systematic effects of the environment our individual finds herself in and all of the noise during development, ²⁴⁷⁰ growth, and the various random insults that life throws at our individual. If a reasonable number of loci contribute to variation in our ²⁴⁷² trait then we can approximate the distribution of $X_{A,i}$ by a normal distribution due to the central limit theorem (see Figure 4.5). Thus if we can approximate the distribution of the effect of environmental ²⁴⁷⁴ variation on our trait ($X_{E,i}$) also by a normal distribution, which is reasonable as there are many small environmental effects, then the ²⁴⁷⁶ distribution of phenotypes within the population (X_i) will be normally distributed (see Figure 4.5).



²⁴⁸⁰ Note that as this is an additive model; we can decompose eqn. 4.3 into the effects of the two alleles at each locus and rewrite it as

$$X_i = \mu + X_{iM} + X_{iP} + X_{iE} \quad (4.4)$$

²⁴⁸² where X_{iM} and X_{iP} are the contribution to the phenotype of the alleles that our individual received from her mother (maternal alleles) and

Figure 4.5: The convergence of the phenotypic distribution to a normal distribution. Each of the three histograms shows the distribution of the phenotype in a large sample, for increasingly large numbers of loci ($L = 1, 4, \text{ and } 10$, with the proportion of variance explained held at $V_A = 1$). I have simulated each individual's phenotype following equations 4.2 and 4.3. Specifically, we've simulated each individual's biallelic genotype at L loci, assuming Hardy-Weinberg proportions and that the allele is at 50% frequency. We assume that all of the alleles have equal effects and combine them additively together. We then add an environmental contribution, which is normally distributed with variance 0.05. Note that in the left two pictures you can see peaks corresponding to different genotypes due to our low environmental noise (in practice we can rarely see such peaks for real quantitative phenotypes). Code here.

father (paternal alleles) respectively. This will come in handy in just
 2484 a moment when we start thinking about the phenotypic covariance of
 relatives.

2486 Now obviously this model seems silly at first sight as alleles don't
 only act in an additive manner, as they interact with alleles at the
 2488 same loci (dominance) and at different loci (epistasis). Later we'll
 relax this assumption, however, we'll find that if we are interested
 2490 in evolutionary change over short time-scales it is actually only the
 "additive component" of genetic variation that will (usually) concern
 2492 us. We will define this more formally later on, but for the moment
 we can offer the intuition that parents only get to pass on a single
 2494 allele at each locus on to the next generation. As such, it is the effect
 of these transmitted alleles, averaged over possible matings, that is
 2496 an individual's average contribution to the next generation (i.e. the
 additive effect of the alleles that their genotype consists of).

2498 4.0.2 Additive genetic variance and heritability

As we are talking about an additive genetic model, we'll talk about
 2500 the additive genetic variance (V_A), the phenotypic variance due to the
 additive effects of segregating genetic variation. This is a subset of the
 2502 total genetic variance if we allow for non-additive effects.

The variance of our phenotype across individuals (V) we can write
 2504 as

$$V = \text{Var}(X_A) + \text{Var}(X_E) = V_A + V_E \quad (4.5)$$

In writing the phenotypic variance as a sum of the additive and environmental contributions, we are assuming that there is no covariance
 2506 between $X_{G,i}$ and $X_{E,i}$ i.e. there is no covariance between genotype
 2508 and environment.

Our additive genetic variance can be written as

$$V_A = \sum_{l=1}^L \text{Var}(G_{i,l}a_l) \quad (4.6)$$

2510 where $\text{Var}(G_{i,l}a_l)$ is the contribution of locus l to the additive variance
 among individuals. Assuming random mating, and that our loci
 2512 are in linkage equilibrium, we can write our additive genetic variance
 as

$$V_A = \sum_{l=1}^L a_l^2 2p_l(1 - p_l) \quad (4.7)$$

2514 where the $2p_l(1 - p_l)$ term follows from the binomial sampling of two
 alleles per individual at each locus.

2516 **Question 1.** You have two biallelic SNPs contributing to variance
 in human height. At the first SNP you have an allele with an additive

2518 effect of 5cm which is found at a frequency of 1/10,000. At the second
 SNP you have an allele with an additive effect of -0.5cm segregat-
 2520 ing at 50% frequency. Which SNP contributes more to the additive
 genetic variance? Explain the intuition of your answer.

2522 *An example of calculating polygenic scores.* Now we don't usually
 get to see the individual loci contributing to highly polygenic traits.
 2524 Instead, we only get to see the distribution of the trait in the popu-
 lation. However, with the advent of GWAS in human genetics we can
 2526 see some of the underlying genetics using the many trait-associated
 loci identified to date. Using the estimated effect sizes at each locus,
 2528 each one of which is tiny, we can calculate the weighted sum over an
 individual's genotype as in equation 4.2. This weighted sum is called
 2530 the individual's polygenic score. To illustrate how polygenic scores
 work, we can take a set of 1700 SNPs, each chosen as the SNP with
 2532 the strongest signal of association with height in 1700 roughly inde-
 pendent bins spaced across the genome. The effects of these SNPs are
 2534 tiny; the medium, absolute additive effect size is 0.07cm. Figure 4.6
 shows the distribution of a thousand individuals' polygenic scores cal-
 2536 culated using these 1700 SNPs (simulated genotypes using the UKBB
 frequencies). The standard deviation of these polygenic scores $\sim 2\text{cm}$.
 2538 The individuals with higher polygenic scores for height are predicted
 to be taller than the individuals with lower polygenic scores.



Figure 4.6: **Left)** The distribution of the number of height-increasing alleles that individuals carry at 1700 SNPs associated with height in the UK Biobank, for a sample of 1000 individuals. **right)** The distribution of the polygenic scores for these 1000 individuals. Plotted on top is a normal distribution with the same mean and variance. The empirical variance of these polygenic scores is 0.13, the additive genetic variance calculated by equation (4.7) is 0.135, so the two are in good agreement. Code here.

2540 *The narrow sense heritability* We would like a way to think about
 what proportion of the variation in our phenotype across individuals
 2542 is due to genetic differences as opposed to environmental differences.
 Such a quantity will be key in helping us think about the evolution of

2544 phenotypes. For example, if variation in our phenotype had no genetic basis, then no matter how much selection changes the mean phenotype
 2546 within a generation the trait will not change over generations.

We'll call the proportion of the variance that is genetic the *heritability*, and denote it by h^2 . We can then write heritability as

$$h^2 = \frac{Var(X_A)}{V} = \frac{V_A}{V} \quad (4.8)$$

Remember that we are thinking about a trait where all of the alleles
 2550 act in a perfectly additive manner. In this case our heritability h^2
 is referred to as the *narrow sense heritability*, the proportion of the
 2552 variance explained by the additive effect of our loci. When we allow
 dominance and epistasis into our model, we'll also have to define the
 2554 *broad sense heritability* (the total proportion of the phenotypic variance
 attributable to genetic variation).

The narrow sense heritability of a trait is a useful quantity; indeed
 2556 we'll see shortly that it is exactly what we need to understand the
 evolutionary response to selection on a quantitative phenotype. We
 2560 can calculate the narrow sense heritability by using the resemblance
 between relatives. For example, if the phenotypic differences between
 individuals in our population were solely determined by environmental
 2562 differences experienced by these different individuals, we should not
 expect relatives to resemble each other any more than random individ-
 uals drawn from the population. Now the obvious caveat here is that
 2564 relatives also share an environment, so may resemble each other due to
 shared environmental effects.

Note that the heritability is a property of a sample from the pop-
 2568 ulation in a particular set of environments at a particular time.

Changes in the environment may change the phenotypic variance.
 2570 Changes in the environment may also change how our genetic alleles
 are expressed through development and so change V_A . Thus estimates
 2572 of heritability are not transferable across environments or populations.

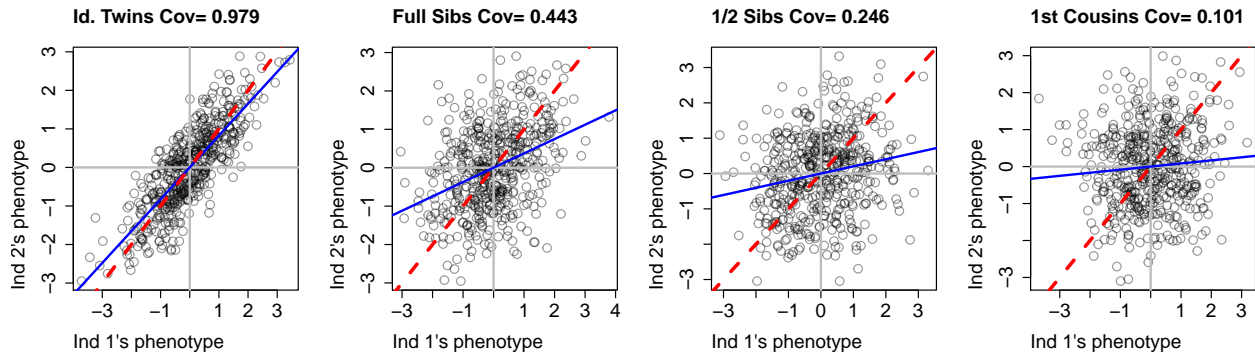
4.0.3 The covariance between relatives

2574 So we'll go ahead and calculate the covariance in phenotype between
 two individuals (1 and 2) who have phenotypes X_1 and X_2 respec-
 2576 tively. To think about imagine plotting the phenotypes of, say, sisters
 against each other. The x and y coordinates of each point will be
 2578 the, say, heights of the pair of siblings. Do tall women tend to have
 tall sisters, do short women tend to have short sisters? How much do
 2580 their phenotypes covary. If some of the variation in our phenotype is
 genetic we expect identical twins to resemble each other more than
 2582 full siblings, who in turn will resemble each other more than half-sibs
 and so on out (see Figure 4.7). Under our simple additive model of

2584 phenotypes we can write the covariance as

$$\text{Cov}(X_1, X_2) = \text{Cov}((X_{1M} + X_{1P} + X_{1E}), ((X_{2M} + X_{2P} + X_{2E})) \quad (4.9)$$

We can expand this out in terms of the covariance between the various
2586 components in these sums.



To make our task easier, we will make two commonly made assumptions:
2588

1. We can ignore the covariance of the environments between individuals (i.e. $\text{Cov}(X_{1E}, X_{2E}) = 0$)
2. We can ignore the covariance between the environment of one individual and the genetic variation in another individual (i.e. $\text{Cov}(X_{1E}, (X_{2M} + X_{2P})) = 0$). (We can actually incorporate these effects in later if we choose too.)

The failure of these assumptions to hold can undermine our estimates of heritability, but we'll return to that later. Moving forward with these assumptions, we can simplify our original expression above
2592 and write our phenotypic covariance between our pair of individuals as
2594

$$\text{Cov}(X_1, X_2) = \text{Cov}((X_{1M}, X_{2M}) + \text{Cov}(X_{1M}, X_{2P}) + \text{Cov}(X_{1P}, X_{2M}) + \text{Cov}(X_{1P}, X_{2P}) \quad (4.10)$$

This equation is saying that, under our simple additive model, we can see the covariance in phenotypes between individuals as the covariance
2600 between the maternal and paternal allelic effects in our individuals.
2602 We can use our results about the sharing of alleles between relatives to obtain these covariance terms. But before we write down the general
2604 case, let's quickly work through some examples.

2606 The covariance between identical twins Let's first consider the case of a pair of identical twins from two unrelated parents. Our pair of

Figure 4.7: Covariance of phenotypes between pairs of individuals of a given relatedness. Each point gives the phenotypes of a different pair of individuals. The additive genetic variance is held constant at $V_A = 1$, such that the expected covariances ($2F_{1,2}V_A$) should be 1, 0.5, 0.25, and 0.125 respectively din good agreement with the empirical covariances reported in the title of each graph. The data were simulated as described in the caption of Figure 4.5. The blue line shows $x = y$ and the red line shows the best fitting linear regression line. Code here.

²⁶⁰⁸ twins share their maternal and paternal allele identical by descent ($X_{1M} = X_{2M}$ and $X_{1P} = X_{2P}$). As their maternal and paternal alleles
²⁶¹⁰ are not correlated draws from the population, i.e. have no probability
²⁶¹² of being *IBD* as we've said the parents are unrelated, the covariance
²⁶¹⁴ between their effects on the phenotype is zero (i.e. $Cov(X_{1P}, X_{2M}) = Cov(X_{1M}, X_{2P}) = 0$). In that case, eqn. 4.10 is

$$Cov(X_1, X_2) = Cov((X_{1M}, X_{2M}) + Cov(X_{1P}, X_{2P}) = 2Var(X_{1M}) = V_A \quad (4.11)$$

²⁶¹⁴ Now in general identical twins are not going to be super helpful for us in estimating h^2 , because under models with non-additive effects,
²⁶¹⁶ identical twins will have higher covariance than we'd expect just based on the alleles they share. This is because identical twins don't just
²⁶¹⁸ share alleles, they share their entire genotypes, and thus resemble each other in phenotype also because of shared dominance effects.

²⁶²⁰ *The covariance in phenotype between mother and child* If a mother and father are unrelated individuals (i.e. are two random draws from
²⁶²² the population) then this mother and her child share one allele IBD at each locus (i.e. $r_1 = 1$ and $r_0 = r_2 = 0$). Half the time our
²⁶²⁴ mother (ind 1) transmits her paternal allele to the child (ind 2), in which case $X_{P1} = X_{M2}$, and so $Cov(X_{P1}, X_{M2}) = Var(X_{P1})$,
²⁶²⁶ and all the other covariances in eqn. 4.10 are zero. The other half of the time she transmits her maternal allele to the child, in which
²⁶²⁸ case $Cov(X_{M1}, X_{M2}) = Var(X_{M1})$ and all the other terms are zero. By this argument, $Cov(X_1, X_2) = \frac{1}{2}Var(X_{M1}) + \frac{1}{2}Var(X_{P1}) = \frac{1}{2}V_A$.

²⁶³⁰ *The covariance between general pairs of relatives under an additive model* The two examples above make clear that to understand
²⁶³² the covariance between phenotypes of relatives, we simply need to think about the alleles they share IBD. Consider a pair of relatives (1 and 2) with a probability r_0 , r_1 , and r_2 of sharing zero, one, or two alleles IBD respectively. When they share zero alleles
²⁶³⁴ $Cov((X_{1M} + X_{1P}), (X_{2M} + X_{2P})) = 0$, when they share one allele
²⁶³⁶ $Cov((X_{1M} + X_{1P}), (X_{2M} + X_{2P})) = Var(X_{1M}) = \frac{1}{2}V_A$, and when they
²⁶³⁸ share two alleles $Cov((X_{1M} + X_{1P}), (X_{2M} + X_{2P})) = V_A$. Therefore, the general covariance between two relatives is

$$Cov(X_1, X_2) = r_0 \times 0 + r_1 \frac{1}{2}V_A + r_2 V_A = 2F_{1,2}V_A \quad (4.12)$$

²⁶⁴⁰ So under a simple additive model of the genetic basis of a phenotype, to measure the narrow sense heritability we need to measure the
²⁶⁴² covariance between pairs of relatives (assuming that we can remove the effect of shared environmental noise). From the covariance between relatives we can calculate V_A , and we can then divide this by the total phenotypic variance to get h^2 .

2646 **Question 2. A)** In polygynous red-winged blackbird populations
 (i.e. males mate with several females), paternal half-sibs can be iden-
 2648 tified. Suppose that the covariance of tarsus lengths among half-sibs
 is 0.25 cm^2 and that the total phenotypic variance is 4 cm^2 . Use these
 2650 data to estimate h^2 for tarsus length in this population.

2652 **B)** Why might paternal half-sibs be preferable for measuring heri-
 2654 tability than maternal half-sibs?

Parent-midpoint offspring regression Another way that we can esti-
 2654 mate the narrow sense heritability is through the regression of child's
 2656 phenotype on the parental mid-point phenotype. The parental mid-
 2658 point phenotype is simply the average of the mum and dad's pheno-
 2660 type. We denote the child's phenotype by X_{kid} and mid-point phe-
 2662 notype by X_{mid} , so that if we take the regression $X_{kid} \sim X_{mid}$ this
 regression has slope $\beta = \text{Cov}(X_{kid}, X_{mid})/\text{Var}(X_{mid})$. The covari-
 2664 ance of $\text{Cov}(X_{kid}, X_{mid}) = \frac{1}{2}V_A$, and $\text{Var}(X_{mid}) = \frac{1}{2}V$, as by taking
 2666 the average of the parents we have halved the variance, such that the
 2668 slope of the regression is

$$\beta_{mid,kid} = \frac{\text{Cov}(X_{kid}, X_{mid})}{\text{Var}(X_{mid})} = \frac{V_A}{V} = h^2 \quad (4.13)$$

i.e. the regression of the child's phenotype on the parental midpoint
 2664 phenotype is an estimate of the narrow sense heritability. This way of
 2666 estimating heritability has the problem of not controlling for environ-
 2668 mental correlations between relatives. But it's a useful way to think
 about heritability and will be directly relevant to our discussion of the
 2670 response to selection in the next chapter.

Our regression allows us to attempt to predict the phenotype of
 2670 the child given the phenotypes of the parents; how well we can do this
 depends on the slope. If the slope is close to zero then the parental
 2672 phenotypes hold no information about the phenotype of the child,
 while if the slope is close to one then the parental mid-point is a good
 2674 guess at the child's phenotype.

More formally, the expected phenotype of the child given the
 2676 parental phenotypes is

$$\mathbb{E}(X_{kid}|X_{mum}, X_{dad}) = \mu + \beta_{mid,kid}(X_{mid} - \mu) = \mu + h^2(X_{mid} - \mu) \quad (4.14)$$

which follows from the definition of linear regression. So to find the
 2678 child's predicted phenotype, we simply take the mean phenotype and
 add on the difference between our parental mid-point and the popula-
 2680 tion mean, multiplied by our narrow sense heritability.

Question 3. Briefly explain what Galton meant by 'regression
 2682 towards mediocrity', and why he observed this pattern in light of
 Mendelian inheritance.



Figure 4.8: Red-winged blackbird and Tricoloured Red-winged blackbirds (*Agelaius phoeniceus* and *Agelaius tricolor*).

Bird-lore (1899). National Association of Audubon Societies for the Protection of Wild Birds and Animals. Image from the Biodiversity Heritage Library. Contributed by American Museum of Natural History Library. Not in copyright.

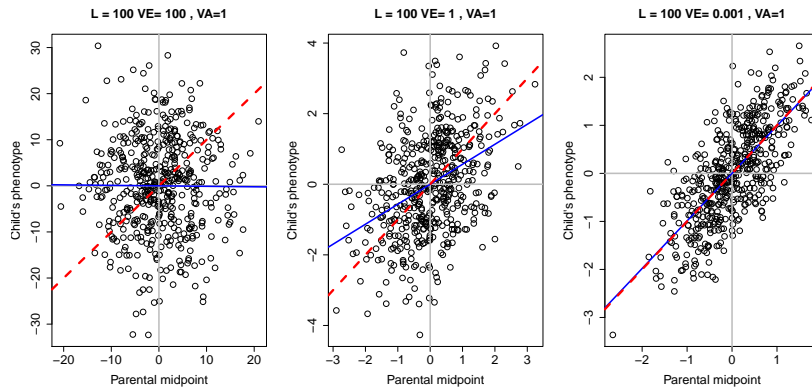


Figure 4.9: Regression of child's phenotype of the parental mid-point phenotype. The three panels show decreasing levels of environmental variance (V_E) holding the additive genetic variance constant ($V_A = 1$). In these figures, we simulate 100 loci, as described in the caption of Figure 4.5. We simulate the genotypes and phenotypes of the two parents, and then simulate the child's genotype following mendelian transmission. The blue line shows $x = y$ and the red line shows the best fitting linear regression line. Code here.

2684 *Estimating additive genetic variance across a variety of different relationships.* In many natural populations we may have access to
 2686 individuals with a range of different relationships to each other (e.g. through monitoring of the paternity of individuals), but relatively few
 2688 pairs of individuals for a specific relationship (e.g. sibs). We can try and use this information on various relatives as fully as possible in a
 2690 mixed model framework. Building from equation 4.3, we can write an individual's phenotype X_i as

$$X_i = \mu + X_{A,i} + X_{E,i} \quad (4.15)$$

2692 where $X_{E,i} \sim N(0, V_E)$ and $X_{A,i}$ is normally distributed across individuals with covariance matrix $V_A A$, where the entries for a pair
 2694 of individuals i and j are $A_{ij} = 2F_{i,j}$ and $A_{ii} = 1$. Given the matrix
 2696 A we can estimate V_A . We can also add fixed effects into this model
 2698 to account for generation effects, additional mixed effects could also be included to account for shared environments between particular individuals (e.g. a shared nest). This approach is sometimes called the “animal model”.

2700 4.1 Multiple traits

Traits often covary with each other, both due to environmentally induced effects (e.g. due to the effects of diet on multiple traits) and due to the expression of underlying genetic covariance between traits.
 2702 Genetic covariance, in turn, can reflect pleiotropy, a mechanistic effect of an allele on multiple traits (e.g. variants that affect skin pigmentation often affect hair color), the genetic linkage of loci independently affecting multiple traits, or the effects of assortative mating.
 2704
 2706

2708 Consider two traits $X_{1,i}$ and $X_{2,i}$ in an individual i . These traits
 could be, say, the individual's leg length and nose length. As before,
 2710 we can write these as

$$\begin{aligned} X_{1,i} &= \mu_1 + X_{1,A,i} + X_{1,E,i} \\ X_{2,i} &= \mu_2 + X_{2,A,i} + X_{2,E,i} \end{aligned} \quad (4.16)$$

As before we can talk about the total phenotypic variance (V_1, V_2),
 2712 environmental variance ($V_{1,E}$ and $V_{2,E}$), and the additive genetic
 variance for trait one and two ($V_{1,A}, V_{2,A}$). But now we also have
 2714 to consider the total covariance between trait one and trait two,
 $V_{1,2} = \text{Cov}(X_1, X_2)$, as well as the environmentally induced covariance
 2716 ($V_{E,1,2} = \text{Cov}(X_{1,E}, X_{2,E})$) and the additive genetic covariance
 $(V_{A,1,2} = \text{Cov}(X_{1,A}, X_{2,A}))$. To better understand the covariance arising
 2718 due to pleiotropy, let's think about a set of L SNPs contributing
 to our two traits. If the additive effect of an allele at the i^{th} SNP is
 2720 $\alpha_{i,1}$ and $\alpha_{i,2}$ on traits 1 and 2, then the additive covariance between
 our traits is

$$V_{A,1,2} = \sum_{i=1}^L 2\alpha_{i,1}\alpha_{i,2}p_i(1-p_i) \quad (4.17)$$

2722 assuming our loci are in linkage disequilibrium. Thus a genetic correlation arises due to pleiotropy, because loci that tend to affect trait 1
 2724 also systematically affect trait 2. For example, alleles associated with later Age at Menarche (AAM) in European females also tend to be
 2726 positively associated with height (see Figure 4.10), thereby creating a genetic correlation between AAM and height.

2728 We can store our variance and covariance values in matrices, a way of gathering these terms that will be useful when we discuss selection:

$$\mathbf{V} = \begin{pmatrix} V_1 & V_{1,2} \\ V_{1,2} & V_2 \end{pmatrix} \quad (4.18)$$

2730 and

$$\mathbf{G} = \begin{pmatrix} V_{1,A} & V_{A,1,2} \\ V_{A,1,2} & V_{2,A} \end{pmatrix} \quad (4.19)$$

Here we've shown the matrices for two traits, but we can generalize
 2732 this to an arbitrary number of traits.

We can estimate these quantities, in a similar way as before, by
 2734 studying the covariance in different traits between relatives:

$$\text{Cov}(X_{1,i}, X_{2,j}) = 2F_{i,j}V_{A,1,2} \quad (4.20)$$

We can also talk about the genetic correlation between two phenotypes
 2736

$$r_g = \frac{V_{A,1,2}}{\sqrt{V_{A,1}V_{A,2}}} \quad (4.21)$$

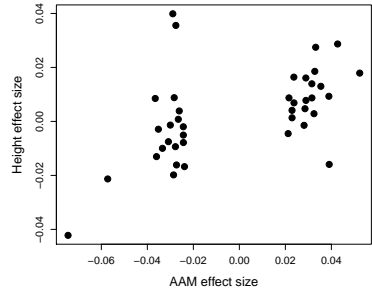


Figure 4.10: The additive effect sizes of loci associated with female Age at Menarche (AAM) and their effect size on Height in a European population. Data from PICKRELL *et al.* (2016). Code here.

where $V_{A,1}$ and $V_{A,2}$ are the additive genetic variance for trait 1 and 2 respectively. Here, r_g tells us to what extent the additive genetic variance in two traits is correlated.

One type of genetic covariance we often think about is the covariance of male and female phenotypes. For example, below is the relationship between the forehead patch size for Pied fly-catcher fathers and their sons and daughters. The phenotype has been standardized to have mean 0 and variance 1 in each group. The phenotypic covariance of the sample of fathers and sons is 0.35, while the phenotypic covariance of fathers and daughter is 0.23.

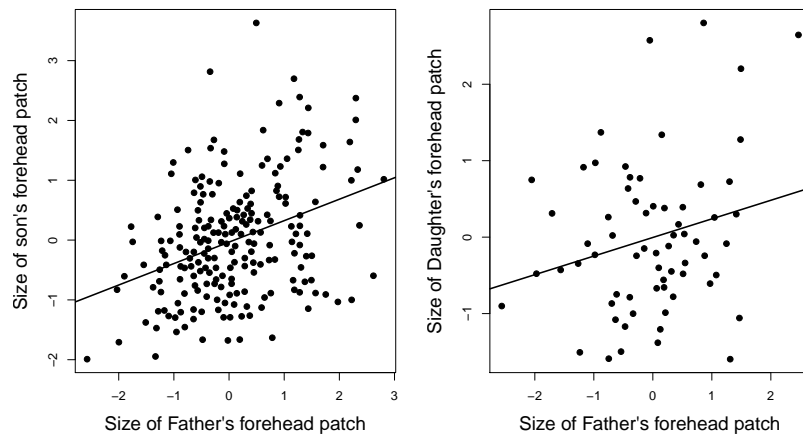


Figure 4.11: Relationship of standardized forehead patch size between fathers and sons and daughters in Pied fly-catchers. Data from POTTI and CANAL. Code here.



Figure 4.12: *Ficedula hypoleuca*, Pied fly-catcher.
Coloured illustrations of British birds, and their eggs (1842-1850). London :G.W. Nicklinson. Image from the Biodiversity Heritage Library. Contributed by Smithsonian Libraries. Not in copyright.

Question 4. Assume we can ignore the effect of the shared environment in our Pied fly-catcher example.

What is the additive genetic covariance between male and female patch size?

What is the additive genetic correlation of male and female patch size? You can assume that the additive genetic variance is the same in males and females.

4.1.1 Non-additive variation.

Up to now we've assumed that our alleles contribute to our phenotype in an additive fashion. However, that does not have to be the case as there may be non-additivity among the alleles present at a locus (*dominance*) or among alleles at different loci (*epistasis*). We can accommodate these complications into our models. We do this by partitioning our total genetic variance into independent variance components.

2762 *Dominance.* To understand the effect of dominance, let's consider
2764 how the allele that a parent transmits influences their offspring's phe-
2766 notype. A parent transmits one of their two alleles at a locus to their
2768 offspring. Assuming that individuals mate at random, this allele is
2770 paired with another allele drawn at random from the population. For
2772 example, assume your mother transmitted an allele 1 to you: with
2774 probability p it would be paired with another allele 1, and you would
2776 be a homozygote; and with probability q it's paired with a 2 allele and
2778 you're a heterozygote.

2772 Now consider an autosomal biallelic locus ℓ , with frequency p for
2774 allele 1, and genotypes 0, 1, and 2 corresponding to how many copies
2776 of allele 1 individuals carry. We'll denote the mean phenotype of an
2778 individual with genotype 0, 1, and 2 as $\bar{X}_{\ell,0}$, $\bar{X}_{\ell,1}$, $\bar{X}_{\ell,2}$ respectively.
2780 This mean is taking an average phenotype over all the environments
2782 and genetic backgrounds the alleles are present on. We'll mean center
2784 (MC) these phenotypic values, setting $\bar{X}'_{\ell,0} = \bar{X}_{\ell,0} - \mu$, and likewise
2786 for the other genotypes.

2780 We can think about the average (marginal) MC phenotype of an
2782 individual who received an allele 1 from their parent as the average
2784 of the MC phenotype for heterozygotes and 11 homozygotes, weighted
2786 by the probability that the individual has these genotypes, i.e. the
2788 probability they receive an additional allele 1 or an allele 2 from their
2790 other parent:

$$a_{\ell,1} = p\bar{X}'_{\ell,2} + q\bar{X}'_{\ell,1}, \quad (4.22)$$

2792 Similarly, if your parent transmitted an 2 allele to you, your average
2794 MC phenotype would be

$$a_{\ell,2} = p\bar{X}'_{\ell,1} + q\bar{X}'_{\ell,0} \quad (4.23)$$

2796 Let's now consider the average phenotype of an offspring of each of
2798 our three genotypes

genotype:	0,	1,	2.
additive genetic value:	$a_{\ell,2} + a_{\ell,2}$,	$a_{\ell,1} + a_{\ell,2}$,	$a_{\ell,1} + a_{\ell,1}$

2798 i.e. the mean phenotype of each genotypes' offspring averaged over
2800 all possible matings to other individuals in the population (assuming
2802 individuals mate at random). These are the additive MC genetic
2804 values (breeding values) of our genotypes. Here we are simply adding
2806 up the additive contributions of the alleles present in each genotype
2808 and ignoring any non-additive effects of genotype.

2810 To illustrate this, in Figure 4.13 we plot two different cases of dom-
2812 inance relationships; in the top row an additive polymorphism and in
2814 the second row a fully dominant allele. The additive genetic values of
2816 the genotypes are shown as red dots. Note that the additive values of
2818 the genotypes line up with the observed MC phenotypic means in the



Figure 4.13: The average mean-centered (MC) phenotypes of each genotype. **Top Row:** Additive relationship between genotype and phenotype. **Bottom Row:** Allele 1 is dominant over allele 2, such that the heterozygote has the same phenotype as the 22 genotype (2). The area of each circle is proportion to the fraction of the population in each genotypic class (p^2 , $2pq$, and q^2). One the left column $p = 0.1$ and the right column is $p = 0.9$. The additive genetic values of the genotypes are shown as red dots. The regression between phenotype and additive genotype is shown as a red line. The black vertical arrows show the difference between the average MC phenotype and additive genetic value for each genotype. Code here.

top row, when our alleles interact in a completely additive manner.

2802 Our additive genetic values always fall along a linear line (the red line in our figure). The additive values are falling along the best fitting line
2804 of linear regression for our population, when phenotype is regressed
2806 against the additive genotype (0, 1, 2 copies of allele 1) across all in-
2808 dividuals in our population. Note in the dominant case the additive
genetic values differ from the observed phenotypic means, and are
closer to the observed values for the genotypes that are most common
in the population.

2810 The difference in the additive effect of the two alleles $a_{\ell,2} - a_{\ell,1}$
2812 can be interpreted as an average effect of swapping an allele 1 for an
allele 2; we'll call this difference $\alpha_{\ell} = a_{\ell,2} - a_{\ell,1}$. Our α_{ℓ} is also the
2814 slope of the regression of phenotype against genotype (the red line
on genotype (α_{ℓ}) does not depend on the population allele frequency
2816 for our completely additive locus (top row of 4.13). In contrast, when
there is dominance, the slope between genotype and phenotype (α_{ℓ})
2818 is a function of allele frequency (bottom row of 4.13). When a domi-
nant allele (1) is rare there is a strong slope of phenotype on genotype,
2820 bottom left Figure 4.13. This strong slope is because replacing a single
copy of the 2 allele with a 1 allele in an individual has a big effect on
2822 average phenotype, as it will most likely move an individual from be-
ing a 22 homozygote to being a 12 heterozygote. In contrast, when the
2824 dominant allele (1) is common in the population, replacing a 2 allele
by a 1 allele in an individual on average has little phenotypic effect,

2826 leading to a weak slope bottom right Figure 4.13. This small effect is
 because as we are mainly turning heterozygotes into homozygotes (11),
 2828 who have the same mean phenotype as each other.

As an example of how dominance and population allele frequencies can change the additive effect of an allele, let's consider the genetics of the age of sexual maturity in Atlantic Salmon. A single allele of large effect segregates in Atlantic Salmon that influences the sexual maturation rate in salmon (AYLLON *et al.*, 2015; BARSON *et al.*, 2015), and hence the timing of their return from the sea to spawn (sea age). The allele falls close to the autosomal gene VGLL3 (COUS-MINER *et al.*, 2013, variation at this gene in humans also influences the timing of puberty). The left side of Figure 4.15 shows the age at sexual maturity in males. The allele (E) associated with slower sexual maturity is recessive in males. While the LL homozygotes mature on average a whole year later, the additive effect of the allele is weak while the L allele is rare in the population. The right panel shows the effect of the L allele in females. Note how the allele is much more dominant in females, and has a much more pronounced additive effect. The dominance of an allele is not a fixed property of the allele but rather a statement of the relationship of genotype to phenotype, such that the dominance relationship between alleles may vary across phenotypes and contexts (e.g. sexes).



The variance in the population phenotype due to these additive breeding values at locus ℓ , assuming HW proportions, is

$$\begin{aligned}
 V_{A,\ell} &= p^2(2a_{\ell,2})^2 + 2pq(a_{\ell,1} + a_{\ell,0})^2 + q^2(2a_{\ell,0})^2 \\
 &= 2(pa_{\ell,1}^2 + qa_{\ell,2}^2) \\
 &= 2pq\alpha_{\ell}^2
 \end{aligned} \tag{4.24}$$

2848 The total additive variance for the whole genotype can be found by

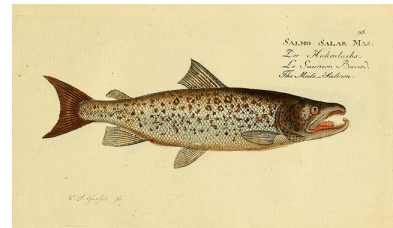


Figure 4.14: Atlantic Salmon (*Salmo salar*).

Histoire naturelle des poissons. 1796. Bloch, M. E. Image from the Biodiversity Heritage Library. Contributed by Ernst Mayr Library, Museum of Comparative Zoology. Not in copyright.

Figure 4.15: The average age at sexual maturity for each genotype, broken down by sex. The area of each circle is proportional to the fraction of the population in each genotypic class. The regression between phenotype and additive genotype is shown as a red line. Data from BARSON *et al.* (2015). Code here.

summing the individual additive genetic variances over loci

$$V_A = \sum_{\ell=1}^L V_{A,\ell} = \sum_{\ell=1}^L 2p_\ell q_\ell \alpha_\ell^2. \quad (4.25)$$

Having assigned the additive genetic variance to be the variance explained by the additive contribution of the alleles at a locus, we define the dominance variance as the population variance among genotypes at a locus due to their deviation from additivity. We can calculate how much each genotypic mean deviates away from its additive prediction at locus ℓ (the length of the arrows in Figure 4.13). For example, the heterozygote deviates

$$d_{\ell,1} = \bar{X}'_{\ell,1} - (a_{\ell,1} + a_{\ell,2}) \quad (4.26)$$

away from its additive genetic value, with similar expressions for each of the homozygotes ($d_{\ell,0}$ and $d_{\ell,2}$). We can then write the dominance variance at our locus as the genotype-frequency weighted sum of our squared dominance deviations

$$V_{D,\ell} = p^2 d_{\ell,0}^2 + 2pq d_{\ell,1}^2 + q^2 d_{\ell,2}^2. \quad (4.27)$$

Writing our total dominance variance as the sum across loci

$$V_D = \sum_{\ell=1}^L V_{D,\ell}. \quad (4.28)$$

Having now partitioned all of the genetic variance into additive and dominant terms, we can write our total genetic variance as

$$V_G = V_A + V_D. \quad (4.29)$$

We can do this because by construction the covariance between our additive and dominant deviations for the genotypes is zero. We can define the narrow sense heritability as before $h^2 = V_A/V_P = V_A/(V_G + V_E)$, which is the proportion of phenotypic variance due to additive genetic variance. We can also define the total proportion of the phenotypic variance due to genetic differences among individuals, as the broad-sense heritability $H^2 = V_G/(V_G + V_E)$.

Relationship (i,j)*	$Cov(X_i, X_j)$
parent-child	$1/2V_A$
full siblings	$1/2V_A + 1/4V_D$
identical (monozygotic) twins	$V_A + V_D$
1 st cousins	$1/8V_A$

Table 4.1: Phenotypic covariance between some pairs of relatives, include the dominance variation. * Assuming this is the only relationship the pair of individuals share (above that expected from randomly sampling individuals from the population).

When dominance is present in the loci influencing our trait ($V_D >$

0), we need to modify our phenotype covariance among relatives to

account for this non-additivity. Specifically, our equation for the
 2874 covariance among a general pair of relatives (eqn. 4.12 for additive variation) becomes

$$\text{Cov}(X_1, X_2) = 2F_{1,2}V_A + r_2V_D \quad (4.30)$$

2876 where r_2 is the probability that the pair of individuals share 2 alleles identical by descent, making the same assumptions (other than
 2878 additivity) that we made in deriving eqn. 4.12. In table 4.1 we show the phenotypic covariance for some common pairs of relatives. The
 2880 regression of offspring phenotype on parental midpoint still has a slope V_A/V_P .

2882 Full sibs and parent-offspring have the same covariance if there
 2884 is no dominance variance (as they have the same kinship coefficient
 $F_{1,2}$). However, when dominance is present ($V_D > 0$), full-sibs re-
 2886 semble each other more than parent-offspring pairs. That's because parents and offspring share precisely one allele, while full-sibs can
 2888 share both alleles (i.e. the full genotype at a locus) identical by de-
 2890 scent. We can attempt to estimate V_D by comparing different sets of relationships. For example, non-identical twins (full sibs born at same
 2892 time) should have 1/2 the phenotypic covariance of identical twins if $V_D = 0$. Therefore, we can attempt to estimate V_D by looking at whether identical twins have more than twice the phenotypic covari-
 2894 ance than non-identical twins.

2894 The most important aspect of this discussion for thinking about evolutionary genetics is that the parent-offspring covariance is still
 2896 only a function of V_A . This is because our parent (e.g. the mother) transmits only a single allele, at each locus, to its offspring. The other
 2898 allele the offspring receives is random (assuming random mating), as it comes from the other unrelated parent (the father). Therefore, the
 2900 average effect on the child's phenotype of an allele the child receives from their mother is averaged over all possible random alleles the child
 2902 could receive from their father (weighted by their frequency in the population). Thus we only care about the additive effect of the allele,
 2904 as parents transmit only alleles (not genotypes) to their offspring.
 This means that the short-term response to selection, as described by
 2906 the breeder's equation, depends only on V_A and the additive effect
 2908 of alleles. Therefore, if we can estimate the narrow-sense heritability
 2910 we can predict the short-term response. However, if alleles display dominance, our value of V_A will change as alleles at our loci change in frequency, e.g. as dominant alleles become common in the population
 2912 their contribution to V_A decreases. Therefore, if there is dominance our value of V_A will not be constant across generations.

Up to this point we have only considered dominance and not epistasis. However, we can include epistasis in a similar manner (for ex-

ample among pairs of loci). This gets a little tricky to think about,
2916 so we will only briefly explain it. We can first estimate the additive
effect of the alleles by considering the effect of the alleles averaging
2918 over their possible genetic backgrounds (including the other interacting
alleles they are possibly paired with), just as before. We can then
2920 calculate the additive genetic variance from this. We can estimate the
dominance variance, by calculating the residual variance among geno-
2922 types at a locus unexplained by the additive effect of the loci. We can
then estimate the epistatic variance by estimating the residual vari-
2924 ance left unexplained among the two locus genotypes after accounting
for the additive and dominant deviations calculated from each locus
2926 separately. In practice these high variance components are hard to
estimate, and usually small as much of our variance is assigned to the
2928 additive effect. Again we would find that we mostly care about V_A for
predicting short-term evolution, but that the contribution of loci to
2930 the additive genetic variance will depend on the epistatic relationships
among loci.

2932 **Question 5.** How could you use 1/2 sibs vs. full-sibs to estimate
 V_D ? Why might this be difficult in practice? Why are identical vs.
2934 non-identical twins better suited for this?

2936 **Question 6.** Can you construct a case where $V_A = 0$ and $V_D > 0$?
You need just describe it qualitatively; you don't need to work out the
math. (tricker question).

The Response to Phenotypic Selection

- 2940 Evolution by natural selection requires:
1. Variation in a phenotype

2942 2. That survival is non-random with respect to this phenotypic variation.

2944 3. That this variation is heritable.

Points 1 and 2 encapsulate our idea of Natural Selection, but evolution by natural selection will only occur if the 3rd condition is also met.

¹ It is the heritable nature of variation that couples change within a generation due to natural selection to change across generations (evolutionary change).

2950 Let's start by thinking about the change within a generation due to directional selection, where selection acts to change the mean phenotype within a generation. For example, a decrease in mean height within a generation, due to taller organisms having a lower chance of surviving to reproduction than shorter organisms. Specifically, we'll denote our mean phenotype at reproduction by μ_S , i.e. after selection has acted, and our mean phenotype before selection acts by μ_{BS} . This second quantity may be hard to measure, as obviously selection acts throughout the life-cycle, so it might be easier to think of this as the mean phenotype if selection hadn't acted. So the change in mean phenotype within a generation is $\mu_S - \mu_{BS} = S$.

We are interested in predicting the distribution of phenotypes in the next generation. In particular, we are interested in the mean phenotype in the next generation to understand how directional selection has contributed to evolutionary change. We'll denote the mean phenotype in offspring, i.e. the mean phenotype in the next generation before selection acts, as μ_{NG} . The change across generations we'll call the response to selection R and put this equal to $\mu_{NG} - \mu_{BS}$.

2968 The mean phenotype in the next generation is

$$\mu_{NG} = \mathbb{E}(\mathbb{E}(X_{kid}|X_{mom}, X_{dad})) \quad (5.1)$$

See LEWONTIN (1970). Note that these requirements are not specific to DNA, i.e. the concept of evolution by natural selection is substrate independent.

¹ Some people consider natural selection to only operate on heritable phenotype variation and so require all three conditions to say that natural selection occurs. This is mostly a semantic point, however, it is useful to be able to distinguish the action of selection from a possible response.

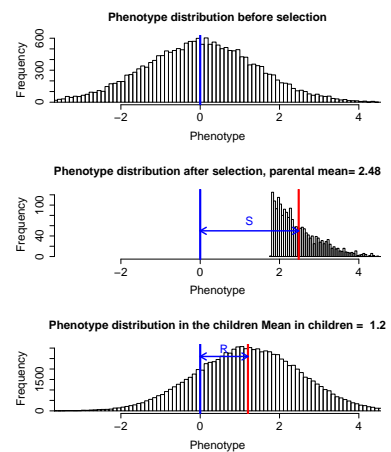


Figure 5.1: **Top.** Distribution of a phenotype in the parental population prior to selection, $V_A = V_E = 1$. **Middle.** Only individuals in the top 10% of the phenotypic distribution are selected to reproduce; the resulting shift in the phenotypic mean is S . **Bottom.** Phenotypic distribution of children of the selected parents; the shift in the mean phenotype is R . Code here.

where the outer expectation is over possible pairs of randomly mating individuals who survive to reproduce. We can use eqn. 4.14 to obtain an expression for this expectation:

$$\mu_{NG} = \mu_{BS} + \beta_{mid,kid}(\mathbb{E}(X_{mid}) - \mu_{BS}) \quad (5.2)$$

So to obtain μ_{NG} we need to compute $\mathbb{E}(X_{mid})$, the expected mid-point phenotype of pairs of individuals who survive to reproduce. Well this is just the expected phenotype in the individuals who survived to reproduce (μ_S), so

$$\mu_{NG} = \mu_{BS} + h^2(\mu_S - \mu_{BS}) \quad (5.3)$$

So we can write our response to selection as

$$R = \mu_{NG} - \mu_{BS} = h^2(\mu_S - \mu_{BS}) = h^2S \quad (5.4)$$

So our response to selection is proportional to our selection differential, and the constant of proportionality is the narrow sense heritability. This equation is sometimes termed the Breeder's equation. It is a statement that the evolutionary change across generations (R) is proportional to the change caused by directional selection within a generation (S), and that the strength of this relationship is determined by the narrow sense heritability (h^2).



Figure 5.2: A visual representation of the Breeder's equation. Regression of child's phenotype on parental midpoint phenotype ($V_A = V_E = 1$). Under truncation selection, only individuals with phenotypes > 1 (red) are bred. [Code here.](#)

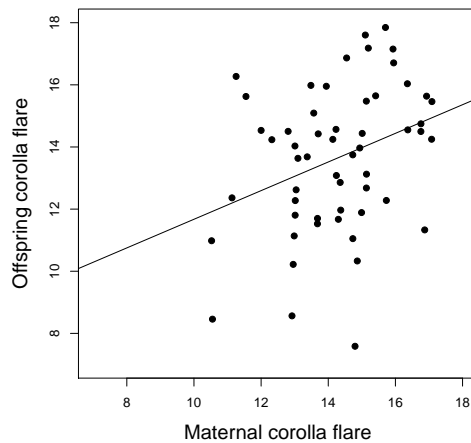


Figure 5.3: The relationship between maternal and offspring corolla flare (flower width) in *P. viscosum*. From GALEN's data the covariance of mother and child is 1.3, while the variance of the mother is 2.8. Data from GALEN (1996). [Code here.](#)



Figure 5.4: Sticky jacob's ladder (*Polemonium viscosum*). Flowers of Mountain and Plain (1920). Clements, E. Image from the Biodiversity Heritage Library. Contributed by New York Botanical Garden, Mertz Library. Not in copyright. Cropped from original.

Question 1. GALEN (1996) explored selection on flower shape in *P. viscosum*. She found that plants with larger corolla flare had more bumblebee visits, which resulted in higher seed set and a 17% increase in corolla flare in the plants contributing to the next generation. Based on the data in the caption of Figure 5.3 what is the expected response in the next generation?

2990 To understand the genetic basis of the response to selection take a look at Figure 5.5. The setup is the same as in our previous simulation figures. The individuals who are selected to form our next

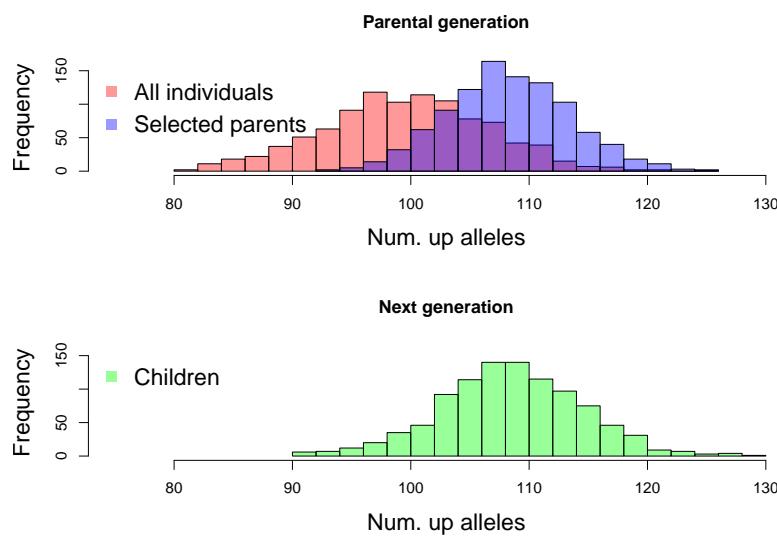


Figure 5.5: **Top.** Distribution of the number of up alleles in the parental population prior to selection (red), for the selected individuals the top 10% of the population (blue) **Bottom.** The same distribution for the offspring of the selected parents in the next generation (green). Code here.

2992 generation carry more alleles that increase the phenotype, in the current range of environments currently experienced by the population.
 2994 The average individual before selection carried 100 of these 'up' alleles, the average individual surviving selection 108 'up' alleles. As
 2996 individuals faithfully transmit their alleles to the next generation the
 2998 average child of the selected parents carries 108 up alleles. Note that
 3000 the variance has changed little, the children have plenty of variation in
 3002 their genotype, such that selection can readily drive evolution in future
 3004 generations. The average frequency of an 'up' allele has changed from
 3006 50% to 54%. Our gains due to selection will be stably inherited to
 3008 future generations.

3004 *The long-term response to selection* If our selection pressure is sustained over many generations, we can use our breeder's equation to
 3006 predict the response. If we are willing to assume that our heritability does not change and we maintain a constant selection gradient, then
 3008 after n generations our phenotype mean will have shifted

$$nh^2S \quad (5.5)$$

i.e. our population will keep up a linear response to selection.

3010 **Question 2.** A population of red deer were trapped on Jersey (an island off of England) during the last inter-glacial period. From the

³⁰¹² fossil record ² we can see that the population rapidly adapted to their new conditions. Within 6,000 years they evolved from an estimated ³⁰¹⁴ mean weight of the population of 200kg to an estimated mean weight of 36kg (a 6 fold reduction)! You estimate that the generation time ³⁰¹⁶ of red deer is 5 years and, from a current day population, that the narrow sense heritability of the phenotype is 0.5.

³⁰¹⁸ **A)** Estimate the mean change per generation in the mean body weight.

³⁰²⁰ **B)** Estimate the change in mean body weight caused by selection within a generation. State your assumptions.

³⁰²² **C)** Assuming we only have fossils from the founding population and the population after 6000 years, should we assume that the calculations ³⁰²⁴ accurately reflect what actually occurred within our population?

² LISTER, A., 1989 Rapid dwarfing of red deer on Jersey in the last interglacial. *Nature* 342(6249): 539

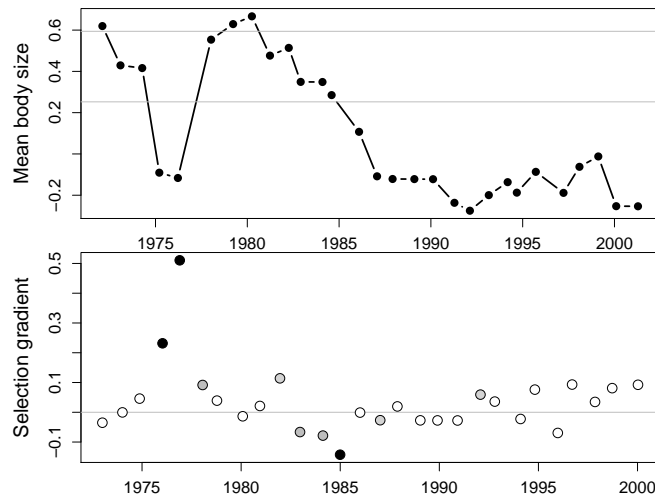


Figure 5.7: Code here.

Figure 5.6: Medium ground-finch (*Geospiza fortis*).
The zoology of the voyage of H.M.S. Beagle. Birds Part 3. (1841) Gould G. Edited by Darwin, C. Illustration by Elizabeth Gould. Image from the Biodiversity Heritage Library. Contributed by Natural History Museum Library, London . Not in copyright.

³⁰²⁶ *Alternative formulations of the Breeder's equation.* A change in mean phenotypic value within a generation occurs because of the differential fitness of our organisms. To think more carefully about this change within ³⁰²⁸ a generation, let's think about a simple fitness model where our phenotype affects the viability of our organisms (i.e. the probability they ³⁰³⁰ survive to reproduce). The probability that an individual has a phenotype X before selection is $p(X)$, so that the mean phenotype before ³⁰³² selection is

$$\mu_{BS} = \mathbb{E}[X] = \int_{-\infty}^{\infty} xp(x)dx \quad (5.6)$$

³⁰³⁴ The probability that an organism with a phenotype X survives to reproduce is $w(X)$, and we'll think about this as the fitness of our

3036 organism. The probability distribution of phenotypes in those who do
survive to reproduce is

$$\mathbb{P}(X|\text{survive}) = \frac{p(x)w(x)}{\int_{-\infty}^{\infty} p(x)w(x)dx}. \quad (5.7)$$

3038 where the denominator is a normalization constant which ensures that
our phenotypic distribution integrates to one. The denominator also
3040 has the interpretation of being the mean fitness of the population,
which we'll call \bar{w} , i.e.

$$\bar{w} = \int_{-\infty}^{\infty} p(x)w(x)dx. \quad (5.8)$$

3042 Therefore, we can write the mean phenotype in those who survive
to reproduce as

$$\mu_S = \frac{1}{\bar{w}} \int_{-\infty}^{\infty} xp(x)w(x)dx \quad (5.9)$$

3044 If we mean center our population, i.e. set the phenotype before
selection to zero, then

$$S = \frac{1}{\bar{w}} \int_{-\infty}^{\infty} xp(x)w(x)dx = \mathbb{E}(Xw(X)) \quad (5.10)$$

3046 where the final part follows from the fact that the integral is taking
the mean of $Xw(X)$ over the population.

3048 As our phenotype is mean centered ($\mathbb{E}(X) = 0$), we can see that
 S has the form of a covariance between our phenotype X and our
3050 relative fitness $w(X)$

$$S = \mathbb{E}(Xw(X)) - \mathbb{E}(X)\mathbb{E}(w(X)) = Cov(X, w(X)/\bar{w}) \quad (5.11)$$

Thus our change in mean phenotype is directly a measure of the co-
3052 variance of our phenotype and our fitness. Rewriting our breeder's
equation using this observation we see

$$R = \frac{V_A}{V} Cov(X, w(X)/\bar{w}) \quad (5.12)$$

3054 we see that the response to selection is due to the fact that our
fitness (viability) of our organisms/parents covaries with our pheno-
3056 type, and that our child's phenotype is correlated with our parent's
phenotype.

Fisher's fundamental theorem of natural selection If we choose fitness
to be our phenotype ($X = w(X)/\bar{w}$), then the response in fitness is

$$\begin{aligned} R &= \frac{V_A}{V} Cov(w(X)/\bar{w}, w(X)/\bar{w}) = \frac{V_A}{V} V \\ &= V_A \end{aligned} \quad (5.13)$$

3058 i.e. the response to selection is equal to the additive genetic variance
for fitness. Or as Fisher put it



Figure 5.8: Red deer (*Cervus elaphus*).
British mammals. Thorburn, A. (1920) Image from the Biodiversity Heritage Library.
Contributed by Field Museum of Natural History Library. Licensed under CC BY-2.0.

3060 “The rate of increase in fitness of any organism at any time is equal to its genetic variance in fitness at that time.” -FISHER (1930) (pg 37)

3062 Fisher called this ‘the fundamental theorem of natural selection’. Our proof here is just a sketch, and more formal approaches are needed
 3064 to show it in generality. There has been much nashing of teeth over exactly how broadly this result holds, and exactly what Fisher meant
 3066 (see EWENS, 2010, for a recent overview).

Fitness Gradients and linear regressions To understand this in more detail let imagine that we calculate the linear regression of an individual i 's mean-centered phenotype (X_i) on fitness (W_i), i.e.

$$W_i \sim \beta X_i + \bar{w} \quad (5.14)$$

3070 The best fitting slope of this regression (β), lets call it the ‘fitness gradient’, is given by

$$\beta = \text{Cov}(X, w(X)/\bar{w})/V \quad (5.15)$$

3072 i.e. the fitness gradient is the covariance of phenotype-fitness covariance divided by the phenotypic variance. Using this result we can
 3074 rewrite the breeder's equation as

$$R = V_A \beta \quad (5.16)$$

3076 i.e. we'll see a directional response to selection if there is a linear relationship of phenotype on fitness, and if there is additive genetic variance for the phenotype. As one example of a fitness gradient, in
 3078 Figure 5.9 the lifetime reproductive success (LRS) of male Red Deer is plotted against the weight of their antlers. The red line gives the linear regression of fitness (LRS) on antler mass and the slope of this
 3080 line is the fitness gradient (β).

3082 *Fitness landscapes* When we talk about evolution we often talk of a population exploring an adaptive landscape with natural selection
 3084 pushing a population towards higher fitness states corresponding to peaks in this landscape (see e.g. Figure ??). LANDE (1976) found
 3086 an evocative formulation of the Breeder's equation which aids our intuition of phenotypic fitness landscapes. LANDE showed that, if the
 3088 phenotype is normally distributed, the response to selection (R) could be written in terms of the gradient (derivative) of the mean fitness (\bar{w})
 3090 of the population as a function of the mean phenotype:

$$R = \frac{V_A}{\bar{w}} \frac{\partial \bar{w}}{\partial \bar{x}} \quad (5.18)$$

What does this mean? Well V_A/\bar{w} is always positive, so the direction
 3092 our population responds to selection is predicted by the sign of the

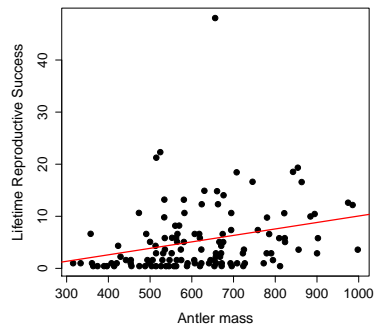


Figure 5.9: Lifetime reproductive success (LRS) of male Red Deer as a function of their antler mass. Data from KRUUK *et al.* (2002), see the paper for discussion of the complexities of equating this selection gradient with the evolutionary response. Code here..

This follows from the fact that we can then move the derivative inside the integral of \bar{w}

$$\begin{aligned} \frac{1}{\bar{w}} \frac{\partial \bar{w}}{\partial \bar{x}} &= \frac{1}{\bar{w}} \int_{-\infty}^{\infty} w(x) \frac{\partial p(x)}{\partial \bar{x}} dx \\ &= \int_{-\infty}^{\infty} \frac{w(x)}{\bar{w}} \frac{(x - \bar{x})}{V} dx \\ &= \frac{\text{cov}(w(x), x)}{\text{var}(x)} \end{aligned} \quad (5.17)$$

which is β . The middle line holds when $p(x)$ is the normal distribution.

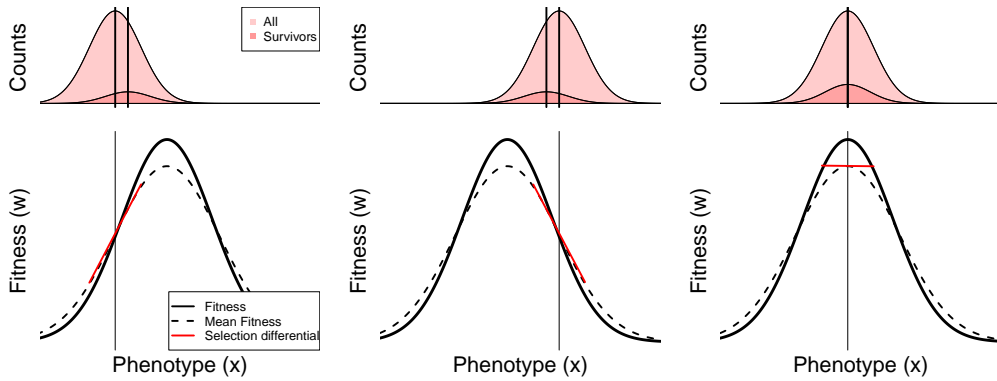
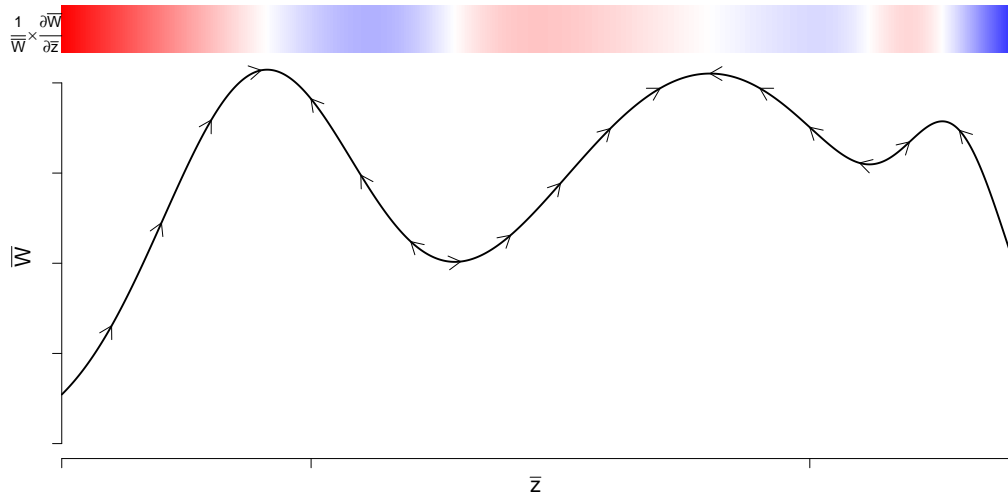


Figure 5.10: A population evolving on a (gaussian) fitness surface. The bottom panel shows the expected individual fitness ($w()$) and mean fitness as a function of phenotype. The red line shows the best fitting linear approximation to the relationship between phenotype and fitness, eqn (??), whose slope is β . The top panel shows the distribution of the phenotype before and after selection.
CAVEATS
Code here..

derivative. If increasing the mean phenotype of the population slightly would increase mean fitness ($\partial \bar{w} / \partial \bar{x} > 0$) our population will respond that generation by evolving toward higher values of the trait ($R > 0$), left panel of Figure 5.10. Conversely if decreasing the population mean phenotype slightly would increase the mean fitness ($\partial \bar{w} / \partial \bar{x} < 0$) the population will that generation evolve towards lower values of the phenotype, middle panel of Figure 5.10. Thus we can think of the population as evolving on an adaptive landscape where the elevation is given by the population mean fitness. Natural selection operates on the basis of individual-level fitness, but as a result of this our population is increasing in its average fitness, it is becoming more adapted.



What happens when it reaches the top? Well at the top of a peak $\partial \bar{w} / \partial \bar{x} = 0$, as it is a local maximum, and so $R = 0$. Assuming that the relationship between fitness and phenotype stays constant, our population will stay at the top of the fitness peak. This view of natural

selection does not imply that the population is evolving to the best possible state. Our population is just marching up the hill of mean fitness end panel Figure 5.10. However, this peak isn't necessarily the highest fitness peak it's just which ever peak was closest and so our population can become trapped on a local, but not global peak of fitness (see, for example Figure ??).

One nice example documenting adaptive evolution to a new fitness optimum is offered by a remarkable time-series of stickleback evolution from a fossil lake-bed in Nevada (BELL *et al.*, 2006). In this lake the layers of sediment are laid down each year allowing a very detailed time series with over five thousand fossils measured. The time-series documents the evolution towards a new set of optimum phenotypes in the fifteen thousand years after the initial invasion of the lake by a heavily armoured stickleback species. In Figure ?? the population mean number of touching pterygiophores, the bones supporting the dorsal spines, through the fossil record. Note how quickly the species evolves toward its new value, presumably a fitness optimum in their new environment, and the long time subsequent time interval over which the population mean phenotype fluctuates about its new value.

HUNT *et al.* (2008) fitted a model of a population adapting to a fitness landscape, with a single peak, to these time-series data. Their fitted fitness surface is shown in the lower panel of Figure 5.12 . The arrows show the moves that the population mean phenotype is making on this inferred fitness surface. The population initially takes large steps up toward the peak of this surface and subsequently fluctuates around the peak. Under the interpretation that there is a single stationary peak these fluctuations represent genetic drift randomly knocking the population off its optimum, with selection acting to restore the population towards this local optimum.

peaks in the fitness landscape

Stabilizing and Disruptive selection Up to now we have just looked at directional selection, where selection acts to change the mean phenotype. However, we can also use quantitative genetic models to describe other modes of selection, extending from effects on the population mean the next natural step is to think about selection which acts on the population variance. Selection might act against more strongly against individuals in the tails of the distribution, with those closer to the mean phenotype having higher fitness, which lowers the variance. Selection could also disfavour individuals close to the population mean, with individuals with extreme phenotypes having higher fitness, which acts to increase the fitness.

Directional selection occurs because of the covariance between our phenotype and fitness, eqn (5.11). Just as we expressing directional

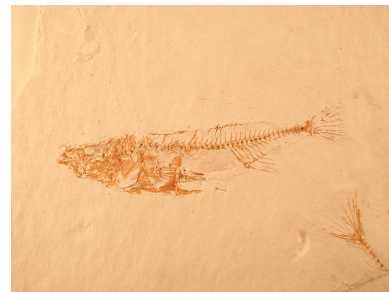


Figure 5.11: Fossil stickleback. Photo by Peter J. Park from LOSOS *et al.* (2013), licensed under CC BY 4.0.

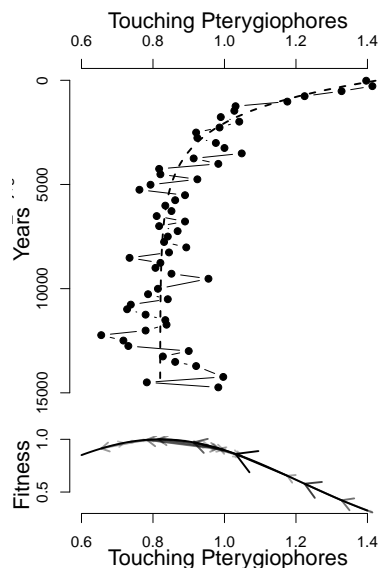


Figure 5.12: **Top)** A time series of stickleback phenotypic evolution from the fossil record. After a heavily armoured stickleback invades the lake it quickly evolves towards touching pterygiophores (the bones supporting the dorsal spines). Fossil measurements means are calculated in 250 year bins. **Bottom)** How our population moves on the Inferred fitness landscape. The arrows show each move made by the population in the 250 intervals. Data from BELL *et al.* (2006) and HUNT *et al.* (2008) Code here.

selection as a covariance allowed us to characterize directional selection as the linear relationship between fitness and phenotype, β , we can summarize the variance reducing selection by including a quadratic term in the regression of fitness on phenotype

$$w_i \sim \beta x_i + 1/2\gamma x_i^2 + \bar{w} \quad (5.19)$$

This γ , the coefficient of the quadratic term in our model, is the quadratic selection gradient: the covariance of fitness and the squared deviation from the phenotypic mean (μ_{BS}), i.e.

$$\gamma = \frac{\text{Cov}(w(X), (X - \mu_{BS})^2)}{V^2} \quad (5.20)$$

Our γ describes the curvature of the fitness surface around the mean.

Values of $\gamma < 0$ are consistent with stabilizing selection, reducing the variance. While values of $\gamma > 0$ are consistent with disruptive selection, increasing the variance.

Under stabilizing selection the individuals with extreme phenotypes in either tail have lower fitness, the result of which is to reduce the phenotypic variance within a generation. A classic case of stabilizing selection is birth weight in humans (KARN and PENROSE, 1951). Mary KARN collected data for nearly fourteen thousand pregnancies from 1935-46 for birth weight and mortality. These data are replotted in Figure 5.13. The variance of all births is 1.575lb^2 , while in live births this was reduced to 1.26lb^2 , a 20% reduction in variance due to stabilizing selection. It is worth noting, that this selection pressure has been greatly reduced over the decades in societies with access to good prenatal care (ULIZZI and TERRENATO, 1992).

In Central Africa, Black-bellied seedcrackers (*P. ostrinus*) show remarkable size polymorphism in their beaks (Figure 5.15). The small-beaked individuals feed on soft seeds from one species of marsh sedge while the big-beaked individuals feed on hard seeds from another sedge, which requires ten times the force to crack. SMITH (1993) recorded the fates of hundreds of juveniles, and found that individuals with intermediate beak sizes survived at much lower rates, Figure 5.15, because they were not well adapted to either seed resource. Break length is subject to disruptive selection, as can also be seen by the significant negative quadratic term in the regression of survival probability on break length. The variance of mandible in the total sample of individuals was 0.5mm^2 in the survivors this variance increased by a factor of almost $\times 2.5$ to 1.3mm^2 .

To illustrate how directional selection and quadratic terms play off during adaptation, lets consider the goldenrod gall fly (*Eurosta solidaginis*), aka the goldenrod ball gallmaker. See Figure 5.17. As it's wonderful name implies this insect lays its eggs in Goldenrod plants,

Just like how β could be interpreted as the mean gradient of the fitness surface, our γ is the mean curvature of the fitness surface

$$\gamma = \mathbb{E} [\partial^2 w(x)/\partial x^2] = \int \partial^2 w(x)/\partial x^2 p(x) dx \quad (5.21)$$

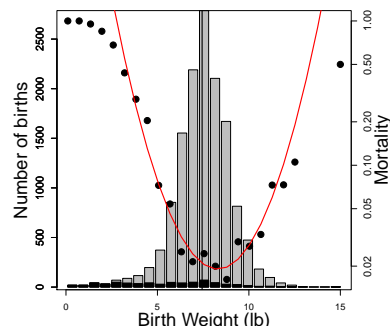


Figure 5.13: Bars show the total number of births with different birth weights (left axis) Dots show the mortality probability for different birth-weight bins (right axis). Data from KARN and PENROSE (1951) Table 2, collapsing male and female births, Code here.



Figure 5.14: Lesser seedcracker *Pyrenestes minor* a close relative of the Black-bellied seedcracker, whose beak is about the same size as the smallest Black-bellied individuals.

The birds of Africa, comprising all the species which occur in the Ethiopian region. (1986) Sclater, W. L Plate by H. Grönvold Image from the Biodiversity Heritage Library. Contributed by Smithsonian Libraries. Not in copyright.

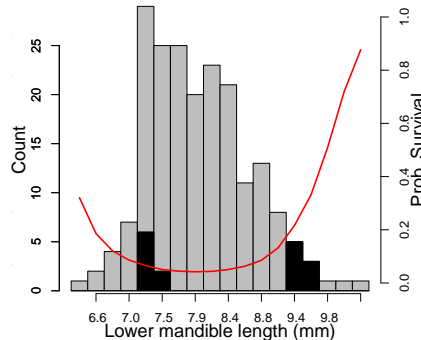
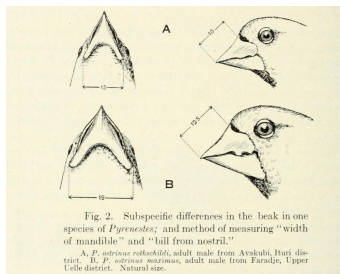


Figure 5.15: **Left** An illustration of the remarkable variation in beak size within Black-bellied seedcrackers (*P. ostrinus*). **Right** A histogram of a beak size measurement in Black-bellied seedcrackers, all juveniles are shown in white the black bars show the survivors. The red curve shows the best fitting linear and quadratic model to the probability of survival, fitted using a binomial generalized linear models with a logit link function.

Left illustration from: Size variation in *Pyrenestes* by Chapin J.P. in the Bulletin of the American Museum of Natural History (Vol. XLIX 1923) Image from the Biodiversity Heritage Library. Contributed by Toronto Library. Not in copyright.

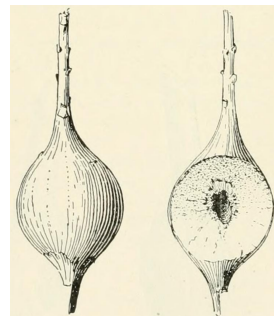


Figure 5.16: The gall formed by the goldenrod ball gallmaker (*Eurosta solidaginis*) in a goldenrod plant. The one on the right is cut to show a partial cross-section.

Annual report of the New York State Museum (1917) Image from the Biodiversity Heritage Library. Contributed by The LuEsther T Mertz Library, the New York Botanical Garden. Not in copyright.

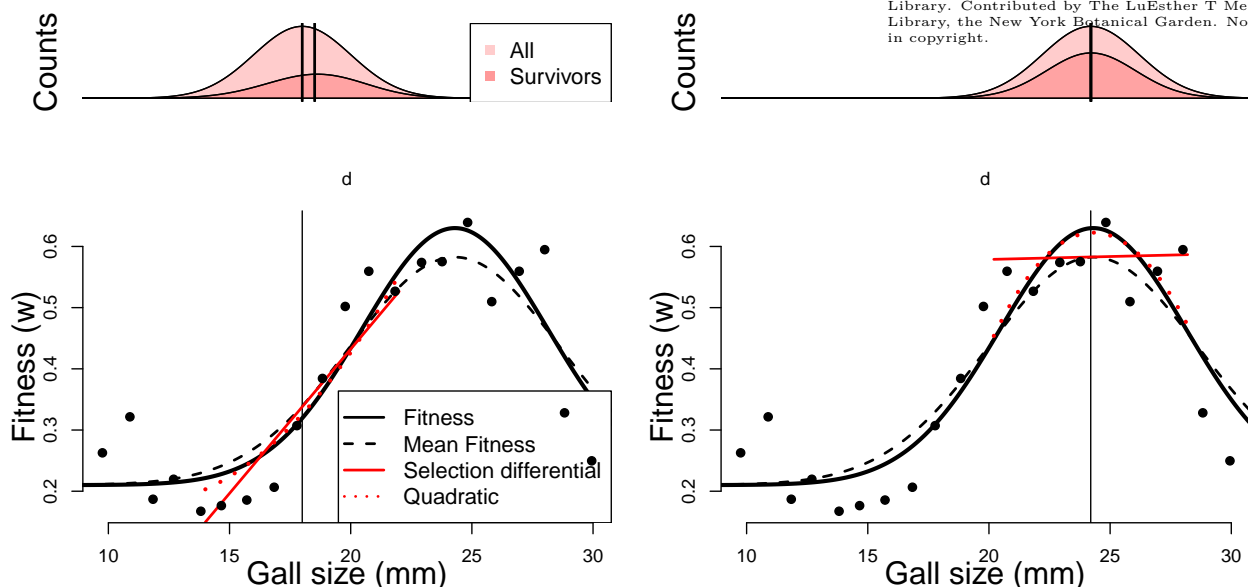


Figure 5.17: Fitness surface for gall diameter in goldenrod ball gall-makers. The dots are the measured survival probabilities of different sized galls. The solid line is a fitted individual fitness surface ($w()$). Dotted line is \bar{w} plotted as a function of the population mean assuming a normal distribution with a standard deviation of 2mm. Data from WEIS and GORMAN (1990), Code here.

5.0.1 The response of multiple traits to selection, the multivariate breeder's equation.

We can generalize these results for multiple traits, to ask how selection on multiple phenotypes plays out over short time intervals.³ Considering two traits we can write our responses in both traits as

$$\begin{aligned} R_1 &= V_{A,1}\beta_1 + V_{A,1,2}\beta_2 \\ R_2 &= V_{A,2}\beta_2 + V_{A,1,2}\beta_1 \end{aligned} \quad (5.22)$$

³ LANDE, R., 1979 Quantitative genetic analysis of multivariate evolution, applied to brain: body size allometry. Evolution 33(1Part2): 402–416

where the 1 and 2 index our two different traits. Here $V_{A,1,2}$ is our additive covariance between our traits. Our selection gradient for trait 1, β_1 , represents the change in fitness changing trait 1 alone holding everything else constant. This is a statement that our response in any one phenotype is modified by selection on other traits that covary with that trait. This offers a good way to think about how genetic trade offs play out over short-term evolution.

We can also write this in matrix form. We can write our change in the mean of our multiple phenotypes within a generation as the vector \mathbf{S} and our response across multiple generations as the vector \mathbf{R} . These two quantities are related by

$$\mathbf{R} = \mathbf{GV}^{-1}\mathbf{S} = \mathbf{G}\boldsymbol{\beta} \quad (5.23)$$

where \mathbf{V} and \mathbf{G} are our matrices of the variance-covariance of phenotypes and additive genetic values (eqn. (4.19) (4.18)) and $\boldsymbol{\beta}$ is a vector of selection gradients (i.e. the change within a generation as a fraction of the total phenotypic variance).

Question 3. You collect observations of red deer within a generation, recording an individual's number of offspring and phenotypes for a number of traits which are known to have additive genetic variation. Using your data, you construct the plots shown in Figure 5.18 (standardizing the phenotypes). Answer the following questions by choosing one of the bold options. Briefly justify each of your answers with reference to the breeder's equation and multi-trait breeder's equation.

A) Looking just at figure 5.18 A, in what direction do you expect male antler size to evolve?

Insufficient information, increase, decrease.

B) Looking just at figures 5.18 B and C, in what direction do you expect male antler size to evolve?

Insufficient information, increase, decrease.

C) Looking at figures 5.18 A, B, and C, in what direction do you expect male antler size to evolve?

Insufficient information, increase, decrease.

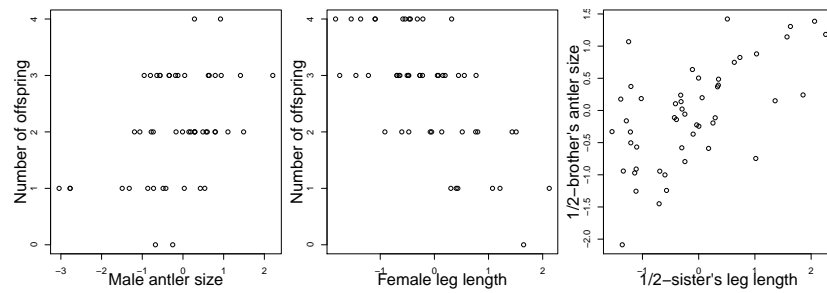


Figure 5.18: Observations of red deer within a generation; recording an individual's number of offspring and phenotypes (simulated data), which are known to have additive genetic variation. The figures left to right are A-C. (Data are simulated. Code here.)

As an example of correlated responses to selection, consider the
3240 WILKINSON (1993) selection experiment on Stalk-eyed flies (*Cyrtodiopsis dalmani*). Stalk-eyed flies have evolved amazingly long
3242 eye-stalks. In the lab, WILKINSON established six populations of
wild-caught flies and selected up and down on males eye-stalk to body
3244 size ratio for 10 generations (left plot in Figure 5.19). Despite the
fact that he did not select on females, he saw a correlated response in
3246 the females from each of the lines (right plot), because of the genetic
correlation between male and female body proportions.

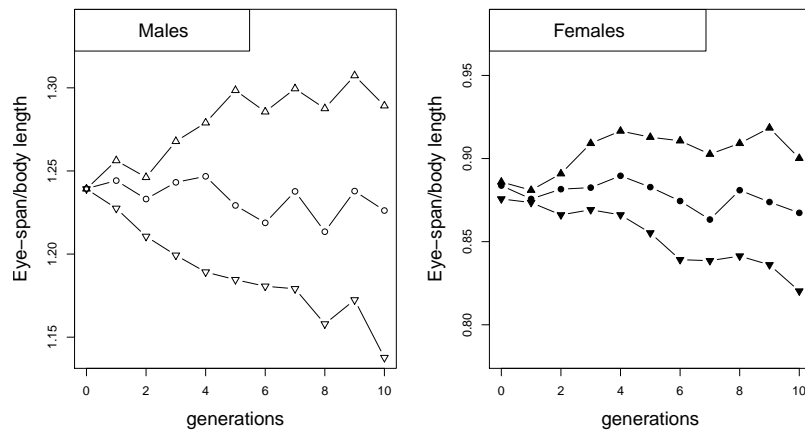


Figure 5.19: WILKINSON selected two of populations for flies for increased and eye-stalk to body length ratio in males (mean shown as up triangles), and two for a decreased ratio (down triangles), by taking the top 10 males with the highest (lowest) ratio out of 50 measures. He also established two control populations (circles). He constructed each generation of females by sampling 10 at random from each population. Data from WILKINSON (1993). Code here.

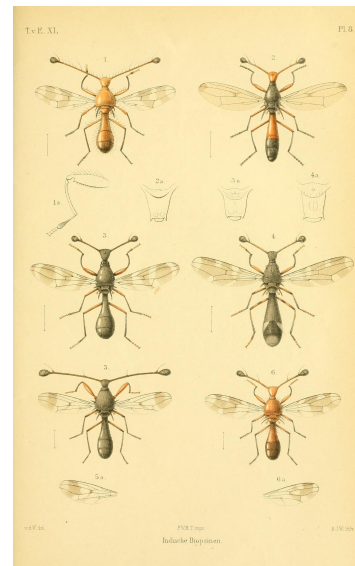


Figure 5.20: Stalk-eyed Flies (*Diopsidae*).

Diptera. van der Wulp. 1898. Image from the Biodiversity Heritage Library. Contributed by Smithsonian Libraries. Not in copyright.

3256 length ratio?

3258 **B)** Assume that the additive genetic variance of male and female phenotypes are equal and that there is no direct selection on female body-proportion in this experiment, i.e. that all of the response in 3260 females is due to correlated selection. Can you estimate the male-female genetic correlation of the eye-stalk ratio?

3262 *Estimating multivariate selection gradients* We can estimate multivariate directional (β) and quadratic selection gradients (γ) just as we 3264 did for a single traits (x_1 and x_2), using linear models. For example, for two traits we can write

$$w_i \sim \beta_1 x_{1,i} + 1/2\gamma_1 x_{1,i}^2 + \beta_2 x_{2,i} + 1/2\gamma_2 x_{2,i}^2 + \gamma_{1,2}x_{1,i}x_{2,i} + \bar{w} \quad (5.24)$$

3266 where β_1 and γ_1 are the directional and quadratic selection gradients for trait one, and similarly for trait two. The covariance selection 3268 gradient between between traits is given by $\gamma_{1,2}$.

3270 BRODIE III (1992)'s work provides a nice example of selection 3272 on multiple predation-avoidance traits in northwestern garter snakes (*Thamnophis ordinoides*). BRODIE III released hundreds on snakes born in the lab into the wild, and then performed mark-recapture 3274 observations to monitor their fate.

3276 Before releasing them he measured how stripey they were, and their behavioural tendency to reversals of direction during simulated flight 3278 from a predator flight. His quadratic fitness surface is shown in Figure 5.22, based on fitting the regression given by eqn (5.24) to juvenile survival. He found that neither single trait directional or quadratic 3280 gradients were significant, ie there was no apparent selection on one trait ignoring the other. However, there was a significant, negative covariance. The individuals with the highest chance of survival are 3282 either highly striped and perform few reversals (top left corner), or have little striping but reverse course frequently (bottom right corner).

3284 5.1 Some applications of the multivariate trait breeder's equation

3286 The multivariate breeders equation has a lot of different uses in understanding the response of multiple traits to selection. It also offers some 3288 insights into kin selection and sexual selection. We'll discuss these next.

3290 *Hamilton's Rule and the evolution of altruistic and selfish behaviours*
Individuals frequently behave in ways that sacrifice their own fitness 3292 for the benefit of others. That selection favours such apparent acts of

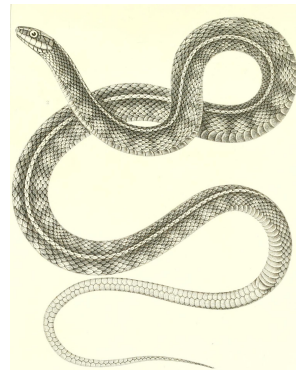


Figure 5.21: Northwestern garter snake (*Eutaenia cooperi*, now *Thamnophis ordinoides*)
The natural history of Washington territory, with much relating to Minnesota, Nebraska, Kansas, Oregon, and California (1859). Cooper J.G. and Suckley, G. Image from the Biodiversity Heritage Library. Contributed by Smithsonian Libraries. Not in copyright.

MAYNARD SMITH (1964) coined the name kin selection to describe Hamilton's approach to this problem. It's also sometimes called the inclusive fitness approach, as we need to include not just one individual's fitness but the weighted sum of all the fitness of all their relatives.

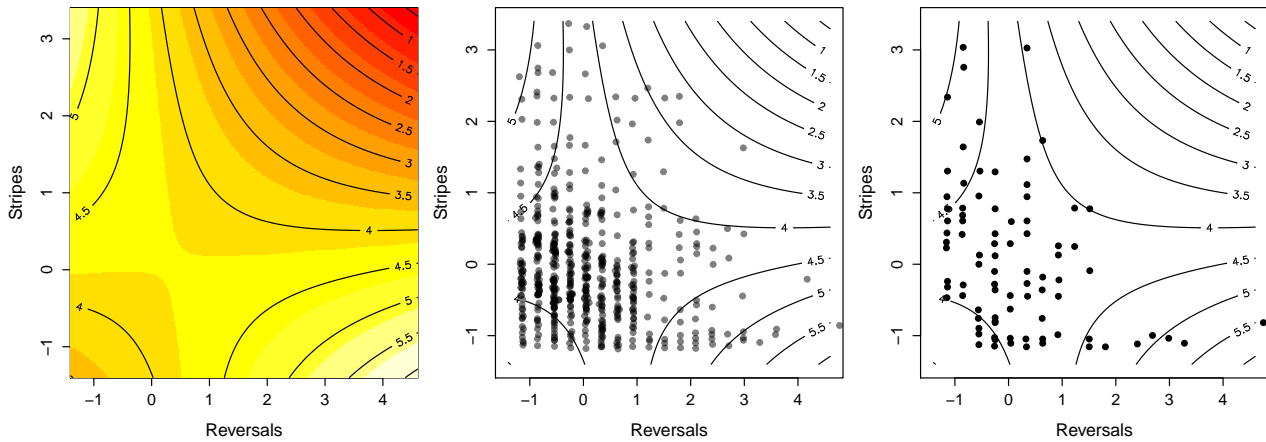


Figure 5.22:

altruism is puzzling at first sight. HAMILTON (1964a,b) supplied the
 3294 first general evolutionary explanation of such altruism. His intuition
 was that while an individual is losing out of some reproductive output,
 3296 the alleles underlying an altruistic behaviour can still spread in the
 population if this cost is outweighed by benefits gained through the
 3298 transmission of these alleles through a related individual. Note that
 this means that the allele is not acting in an self-sacrificing manner,
 3300 even though individuals may as a result.

Altruism reflects social interactions. So as a simple model let's
 3302 imagine that individuals interact in pairs, with our focal individual
 i being paired with an individual j . This could be pairs of siblings
 3304 interacting. Imagine that individuals have two possible phenotypes
 $X = 1$ or 0 , corresponding to providing or withholding some small
 3306 act of 'altruism' (we could just as easily flip these labels and call them
 an unselfish act and a selfish act respectively). Our pairs of individ-
 3308 uals interacting could, for example, be siblings sharing a nest. The
 altruistic trait could be as simple as growing at a slightly slower rate
 3310 so as to reducing sibling-competition for food from parents, or more
 complicated acts of altruism such as children foregoing their own re-
 3312 production so as to help their parents raise their siblings.

Providing the altruistic act has a cost C to the fitness of our in-
 3314 dividual and failing to provide this act has no cost. Receiving this
 altruistic act confers a fitness benefit B over individuals who did not
 3316 receive this act. HAMILTON's rule states that such a trait will spread
 through the population if

$$2FB > C \quad (5.25)$$

3318 where F is the average kinship coefficient between the interacting
 individuals (i and j). In the usual formulation of Hamilton's Rule
 3320 our $2F$ is replaced by the 'Coefficient of relationship', which is the

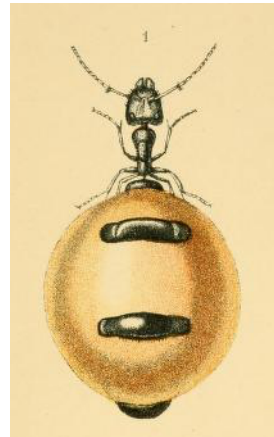


Figure 5.23: Australian Honey-pot Ant (*Camponotus inflatus*). Honey ants are gorged with honeydew collected by their nest mates, till they swell to the size of grapes, and used as a food storage device.
 Ants, bees, and wasps: a record of observations on the habits of the social Hymenoptera (1897) Lubbock, J. Image from the Biodiversity Heritage Library. Contributed by Smithsonian Libraries. Not in copyright.

proportion of alleles shared between the individuals. Here we use two times the kinship coefficient to keep things inline with our notation for these chapters. Note that if our individuals are themselves inbred we need to do a little more careful to reconcile these two measures. So the altruistic behaviour will spread even if it is costly to the individual if its cost is paid off by the benefit to sufficiently related individuals.

As one example of kin-selection consider KRAKAUER (2005)'s work on co-operative courtship in wild turkeys (*Meleagris gallopavo*). Male turkeys often form display partnerships, with a subordinate male helping a dominant male with displaying to females and defending the females from other groups of males.

These pairs are often full brothers ($F = 0.25$), with the subordinate male often being the younger of the two. The subordinate male often loses out on mating opportunities over their entire lifetime by acting as a wingman to their older brothers. KRAKAUER (2005) estimated that dominant males gained an extra 6.1 offspring when they display with a partner than males who display alone. While the subordinate males lose out on fathering 0.9 offspring compared to solitary males. Thus the costs of helping by subordinate males is more than compensated by the fitness gains of their brothers ($(2 \times 0.25) \times 6.1 > 0.9$), and so the evolution of this altruistic helping in co-operative courtship is potentially well explained by kin-selection (see AKÇAY and VAN CLEVE, 2016, for more analysis).

Question 5. How would this answer be changed if the male Turkey partnerships were only $1/2$ sibs, or first cousins?

Where does this result come from? Well, we can use our quantitative genetics framework to gain some intuition by deriving a simple version of Hamilton's Rule by thinking about the phenotypes of an individual's kin as genetically correlated phenotypes. To sketch a proof of this result, let's assume that our focal i individual's fitness can be written as

$$W(i, j) = W_0 + W_i + W_j \quad (5.26)$$

where W_i is the contribution of the fitness of the individual i due to their own phenotype, and W_j is the contribution to our individual i 's fitness due to the interacting individual j 's behaviour (i.e. j 's phenotype). With the benefit B and cost C , our $W(i, j)$ are depicted in Figure 5.25.

Following our multivariate breeder's equation, we can write the expected change of our behavioural phenotype as

$$R = \beta_i V_A + \beta_j V_{A,i,j}, \quad (5.27)$$

Our altruistic phenotype is increasing in the population if $R > 0$, i.e. if



Figure 5.24: Turkey (*Meleagris gallopavo*).

Bilder-atlas zur Wissenschaftlich-populären Naturgeschichte der Vögel in ihren sämtlichen Hauptformen (1864). Wien, K.K. Hof Image from the Biodiversity Heritage Library. Contributed by Smithsonian Libraries. Not in copyright.

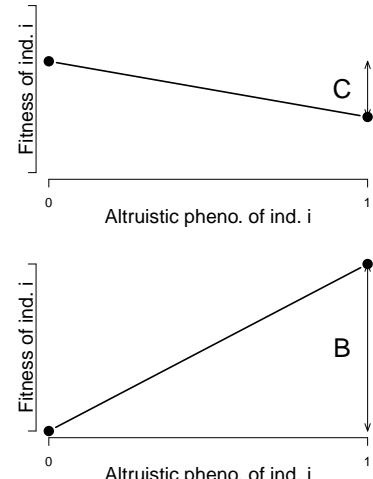


Figure 5.25: **Top)** The fitness of individual i as a function of their behavioural phenotype, where altruistic/non-altruistic behavioural phenotypes are encoded as 1 and 0 respectively. The direct fitness cost of behaving altruistically is C . **Bottom)** The fitness of our focal individual i as a function of the behavioural phenotype of their interacting partner (j). Our focal individual gets an increase B in fitness if their partner behaves altruistically. Code here.

3360

$$\beta_i V_A + \beta_j V_{A,i,j} > 0 \quad (5.28)$$

The slope β_i of the regression of our focal individual's behavioural phenotype on fitness is proportional to $-C$. The slope β_j of the regression of our interacting partner's phenotype on our focal individual's fitness is proportional to B (with the same constant of proportionality). Therefore, our altruistic phenotype is increasing in the population if

$$\begin{aligned} \beta_i V_A + \beta_j V_{A,i,j} &> 0 \\ B \frac{V_{A,i,j}}{V_A} &> C \end{aligned} \quad (5.29)$$

Here we're following a simplified version of QUELLER (1992)'s treatment, to re-derive Hamilton's rule in a quantitative genetics framework (Hamilton's original papers did this in a population genetics framework).

So what's the average genetic covariance between individual i and j 's altruistic phenotype? Well it's the same behavioural phenotype in both individuals, so the phenotypes are genetically correlated if our individuals are related to each other. The covariance of the same phenotype between two individuals is just $2F_{i,j}V_A$ (see (4.12)). So our altruistic phenotype is increasing in the population if

$$\begin{aligned} B \frac{2F_{i,j}V_A}{V_A} &> C \\ 2F_{i,j}B &> C \end{aligned} \quad (5.30)$$

Seen from this perspective, HAMILTON's rule is simply a statement that altruistic behaviours can spread via kin-selection, if the average cost to an individual of carrying altruistic alleles is paid back through the average benefit of interacting with altruistic relatives (kin)

Sexual selection and the evolution of mate preference by indirect benefits. Organisms often put an enormous effort into finding and attracting mates, sometimes at a considerable cost to their chances of survival. Why are individuals so choosy about who they mate with, particularly when their choice seems to be based on elaborate characters and arbitrary displays that surely lower the viability of their mates?

One major reason why individuals evolve to be choosy about who they mate with is that it can directly impact their fitness. By choosing a mate with particular characteristics, individuals can gain more parental care for their offspring, avoid parasites, or be choosing a mate with higher fertility. For example, female glow-worms flash at night to attract males flying by. Females with larger, brighter lanterns have higher fecundity, so males with a preference for brighter flashes will gain a direct benefit to their own fitness. (Note that males will benefit even if these differences in female fecundity are entirely driven by differences in environment, and so non-heritable.) Indeed male glow worms have evolved to be attracted to brighter flashing lures.

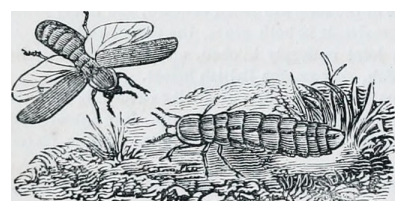


Figure 5.26: Male (left) and female (right) common glow worm (*Lampyris noctiluca*).

The animal kingdom : arranged after its organization; forming a natural history of animals, and an introduction to comparative anatomy. (1863) Cuvier, G. Image from the Biodiversity Heritage Library. Contributed by University of Toronto - Gerstein Science Information Centre. Not in copyright.

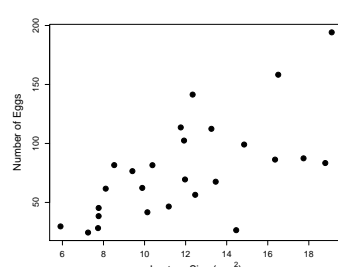


Figure 5.27: Female Glow worms who have the largest, and therefore brightest, lanterns have the highest fecundity. Data from HOPKINS *et al.* (2015). Code here.

However, even in the absence of direct benefits of choice, selection
 3396 can still indirectly favour the evolution of choosiness. These indirect
 benefits occur because individuals can have higher fitness offspring
 3398 by choosing a mate whose phenotype indicates high viability (the so-
 called good genes hypothesis), or by choosing a mate whose phenotype
 3400 is simply attractive, and likely to produce similarly attractive offspring
 (the ‘runaway’ or sexy sons hypothesis).

3402 We'll denote a display trait, e.g. tail length, in males by σ and
 a preference trait in females by φ . Our display trait is under direct
 3404 selection in males, such that its response to selection can be written as

$$R_\sigma = \beta_\sigma V_{A,\sigma} \quad (5.31)$$

3406 Let's assume that the female preference trait, the degree to which
 females are attracted to long tails, is not under direct selection $\beta_\varphi = 0$.
 3408 Then the response to selection of the preference trait can be written as

$$R_\varphi = \beta_\varphi V_{A,\varphi} + \beta_\sigma V_{A,\varphi\sigma} = \beta_\sigma V_{A,\varphi\sigma} \quad (5.32)$$

So the female preference will respond to selection if it is genetically
 3410 correlated with the male trait, i.e. if $V_{A,\varphi\sigma}$ is not zero. There's a
 number of different ways this genetic correlation could arise; the sim-
 3412 plest is that the loci underlying the male trait may have a pleiotropic
 effect on female preference. However, female preference may often
 have quite a distinct genetic basis from male display traits.

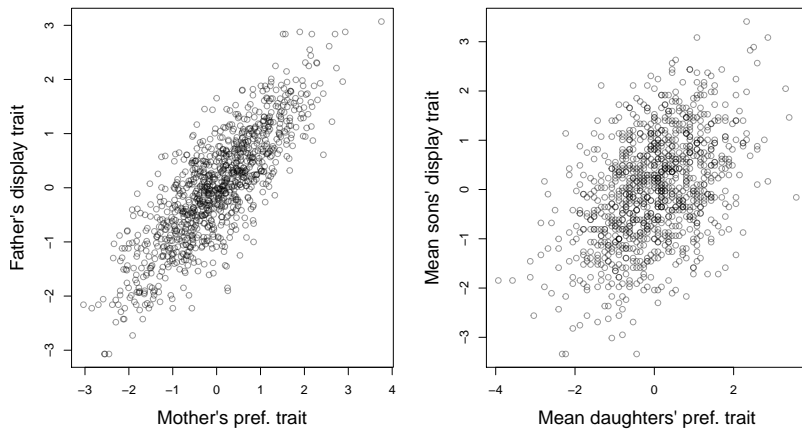


Figure 5.28: **Left)** Assortative mating between males and females. Males vary in a display trait (e.g. tail length), females vary in their preference for this trait. We see evidence of assortative mating as females with a preference for a particular value of the male trait tend to mate with those males. **Right)** As both male trait and female preference are genetic this establishes a genetic correlation in the next generation. This is simulated data. Code here.

3414 A more general way in which trait-preference genetic correlations
 3416 may arise is through assortative mating. As females vary in their tail-
 length preference, the ones with a preference for longer tails will mate
 3418 with long-tailed males and the opposite for females with a preference

for shorter-tails. Therefore, a genetic correlation between mates display and preference traits will become established (see Figure 5.28).
 3420

The males with the longer tails will also carry the alleles associated
 3422 with the preference for longer tails, as their long-tailed dads tended
 to mate with females with a genetic preference for long tails. Simi-
 3424 larly, the the males with shorter tails will carry alleles associated with
 the preference for shorter tails. Thus if there is direct selection for
 3426 males with longer tails, then the female preference for longer tails will
 increase too, as it is genetically correlated via assortative mating.

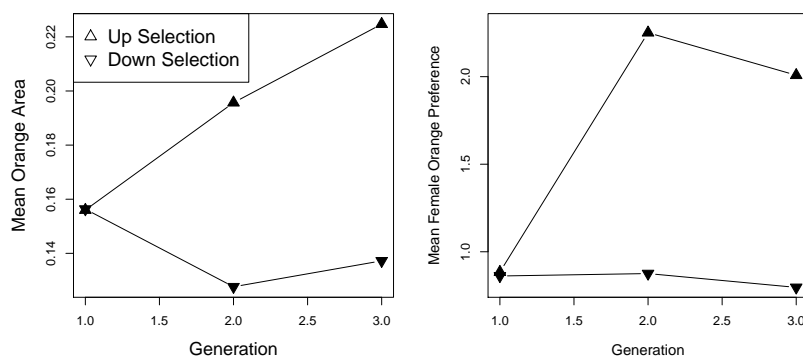


Figure 5.29: Mean phenotypes for the two up- and two down-selected populations of Guppies. Left panel: A response to selection was seen due to the direct selection on male colouration. Right panel: An indirect, correlated response was also seen in female preference. Data from HOUDE (1994). Code here.

3428 As an example of how direct selection on display traits can drive
 the evolution of preference traits, let's consider some data from gup-
 3430 pies. Guppies (*Poecilia reticulata*) are a classic system for studying
 the interplay of natural and sexual selection. In some populations
 3432 of guppies, females show a preference for males with more orange
 colouration.

3434 HOODE established four replicate population pairs of guppies and
 selected one of each pair for an increased or decreased orange col-
 3436 ouration in males, selecting the top/bottom 20 out of 50 males. She
 randomly chose females from each population to form the next gener-
 3438 ation, and so did not exert direct selection on females. She measured
 the response to selection on male colouration and on female prefer-
 3440 ence for orange (left and right panels of Figure 5.1 respectively). In
 the lines that were selected for more orange males females showed an
 3442 increased preference for orange. While in those lines that she selected
 males for less orange in their display females showed a decreased pref-
 3444 erence for orange. This is consistent with indirect selection on female
 orange preference as a response to selection on male trait. It is
 3446 *a priori* unlikely that pleiotropy is the source of the genetic correlation
 between these traits, rather it is likely caused by females assortative



Figure 5.30: Guppy (*Poecilia reticulata*).

From a set of 1962 stamps of Hungary.
 Contributed to wikimedia by Darjac, not
 covered by copyright

mating with males that match their colour preference.

3450 Returning to our bird tail example, what could drive the direct selection on male tail length? The selection for longer tails in males
3452 could come about because longer tails are genetic correlated with higher male viability, for example perhaps only males who gather an
3454 excess of food have the resources to invest in growing long tail, i.e. a long tail is an honest signal. This would be a good genes explanation
3456 of female mate choice evolution.

3458 There's another subtler way that selection could favour our male trait. Imagine that the variation in female preference trait is because some females have no strong preference for the male-tail length, but
3460 some females have a strong preference for males with longer tails.

3462 Males with longer tails would then have higher fecundity than the short-tailed males as there's a subset of females who are strongly attracted to long tails, and these males also get to mate with the other
3464 females. Thus selection favours long-tailed males, and so indirectly favours female preference for longer tails; females with a preference
3466 for longer-tails have sons who in turn who are more attractive. This model is sometimes called the sexy-son model. It is also called the
3468 Fisherian runaway model (FISHER, 1915), as female preference and male trait can coevolve in an escalating fashion driving more and more
3470 extreme preferences for arbitrary traits. Thus many extravagant display traits in males and females may exist purely because individuals
3472 find them beautiful and are attracted to them.

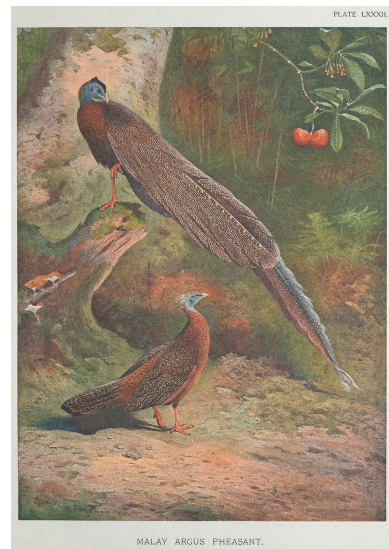


Figure 5.31: Argus Pheasant.
A monograph of the pheasants. (1918). Beebe, W. Image from the Biodiversity Heritage Library. Contributed by Smithsonian Institution Libraries. Licensed under CC BY-2.0.

“The case of the male Argus Pheasant is eminently interesting, because it affords good evidence that the most refined beauty may serve as a sexual charm, and for no other purpose.” – DARWIN (1888)

6

One-Locus Models of Selection

3476 "Socrates consisted of the genes his parents gave him, the experiences
they and his environment later provided, and a growth and development mediated by numerous meals. For all I know, he may have been
3478 very successful in the evolutionary sense of leaving numerous offspring.
His phenotype, nevertheless, was utterly destroyed by the hemlock
3480 and has never since been duplicated. The same argument holds also
for genotypes. With Socrates' death, not only did his phenotype dis-
3482 appear, but also his genotype.[...] The loss of Socrates' genotype is
not assuaged by any consideration of how prolifically he may have
3484 reproduced. Socrates' genes may be with us yet, but not his genotype,
because meiosis and recombination destroy genotypes as surely as
3486 death." —WILLIAMS (1966)

3488 Individuals are temporary, their phenotypes are temporary, and
their genotypes are temporary. However, the alleles that individuals
transmit across generations have permanence. Sustained phenotypic
3490 evolutionary change due to natural selection occurs because of changes
in the allelic composition of the population. To understand these
3492 changes, we need to understand how the frequency of alleles (genes)
changes over time due to natural selection.

3494 As we have seen, natural selection occurs when there are differences
between individuals in fitness. We may define fitness in various ways.
3496 Most commonly, it is defined with respect to the contribution of a
phenotype or genotype to the next generation. Differences in fitness
3498 can arise at any point during the life cycle. For instance, different
genotypes or phenotypes may have different survival probabilities from
3500 one stage in their life to the stage of reproduction (viability), or they
may differ in the number of offspring produced (fertility), or both.
3502 Here, we define the absolute fitness of a genotype as the expected
number of offspring of an individual of that genotype. Differences in
3504 fitness among genotypes drive allele frequency change. In this chapter
we'll study the dynamics of alleles at a single locus. In this chapter
3506 we'll ignore the effects of genetic drift, and just study the deterministic
dynamics of selection. We'll return to discuss the interaction of

3508 selection and drift in the next chapter.

6.0.1 Haploid selection model

3510 We start out by modeling selection in a haploid model, as this is
 3512 mathematically relatively simple. Let the number of individuals carry-
 3514 ing alleles A_1 and A_2 in generation t be P_t and Q_t . Then, the relative
 3516 frequencies at time t of alleles A_1 and A_2 are $p_t = P_t/(P_t + Q_t)$ and
 $q_t = Q_t/(P_t + Q_t) = 1 - p_t$. Further, assume that individuals of
 type A_1 and A_2 on average produce W_1 and W_2 offspring individuals,
 respectively. We call W_i the absolute fitness.

3518 Therefore, in the next generation, the absolute number of carriers
 3520 of A_1 and A_2 are $P_{t+1} = W_1 P_t$ and $Q_{t+1} = W_2 Q_t$, respectively. The
 mean absolute fitness of the population at time t is

$$\bar{W}_t = W_1 \frac{P_t}{P_t + Q_t} + W_2 \frac{Q_t}{P_t + Q_t} = W_1 p_t + W_2 q_t, \quad (6.1)$$

3520 i.e. the sum of the fitness of the two types weighted by their relative
 3522 frequencies. Note that the mean fitness depends on time, as it is a
 function of the allele frequencies, which are themselves time depen-
 dent.

3524 As an example of a rapid response to selection on an allele in a
 3526 haploid population, we can consider some data on the evolution of
 3528 drug resistant viruses. FEDER *et al.* (2017) studied viral dynamics
 in a macaque infected with a strain of simian immunodeficiency virus
 (SHIV) that carries the HIV-1 reverse transcriptase coding region.
 The viral load of the macaque's blood plasma is shown as a black line
 3530 in Figure 6.1. Twelve weeks after infection, the macaque was treated
 with an anti-retroviral drug that targeted the the virus' reverse tran-
 3532 scriptase protein. Note how the viral load initially starts to drop once
 the drug is administered, suggesting that the absolute fitness of the
 3534 original strain is less than one ($W_2 < 1$) in the presence of the drug (as
 their numbers are decreasing). However, the viral population rebounds
 3536 as a mutation that confers drug resistance to the anti-retroviral drug
 arises in the SHIV and starts to spread. Viruses carrying this mu-
 3538 tation (let's call them allele 1) likely have absolute fitness $W_1 > 1$.
 The frequency of the drug-resistant allele is shown in red; it quickly
 3540 spreads from being undetectable in week 13, to being fixed in the
 SHIV population in week 20.

3542 The rapid spread of this drug-resistant allele through the popula-
 3544 tion is driven by the much greater relative fitness of the drug-resistant
 allele over the original strain in the presence of the anti-retroviral
 drug.

The main focus of FEDER *et al.*'s work was modeling the complicated spatial dynamics of drug-resistant SHIV adaptation in different organ systems.

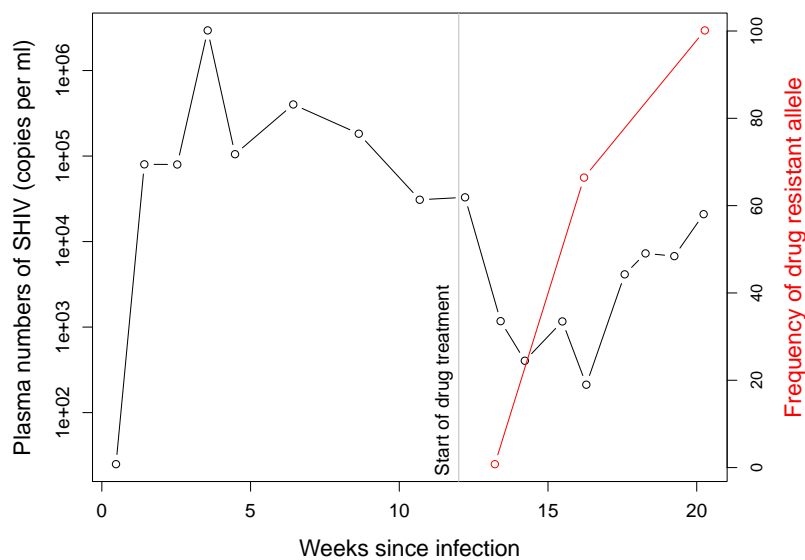


Figure 6.1: The rapid evolution of drug-resistant SHIV. The viral load of SHIV in the blood of a macaque (black line), the frequency of a drug resistance mutation (red line). Data from FEDER *et al.* (2017). Code here.

3546 The frequency of allele A_1 in the next generation is given by

$$p_{t+1} = \frac{P_{t+1}}{P_{t+1} + Q_{t+1}} = \frac{W_1 P_t}{W_1 P_t + W_2 Q_t} = \frac{W_1 p_t}{W_1 p_t + W_2 q_t} = \frac{W_1}{\bar{W}_t} p_t. \quad (6.2)$$

Importantly, eqn. (6.2) tells us that the change in p only depends

3548 on a ratio of fitnesses. Therefore, we need to specify fitness only up to an arbitrary constant. As long as we multiply all fitnesses by the same value, that constant will cancel out and eqn. (6.2) will hold.

3550 Based on this argument, it is very common to scale absolute fitnesses by the absolute fitness of one of the genotypes, e.g. the most or the least fit genotype, to obtain relative fitnesses. Here, we will use w_i for 3552 the relative fitness of genotype i . If we choose to scale by the absolute fitness of genotype A_1 , we obtain the relative fitnesses $w_1 = W_1/W_1 = 1$ and $w_2 = W_2/W_1$.

3554 Without loss of generality, we can therefore rewrite eqn. (6.2) as

$$p_{t+1} = \frac{w_1}{\bar{w}} p_t, \quad (6.3)$$

3556 dropping the subscript t for the dependence of the mean fitness on time in our notation, but remembering it. The change in frequency from one generation to the next is then given by

$$\Delta p_t = p_{t+1} - p_t = \frac{w_1 p_t}{\bar{w}} - p_t = \frac{w_1 p_t - \bar{w} p_t}{\bar{w}} = \frac{w_1 p_t - (w_1 p_t + w_2 q_t) p_t}{\bar{w}} = \frac{w_1 - w_2}{\bar{w}} p_t q_t, \quad (6.4)$$

recalling that $q_t = 1 - p_t$.

3562 Assuming that the fitnesses of the two alleles are constant over time, the number of the two allelic types τ generations after time t are

³⁵⁶⁴ $P_{t+\tau} = (W_1)^\tau P_t$ and $Q_{t+\tau} = (W_2)^\tau Q_t$, respectively. Therefore, the relative frequency of allele A_1 after τ generations past t is

$$p_{t+\tau} = \frac{(W_1)^\tau P_t}{(W_1)^\tau P_t + (W_2)^\tau Q_t} = \frac{(w_1)^\tau P_t}{(w_1)^\tau P_t + (w_2)^\tau Q_t} = \frac{p_t}{p_t + (w_2/w_1)^\tau q_t}, \quad (6.5)$$

³⁵⁶⁶ where the last step includes dividing the whole term by $(w_1)^\tau$ and switching from absolute to relative allele frequencies.

³⁵⁶⁸ Rearranging eqn. (6.5) and setting $t = 0$, we can work out the time τ for the frequency of A_1 to change from p_0 to p_τ . First, we write

$$p_\tau = \frac{p_0}{p_0 + (w_2/w_1)^\tau q_0} \quad (6.6)$$

³⁵⁷⁰ and rearrange this to obtain

$$\frac{p_\tau}{q_\tau} = \frac{p_0}{q_0} \left(\frac{w_1}{w_2} \right)^\tau. \quad (6.7)$$

Solving this for τ yields

$$\tau = \log \left(\frac{p_\tau q_0}{q_\tau p_0} \right) / \log \left(\frac{w_1}{w_2} \right). \quad (6.8)$$

³⁵⁷² In practice, it is often helpful to parametrize the relative fitnesses w_i in a specific way. For example, we may set $w_1 = 1$ and $w_2 = 1 - s$,
³⁵⁷⁴ where s is called the selection coefficient. Using this parametrization,
 s is simply the difference in relative fitnesses between the two alleles.
³⁵⁷⁶ Equation (6.5) becomes

$$p_{t+\tau} = \frac{p_t}{p_t + q_t(1-s)^\tau}, \quad (6.9)$$

as $w_2/w_1 = 1 - s$. Then, if $s \ll 1$, we can approximate $(1 - s)^\tau$ in the denominator by $\exp(-s\tau)$ to obtain

$$p_{t+\tau} \approx \frac{p_t}{p_t + q_t e^{-s\tau}}. \quad (6.10)$$

This equation takes the form of a logistic function. That is because we
³⁵⁸⁰ are looking at the relative frequencies of two ‘populations’ (of alleles
 A_1 and A_2) that are growing (or declining) exponentially, under the
³⁵⁸² constraint that p and q always sum to 1.

Moreover, eqn. (6.7) for the number of generations τ it takes for a
³⁵⁸⁴ certain change in frequency to occur becomes

$$\tau = -\log \left(\frac{p_\tau q_0}{q_\tau p_0} \right) / \log(1 - s). \quad (6.11)$$

Assuming again that $s \ll 1$, this simplifies to

$$\tau \approx \frac{1}{s} \log \left(\frac{p_\tau q_0}{q_\tau p_0} \right). \quad (6.12)$$

3586 One particular case of interest is the time it takes to go from an
 absolute frequency of 1 to near fixation in a population of size N . In
 3588 this case, we have $p_0 = 1/N$, and we may set $p_\tau = 1 - 1/N$, which is
 very close to fixation. Then, plugging these values into eqn. (6.12), we
 3590 obtain

$$\begin{aligned}\tau &= \frac{1}{s} \log \left(\frac{1 - 2/N + 1/N^2}{1/N^2} \right) \\ &\approx \frac{1}{s} (\log(N) + \log(N - 2)) \\ &\approx \frac{2}{s} \log(N)\end{aligned}\tag{6.13}$$

where we make the approximations $N^2 - 2N + 1 \approx N^2 - 2N$ and later
 3592 $N - 2 \approx N$.

Question 1. In our example of the evolution of drug resistance,
 3594 the drug-resistant SHIV virus spread from undetectable frequencies to
 $\sim 65\%$ frequency by 16 weeks post infection. An estimated effective
 3596 population size of SHIV is 1.5×10^5 , and its generation time is ~ 1
 day. Assuming that the mutation arose as a single copy allele very
 3598 shortly the start of drug treatment at 12 weeks, what is the selection
 coefficient favouring the drug resistance allele?

3600 *Haploid model with fluctuating selection* Selection pressures may
 change while a polymorphism persists in the population due to en-
 3602 vironmental changes. We can use our haploid model to consider this
 case where the fitnesses depend on time (DEMPSTER, 1955), and say
 3604 that $w_{1,t}$ and $w_{2,t}$ are the fitnesses of the two types in generation t .
 The frequency of allele A_1 in generation $t + 1$ is

$$p_{t+1} = \frac{w_{1,t}}{\bar{w}_t} p_t,\tag{6.14}$$

3606 which simply follows from eqn. (6.3). The ratio of the frequency of
 allele A_1 to that of allele A_2 in generation $t + 1$ is

$$\frac{p_{t+1}}{q_{t+1}} = \frac{w_{1,t}}{w_{2,t}} \frac{p_t}{q_t}.\tag{6.15}$$

3608 Therefore, if we think of the two alleles starting in generation t at
 frequencies p_t and q_t , then τ generations later,

$$\frac{p_{t+\tau}}{q_{t+\tau}} = \left(\prod_{i=t}^{\tau-1} \frac{w_{1,i}}{w_{2,i}} \right) \frac{p_t}{q_t}.\tag{6.16}$$

3610 The question of which allele is increasing or decreasing in frequency
 comes down to whether $\left(\prod_{i=t}^{\tau-1} w_{1,i}/w_{2,i} \right)$ is > 1 or < 1 . As it is a little

³⁶¹² hard to think about this ratio, we can instead take the τ^{th} root of it
and consider

$$\sqrt[\tau]{\left(\prod_{i=t}^{\tau-1} \frac{w_{1,i}}{w_{2,i}}\right)} = \frac{\sqrt[\tau]{\prod_{i=t}^{\tau-1} w_{1,i}}}{\sqrt[\tau]{\prod_{i=t}^{\tau-1} w_{2,i}}} \quad (6.17)$$

³⁶¹⁴ The term

$$\sqrt[\tau]{\prod_{i=t}^{\tau-1} w_{1,i}} \quad (6.18)$$

is the geometric mean fitness of allele A_1 over the τ generations past
³⁶¹⁶ generation t . Therefore, allele A_1 will only increase in frequency if
it has a higher geometric mean fitness than allele A_2 (at least in our
³⁶¹⁸ simple deterministic model).

Evolution of bet hedging Don't put your eggs in one basket. It makes
³⁶²⁰ a lot of sense to spread your bets. Financial advisors often advise you
to diversify your portfolio, rather than placing all your investments
³⁶²² in one stock. Even if that stock looks very strong, you can come a
cropper that $1/20$ times some particular part of the market crashes.
³⁶²⁴ Likewise, evolution can result in risk averse strategies. Some species
of bird lay multiple eggs of nests; some plants don't put all of their
³⁶²⁶ energy into seeds for next year. It can even make sense to spread your
bets even if that comes at an average cost.

³⁶²⁸ To see this let's think more about geometric fitness. We can write
the fitness in a given generation i as $w_i = 1 + s_i$, such that we can
³⁶³⁰ write your geometric fitness as

$$\bar{g} = \sqrt[\tau]{\prod_{i=t}^{\tau-1} 1 + s_i} \quad (6.19)$$

when we think about products it's often natural to take the log to
turn it into a sum

$$\begin{aligned} \log(\bar{g}) &= \frac{1}{\tau} \sum_{i=t}^{\tau-1} \log(1 + s_i) \\ &= \mathbb{E} \left[\log(1 + s_i) \right] \end{aligned} \quad (6.20)$$

equating the mean and the expectation. Assuming that s_i is small
 $\log(1 + s_i) \approx s_i - s_i^2/2$, ignoring terms s_i^3 and higher then this is

$$\begin{aligned} \log(\bar{g}) &\approx \mathbb{E} \left[s_i - s_i^2/2 \right] \\ &= \mathbb{E} \left[s_i \right] - \text{var}(s_i)/2 \end{aligned} \quad (6.21)$$

So genotypes with high arithmetic mean fitness can be selected against,
 3632 i.e. have low geometric mean fitness against, if their fitness has too
 high a variance across generations.

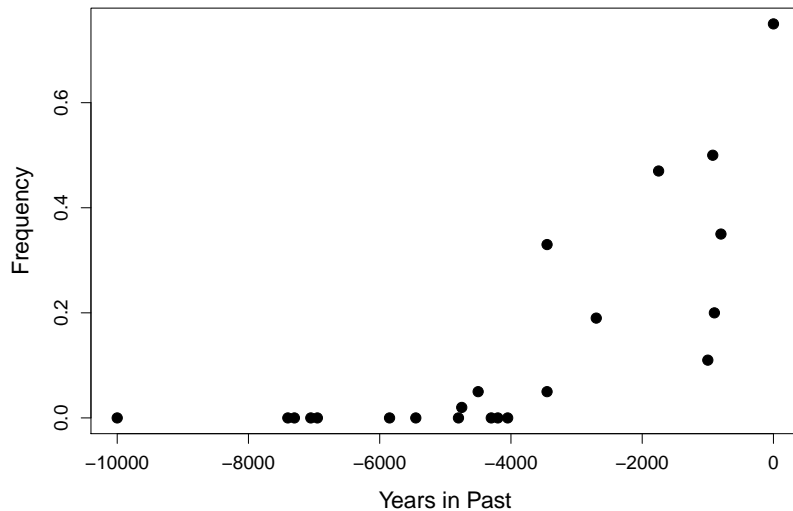


Figure 6.2: Frequency of the Lactase persistence allele in ancient and modern samples from Central Europe. Data compiled by MARCINIAK and PERRY (2017) from various sources. Thanks to Stephanie Marcinak for sharing these data. Code here.



Figure 6.3: Auroch (*Bos primigenius*). Aurochs are an extinct species of large wild cattle that cows were domesticated from.
Dictionnaire des sciences naturelles. 1816
 Cuvier, F.G. Image from the Internet Archive.
 Contributed by NCSU Libraries. No known
 copyright restrictions.

3634 6.0.2 Diploid model

We will now move on to a diploid model of a single locus with two
 3636 segregating alleles. As an example of the change in the frequency of an
 allele driven by selection, let's consider the evolution of Lactase persis-
 3638 tance. A number of different human populations that historically have
 raised cattle have convergently evolved to maintain the expression
 3640 of the protein Lactase into adulthood (in most mammals the pro-
 tein is switched off after childhood), with different lactase-persistence
 3642 mutations having arisen and spread in different pastoral human pop-
 3644 ulations. This continued expression of Lactase allows adults to break
 down Lactose, the main carbohydrate in milk, and so benefit nutri-
 3646 tionally from milk-drinking. This seems to have offered a strong fitness
 benefit to individuals in pastoral populations.

With the advent of techniques to sequence ancient human DNA,
 3648 researchers can now potentially track the frequency of selected muta-
 3650 tions over thousands of years. The frequency of a Lactase persistence
 allele in ancient Central European populations is shown in Figure
 3652 6.2. The allele is absent more than 5,000 years ago, but now found at
 frequency of upward of 70% in many European populations.

We will assume that the difference in fitness between the three
 3654 genotypes comes from differences in viability, i.e. differential survival

of individuals from the formation of zygotes to reproduction. We
 3656 denote the absolute fitnesses of genotypes A_1A_1 , A_1A_2 , and A_2A_2
 by W_{11} , W_{12} , and W_{22} . Specifically, W_{ij} is the probability that a
 3658 zygote of genotype A_iA_j survives to reproduction. Assuming that
 individuals mate at random, the number of zygotes that are of the
 3660 three genotypes and form generation t are

$$Np_t^2, \quad N2p_tq_t, \quad Nq_t^2. \quad (6.22)$$

The mean fitness of the population of zygotes is then

$$\bar{W}_t = W_{11}p_t^2 + W_{12}2p_tq_t + W_{22}q_t^2. \quad (6.23)$$

3662 Again, this is simply the weighted mean of the genotypic fitnesses.

How many zygotes of each of the three genotypes survive to re-
 3664 produce? An individual of genotype A_1A_1 has a probability of W_{11}
 of surviving to reproduce, and similarly for other genotypes. There-
 3666 fore, the expected number of A_1A_1 , A_1A_2 , and A_2A_2 individuals who
 survive to reproduce is

$$NW_{11}p_t^2, \quad NW_{12}2p_tq_t, \quad NW_{22}q_t^2. \quad (6.24)$$

3668 It then follows that the total number of individuals who survive to
 reproduce is

$$N(W_{11}p_t^2 + W_{12}2p_tq_t + W_{22}q_t^2). \quad (6.25)$$

3670 This is simply the mean fitness of the population multiplied by the
 population size (i.e. \bar{W}).

3672 The relative frequency of A_1A_1 individuals at reproduction is
 simply the number of A_1A_1 genotype individuals at reproduction
 3674 ($NW_{11}p_t^2$) divided by the total number of individuals who survive to
 reproduce (\bar{W}), and likewise for the other two genotypes. Therefore,
 3676 the relative frequency of individuals with the three different genotypes
 at reproduction is

$$\frac{NW_{11}p_t^2}{\bar{W}}, \quad \frac{NW_{12}2p_tq_t}{\bar{W}}, \quad \frac{NW_{22}q_t^2}{\bar{W}} \quad (6.26)$$

3678 (see Table 6.1).

	A_1A_1	A_1A_2	A_2A_2
Absolute no. at birth	Np_t^2	$N2p_tq_t$	Nq_t^2
Fitnesses	W_{11}	W_{12}	W_{22}
Absolute no. at reproduction	$NW_{11}p_t^2$	$NW_{12}2p_tq_t$	$NW_{22}q_t^2$
Relative freq. at reproduction	$\frac{W_{11}}{\bar{W}}p_t^2$	$\frac{W_{12}}{\bar{W}}2p_tq_t$	$\frac{W_{22}}{\bar{W}}q_t^2$

As there is no difference in the fecundity of the three genotypes, the
 3680 allele frequencies in the zygotes forming the next generation are simply

Table 6.1: Relative genotype frequencies after one episode of viability selection.

the allele frequency among the reproducing individuals of the previous generation. Hence, the frequency of A_1 in generation $t + 1$ is

$$p_{t+1} = \frac{W_{11}p_t^2 + W_{12}p_tq_t}{\bar{W}}. \quad (6.27)$$

Note that, again, the absolute value of the fitnesses is irrelevant to the frequency of the allele. Therefore, we can just as easily replace the absolute fitnesses with the relative fitnesses. That is, we may replace W_{ij} by $w_{ij} = W_{ij}/\bar{W}$, for instance.

Each of our genotype frequencies is responding to selection in a manner that depends just on its fitness compared to the mean fitness of the population. For example, the frequency of the 11 homozygotes increases from birth to adulthood in proportion to W_{11}/\bar{W} . In fact, we can estimate this fitness ratio for each genotype by comparing the frequency at birth compared to adults. As an example of this calculation, we'll look at some data from sticklebacks.

Marine threespine stickleback (*Gasterosteus aculeatus*) independently colonized and adapted to many freshwater lakes as glaciers receded following the last ice age, making sticklebacks a wonderful system for studying the genetics of adaptation. In marine habitats, most of the stickleback have armour plates to protect them from predation, but freshwater populations repeatedly evolve the loss of armour plates due to selection on an allele at the Ectodysplasin gene (EDA). This allele is found as a standing variant at very low frequency marine populations; BARRETT *et al.* took advantage of this fact and collected and bred a population of marine individuals carrying both the low- (L) and completely-plated (C) alleles. They introduced the offspring of this cross into four freshwater ponds and monitored genotype frequencies¹ over their life courses:

	CC	LC	LL
Juveniles	0.55	0.23	0.22
Adults	0.21	0.53	0.26
Adults/Juv. (W_{\bullet}/\bar{W})	0.4	2.3	1.2
rel. fitness (W_{\bullet}/W_{12})	0.17	1.0	0.54

The heterozygotes have increased in frequency dramatically in the population as their fitness is more than double the mean fitness of the population. We can also calculate the relative fitness of each genotype by dividing through by the fitness of the fittest genotype, the heterozygote in this case (doing this cancels through \bar{W}). The relative fitness of the CC is $\sim 1/5$ of the heterozygote. Note that this calculation does not rely on the genotype frequencies being at their HWE in the juveniles.

Question 2. A What is the frequency of the low-plated EDA allele (L) at the start of the stickleback experiment?

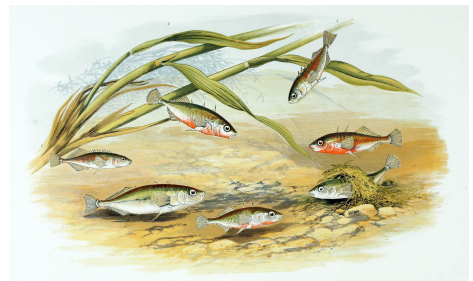


Figure 6.4: Freshwater threespine Stickleback (*G. aculeatus*). British fresh-water fishes. Houghton W 1879. Image from the Biodiversity Heritage Library. Contributed by Ernst Mayr Library, Harvard.. Not in copyright.

¹ The actual dynamics observed by BARRETT *et al.* are more complicated as in the very young fish selection reverses direction.

³⁷¹⁸ **B** What is the frequency in the adults?

Question 3. For many generations you have been studying an ³⁷²⁰ annual wildflower that has two color morphs, orange and white. You have discovered that a single bi-allelic locus controls flower color, with ³⁷²² the white allele being recessive. The pollinator of these plants is an almost blind bat, so individuals are pollinated at random with respect ³⁷²⁴ to flower color. Your population census of 200 individuals showed that the population consisted of 168 orange-flowered individuals, and 32 ³⁷²⁶ white-flowered individuals.

Heavy February rainfall creates optimal growing conditions for ³⁷²⁸ an exotic herbivorous beetle with a preference for orange-flowered individuals. This year it arrives at your study site with a ravenous ³⁷³⁰ appetite. Only 50% of orange-flowered individuals survive its wrath, while 90% of white-flowered individuals survive until the end of the ³⁷³² growing season.

A What is the initial frequency of the white allele, and what do you ³⁷³⁴ have to assume to obtain this?

B What is the frequency of the white allele in the seeds forming the ³⁷³⁶ next generation?

The change in frequency from generation t to $t + 1$ is

$$\Delta p_t = p_{t+1} - p_t = \frac{w_{11}p_t^2 + w_{12}p_tq_t}{\bar{w}} - p_t. \quad (6.28)$$

³⁷³⁸ To simplify this equation, we will first define two variables \bar{w}_1 and \bar{w}_2 as

$$\bar{w}_1 = w_{11}p_t + w_{12}q_t, \quad (6.29)$$

$$\bar{w}_2 = w_{12}p_t + w_{22}q_t. \quad (6.30)$$

³⁷⁴⁰ These are called the marginal fitnesses of allele A_1 and A_2 , respectively. They are so called as \bar{w}_1 is the average fitness of an allele A_1 , ³⁷⁴² i.e. the fitness of A_1 in a homozygote weighted by the probability it is in a homozygote (p_t) plus the fitness of A_1 in a heterozygote weighted ³⁷⁴⁴ by the probability it is in a heterozygote (q_t). We further note that the mean relative fitness can be expressed in terms of the marginal ³⁷⁴⁶ fitnesses as

$$\bar{w} = \bar{w}_1p_t + \bar{w}_2q_t, \quad (6.31)$$

where, for notational simplicity, we have omitted subscript t for the ³⁷⁴⁸ dependence of mean and marginal fitnesses on time.

We can then rewrite eqn. (6.28) using \bar{w}_1 and \bar{w}_2 as

$$\Delta p_t = \frac{(\bar{w}_1 - \bar{w}_2)}{\bar{w}}p_tq_t. \quad (6.32)$$

³⁷⁵⁰ The sign of Δp_t , i.e. whether allele A_1 increases or decreases in frequency, depends only on the sign of $(\bar{w}_1 - \bar{w}_2)$. The frequency of A_1

³⁷⁵² will keep increasing over the generations so long as its marginal fitness is higher than that of A_2 , i.e. $\bar{w}_1 > \bar{w}_2$, while if $\bar{w}_1 < \bar{w}_2$, the ³⁷⁵⁴ frequency of A_1 will decrease. Note the similarity between eqn. (6.32) and the respective expression for the haploid model in eqn. (6.4). (We ³⁷⁵⁶ will return to the special case where $\bar{w}_1 = \bar{w}_2$ shortly).

We can also rewrite (6.28) as

$$\Delta p_t = \frac{1}{2} \frac{p_t q_t}{\bar{w}} \frac{d\bar{w}}{dp}, \quad (6.33)$$

³⁷⁵⁸ the demonstration of which we leave to the reader. This form shows that the frequency of A_1 will increase ($\Delta p_t > 0$) if the mean fitness is ³⁷⁶⁰ an increasing function of the frequency of A_1 (i.e. if $\frac{d\bar{w}}{dp} > 0$). On the other hand, the frequency of A_1 will decrease ($\Delta p_t < 0$) if the mean ³⁷⁶² fitness is a decreasing function of the frequency of A_1 (i.e. if $\frac{d\bar{w}}{dp} < 0$). Thus, although selection acts on individuals, under this simple model, ³⁷⁶⁴ selection is acting to increase the mean fitness of the population. The rate of this increase is proportional to the variance in allele frequencies ³⁷⁶⁶ within the population ($p_t q_t$).

Question 4. Show that eqns. (6.33) and (6.32) are equivalent.

³⁷⁶⁸ (Trickier question.)

So far, our treatment of the diploid model of selection has been in ³⁷⁷⁰ terms of generic fitnesses w_{ij} . In the following, we will use particular parametrizations to gain insight about two specific modes of selection: ³⁷⁷² directional selection and heterozygote advantage.

6.0.3 Diploid directional selection

³⁷⁷⁴ Directional selection means that one of the two alleles always has higher marginal fitness than the other one. Let us assume that A_1 is ³⁷⁷⁶ the fitter allele, so that $w_{11} \geq w_{12} \geq w_{22}$, and hence $\bar{w}_1 > \bar{w}_2$. As we are interested in changes in allele frequencies, we may use relative ³⁷⁷⁸ fitnesses. We parameterize the reduction in relative fitness in terms of a selection coefficient, similar to the one we met in the haploid ³⁷⁸⁰ selection section, as follows:

genotype	$A_1 A_1$	$A_1 A_2$	$A_2 A_2$
absolute fitness	W_{11}	$\geq W_{12} \geq$	W_{22}
relative fitness (generic)	$w_{11} = W_{11}/W_{11}$	$w_{12} = W_{12}/W_{11}$	$w_{22} = W_{22}/W_{11}$
relative fitness (specific)	1	$1 - sh$	$1 - s$.

Here, the selection coefficient s is the difference in relative fitness ³⁷⁸⁴ between the two homozygotes, and h is the dominance coefficient. For selection to be directional, we require that $0 \leq h \leq 1$ holds. The ³⁷⁸⁶ dominance coefficient allows us to move between two extremes. One

is when $h = 0$, such that allele A_1 is fully dominant and A_2 fully recessive. In this case, the heterozygote A_1A_2 is as fit as the A_1A_1 homozygote genotype. The inverse holds when $h = 1$, such that allele A_1 is fully recessive and A_2 fully dominant.

3790 We can then rewrite eqn. (6.32) as

$$\Delta p_t = \frac{p_t h s + q_t s(1-h)}{\bar{w}} p_t q_t, \quad (6.34)$$

3792 where

$$\bar{w} = 1 - 2p_t q_t s h - q_t^2 s. \quad (6.35)$$

Question 5. Throughout the Californian foothills are old copper and gold-mines, which have dumped out soils that are polluted with heavy metals. While these toxic mine tailings are often depauperate of plants, *Mimulus guttatus* and a number of other plant species have managed to adapt to these harsh soils. WRIGHT *et al.* (2015) have mapped one of the major loci contributing to the adaptation to soils at two mines near Copperopolis, CA. WRIGHT *et al.* planted homozygote seedlings out in the mine tailings and found that only 10% of the homozygotes for the non-copper-tolerant allele survived to flower, while 40% of the copper-tolerant seedlings survived to flower.

3804 A) What is the selection coefficient acting against the non-copper-tolerant allele on the mine tailing?

B) The copper-tolerant allele is fairly dominant in its action on fitness. If we assume that $h = 0.1$, what percentage of heterozygotes should survive to flower?

3808 **Question 6.** Comparing the red ($h = 0$) and black ($h = 0.5$) trajectories in Figure 6.5, provide an explanation for why A_1 increases faster initially if $h = 0$, but then approaches fixation more slowly compared to the case of $h = 0.5$.

3812 To see how dominance affects the trajectory of a real polymorphism, we'll consider an example from a colour polymorphism in red foxes (*Vulpes vulpes*). There are three colour morphs of red foxes: silver, cross, and red (see Figure 6.8), with this difference primarily controlled by a single polymorphism with genotypes RR, Rr, and rr respectively. The fur pelts of the silver morph fetched three times 3818 the price for hunters compared to cross (a smoky red) and red pelts, the latter two being seen as roughly equivalent in worth. Thus the 3820 desirability of the pelts acts as a recessive trait, with much stronger selection against the silver homozygotes. As a result of this price difference, silver foxes were hunted more intensely and declined as a 3822 proportion of the population in Eastern Canada, see Figure 6.7, as 3824 documented by ELTON, from 16% to 5% from 1834 to 1937. HAL-

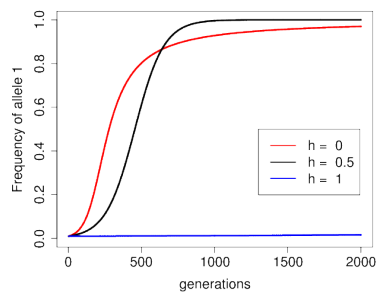
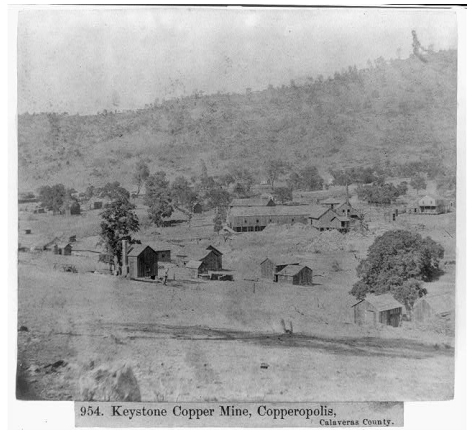


Figure 6.5: The trajectory of the frequency of allele A_1 , starting from $p_0 = 0.01$, for a selection coefficient $s = 0.01$ and three different dominance coefficients. The recessive beneficial allele ($h = 1$) will eventually fix in the population, but it takes a long time. Code here.



954. Keystone Copper Mine, Copperopolis, Calaveras County.
1866, Copperopolis, Calaveras County.
Image from picryl. Source Library of Congress, Public Domain.

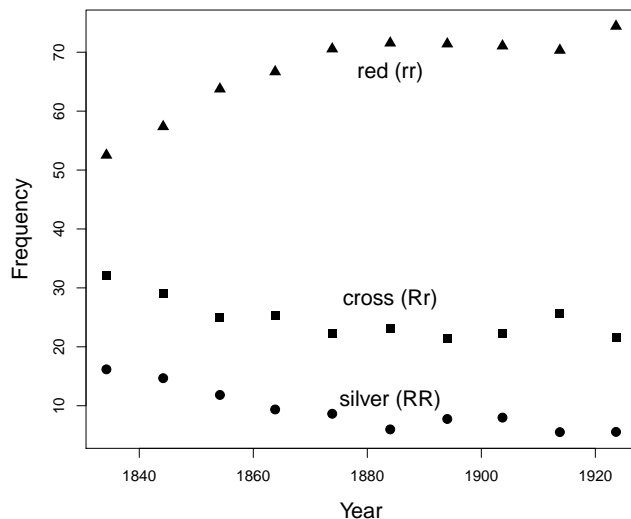


Figure 6.7: The frequency of red, cross, and silver fox morphs over the decades in Eastern Canada. These data are well described by recessive selection acting against the silver fox morph. Data from ELTON (1942), compiled by ALLENDORF and HARD (2009). [Code here.](#)

DANE reanalyzed these data and showed that they were consistent
3826 with recessive selection acting against the silver morph alone.

Note how the heterozygotes (cross) decline somewhat as a result of
3828 selection on the silver homozygotes, but overall the R allele is slow to
respond to selection as it is ‘hidden’ from selection in the heterozygote
3830 state.

Directional selection on an additive allele. A special case is when
3832 $h = 0.5$. This case is the case of no dominance, as the interaction
among alleles with respect to fitness is strictly additive. Then, eqn.
3834 (6.34) simplifies to

$$\Delta p_t = \frac{1}{2} \frac{s}{\bar{w}} p_t q_t. \quad (6.36)$$

If selection is very weak, i.e. $s \ll 1$, the denominator (\bar{w}) is close to
3836 1 and we have

$$\Delta p_t = \frac{1}{2} s p_t q_t. \quad (6.37)$$

It is instructive to compare eqn. (6.37) to the respective expression
3838 under the haploid model. To this purpose, start from the generic term
for Δp_t under the haploid model in eqn. (6.4) and set $w_1 = 1$ and
3840 $w_2 = 1 - s$. Again, assume that s is small, so that eqn. (6.4) becomes
 $\Delta p_t = s p_t q_t$. Hence, if s is small, the diploid model of directional
3842 selection without dominance is identical to the haploid model, up to a
factor of 1/2. That factor is due to the choice of the parametrisation;
3844 we could have set $w_{11} = 1$, $w_{12} = 1 - s$, and $w_{22} = 1 - 2s$ in our diploid



Figure 6.8: Three colour morphs in red fox *V. vulpes*, cross, red, and silver foxes from left to right.
The larger North American mammals” Nelson,
E.W. Fuertes, L.A. 1916. Image from the
Biodiversity Heritage Library. Contributed
by Cornell University Library. No known
copyright restrictions.

model instead, in which case the agreement with the haploid model
 3846 would be perfect.

From this analogy, we can borrow some insight we gained from the
 3848 haploid model. Specifically, the trajectory of the frequency of allele
 A_1 in the diploid model without dominance follows a logistic growth
 3850 curve similar to (6.10). From this similarity, we can extrapolate from
 Equation (6.12) to find the time it takes for our diploid, beneficial,
 3852 additive allele (A_1) to move from frequency p_0 to p_τ :

$$\tau \approx \frac{2}{s} \log \left(\frac{p_\tau q_0}{q_\tau p_0} \right) \quad (6.38)$$

generations; this just differs by a factor of 2 from our haploid model.

3854 Using this result we can find the time it takes for our favourable,
 additive allele (A_1) to transit from its entry into the population ($p_0 =$
 3856 $1/(2N)$) to close to fixation ($p_\tau = 1 - 1/(2N)$):

$$\tau \approx \frac{4}{s} \log(2N) \quad (6.39)$$

generations. Note the similarity to eqn. 6.13 for the haploid model,
 3858 with a difference by a factor of 2 due to the choice of parametrization
 (and that the number of alleles is $2N$ in the diploid model, rather than
 3860 N). Doubling our selection coefficient halves the time it takes for our
 allele to move through the population.

3862 **Question 7.** Gulf killifish (*Fundulus grandis*) have rapidly adapted
 to the very high pollution levels in the Houston shipping canal since
 3864 the 1950s. One of the ways that they've adapted is through the dele-
 tion of their aryl hydrocarbon receptor (AHR) gene. Oziolor et al.
 3866 estimated that individuals who were homozygote for the intact AHR
 gene had a relative fitness of 20% of that of homozygotes for the dele-
 3868 tion. Assuming an effective population size of 200 thousand individ-
 uals, how long would it take for the deletion to reach fixation, starting
 3870 as a single copy in this population?

3872 Directional selection on genotypes is expected to remove variation
 from populations, yet we see plentiful phenotypic and genetic variation
 in every natural population. Why is this? Three broad explanations
 3874 for the maintenance of polymorphisms are

1. Variation is maintained by a balance of genetic drift and mutation
 3876 (we discussed this explanation in Chapter 3).
2. Selection can sometimes act to maintain variation in populations
 3878 (balancing selection).
3. Deleterious variation can be maintained in the population as a bal-
 3880 ance between selection removing variation and mutation constantly
 introducing new variation into the population.

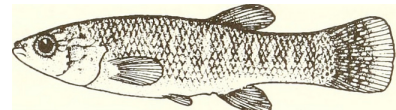


Figure 6.9: Gulf killifish (*Fundulus grandis*).

Distribution and abundance of fishes and invertebrates in Gulf of Mexico estuaries. Nelson D M and Pattiilo M E Image from the Biodiversity Heritage Library. Contributed by MBLWHOI Library. No known copyright restrictions.

³⁸⁸² We'll turn to these latter two explanations through the rest of the chapter. Note that these explanations are not mutually exclusive, and ³⁸⁸⁴ each of them will explain some proportion of the variation.

6.0.4 Heterozygote advantage

³⁸⁸⁶ One form of balancing selection occurs when the heterozygotes are fitter than either of the homozygotes. In this case, it is useful to parameterize the relative fitnesses as follows:

genotype	A_1A_1	A_1A_2	A_2A_2
absolute fitness	w_{11}	$< w_{12} >$	w_{22}
relative fitness (generic)	$w_{11} = W_{11}/W_{12}$	$w_{12} = W_{12}/W_{12}$	$w_{22} = W_{22}/W_{12}$
relative fitness (specific)	$1 - s_1$	1	$1 - s_2$

³⁸⁹² Here, s_1 and s_2 are the differences between the relative fitnesses of the two homozygotes and the heterozygote. Note that to obtain ³⁸⁹⁴ relative fitnesses we have divided absolute fitness by the heterozygote fitness. We could use the same parameterization as in the model of directional selection, but the reparameterization we have chosen here ³⁸⁹⁶ makes the math easier.

In this case, when allele A_1 is rare, it is often found in a heterozygous state, while the A_2 allele is usually in the homozygous state, and so A_1 is more fit and increases in frequency. However, when the allele ³⁹⁰⁰ A_1 is common, it is often found in a less fit homozygous state, while the allele A_2 is often found in a heterozygous state; thus it is now allele A_2 that increases in frequency at the expense of allele A_1 . Thus, at least in the deterministic model, neither allele can reach fixation ³⁹⁰⁴ and both alleles will be maintained at an equilibrium frequency as a balanced polymorphism in the population.

³⁹⁰⁶ We can solve for this equilibrium frequency by setting $\Delta p_t = 0$ in eqn. (6.32), i.e. $p_t q_t (\bar{w}_1 - \bar{w}_2) = 0$. Doing so, we find that there ³⁹⁰⁸ are three equilibria, all of which are stable. Two of them are not very interesting ($p = 0$ or $q = 0$), but the third one is the polymorphic equilibrium, where $\bar{w}_1 - \bar{w}_2 = 0$ holds. Using our s_1 and s_2 parametrization above, we see that the marginal fitnesses of the two alleles are equal ³⁹¹⁰ when

$$p_e = \frac{s_2}{s_1 + s_2} \quad (6.40)$$

³⁹¹² for the equilibrium frequency of interest. This is also the frequency of A_1 at which the mean fitness of the population is maximized. The highest possible fitness of the population would be achieved if every ³⁹¹⁶ individual was a heterozygote. However, Mendelian segregation of alleles in the gametes of heterozygotes means that a sexual population

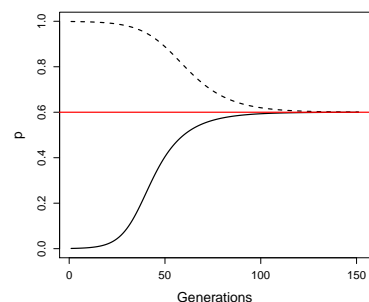


Figure 6.10: Two allele frequency trajectories of the A_1 allele subject to heterozygote advantage ($w_{11} = 0.9$, $w_{12} = 1$, and $w_{22} = 0.85$). In one simulation the allele is started from being rare in the population ($p = 1/1000$, solid line) and increases in frequency/³⁹⁰⁸ In the other simulation the allele is almost fixed ($p = 999/1000$, dashed line). In both cases the frequency moves toward the equilibrium frequency. The red line shows the equilibrium frequency (p_e). Code here.

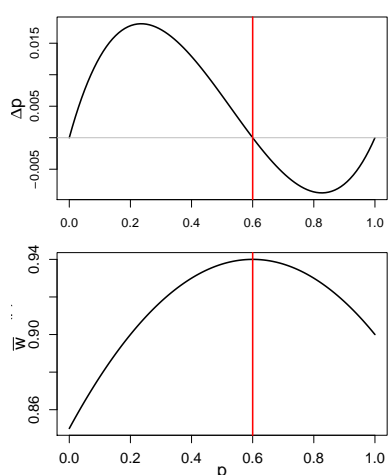
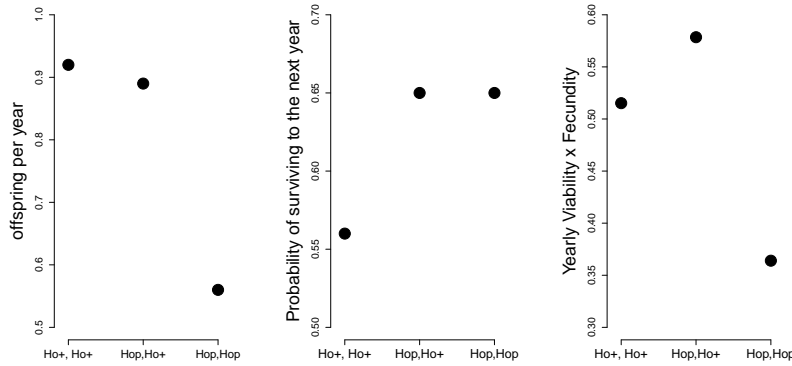


Figure 6.11: **Top**) The change in frequency of an allele with heterozygote advantage within a generation (Δp) as a function of the allele frequency. Fitnesses as in Figure 6.10. Note how the frequency changes in opposite directions depending on whether the allele is rare or common.

3918 can never achieve a completely heterozygote population. This equilibrium frequency represents an evolutionary compromise between the
 3920 advantages of the heterozygote and the comparative costs of the two homozygotes.



3922 One example of a polymorphism maintained by heterozygote advantage is a horn-size polymorphism found in Soay sheep, a population of
 3924 feral sheep on the island of Soay (about 40 miles off the coast of Scotland). The horns of the soay sheep resemble those of the wild Mouflon
 3926 sheep, and the male Soay sheep use their horns to defend females during the rut. JOHNSTON *et al.* (2013) found a large-effect locus, at the
 3928 RXFP2 gene, that controls much of the genetic variation for horn size.
 Two alleles Ho^p and Ho^+ segregate at this locus. The Ho^+ allele is
 3930 associated with growing larger horns, while the Ho^p allele is associated with smaller horns, with a reasonable proportion of Ho^p homozygotes
 3932 developing no horns at all. JOHNSTON *et al.* (2013) found that the
 3934 Ho locus had substantial effects on male, but not female, fitness (see Figure 6.13).

The Ho^p allele has a mostly recessive effect on male fecundity, with
 3936 the Ho^p homozygotes having lower yearly reproductive success presumably due to the fact that they perform poorly in male-male competition (left plot Figure 6.13). Conversely, the Ho^+ has a mostly recessive effect on viability, with Ho^+ homozygotes having lower yearly
 3938 survival (middle plot Figure 6.13), likely because they spend little time feeding during the rut and so lose substantial body weight. Thus
 3940 both of the homozygotes suffer from trade-offs between viability and fecundity. As a result, the Ho^pHo^+ heterozygotes have the highest
 3942 fitness (right plot Figure 6.13). The allele is thus balanced at intermediate frequency (~ 50%) in the population due to this trade off between
 3944 fitness at different life history stages.

Question 8. Assume that the frequency of the Ho^P allele is 10%,

Figure 6.12: For the three Soay sheep genotypes: the offspring per year (left), the probability of surviving a year (middle), and the product of the two (right). Thanks to Susan Johnston for supplying these simplified numbers from JOHNSTON *et al.* (2013). Code here.

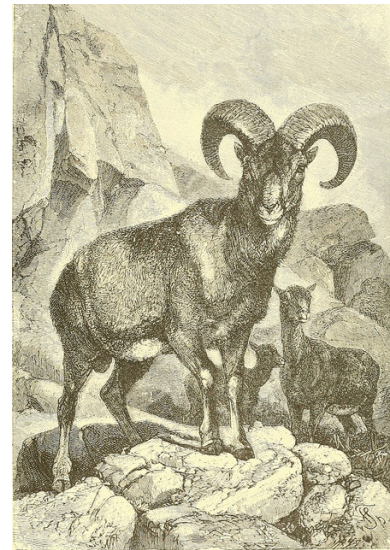


Figure 6.13: Mouflon (*Ovis orientalis orientalis*).
 Animate creation. (1898). Wood, J. G. Image from the Biodiversity Heritage Library. Contributed by Smithsonian Libraries. Not in copyright.

The fitnesses here are chosen to roughly match those of the real Soay sheep example, as a full model would require us to more carefully model the life-histories of the sheep.

3948 that there are 1000 males at birth, and that individual adults mate at random.

3950 **A)** What is the expected number of males with each of the three genotypes in the population at birth?

3952 **B)** Assume that a typical male individual of each genotypes has the following probability of surviving to adulthood:

$$\begin{array}{cccccc} \text{Ho}^+ & \text{Ho}^+ & \text{Ho}^+ & \text{Ho}^p & \text{Ho}^p & \text{Ho}^p \\ 0.5 & & 0.8 & & & 0.8 \end{array}$$

Making the assumptions from above, how many males of each genotype survive to reproduce? **C)** Of the males who survive to reproduce, let's say that males with the Ho^+Ho^+ and Ho^+Ho^p genotype have on average 2.5 offspring, while Ho^pHo^p males have on average 1 offspring. Taking into account both survival and reproduction, how many offspring do you expect each of the three genotypes to contribute to the total population in the next generation?

3962 **D)** What is the frequency of the Ho^+ allele in the sperm that will form this next generation?

3964 **E)** How would your answers to B-D change if the Ho^p allele was at 90% frequency?

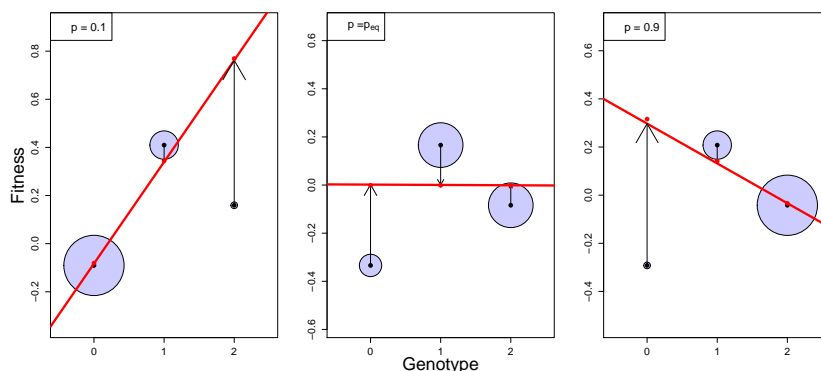


Figure 6.14: The deviation of the fitness of each genotype away from the mean population fitness (0) is shown as black dots. The area of each circle is proportion to the fraction of the population in each genotypic class (p^2 , $2pq$, and q^2). The additive genetic fitness of each genotype is shown as a red dot. The linear regression between fitness and additive genotype is shown as a red line. The black vertical arrows show the difference between the average mean-centered phenotype and additive genetic value for each genotype. The left panel shows $p = 0.1$ and the right panel shows $p = 0.9$; in the middle panel the frequency is set to the equilibrium frequency. Code here.

3966 To push our understanding of heterozygote advantage a little further, note that the marginal fitnesses of our alleles are equivalent to the additive effects of our alleles on fitness. Recall from our discussion of non-additive variation (Section 4.1.1) that the difference in the additive effects of the two alleles gives the slope of the regression of additive genotypes on fitness, and that there is additive variance in fitness when this slope is non-zero. So what's happening here in our heterozygote advantage model is that the marginal fitness of the A_1 allele, the additive effect of allele A_1 on fitness, is greater than the marginal fitness of the A_2 allele ($\bar{w}_1 > \bar{w}_2$) when A_1 is at low frequency in the population. In this case, the regression of fitness on the number of A_1 alleles in a genotype has a positive slope. This is true

3978 when the frequency of the A_1 allele is below the equilibrium frequency.
 If the frequency of A_1 is above the equilibrium frequency, then the
 3980 marginal fitness of allele A_2 is higher than the marginal fitness of allele
 A_1 ($\bar{w}_1 < \bar{w}_2$) and the regression of fitness on the number of copies
 3982 of allele A_1 that individuals carry is negative. In both cases there is
 additive genetic variance for fitness ($V_A > 0$) and the population has
 3984 a directional response. Only when the population is at its equilibrium
 frequency, i.e. when $\bar{w}_1 = \bar{w}_2$, is there no additive genetic variance
 3986 ($V_A = 0$), as the linear regression of fitness on genotype is zero.

3988 *Underdominance.* Another case that is of potential interest is the
 case of fitness underdominance, where the heterozygote is less fit than
 either of the two homozygotes. Underdominance can be parametrized
 3990 as follows:

genotype	A_1A_1	A_1A_2	A_2A_2
absolute fitness	w_{11}	$> w_{12} <$	w_{22}
relative fitness (generic)	$w_{11} = W_{11}/W_{12}$	$w_{12} = W_{12}/W_{12}$	$w_{22} = W_{22}/W_{12}$
relative fitness (specific)	$1 + s_1$	1	$1 + s_2$

3992 Underdominance also permits three equilibria: $p = 0$, $p = 1$, and
 3994 a polymorphic equilibrium $p = p_U$. However, now only the first two
 equilibria are stable, while the polymorphic equilibrium is unstable. If
 3996 $p < p_U$, then Δp_t is negative and allele A_1 will be lost, while if $p > p_U$,
 allele A_1 will become fixed.

3998 While strongly-selected, underdominant alleles might not spread
 within populations (if $p_U \gg 0$), they are of special interest in the
 4000 study of speciation and hybrid zones. That is because alleles A_1 and
 A_2 may have arisen in a stepwise fashion, i.e. not by a single mutation,
 4002 but in separate subpopulations. In this case, heterozygote disadvan-
 tage will play a potential role in species maintenance, if isolation of
 4004 the subpopulations is not complete.

4006 **Question 9.** You are studying the polymorphism that affects
 flight speed in butterflies. The polymorphism does not appear to affect
 fecundity. Homozygotes for the B allele are slow in flight and so only
 4008 40% of them survive to have offspring. Heterozygotes for the poly-
 morphism (Bb) fly quickly and have a 70% probability of surviving
 4010 to reproduce. The homozygotes for the alternative allele (bb) fly very
 quickly indeed, but often die of exhaustion, with only 10% of them
 4012 making it to reproduction.

- 4014 A) What is the equilibrium frequency of the B allele?
 B) Calculate the marginal absolute fitnesses of the B and the b
 allele at the equilibrium frequency.

4016 **Question 10.** OPTIONAL trickier question.



Figure 6.15: In *Pseudacraea eurytus* there are two homozygotes morphs that mimic a different blue and orange butterfly; the heterozygote fails to mimic either successfully and so suffers a high rate of predation (OWEN and CHANTER, 1972). Illustrations of new species of exotic butterflies (1868) Hewitson. Image from the Biodiversity Heritage Library. Contributed by Smithsonian Libraries. Not in copyright.

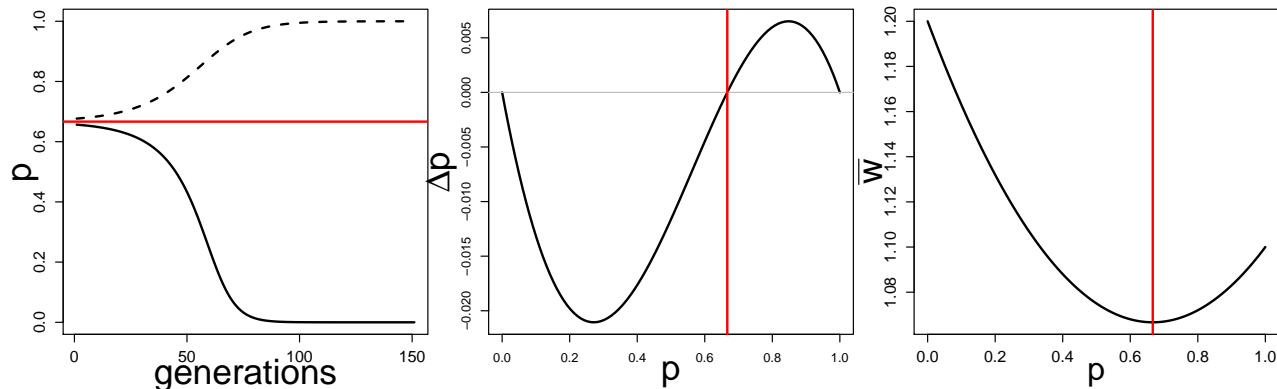


Figure 6.16: Two allele frequency trajectories of an A_1 allele subject to heterozygote disadvantage ($w_{11} = 1.1$, $w_{12} = 1$, and $w_{22} = 1.2$). The allele is started from just above and below the equilibrium frequency, in both cases the frequency move away the equilibrium frequency. The red line shows the unstable equilibrium frequency (p_e). **Top**) The change in frequency of an allele with heterozygote disadvantage within a generation (Δp) as a function of the allele frequency (p). Fitnesses as in Figure 6.10. Note how the frequency change is negative below the equilibrium frequency (p_e) and positive above. **Bottom**) Mean fitness (\bar{w}) as a function of the allele frequency. The red line shows the unstable equilibrium frequency (p_e). Code here.

Imagine a randomly-mating population of hermaphrodites. In this population, a derived allele (D) segregates that distorts transmission in its favour over the ancestral allele (d) in the production of all the gametes of heterozygotes. The drive leads to a fraction r of the gametes of heterozygotes (D/d) to carry the D allele ($r > 0.5$). The D allele causes viability problems in the homozygous state, such that the relative fitnesses are $w_{dd} = 1$, $w_{Dd} = 1$, $w_{DD} = 1 - e$. The D allele is currently at frequency p in the population at birth. Assume that the population is very large and no mutation occurs:

- A)** What is the frequency of the D allele in the next generation, before selection has had a chance to act?
- B)** What conditions do you need for a polymorphic equilibrium to be maintained? What is the equilibrium frequency of this balanced polymorphism?
- C)** Imagine the cost of the driver were additive: $w_{dd} = 1$, $w_{Dd} = 1 - e$, $w_{DD} = 1 - 2e$. Under what conditions can the driver invade the population? Can a polymorphic equilibrium be maintained?

Diploid fluctuating fitness Selection pressures fluctuate over time and can potentially maintain polymorphisms in the population. Two examples of polymorphisms fluctuating in frequency in response to temporally-varying selection are shown in Figure 6.17; thanks to the short lifespan of *Drosophila* we can see seasonally-varying selection. The first example is an inversion allele in *Drosophila pseudoobscura* populations. Throughout western North America, two orientations of the chromosome, two ‘inversion alleles’, exist: the Chiricahua and Standard alleles. DOBZHANSKY (1943) and WRIGHT and DOBZHANSKY (1946) investigated the frequency of these inversion alleles over four years at a number of locations and found that their frequency fluctuated systematically over the seasons in response to se-

lection (left side of 6.17). If you're still reading these notes send Prof. Coop a picture of Dobzhansky; Dobzhansky was one of the most important evolutionary geneticists of the past century and spent a bunch of time at UC Davis in his later years. Our second example is an insertion-deletion polymorphism in the Insulin-like Receptor gene in *Drosophila melanogaster*. PAABY *et al.* (2014) tracked the frequency of this allele over time and found it oscillated with the seasons (right side of 6.17). She and her coauthors also determined that these alleles had large effects on traits such as developmental time and fecundity, which could mediate the maintenance of this polymorphism through life-history trade-offs.

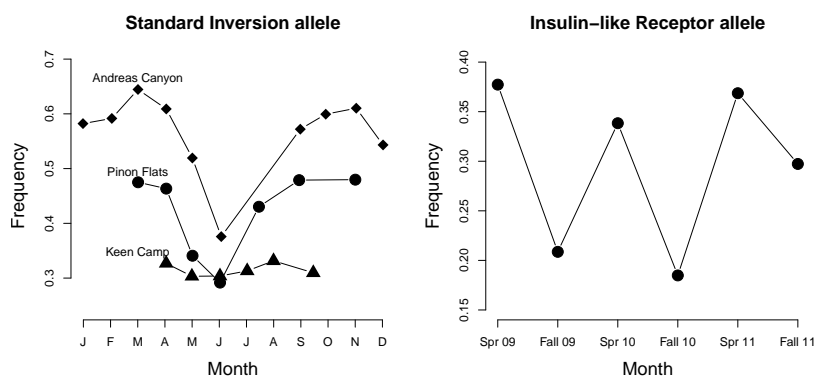


Figure 6.17: **Left**) Seasonal variation in the frequency of the ‘Standard’ inversion allele in *Drosophila pseudobscura* for three populations from Mount San Jacinto, CA. These frequencies are an average over four years. Data from WRIGHT and DOBZHANSKY (1946). **Right**) The frequency of an allele at the Insulin-like Receptor gene over three years in *Drosophila melanogaster* samples from an Orchard in Pennsylvania. Data from PAABY *et al.* (2014). Code here.

To explore temporal fluctuations in fitness, we'll need to think

about the diploid absolute fitnesses being time-dependent, where the three genotypes have fitnesses $w_{11,t}$, $w_{12,t}$, and $w_{22,t}$ in generation t . Modeling the diploid case with time-dependent fitness is much less tractable than the haploid case, as segregation makes it tricky to keep track of the genotype frequencies. However, we can make some progress and gain some intuition by thinking about how the frequency of allele A_1 changes when it is rare (following the work of HALDANE and JAYAKAR, 1963).

When A_1 is rare, i.e. $p_t \ll 1$, the frequency of A_1 in the next generation (6.27) can be approximated as

$$p_{t+1} \approx \frac{w_{12}}{\bar{w}} p_t. \quad (6.41)$$

To obtain this equation, we have ignored the p_t^2 term (because it is very small when p_t is small) and we have assumed that $q_t \approx 1$ in the numerator. Following a similar argument to approximate q_{t+1} , we can write

$$\frac{p_{t+1}}{q_{t+1}} = \frac{w_{12,t}}{w_{22,t}} \frac{p_t}{q_t}. \quad (6.42)$$

⁴⁰⁷² Starting from out from p_0 and q_0 in generation 0, then $t+1$ generations later we have

$$\frac{p_{t+1}}{q_{t+1}} = \left(\prod_{i=0}^t \frac{w_{12,i}}{w_{22,i}} \right) \frac{p_0}{q_0}. \quad (6.43)$$

⁴⁰⁷⁴ From this we can see, following our haploid argument from above, that the frequency of allele A_1 will increase when rare only if

$$\frac{\sqrt[t]{\prod_{i=0}^t w_{12,i}}}{\sqrt[t]{\prod_{i=0}^t w_{22,i}}} > 1, \quad (6.44)$$

⁴⁰⁷⁶ i.e. if the heterozygote has higher geometric mean fitness than the A_2A_2 homozygote.

⁴⁰⁷⁸ The question now is whether allele A_1 will approach fixation in the population, or whether there are cases in which we can obtain a balanced polymorphism. To investigate that, we can simply repeat our analysis for $q \ll 1$, and see that in that case

$$\frac{p_{t+1}}{q_{t+1}} = \left(\prod_{i=0}^t \frac{w_{11,i}}{w_{12,i}} \right) \frac{p_0}{q_0}. \quad (6.45)$$

⁴⁰⁸² Now, for allele A_1 to carry on increasing in frequency and to approach fixation, the A_1A_1 genotype has to be out-competing the heterozygotes. For allele A_1 to approach fixation, we need the geometric mean of $w_{11,i}$ to be greater than the geometric mean fitness of heterozygotes ($w_{12,i}$). At the same time, if heterozygotes have higher geometric mean fitness than the A_1A_1 homozygotes, then the A_2 allele will increase in frequency when it is rare.

Intriguingly, we can thus have a balanced polymorphism even if the ⁴⁰⁹⁰ heterozygote is never the fittest genotype in any generation, as long as the heterozygote has a higher geometric mean fitness than either of ⁴⁰⁹² the homozygotes. In this case, the heterozygote comes out ahead when we think about long-term fitness across heterogeneous environmental ⁴⁰⁹⁴ conditions, despite never being the fittest genotype in any particular environment.

⁴⁰⁹⁶ As a toy example of this type of balanced polymorphism, consider a plant population found in one of two different environments each generation. These occur randomly; $1/2$ of time the population experiences the dry environment and with probability $1/2$ it experiences the wet ⁴⁰⁹⁸ environment. The absolute fitnesses of the genotypes in the different environments are as follows:

Environment	AA	Aa	aa
Wet	6.25	5.0	3.75
Dry	3.85	5.0	6.15
arithmetic mean	5.05	5.0	4.95

Let's write $w_{AA,\text{dry}}$ and $w_{AA,\text{wet}}$ for the fitnesses of the AA homozygote in the two environments. Then, if the two environments are equally common, $\prod_{i=0}^t w_{AA,i} \approx w_{AA,\text{dry}}^{t/2} w_{AA,\text{wet}}^{t/2}$ for large values of t . To obtain an estimate of this product normalized over the t generations, we can take the t^{th} root to obtain the geometric mean fitness. Taking the t^{th} root, we find the geometric mean fitness of the AA allele is $w_{AA,\text{dry}}^{1/2} w_{AA,\text{wet}}^{1/2}$. Doing this for each of our genotypes, we find the geometric mean fitnesses of our alleles to be:

	AA	Aa	aa
Geometric mean	4.91	5.0	4.80

i.e. the heterozygote has higher geometric mean fitnesses than either of the homozygotes, despite not being the fittest genotype in either environment (nor having the highest arithmetic mean fitness). So the A_1 allele can invade the population when it is rare as it spread thanks to the higher fitness of the heterozygotes. Similarly the A_2 allele can invade the population when it is rare. Thus both alleles will persist in the population due to the environmental fluctuations, and the higher geometric mean fitness of the heterozygotes.

Negative frequency-dependent selection. In the models and examples above, heterozygote advantage maintains multiple alleles in the population because the common allele has a disadvantage compared to the other rarer allele. In the case of heterozygote advantage, the relative fitnesses of our three genotypes are not a function of the other genotypes present in the population. However, there's a broader set of models where the relative fitness of a genotype depends on the genotypic composition of the population; this broad family of models is called frequency-dependent selection. Negative frequency-dependent selection, where the fitness of an allele (or phenotype) decreases as it becomes more common in the population, can act to maintain genetic and phenotypic diversity within populations. While cases of long-term heterozygote advantage may be somewhat rare in nature, negative frequency-dependent selection is likely a common form of balancing selection.

One common mechanism that may create negative frequency-dependent selection is the interaction between individuals within or among species. For example, negative frequency-dependent dynamics can arise in predator-prey or pathogen-host dynamics, where alleles conferring common phenotypes are at a disadvantage because predators or pathogens learn or evolve to counter the phenotypic effects of common alleles.

As one example of negative frequency-dependent selection, consider the two flower colour morphs in the deceptive Elderflower orchid

This example is loosely based on the work of SCHEMSKE and BIERZYCHUDEK (2001) on *Linanthus parryae*, a desert annual, endemic to California. There are blue- and a white-flowered colour morphs polymorphic many populations, with this polymorphism being controlled by a single dominant allele. The blue-flowered plants produce more seeds in dry years, i.e. they have higher fitness in these years, while the white-flowered plants have higher seed production in wet years. Thus both morphs can potentially be maintained in the population. See TURELLI *et al.* (2001) for a more detailed analysis.



Figure 6.18: Elderflower orchid (*Dactylorhiza sambucina*).

Abbildungen der in Deutschland und den angrenzenden gebieten vorkommenden grundformen der orchideenarten (1904). Müller, W.

(*Dactylorhiza sambucina*). Throughout Europe, there are populations of these orchids polymorphic for yellow- and purple-flowered individuals, with the yellow flower corresponding to a recessive allele. Neither of these morphs provide any nectar or pollen reward to their bumblebee pollinators. Thus these plants are typically pollinated by newly emerged bumblebees who are learning about which plants offer food rewards, with the bees alternating to try a different coloured flower if they find no food associated with a particular flower-colour morph (SMITHSON and MACNAIR, 1997). GIGORD *et al.* (2001) explored whether this behaviour by bees could result in negative frequency-dependent selection; out in the field, the researchers set up experimental orchid plots in which they varied the frequency of the two colour morphs. Figure 6.19 shows their measurements of the relative male and female reproductive success of the yellow morph across these experimental plots. When the yellow morph is rare, it has higher reproductive success than the purple morph, as it receives a disproportionate number of visits from bumblebees that are dissatisfied with the purple flowers. This situation is reversed when the yellow morph becomes common in the population; now the purple morph outperforms the yellow morph. Therefore, both colour morphs are maintained in this population, and presumably Europe-wide, due to this negative frequency-dependent selection.

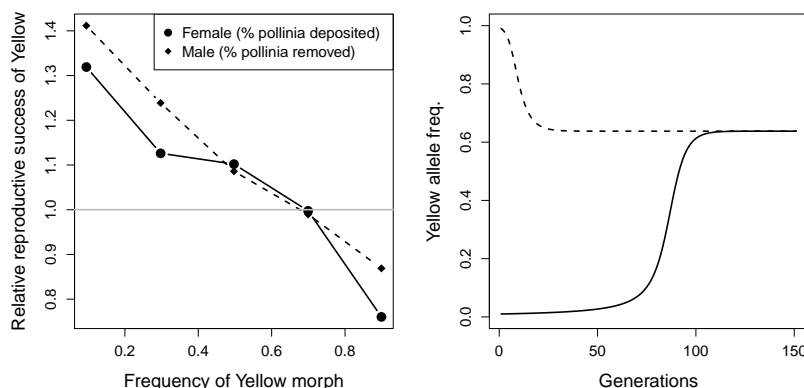


Figure 6.19: **Left)** Measures of the relative male- and female- reproductive success of the yellow Elderflower orchid morph as a function of the yellow morph in experimental plots. **Right)** Two allele frequency trajectories of the Yellow allele subject to negative frequency scheme given in the left plot (for an initial frequency of 0.01 and 0.99, solid and dotted line respectively). Note that the yellow Male reproductive success is measured in terms of the % of pollinia removed front a plant and female reproductive success is measured in terms of the % of stigmas receiving pollinia on a plant. These measures are made relative by dividing the reproductive success of the yellow morph by the mean of the yellow and purple morphs. Pollinia are the pollen masses of orchids, and other plants, where individual pollinium are transferred as a single unit by pollinators. Data from GIGORD *et al.* (2001). Code here.

Negative frequency-dependent selection can also maintain different breeding strategies due to interactions amongst individuals within a population. One dramatic example of this occurs in ruffs (*Philomachus pugnax*), a marsh-wading sandpiper that summers in Northern Eurasia. The males of this species lek, with the males gathering on open ground to display and attract females. There are three different male morphs differing in their breeding strategy. The large majority of

males are ‘Independent’, with black or chestnut ruff plumage, and try
 4174 to defend and display on small territories. ‘Satellite’ males, with white
 ruff plumage, make up ~ 16% of males and do not defend territories,
 4176 but rather join in displays with Independent males and opportunistically
 mate with females visiting the lek. Finally, the rare ‘Faeder’
 4178 morph was only discovered in 2006 (JUKEMA and PIERSMA, 2006)
 and makes up less than 1% of males. These Faeder males are female
 4180 mimics who hang around the territories of Independents and try to
 ‘sneak’ in matings with females. Faeder males have plumage closely
 4182 resembling that of females and a smaller body size than other males,
 but with larger testicles (presumably to take advantage of rare mating
 4184 opportunities). All three of these morphs, with their complex behav-
 ioural and morphological differences, are controlled by three alleles
 4186 at a single autosomal locus, with the Satellite and Faeder alleles being
 genetically dominant over the high frequency Independent allele. The



Figure 6.20: Lekking Ruffs (*Philomachus pugnax*). Three Independent males, one Satellite male, and one female (or Faeder male?).
 Painting by Johann Friedrich Naumann (1780–1857). Public Domain, wikimedia.

4188 genetic variation for these three morphs is potential maintained by
 negative frequency-dependent selection, as all three male strategies are
 4190 likely at an advantage when they are rare in the population. For ex-
 ample, while the Satellites mostly lose out on mating opportunities to
 4192 Independents, they may have longer life-spans and so may have equal
 life-time reproductive success (WIDEMO, 1998). However, Satellite
 4194 and Faeder males are totally reliant on the lekking Independent males,
 and so both of these alternative strategies cannot become overly com-
 4196 mon in the population. The locus controlling these differences has
 been mapped, and the underlying alleles have persisted for roughly
 4198 four million years (KÜPPER *et al.*, 2016; LAMICHHANEY *et al.*,
 2016). While this mating system is bizarre, the frequency dependent
 4200 dynamics mean that it has been around longer than we’ve been using
 stone tools.

4202 While these examples may seem somewhat involved, they must be

simple compared to the complex dynamics that maintain the hundreds
 4204 of alleles present at the genes in the Major histocompatibility complex
 (MHC). MHC genes are key to the coordination of the vertebrate
 4206 immune system in response to pathogens, and are likely caught in an
 4208 endless arms race with pathogens adapting to common MHC alleles,
 4208 allowing rare MHC alleles to be favoured. Balancing selection at the
 4210 MHC locus has maintained some polymorphisms for tens of millions
 4210 of years, such that some of your MHC alleles may be genetically more
 4212 closely related to MHC alleles in other primates than they are to
 4212 alleles in your close human friends.

6.0.5 Mutation-selection balance

4214 Mutation is constantly introducing new alleles into the population.
 Therefore, variation can be maintained within a population not only
 4216 if selection is balancing (e.g. through heterozygote advantage or fluctuating selection over time, as we have seen in the previous section),
 4218 but also due to a balance between mutation introducing deleterious
 alleles and selection acting to purge these alleles from the population
 4220 (HALDANE, 1937). To study mutation-selection balance, we return to
 the model of directional selection, where allele A_1 is advantageous, i.e.

genotype	A_1A_1	A_1A_2	A_2A_2
absolute fitness	W_{11}	$\geq W_{12} \geq$	W_{22}
relative fitness	$w_{11} = 1$	$w_{12} = 1 - sh$	$w_{22} = 1 - s.$

We'll begin by considering the case where allele A_2 is not completely
 4224 recessive ($h > 0$), so that the heterozygotes suffer at least some dis-
 advantage. We denote by $\mu = \mu_{1 \rightarrow 2}$ the mutation rate per generation
 4226 from A_1 to the deleterious allele A_2 , and assume that there is no re-
 4228 verse mutation ($\mu_{2 \rightarrow 1} = 0$). Let us assume that selection against A_2 is
 4228 relatively strong compared to the mutation rate, so that it is justified
 4230 to assume that A_2 is always rare, i.e. $q_t = 1 - p_t \ll 1$. Compared to
 4230 previous sections, for mathematical clarity, we also switch from fol-
 4232 lowing the frequency p_t of A_1 to following the frequency q_t of A_2 . Of
 course, this is without loss of generality. The change in frequency of
 4232 A_2 due to selection can be written as

$$\Delta_S q_t = \frac{\bar{w}_2 - \bar{w}_1}{\bar{w}} p_t q_t \approx -hsq_t. \quad (6.46)$$

4234 This approximation can be found by assuming that $q^2 \approx 0$, $p \approx 1$,
 and that $\bar{w} \approx w_1$. All of these assumptions make sense if $q \ll 1$.
 4236 From eqn. (6.46) we see that selection acts to reduce the frequency of
 4238 A_2 (as both h and s are positive), and it does so geometrically across
 the generations. That is, if the initial frequency of A_2 is q_0 , then its
 frequency at time t is approximately

$$q_t = q_0(1 - hs)^t. \quad (6.47)$$

⁴²⁴⁰ We will now consider the change in frequency induced by mutation.
 Recalling that μ is the mutation rate from A_1 to A_2 per generation,
⁴²⁴² the frequency of A_2 after mutation is

$$q' = \mu p_t + q_t = \mu(1 - q_t) + q_t. \quad (6.48)$$

⁴²⁴⁴ Assuming that $\mu \ll 1$ and that $q \ll 1$, the change in the frequency of allele A_2 due to mutation ($\Delta_M q_t$) can be approximated by

$$\Delta_M q_t = q' - q_t = \mu. \quad (6.49)$$

⁴²⁴⁶ Hence, when A_2 is rare and the mutation rate is low, mutation acts to linearly increase the frequency of the deleterious allele A_2 .

⁴²⁴⁸ If selection is to balance deleterious mutation, their combined effect over one generation has to be zero. Therefore, to find the mutation–selection equilibrium, we set

$$\Delta_M q_t + \Delta_S q_t = 0, \quad (6.50)$$

⁴²⁵⁰ insert eqns. (6.46) and (6.49), and solve for q to obtain

$$q_e = q_t = \frac{\mu}{hs}. \quad (6.51)$$

We see that the frequency of the deleterious allele A_2 is balanced at a frequency equal to the mutation rate (μ) divided by the reduction in relative fitness in the heterozygote (hs).

⁴²⁵⁴ It is worth pointing out that the fitness of the $A_2 A_2$ homozygote has not entered this calculation, as A_2 is so rare that it is hardly ever found in the homozygous state. Therefore, if A_2 has any deleterious effect in a heterozygous state (i.e. if $h > 0$), it is this effect that determines the frequency at which A_2 is maintained in the population. Also, note that by writing the total change in allele frequency as $\Delta_M q_t + \Delta_S q_t$ we have implicitly assumed that we can ignore terms of order $\mu \times s$. That is, we have assumed that mutation and selection are both relatively weak. This assumption is valid under our prior assumption that both μ and s are small.

⁴²⁶⁴ If an allele is truly recessive (although few likely are), we have $h = 0$, and so eqn. (6.51) is not valid. However, we can make an argument similar to the one above to show that, for truly recessive alleles,

$$q_e = \sqrt{\frac{\mu}{s}}. \quad (6.52)$$

⁴²⁶⁸ **Question 11.** Oblong-winged katydids (*Amblycorypha oblongifolia*) are usually green. However, some are bright pink, thanks to an erythrism mutation (a nice example of early Mendelian reasoning in a wonderfully titled paper²). This pink condition is thought to be due



Figure 6.21: Oblong-winged katydid. Field book of insects (1918). Lutz, F.E. Illustrations by Edna L. Beutemüller. Image from the Biodiversity Heritage Library. Contributed by MBLWHOI Library. Not in copyright.

² WHEELER, W. M., 1907 Pink Insect Mutants. The American Naturalist 41(492): 773–780

4272 to a dominant mutation (Crew, 2013). Assume that roughly one in
 4274 ten thousand katydids is bright pink and that the mutation rate at the
 gene underlying this condition is 10^{-5} . What is the relative fitness of
 heterozygotes for the pink mutation?

4276 *The genetic load of deleterious alleles* What effect do such deleterious
 mutations at mutation-selection balance have on the population? It
 4278 is common to quantify the effect of deleterious alleles in terms of a
 reduction of the mean relative fitness of the population. For a single
 4280 site at which a deleterious mutation is segregating at frequency $q_e =$
 $\mu/(hs)$, the population mean relative fitness is reduced to

$$\bar{w} = 1 - 2p_e q_e hs - q_e^2 s \approx 1 - 2\mu. \quad (6.53)$$

4282 Somewhat remarkably, the drop in mean fitness due to a site segregating at mutation-selection balance is independent of the selection
 4284 coefficient against the heterozygote; it depends only on the mutation rate. Intuitively this is because, given a fixed mutation rate, less deleterious alleles can rise to a higher equilibrium frequency, and thus contribute the same total load as more deleterious (rarer) alleles, but
 4286 this load is spread across more individuals in the population. Note
 4288 that this result applies only if the mutation is not totally recessive, i.e.
 4290 if $h > 0$.

A fitness reduction of 2μ is very small, given that the mutation
 4292 rate of a gene is likely $< 10^{-5}$. However, if there are many loci segregating at mutation-selection balance, small fitness reductions can
 4294 accumulate to a substantial so-called genetic load, a major cause of variation in fitness-related traits among individuals. For example,
 4296 the human genome contains over twenty thousand genes, and many other functional regions, the vast majority of which will be subject
 4298 to purifying selection against mutations that disrupt their function. In humans, most loss of function (LOF) variants, which severely disrupt a protein-coding gene, are found at low frequencies. However,
 4300 each human genome typically carries over a hundred LOF variants (MACARTHUR *et al.*, 2012; LEK *et al.*, 2016). Not every LOF allele will be deleterious; some could even be advantageous. However, the
 4302 combined load of these LOF alleles must on average lower our fitness, otherwise selection wouldn't be removing them from the population.
 4304 Each one of us carries a unique set of these LOF alleles, usually in a heterozygous state. We differ slightly in how many of these alleles we
 4306 carry. For example, the left side of Figure 6.22 shows the distribution
 4308 of the number of LOF alleles carried by 769 individuals of Dutch ancestry. The individuals who carry fewer of these LOF alleles will on average have higher fitness than those individuals with more.

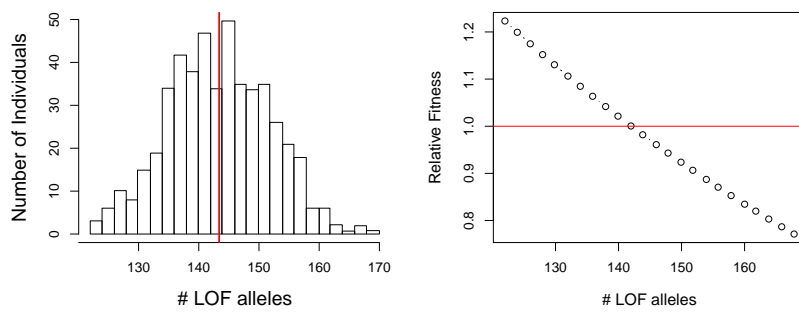


Figure 6.22: **Left)** The distribution of LOF alleles in 769 individuals from the Genome of the Netherlands project. Data from FRANCIOLI *et al.*. The average individual (red line) carries 144 LOF alleles. **Right).** The relative fitness of individuals carrying these varying numbers of LOF alleles, assuming multiplicative selection and a selection coefficient of $sh = 10^{-2}$ acting against these alleles (CASSA *et al.*, 2017). Code here.

4312 How do these differences across individuals in total LOF mutations mount up? Well, if we are willing to assume that the fitness
 4314 costs of deleterious alleles interact multiplicatively, we can make some progress. If an individual who carries one LOF mutation has a fitness
 4316 $1 - hs$, then an individual who's heterozygote for two LOF mutations would have fitness $(1 - hs)^2$, and an individual who is heterozygote
 4318 for L LOF alleles would have fitness $(1 - hs)^L$. The right-hand side of Figure 6.22 shows the predicted fitness of individuals carrying varying
 4320 number of LOF alleles, relative to the mean fitness of the sample, using this multiplicative model. We don't yet know how much lower the
 4322 fitness of these individuals really is, nor do we know how most of these LOF alleles manifest their fitness consequences through disease and
 4324 other mechanisms. However, it's a reasonable guess that this variation in LOF alleles, presumably maintained by mutation-selection balance,
 4326 is a major source of variation in fitness.

6.0.6 Inbreeding depression

4328 All else being equal, eqn. (6.51) suggests that mutations that have a smaller effect in the heterozygote can segregate at higher frequency
 4330 under mutation-selection balance. As a consequence, alleles that have strongly deleterious effects in the homozygous state can still segregate
 4332 at low frequencies in the population, as long as they do not have too strong a deleterious effect in heterozygotes. Thus, outbred populations
 4334 may have many alleles with recessive deleterious effects segregating within them.

4336 **Question 12.** Assume that a deleterious allele has a relative fitness .99 in heterozygotes and a relative fitness 0.2 when present in
 4338 the homozygote state. Assume that the deleterious allele is at a frequency 10^{-3} at birth and the genotype frequencies follow from HWE.
 4340 Only considering the fitness effects of this locus, and measuring fitness

relative to the most fit genotype, answer the following questions:

- 4342 A) What is the average fitness of an individual in the population?
 B) What is the average fitness of the child of a full-sib mating?

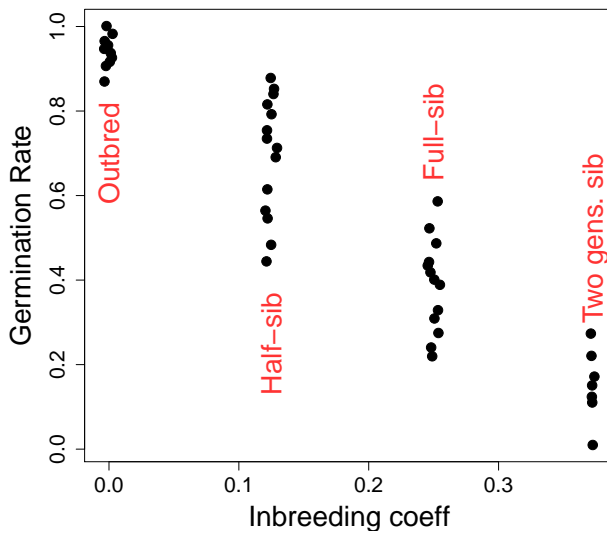


Figure 6.23: Data showing inbreeding depression over different degrees of inbreeding in *S. latifolia*. Each point is the mean seed germination rates for different family crosses. Data from RICHARDS. Code here.

4344 One consequence of segregating for low-frequency recessive deleterious alleles is that inbreeding can reduce fitness. In typically outbred populations, the mean fitness of individuals decreases with the inbreeding coefficient, i.e. so-called 'inbreeding depression' is a common observation. This wide-spread observation dates back to systematic surveys of inbreeding depression by DARWIN (1876). Inbreeding depression is likely primarily a consequence of being homozygous at many loci for alleles with recessive deleterious effects.

4352 One example of inbreeding depression is shown in Figure 6.23. White campion (*Silene latifolia*) is a dioecious flowering plant; dioecious means that the males and females are separate individuals. RICHARDS performed crosses to create offspring who were outbred, the offspring of half-sibs, full-sibs, and of two generations of full-sib mating. He measured their germination success, which is plotted in Figure 6.23. Note how the fitness of individuals declines with increased inbreeding.

4360 *Purging the inbreeding load.* Populations that regularly inbreed over sustained periods of time are expected to partially purge this load of deleterious alleles. This is because such populations have exposed many of these alleles in a homozygous state, and so selection can more readily remove these alleles from the population.

If the population has sustained inbreeding, such that individuals in the population have an inbreeding coefficient F , deleterious alle-

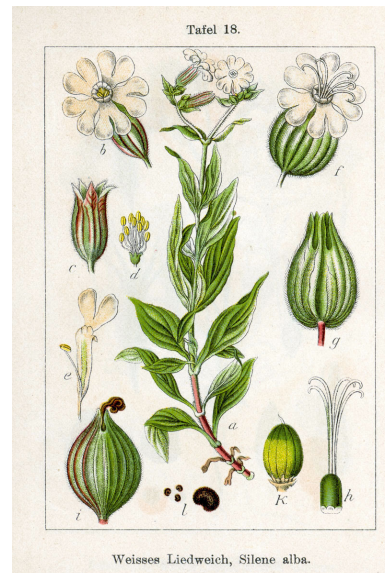


Figure 6.24: White campion (*S. latifolia*).
 Deutschlands Flora in Abbildungen (1796). Johann Georg Sturm (Painter: Jacob Sturm). Public Domain, wikimedia.

les at each locus will find a new equilibrium frequency. Assuming
 4368 the mutation-selection model, now with inbreeding, the equilibrium
 frequency is

$$q_e = \frac{\mu}{(h(1 - F) + F)s} \quad (6.54)$$

4370 The frequency of the deleterious allele is decreased due to the al-
 lele now being expressed in homozygotes, and therefore exposed to
 4372 selection, more often due to inbreeding. Thus, all else being equal,
 populations with a high degree of inbreeding will purge their load.

4374 6.0.7 Migration-selection balance

Another reason for the persistence of deleterious alleles in a population
 4376 is that there is a constant influx of maladaptive alleles from other pop-
 ulations where these alleles are locally adaptive. Migration-selection
 4378 balance seems unlikely to be as broad an explanation for the persis-
 tence of deleterious alleles genome-wide as mutation-selection balance.
 4380 However, a brief discussion of such alleles is worthwhile, as it helps to
 inform our ideas about local adaptation.

4382 Local adaptation can occur over a range of geographic scales. Lo-
 cal adaptation is relatively unimpeded by migration at broad geo-
 4384 graphically scales, where selection pressures change more slowly than
 distances over which individuals typically migrate over a number of
 4386 generations. Adaptation can, however, potentially occur on much finer
 geographic scales, from kilometers down to meters in some species. On
 4388 such small scales, dispersal is surely rapidly moving alleles between
 environments, but local adaptation is maintained by the continued
 4390 action of selection. An example of adaptation at fine-scales is shown in
 Figure 6.26 . JAIN and BRADSHAW (1966) studied the patterns of
 4392 heavy-metal resistance in plants on mine tailings and in nearby mead-
 ows, a set of classic studies of population differences maintained by
 4394 local adaptation to different soils. Even at these very short geo-
 graphically scales, over which seed and pollen will definitely move, we see
 4396 strong local adaptation. Zinc-intolerant alleles are nearly absent from
 the mine tailings because they prevent plants from growing on these
 4398 zinc-heavy soils; conversely, zinc-tolerant alleles do not spread into
 the meadow populations, likely due to some trade-off or fitness cost of
 4400 zinc-tolerance.

As a first pass at developing a model of local adaptation, let's con-
 4402 sider a haploid two-allele model with two different populations, see
 Figure 6.27, where the relative fitnesses of our alleles are as follows

allele	1	2
population 1	1	1-s
population 2	1-s	1



Figure 6.25: Sweet vernal grass (*Anthoxanthum odoratum*).
 Billeder af nordens flora (1917). Mentz, A & Ostenfeld, C H. Image from the Biodiversity Heritage Library. Contributed by New York Botanical Garden. Not in copyright.

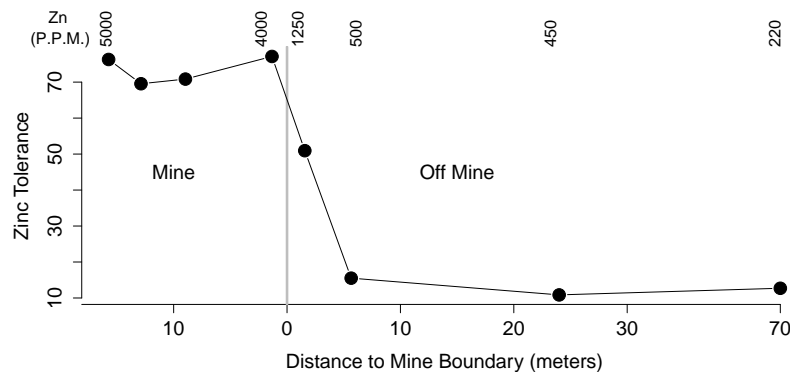


Figure 6.26: Data showing the Zinc tolerance of *Anthoxanthum odoratum* on and off of the Trelogan Mine, Flintshire, North Wales. The numbers along the top give the soil contamination of Zinc in parts per million. Data from JAIN and BRADSHAW (1966). Code here.

As a simple model of migration, let's suppose within a population a fraction of m individuals are migrants from the other population, and $1 - m$ individuals are from the same population.

To quickly sketch an equilibrium solution to this scenario, we'll take an approach analogous to our mutation-selection balance model. To do this, let's assume that selection is strong compared to migration ($s \gg m$), such that allele 1 will be almost fixed in population 1 and allele 2 will be almost fixed in population 2. If that is the case, migration changes the frequency of allele 2 in population 1 (q_1) by

$$\Delta_{Mig.} q_1 \approx m \quad (6.55)$$

while as noted above $\Delta_S q_1 = -sq_1$, so that migration and selection are at an equilibrium when $0 = \Delta_S q_1 + \Delta_{Mig.} q_1$, i.e. an equilibrium frequency of allele 2 in population 1 of

$$q_{e,1} = \frac{m}{s} \quad (6.56)$$

Here, migration is playing the role of mutation and so migration-selection balance (at least under strong selection) is analogous to mutation-selection balance.

We can use this same model by analogy for the case of migration-selection balance in a diploid model. For the diploid case, we replace our haploid s by the cost to heterozygotes hs from our directional selection model, resulting in a diploid migration-selection balance equilibrium frequency of

$$q_{e,1} = \frac{m}{hs} \quad (6.57)$$

As an example of fine-scale local adaptation due to a single locus, consider the case of the rock pocket mice adapting to lava flows. Throughout the deserts of the American Southwest there are old lava flows, where the rocks and soils are much dark than the surrounding desert.

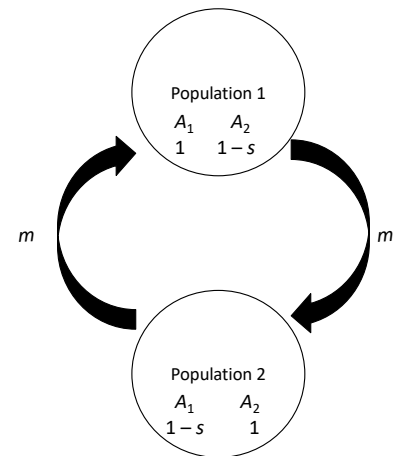


Figure 6.27: Setup of a two-population haploid model of local adaptation.

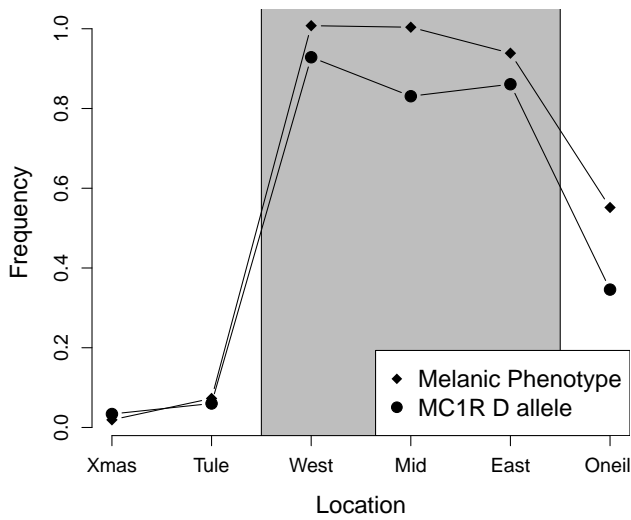


Figure 6.28: Frequency of melanic mice on the lava flow, and at nearby locations (diamonds). Frequency of MC1R melanic allele at same locations. Data from HOEKSTRA *et al.* (2004). Code here.

Many populations of small animals that live on these flows have evolved darker pigmentation to be cryptic against this dark substrate and better avoid visual predators. One example of such a locally adapted population are the rock pocket mice (*Chaetodipus intermedius*) who live on the Pinacate lava flow on the Arizona-Mexico border, studied by HOEKSTRA *et al.* (2004). These mice have much darker, more melanic pelts than the mice who live on nearby rocky outcrops (see Figure 6.28). NACHMAN *et al.* (2003) determined that a dominant allele (*D*) at MC1R is the primary determinant of this melanic phenotype. The frequency of this allele across study sites is shown in Figure 6.28. HOEKSTRA *et al.* (2004) found that other, unlinked markers showed little differentiation over these populations, suggesting that the migration rate is high.

Question 13. HOEKSTRA *et al.* (2004) found that the dark *D* allele was at 3% frequency at the Tule Mountains study site. Using F_{ST} -based approaches, for unlinked markers, they estimated that the per individual migration rate was $m = 7.0 \times 10^{-4}$ per generation between this site and the Pinacate lava flow. What is the selection coefficient acting against the dark *D* allele at the Tule Mountains site?

The width of a genetic cline. We can also extend these ideas beyond our discrete model to a model of a population spread out on a land-



Figure 6.29: Two species from the genus *Chaetodipus*, pocket mice, formerly known as *Perognathus*. Wild animals of North America, intimate studies of big and little creatures of the mammal kingdom (1918), Nelson, E. W. Image from the Biodiversity Heritage Library. Contributed by American Museum of Natural History Library. Not in copyright.

4452 scape where individuals migrate in a more continuous fashion. For
 4453 simplicity, let's assume a one dimensional habitat, where the habitat
 4454 makes a sharp transition in the middle of our region. You could imagine
 4455 this to be a set of populations sampled along a transect through
 4456 some environmental transition. Our individuals disperse to live on
 4457 average σ miles away from where they were born (we can think of this
 4458 as our individuals migrating a random distance drawn from a normal
 4459 distribution, with mean zero, and σ being the standard deviation of
 4460 this distribution). . We'll think of a bi-allelic model where the ho-
 4461 mozygotes for allele 1 have an additive selective advantage s over allele
 4462 2 homozygotes to the east of our habitat transition (left of zero in
 4463 Figure 6.30). This flips to allele 2 having the same advantage s west
 4464 of the transition (right of zero). If you've read this send Prof Coop a
 4465 picture of the East and West Beast.

"Upon an island hard to reach, the
 East Beast sits upon his beach. Upon
 the west beach sits the West Beast.
 Each beach beast thinks he's the best
 beast." – Theodor Seuss Geisel

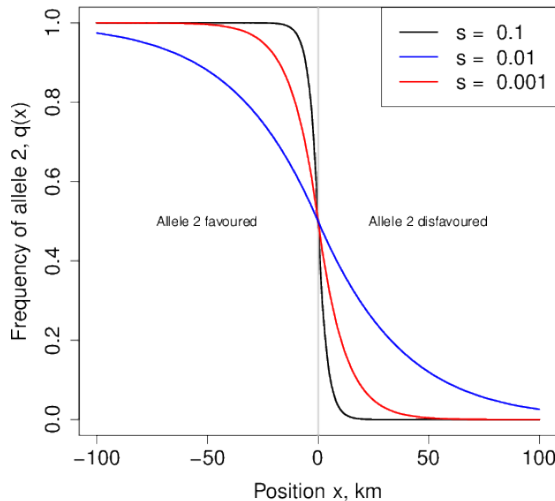


Figure 6.30: An equilibrium cline in allele frequency (the frequency of allele 2, $q(\cdot)$) is shown). Our individuals disperse an average distance of $\sigma = 1$ miles per generation, and our allele 2 has a relative fitness of $1 + s$ and $1 - s$ on either side of the environmental change at $x = 0$. Code here.

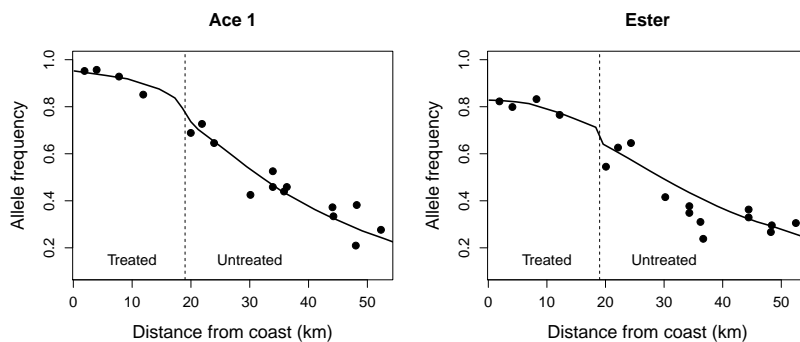
4466 With this setup, we get an equilibrium distribution of our two alle-
 4467 les, where to the left of zero our allele 2 is at higher frequency, while
 4468 to the right of zero allele 1 predominates. As we cross from the left to
 4469 the right side of our range, the frequency of our allele 2 decreases in
 4470 a smooth cline. The frequency of allele 2, $q(\cdot)$, is shown as a function
 4471 of location along the cline for a variety of selection coefficients (s) in
 4472 Figure 6.30. The width of this cline, i.e. the geographic distance over
 4473 which the allele frequency changes, depends on the relative strengths
 4474 of dispersal and selection. If selection is strong compared to dispersal,
 4475 then selection acts to remove maladaptive alleles much faster than
 4476 migration acts to move alleles across the environmental transition.
 Thus the allele frequency transition would be very rapid, and the cline

4478 narrow, as we move across the environmental transition. In contrast,
 4480 if individuals disperse long distances and selection is weak, many alleles
 4482 are being moved back and forth over the environmental transition
 much faster than selection can act against these alleles and so the cline
 would be very wide.

4484 The width of our cline, i.e. the distance over which we make this
 shift from allele 2 to allele 1 predominating, can be defined in a num-
 4486 ber of different ways. One way to define the cline width, which is
 simple to define but perhaps hard to measure accurately, is via the
 slope (i.e. the tangent) of $q(x)$ at $x = 0$. See Figure 6.31. Under this
 4488 definition, the cline width is approximately

$$0.6\sigma/\sqrt{s} \text{ miles}, \quad (6.58)$$

4490 note that the units are miles here just because we defined the average
 dispersal distance (σ) in miles above. Thus the cline will be wider
 4492 if individuals disperse further, higher σ , and if selection is weaker,
 smaller s . The appendix below talks through the math underlying
 these ideas in more detail.



4494 LENORMAND *et al.* (1999) collected mosquitoes (*Culex pipiens*)
 in a north-south transect moving away from the Southern French
 4496 coast. Areas near the coast were treated with pesticides, and the
 mosquitoes have evolved resistance, but areas just a few tens of kilo-
 4498 meters from the coast were untreated. LENORMAND *et al.* estimated
 the frequency of two unlinked, pesticide-resistance alleles, and found
 4500 them at high frequency near the coast but found that their frequencies
 declined rapidly moving inland. LENORMAND *et al.* fit migration-
 4502 selection cline models to their data, similar to those in Figure 6.30,
 with the pesticide-resistance alleles having an selection advantage (s)
 4504 in treated areas an a cost (c) in untreated areas (they didn't enforce
 the selective advantage and cost being symmetric).

4506 They estimated that a higher selective advantage for the Ace 1
 allele than Ester allele ($s = 0.33$ and $s = 0.19$ respectively) and a

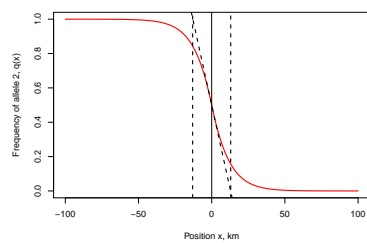


Figure 6.31: An equilibrium cline in allele frequency from Figure 6.30, $s = 0.01$. Vertical lines show the cline width. The diagonal line show the tangent to the cline at its midpoint. Code here.

Figure 6.32: Allele frequency clines of two pesticide resistance alleles, at the Ace 1 and Ester genes, in the mosquito *Culex pipiens*. The dotted line shows where we move from pesticide-treated to untreated areas as we move away from the French coast. The dots show observed allele frequencies, the solid lines clines fit under a migration-selection balance model of a cline. These allele frequencies represent collections over two summers, the frequencies of the alleles are substantially reduced in the winter due to the reduced use of pesticides. Data from LENORMAND *et al.* (1999). Code here.

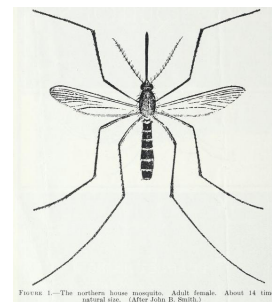


Figure 6.33: mosquito (*Culex pipiens*). Domestic mosquitoes (1939). Bishopp, F. C. Image from the Biodiversity Heritage Library. Contributed by U.S. Department of Agriculture, National Agricultural Library. Not in copyright.

higher cost to the Ace 1 allele than Ester allele in untreated areas ($c = 0.11$ and $c = 0.7$ respectively) potentially explaining the less extreme cline for Ester allele than the Ace 1 allele. Despite these strong selection pressures we still see a cline over tens of kilometers because dispersal is relatively high ($\sigma = 6.6\text{km}$ per generation).

Hybrid zones Local adaptation isn't the only way that selection can generate strong spatial patterns. We can also see strong selection-driven clines when partially-reproductively isolated species spread back in to secondary contact they can hybridize bringing alleles together that may not work well with each other. One simple model of is to think about an under-dominant polymorphism, i.e. where the heterozygote has lower fitness. The two ancestral populations are alternatively fixed for the two fitter homozygote states, e.g. ancestral population 1 fixed A_1A_1 and ancestral population two the A_2A_2 . The hybrid population forming at the mating edge between the two ancestral populations has a high frequency of the less fit heterozygotes. Thus hybrids are at a disadvantage, potentially acting to keep the two populations from collapsing into each other.

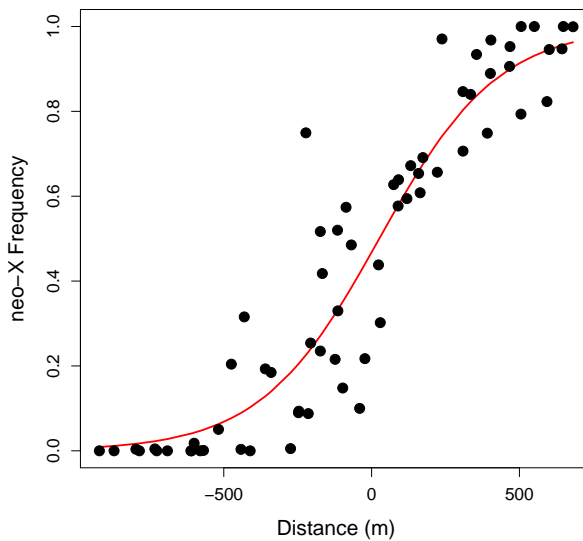
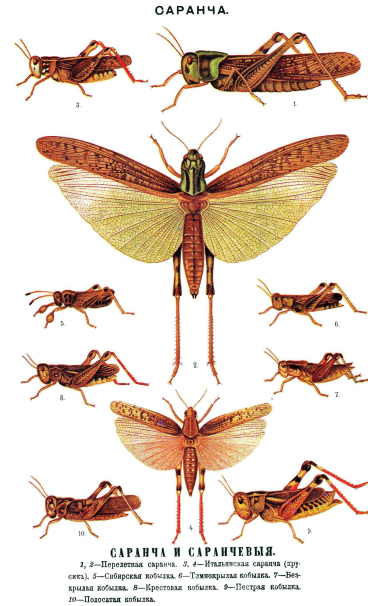


Figure 6.34: The frequency of the southern neo-X chromosome moving along a valley transect (more southern locations to the right of the graph). This represents data from four different valleys in the French Alps over less than a kilometer, each point represents a sample of 20 males. The red curve is the fitted cline under a model of heterozygote disadvantage (BAZIKIN, 1969). Data from BARTON and HEWITT (1981), Code here.



Two previously isolated populations of the short-horned grasshopper *Podisma pedestris* have spread into secondary contact in the French Alps, probably after the last ice age. The population that has spread into the Alps from the south has a large section of novel X chromosome, due to a chromosomal fusion. This 'neo-X' is absent in the populations that spread from the North into the Alps. The two

Figure 6.35: 7. *Podisma pedestris*, a species of short-horned grasshoppers; from a page illustrating *Orthoptera*. Illustration from Brockhaus and Efron Encyclopedic Dictionary (1890) Image wikimedia, public domain.

4532 populations meet in many valleys running through the Alps, and re-
 peated form a narrow hybrid zone, with the frequency of the neo-X
 4534 chromosome forming a very steep cline transitioning in frequency over
 a few hundred meters (BARTON and HEWITT, 1981). One potential
 4536 reason for this steep cline is that females who are heterozygous for
 the neo-X (neo-X/old-X) may have reduced fitness, consistent with an
 4538 underdominant polymorphism. The neo-X allele cannot spread into
 the northern population as it cannot increase in frequency when rate.
 4540 Conversely the northern population cannot displace the neo-X, as the
 old-X is at a disadvantage. This spatial distribution at this locus is a
 4542 tension zone between the two populations, where neither population
 can make ground on the other due to the low fitness of the hybrid.

4544 We can use our same continuous model of migration and selection
 to study this setup. Assuming that the homozygotes are equally fit,
 4546 and that the heterozygotes relative fitness is reduced by a selection
 coefficient s_h , the width of the cline is

$$\frac{\sigma}{\sqrt{s_h}} \quad (6.59)$$

4548 The stronger the selection the more abrupt the transition between
 the populations. These wingless grasshoppers move $\sigma \sim 20$ meters
 4550 a generation. Thus a reduction in the relative fitness of the hybrid
 would be needed to explain this hybrid zone with a width of ~ 800 m.

4552 More generally we can see tension zones arise when hybrids have re-
 duced fitness compared to either species. For example, this can occur
 4554 due to be due to bad epistatic interactions between alleles from each
 species. If selection is strong enough on hybrids, often because many
 4556 loci are involved in incompatibilities between the species, the entire
 genome can be tied up in a tension zone between the two species.

4558 *Appendix: Some theory of the spatial distribution of allele frequen-
 cies under deterministic models of selection*

4560 Imagine a continuous haploid population spread out along a line. Each
 individual disperses a random distance Δx from its birthplace to the
 4562 location where it reproduces, where Δx is drawn from the probabili-
 ty density $g(\cdot)$. To make life simple, we will assume that $g(\Delta x)$ is
 4564 normally distributed with mean zero and standard deviation σ , i.e.
 migration is unbiased and individuals migrate an average distance of
 4566 σ .

The frequency of allele 2 at time t in the population at spatial lo-
 4568 cation x is $q(x, t)$. Assuming that only dispersal occurs, how does our
 allele frequency change in the next generation? Our allele frequency in
 4570 the next generation at location x reflects the migration from different
 locations in the proceeding generation. Our population at location x

4572 receives a contribution $g(\Delta x)q(x + \Delta x, t)$ of allele 2 from the popula-
tion at location $x + \Delta x$, such that the frequency of our allele at x in
4574 the next generation is

$$q(x, t + 1) = \int_{-\infty}^{\infty} g(\Delta x)q(x + \Delta x, t)d\Delta x. \quad (6.60)$$

To obtain $q(x + \Delta x, t)$, let's take a Taylor series expansion of $q(x, t)$:

$$q(x + \Delta x, t) = q(x, t) + \Delta x \frac{dq(x, t)}{dx} + \frac{1}{2}(\Delta x)^2 \frac{d^2q(x, t)}{dx^2} + \dots \quad (6.61)$$

4576 then

$$q(x, t+1) = q(x, t) + \left(\int_{-\infty}^{\infty} \Delta x g(\Delta x) d\Delta x \right) \frac{dq(x, t)}{dx} + \frac{1}{2} \left(\int_{-\infty}^{\infty} (\Delta x)^2 g(\Delta x) d\Delta x \right) \frac{d^2q(x, t)}{dx^2} + \dots \quad (6.62)$$

Because $g(\)$ has a mean of zero, $\int_{-\infty}^{\infty} \Delta x g(\Delta x) d\Delta x = 0$, and has
4578 because $g(\)$ has variance σ^2 , $\int_{-\infty}^{\infty} (\Delta x)^2 g(\Delta x) d\Delta x = \sigma^2$. All higher
order terms in our Taylor series expansion cancel out (as all high
4580 moments of the normal distribution are zero). Looking at the change
in allele frequency, $\Delta q(x, t) = q(x, t + 1) - q(x, t)$, so

$$\Delta q(x, t) = \frac{\sigma^2}{2} \frac{d^2q(x, t)}{dx^2} \quad (6.63)$$

4582 This is a diffusion equation, so that migration is acting to smooth
out allele frequency differences with a diffusion constant of $\frac{\sigma^2}{2}$. This is
4584 exactly analogous to the equation describing how a gas diffuses out to
equal density, as both particles in a gas and our individuals of type 2
4586 are performing Brownian motion (blurring our eyes and seeing time as
continuous).

4588 We will now introduce fitness differences into our model and set the
relative fitnesses of allele 1 and 2 at location x to be 1 and $1 + s\gamma(x)$.
4590 To make progress in this model, we'll have to assume that selection
isn't too strong, i.e. $s\gamma(x) \ll 1$ for all x . The change in frequency of
4592 allele 2 obtained within a generation due to selection is

$$q'(x, t) - q(x, t) \approx s\gamma(x)q(x, t)(1 - q(x, t)) \quad (6.64)$$

i.e. logistic growth of our favoured allele at location x . Putting our
4594 selection and migration terms together, we find the total change in
allele frequency at location x in one generation is

$$q(x, t + 1) - q(x, t) = s\gamma(x)q(x, t)(1 - q(x, t)) + \frac{\sigma^2}{2} \frac{d^2q(x, t)}{dx^2} \quad (6.65)$$

4596 In deriving this result, we have essentially assumed that migration
acted upon our original allele frequencies before selection, and in doing
4598 so have ignored terms of the order of σs .

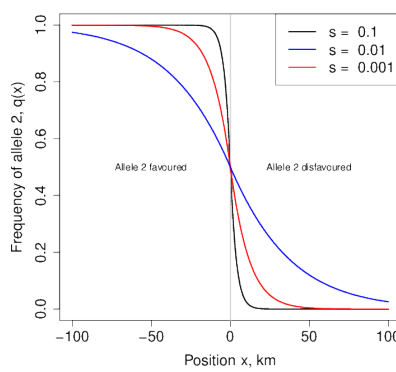


Figure 6.36: An equilibrium cline in allele frequency. Our individuals disperse an average distance of $\sigma = 1\text{km}$ per generation, and our allele 2 has a relative fitness of $1 + s$ and $1 - s$ on either side of the environmental change at $x = 0$.

The cline in allele frequency associated with a sharp environmental transition. To make progress, let's consider a simple model of local adaptation where the environment abruptly changes. Specifically, we assume that $\gamma(x) = 1$ for $x < 0$ and $\gamma(x) = -1$ for $x \geq 0$, i.e. our allele 2 has a selective advantage at locations to the left of zero, while this allele is at a disadvantage to the right of zero. In this case we can get an equilibrium distribution of our two alleles, where to the left of zero our allele 2 is at higher frequency, while to the right of zero allele 1 predominates. As we cross from the left to the right side of our range, the frequency of our allele 2 decreases in a smooth cline.

Our equilibrium spatial distribution of allele frequencies can be found by setting the left-hand side of eqn. (6.65) to zero to arrive at

$$s\gamma(x)q(x)(1-q(x)) = -\frac{\sigma^2}{2} \frac{d^2q(x)}{dx^2} \quad (6.66)$$

We then could solve this differential equation with appropriate boundary conditions ($q(-\infty) = 1$ and $q(\infty) = 0$) to arrive at the appropriate functional form for our cline. While we won't go into the solution of this equation here, we can note that by dividing our distance x by $\ell = \sigma/\sqrt{s}$, we can remove the effect of our parameters from the above equation. This compound parameter ℓ is the characteristic length of our cline, and it is this parameter which determines over what geographic scale we change from allele 2 predominating to allele 1 predominating as we move across our environmental shift.

Cline arising from an underdominant polymorphism

7

The Impact of Genetic Drift on Selected Alleles

4622 “Natural selection is a mechanism for generating an exceedingly high
4624 degree of improbability.” –R.A. Fisher

In the previous chapter we assumed that the selection acting on our
4626 alleles was strong enough that we could ignore the action of genetic
drift in shaping allele frequencies. However, genetic drift affects all al-
4628 leles, and so in this chapter we explore the interaction of selection and
drift. Strongly selected alleles can be lost from the population via drift
4630 when they are rare in the population, while both weakly beneficial and
weakly deleterious alleles are subject to the random whims of genetic
4632 drift throughout their entire time in the population. Understanding
the interaction of selection and genetic drift is key to understand-
4634 ing the extent to which small populations may be mutation-limited
in their rates of adaptation, and how rates of molecular and genome
4636 evolution may differ across taxa.

7.1 Stochastic loss of strongly selected alleles

4638 Even strongly beneficial alleles can be lost from the population when
they are sufficiently rare. This is because the number of offspring left
4640 by individuals to the next generation is fundamentally stochastic. A
selection coefficient of $s=1\%$ is a strong selection coefficient, which can
4642 drive an allele through the population in a few hundred generations
once the allele is established. However, if individuals have on average a
4644 small number of offspring per generation, the first individual to carry
our beneficial allele, who has on average 1% more children than their
4646 peers, could easily have zero offspring, leading to the loss of our allele
before it ever gets a chance to spread.

4648 To take a first stab at this problem, let’s think of a very large hap-
loid population in which a single individual starts with the selected
4650 allele, and ask about the probability of eventual loss of our selected
allele starting from this single copy. To derive this probability of loss
4652 (p_L), we’ll make use of a simple argument (derived from branching

processes FISHER, 1923; HALDANE, 1927). Our selected allele will be eventually lost from the population if every individual with the allele fails to leave descendants. Well we can think about different cases:

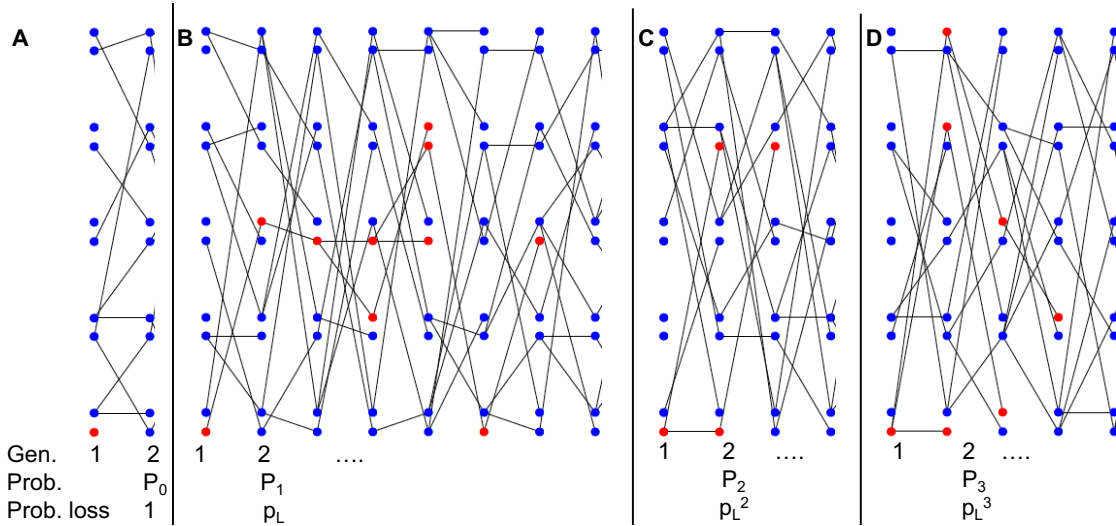


Figure 7.1: Four different outcomes of a selected allele present as a single copy in the population, leaving zero, one, two, three offspring in the next generation.

- 4654 1. In our first generation, with probability P_0 our individual allele leaves no copies of itself to the next generation, in which case our allele is lost (Figure 7.1A).
- 4658 2. Alternatively, our allele could leave one copy of itself to the next generation (with probability P_1), in which case with probability p_L this copy eventually goes extinct (Figure 7.1B).
- 4662 3. Our allele could leave two copies of itself to the next generation (with probability P_2), in which case with probability p_L^2 both of these copies eventually go extinct (Figure 7.1C).
- 4664 4. More generally, our allele could leave k copies ($k > 0$) of itself to the next generation (with probability P_k), in which case with probability p_L^k all of these copies eventually go extinct (e.g. Figure 7.1D).

Summing over these probabilities, we see that

$$p_L = \sum_{k=0}^{\infty} P_k p_L^k \quad (7.1)$$

- 4670 5. We'll now need to specify P_k , the probability that an individual carrying our selected allele has k offspring. In order for this population to stay constant in size, we'll assume that individuals without the selected mutation have on average one offspring per generation, while

⁴⁶⁷⁴ individuals with our selected allele have on average $1 + s$ offspring per generation. We'll assume that the number of offspring an individual has is Poisson distributed with mean given by 1 or $1 + s$, i.e. the probability that an individual with the selected allele has i children is

$$P_i = \frac{(1+s)^i e^{-(1+s)}}{i!} \quad (7.2)$$

Substituting P_k into the equation above, we see

$$\begin{aligned} p_L &= \sum_{k=0}^{\infty} \frac{(1+s)^k e^{-(1+s)}}{k!} p_L^k \\ &= e^{-(1+s)} \left(\sum_{k=0}^{\infty} \frac{(p_L(1+s))^k}{k!} \right) \end{aligned} \quad (7.3)$$

⁴⁶⁷⁸ The term in the brackets is itself an exponential expansion, so we can rewrite this equation as

$$p_L = e^{(1+s)(p_L - 1)} \quad (7.4)$$

⁴⁶⁸⁰ Solving for p_L would give us our probability of loss for any selection coefficient. Let's rewrite our result in terms of the probability of escaping loss, $p_F = 1 - p_L$. We can rewrite eqn. (7.4) as

$$1 - p_F = e^{-p_F(1+s)} \quad (7.5)$$

To gain an approximate solution for this result, let's consider a small selection coefficient $s \ll 1$ such that $p_F \ll 1$ and then use a Taylor series to expand out the exponential on the right hand side (ignoring terms of higher order than s^2 and p_F^2):

$$1 - p_F \approx 1 - p_F(1 + s) + p_F^2(1 + s)^2/2 \quad (7.6)$$

Solving this we find that

$$p_F = 2s. \quad (7.7)$$

⁴⁶⁸⁸ Thus even an allele with a 1% selection coefficient has a 98% probability of being lost when it is first introduced into the population by mutation.

If the mutation rate towards our advantageous allele is μ , and there are N individuals in our haploid population, then $N\mu$ advantageous mutations arise per generation. Each of these new beneficial mutations has a probability p_F of fixing. Thus the number of advantageous mutations arising per generation that will eventually fix in the population is $N\mu p_F$, and the waiting time for a mutation that will fix to arise is the reciprocal of this: $1/N\mu p_F$. Thus, in adapting to a novel selection pressure via new mutations, the population size, the mutational target size, and the selective advantage of new mutations all matter. One

4700 reason why combinations of drugs are used against viruses like HIV
 4701 and malaria is that, even if the viruses adapt to one of the drugs, the
 4702 viral load (N) of the patient is greatly reduced, making it very un-
 4703 likely that the population will manage to fix a second drug-resistant
 4704 allele.

Diploid model of stochastic loss of strongly selected alleles. We can
 4706 also adapt this result to a diploid setting. Assuming that heterozy-
 4707 gotes for the 1 allele have on average $1 + hs$ children, the probability
 4708 allele 1 is not lost, starting from a single copy in the population, is

$$p_F = 2hs \quad (7.8)$$

for $h > 0$. Note this is a slightly different parameterization from our
 4710 diploid model in the previous chapter; here h is the dominance of our
 4711 positively selected allele, with $h = 1$ corresponding to the full se-
 4712 lective advantage expressed in an individual with only a single copy.
 Thus the probability that a beneficial allele is not lost depends just
 4714 on the relative fitness advantage of the heterozygote; this is because
 4716 when the allele is rare it is usually present in heterozygotes and so its
 4718 probability of escaping loss just depends on the fitness of these indi-
 viduals compared to homozygotes for the ancestral allele (assuming an
 outbred population).

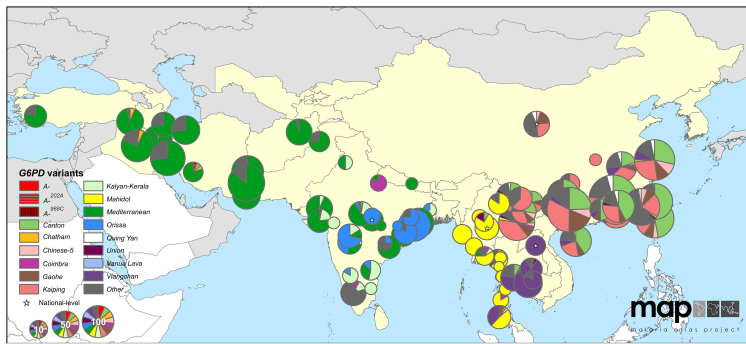


Figure 7.2: Map of G6PD-deficiency allele frequencies across Asia. The pie chart shows the frequency of G6PD-deficiency alleles. The size of the pie chart indicates the number of G6PD-deficient individuals sampled. Countries with endemic malaria are colored yellow. Figure from HOWES *et al.* (2013), licensed under CC BY 4.0.

Over roughly the past ten thousand years, adaptive alleles con-
 4720 ferring resistance to malaria have arisen in a number of genes and
 spread through human populations in areas where malaria is en-
 4722 demic (KWIATKOWSKI, 2005). One particularly impressive case of
 convergent evolution in response to selection pressures imposed by
 4724 malaria are the numerous changes throughout the G6PD gene, which
 include at least 15 common variants in Central and Eastern Asia
 4726 alone that lower the activity of the enzyme (HOWES *et al.*, 2013).
 These alleles are now found at a combined frequency of around 8%
 4728 frequency in malaria endemic areas, rarely exceeding 20% (HOWES

et al., 2012). Whether these variants *all* confer resistance to malaria is unknown, but a number of these alleles have demonstrated effects against malaria and are thought to have a selective advantage to heterozygotes $sh > 5\%$ where malaria is endemic (RUWENDE *et al.*, 1995; TISHKOFF *et al.*, 2001; LOUICHAROEN *et al.*, 2009).

With a 5% advantage in heterozygotes, a G6PD allele present as a single copy would only have a 10% probability of fixing in the population. If that's so, how come malaria adaptation has repeatedly occurred via changes at G6PD? Well, maybe adaptation didn't start from a single copy of the selected allele. How many copies of the G6PD-deficiency alleles do we expect were segregating in the population before selection pressures changed?

In the absence of malaria, these G6PD alleles are deleterious with carriers suffering from G6PD deficiency, leading to hemolytic anemia when individuals are exposed to a variety of different compounds, notably those present in fava beans. There's upward of one hundred bases where G6PD-deficiency alleles can arise, so assuming a mutation rate of $\approx 10^{-8}$ per base pair per generation, we can roughly estimate the rate of mutations arising that affect the G6PD gene as $\mu \approx 10^{-6}$ per generation. In the absence of malaria, the selective cost of being a heterozygote carrier of a G6PD-deficient allele must have been on the order of 5% or more, and thus the frequency of the allele under mutation-selection balance would have been $\approx 10^{-6}/0.05 = 2 \times 10^{-5}$.

Assuming an effective population size of 2 – 20 million individuals, roughly five to ten thousand years ago that means that there would have been forty to four hundred copies of the G6PD-deficiency allele present in the population when selection pressures shifted at the introduction of malaria. The chance that one of these newly adaptive alleles is lost is 90% but the chance that they're all lost is $< (0.9)^{40} \approx 0.02$, i.e. there would have been a greater than 98% chance that adaptation would occur via one or more alleles at G6PD. How many alleles would escape drift? Well with 40 – 400 copies of the allele pre-malaria, and each of them having a 10% probability of escaping drift, we expect between 4 and 40 G6PD alleles to escape drift and contribute to adaptation. We see 15 common G6PD alleles in Eurasia, so our simple model of adaptation from mutation-selection balance seems reasonable.

Question 1. ‘Haldane’s sieve’ is the name for the idea that the mutations that contribute to adaptation are likely to be dominant or at least co-dominant.

A) Briefly explain this argument with a verbal model relating to the results we’ve developed in the last two chapters.

B) Haldane’s sieve is thought to be less important for adaptation from previously deleterious standing variation, than adaptation from



Figure 7.3: Pythagoras’s “just say no to fava beans” campaign. Pythagoras prohibited the consumption of fava beans by his followers; perhaps because favism, the anemia induced in G6PD-deficient individuals by fava beans, is relatively common in the Mediterranean due to adaptation to endemic malaria. French early 16th Century. Woodner Collection, National Gallery of Art. Public Domain, wikimedia.

A full analysis of this case requires modeling of G6PD’s X chromosome inheritance, and the randomness in the number of copies of the allele present at mutation-selection balance (RALPH and COOP, 2015).



Figure 7.4: Haldane’s sieve. To our knowledge Haldane never wore a sieve, but we assume he owned one. Sieve, Flickr licensed under CC BY 2.0. Haldane, Public Domain, wikimedia.

new mutation. Can you explain the intuition behind of this idea?

C) Haldane's sieve is likely to be less important in inbred, e.g. selfing, populations. Why is this?

Question 2. Melanic squirrels suffer a higher rate of predation (due to hawks) than normally pigmented squirrels. Melanism is due to a dominant, autosomal mutation. The frequency of melanic squirrels at birth is 4×10^{-5} .

A) If the mutation rate to new melanic alleles is 10^{-6} , assuming the melanic allele is at mutation-selection equilibrium, what is the reduction in fitness of the heterozygote?

Suddenly levels of pollution increase dramatically in our population, and predation by hawks now offers an equal (and opposite) advantage to the dark individuals as it once offered to the normally pigmented individuals.

B) What is the probability that a single copy of this allele (present just once in the population) is lost?

C) If the population size of our squirrels is a million individuals, and is at mutation-selection balance, what is the probability that the population adapts from one or more allele(s) from the standing pool of melanic alleles?

7.2 The interaction between genetic drift and weak selection.

For strongly selected alleles, once the allele has escaped initial loss at low frequencies, its path will be determined deterministically by its selection coefficients. However, if selection is weak compared to genetic drift, the stochasticity of reproduction can play a role in the trajectory an allele takes even when it is common in the population. If selection is sufficiently weak compared to genetic drift, then genetic drift will dominate the dynamics of alleles and they will behave like they're effectively neutral. Thus, the extent to which selection can shape patterns of molecular evolution will depend on the relative strengths of selection and genetic drift. But how weak must selection on an allele be for drift to overpower selection? And do these interactions between selection and drift have longterm consequences for genome-wide patterns evolution?

To model selection and drift each generation, we can first calculate the deterministic change in our allele frequency due to selection using our deterministic formula. Then, using our newly calculated expected allele frequency, we can binomially sample two alleles for each of our offspring to construct the next generation. This approach to jointly modeling genetic drift and selection is called the Wright-Fisher model.

Under the Wright-Fisher model, we will calculate the expected



Figure 7.5: cress bug (*Asellus aquaticus*) in the isopod family *Asellidae*. Brehms Tierleben. Allgemeine kunde des Tierreichs (1911). Brehm A.E. Image from the Biodiversity Heritage Library. Contributed by Smithsonian Libraries. Not in copyright.

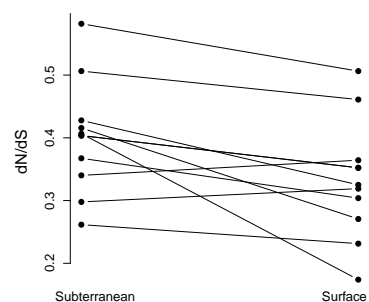


Figure 7.6: Asellid isopods have repeatedly invaded subterranean, ground-water habitats from surface-water habitats, and leading to a genome-wide increase in dN/dS and larger genomes (Data from LEFÉBURE *et al.*, 2017, comparing independent isopod species pairs). One possible explanation of this is that the longterm effective population sizes of the subterranean species are lower and so these species are less able to prevent mildly deleterious

4814 change in allele frequency due to selection and the variance around
this expectation due to drift. To make our calculations simpler, let's
4816 assume an additive model, i.e. $h = 1/2$, and that $s \ll 1$ so that $\bar{w} \approx 1$.
Using our directional selection deterministic model, from Chapter 6,
4818 and these approximations gives us our deterministic change due to
selection

$$\Delta_{SP} = \mathbb{E}(\Delta p) = \frac{s}{2}p(1-p) \quad (7.9)$$

4820 To obtain our new frequency in the next generation, p_1 , we binomially
sample from our new deterministic frequency $p' = p + \Delta_{SP}$, so the
4822 variance in our allele frequency change from one generation to the
next is given by

$$Var(\Delta p) = Var(p_1 - p) = Var(p_1) = \frac{p'(1-p')}{2N} \approx \frac{p(1-p)}{2N}. \quad (7.10)$$

4824 where the previous allele frequency p drops out because it is a con-
stant and the variance in our new allele frequency follows from the
4826 fact that we are binomially sampling $2N$ new alleles from a frequency
 p' to form the next generation.

4828 To get our first look at the relative effects of selection vs. drift we
can simply look at when our change in allele frequency caused by se-
4830 lection within a generation is reasonably faithfully passed down through
the generations. In particular, if our expected change in allele fre-
4832 quency is much greater than the variance around this change, genetic
drift will play little role in the fate of our selected allele (once the al-
4834 lele is not at low copy number within the population). When does se-
lection dominant genetic drift? This will happen if $\mathbb{E}(\Delta p) \gg Var(\Delta p)$,
4836 i.e. when $|Ns| \gg 1$. Conversely, any hope of our selected allele follow-
ing its deterministic path will be quickly undone if our change in allele
4838 frequencies due to selection is much less than the variance induced by
drift. So if the absolute value of our population-size-scaled selection
4840 coefficient $|Ns| \ll 1$, then drift will dominate the fate of our allele.

To make further progress on understanding the fate of alleles with
4842 selection coefficients of the order $1/N$ requires more careful modeling.
However, under our diploid model, with an additive selection coef-
4844 ficient s , we can obtain the probability that allele 1 fixes within the
population, starting from a frequency p :

$$p_F(p) = \frac{1 - e^{-2Ns}}{1 - e^{-2Ns}} \quad (7.11)$$

4846 The proof of this result is sketched out below (see Section 7.2.1). A
new allele that arrives in the population at frequency $p = 1/(2N)$ has
4848 a probability of reaching fixation of

$$p_F\left(\frac{1}{2N}\right) = \frac{1 - e^{-s}}{1 - e^{-2Ns}} \quad (7.12)$$

To see this denote our new count of
allele 1 by i , then

$$\begin{aligned} Var(p_1 - p) &= Var\left(\frac{i}{2N} - p\right) = Var\left(\frac{i}{2N}\right) \\ &= \frac{Var(i)}{(2N)^2} \end{aligned}$$

and from binomial sampling $Var(i) = 2Np'(1-p')$ and so we arrive at our
answer. Assuming that $s \ll 1$, $p' \approx p$, then in practice we can use

$$Var(\Delta p) = Var(p' - p) \approx p(1-p)/2N.$$

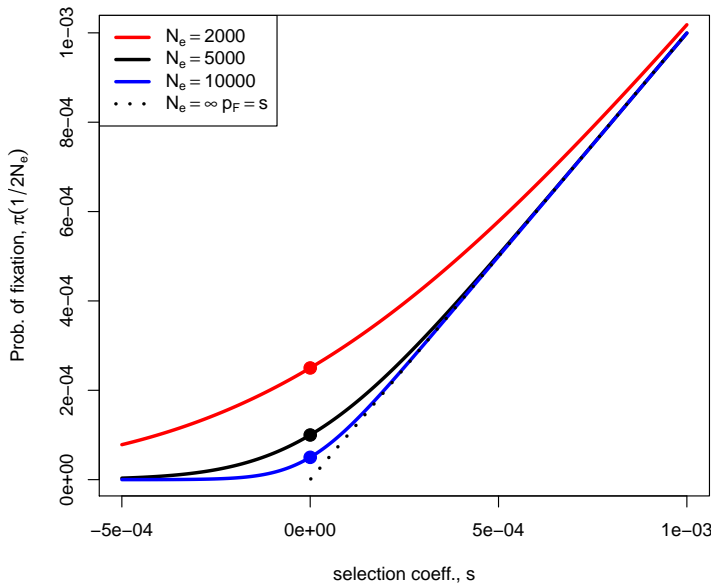


Figure 7.7: The probability of the fixation of a new mutation with selection coefficient s ($h = 1/2$) in a diploid population of effective size N_e . The dashed line gives the infinite population solution. The dots give the solution for $s \rightarrow 0$, i.e. the neutral case, where the probability of fixation is $1/(2N_e)$. Code here.

If $s \ll 1$ but $Ns \gg 1$ then $p_F(\frac{1}{2N}) \approx s$, which nicely gives us back the result that we obtained above for an allele under strong selection (eqn. (7.8)). Our probability of fixation (eqn. (7.12)) is plotted as a function of s and N in Figure 7.8. To recover our neutral result, we can take the limit $s \rightarrow 0$ to obtain our neutral fixation probability, $1/(2N)$.

In the case where Ns is close to 1, then

$$p_F\left(\frac{1}{2N}\right) \approx \frac{s}{1 - e^{-2Ns}} \quad (7.13)$$

This is greater than our earlier result $p_F = s$ from the branching process argument (using our additive model of $h = 1/2$), increasingly so for smaller N . Why is this? The reason why is that p_F is really the probability of "never being lost" in an infinitely large population. So to persist indefinitely, the allele has to escape loss permanently, by never being absorbed by the zero state. When the population size is finite, to fix we only need to reach a size $2N$ individuals. Weakly beneficial mutations ($Ns > 1$) are slightly more likely to fix than the s probability, as they only have to reach $2N$ to never be lost.

If, for selection to operate on an allele, we need the selection coefficient to satisfy $|Ns| \gg 1$, then that holds if $|s| \gg 1/N$. Well, effective population sizes are often reasonably large, on the order of hundreds of thousands or millions of individuals, thus selection coefficients on the order of 10^{-5} to 10^{-6} can be effectively selected upon, i.e. selection equivalent to individuals have incredibly slight advantages in

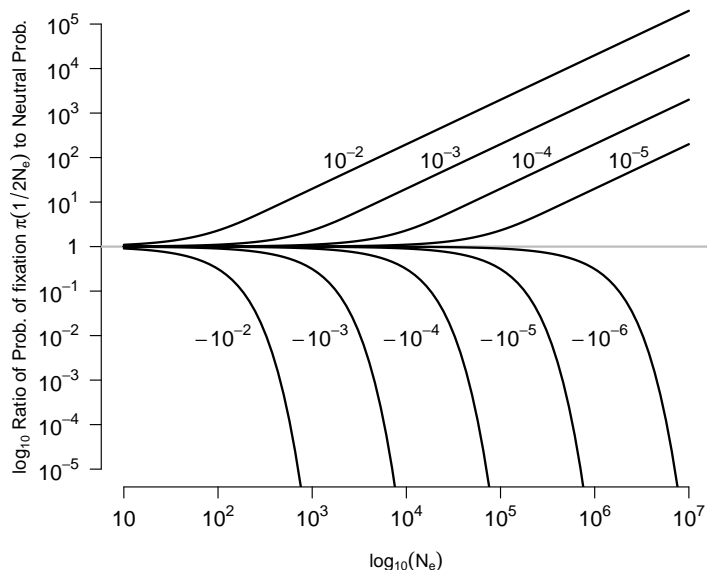


Figure 7.8: The probability of the fixation of a new mutation with selection coefficient s relative to the neutral fixation probability ($1/2N_e$) as a function of the effective size N_e . The selection coefficient is shown next to the line. Note how quickly the probabilities move away from the neutral expectation as $N_e s$ moves passed 1. Code here.

4870 terms of the number of offspring they leave to the next generation.
 While we are incapable of detecting measuring all but the large fitness
 4872 effect sizes, except in some elegant experiments (e.g. in microbes),
 such small effects are visible to selection in large populations. Thus, if
 4874 consistent selection pressures are exerted over long time periods, natural
 selection can potentially finely tune various aspects of an organism.

4876 As one example of this fine-tuning, consider how carefully crafted
 and optimized the sequence of codons is for translation. Due to the
 4878 degeneracy of the protein code, multiple codons code for the same
 amino-acid. For example, there are six different codons that can code
 4880 leucine. While these synonymous codons are equivalent at the protein
 level, cells do differ in the number of tRNA molecules that bind these
 4882 codons and so the efficacy and accuracy with which proteins can be
 formed through translation and folding. These slight differences in
 4884 translation rates likely often correspond to tiny differences in fitness,
 but do they matter?

4886 In many organisms there is a strong bias in the codons to encode
 particular amino-acids, see Figure 7.9, with the most abundant codon
 4888 matching the most abundant tRNA in cells. This 'codon bias' likely
 reflects the combined action of weak selection and mutational pressure,
 4890 pushing the codon composition of the genome and tRNA abundances
 towards an adaptive compromise. These selection pressures have acted
 4892 over long time periods, as codon usage patterns are often very simi-

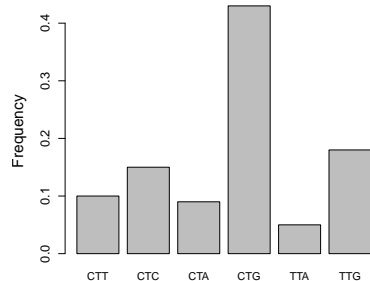


Figure 7.9: Data from *Drosophila melanogaster* on the frequency of different codons for Leucine. Data from Genscript. Code here.

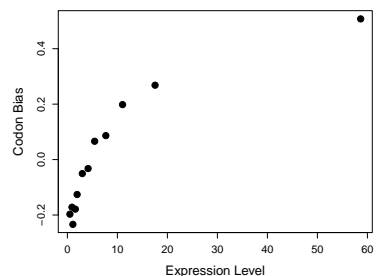


Figure 7.10: A measure of unequal codon frequencies (F) plotted in bins of gene expression (E) for genes across the *Drosophila melanogaster* genome. Data from HEY and KLIMAN (2002). Code here.

lar for species that diverged over many tens of millions of years ago.

4894 Compared to other genes, highly expressed genes show a strong bias towards using codons matching abundant tRNAs, consistent with the

4896 idea that the synonymous codon content of highly expressed genes

is evolving to optimize their translation (see Figure 7.10 for an early

4898 example). These patterns likely represent the action of selection pres-

ures that are incredibly weak on average, but that have played out

4900 over vast time-periods.

The fixation of slightly deleterious alleles. From Figure 7.8 we can

4902 see that weakly deleterious alleles can also fix, especially in small

populations. To understand how likely it is that deleterious alleles by

4904 chance reach fixation by genetic drift, let's assume a diploid model

with additive selection (with a selection coefficient of $-s$ against our

4906 allele 2).

If $Ns \gg 1$ then our deleterious allele (allele 2) cannot possibly reach

4908 fixation. However, if Ns is not large, then the probability of fixation

$$p_F \left(\frac{1}{2N} \right) \approx \frac{s}{e^{2Ns} - 1} \quad (7.14)$$

for our single-copy deleterious allele. So deleterious alleles can fix

4910 within populations (albeit at a low rate) if Ns is not too large. As

above, this is because while deleterious mutations will never escape

4912 loss in infinite populations, they can become fixed in finite population

by reaching $2N$ copies.

Question 3. An additive mutation arises that lowers the relative fitness of heterozygotes by 10^{-5} . What is the probability that this

4914 mutation fixes in a diploid population with effective size of 10^4 ? What

is the probability it fixes in a population of effective size 10^6 ? By

4918 comparing both to their neutral probability describe the intuition

behind this result.

OHTA proposed the ‘nearly-neutral’ theory of molecular evolution in a series of papers¹. She suggested that a reasonable fraction

4920 of newly arising functional mutations may have very weak selection

coefficients, such that species with smaller effective population sizes

4924 may have higher rates of fixation of these very weakly deleterious

alleles. In effect, her suggestion is that the constraint parameter C of

4926 a functional region is not a fixed property, but rather depends on the

ability of the population to resist the influx of very weakly deleterious

4928 mutations.

¹ OHTA, T., 1972 Population size and rate of evolution. *Journal of Molecular Evolution* 1(4): 305–314; OHTA, T., 1973 Slightly deleterious mutant substitutions in evolution. *Nature* 246(5428): 96; and OHTA, T., 1987 Very slightly deleterious mutations and the molecular clock. *Journal of Molecular Evolution* 26(1-2): 1–6

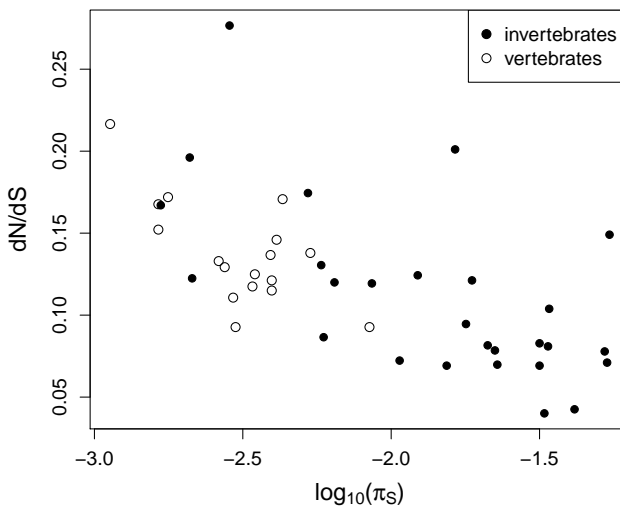


Figure 7.11: Data from 44 metazoan species from Cuttlefish to Sifakas. Each dot represents the average of over many genes plotting d_N/d_S against synonymous diversity (π_S). Data from GALTIER (2016). Code here.

Across species, genome-wide averages of d_N/d_S do seem to be correlated with measures of the effective population size (such as synonymous diversity), see Figure 7.11. This evidence supports the idea that in species with smaller effective population sizes (lower π_S), proteins may be subject to lower degrees of constraint, as very weakly deleterious mutations are able to fix. Thus, some reasonable proportion of functional substitutions in populations with small effective population sizes, such as humans, may be mildly deleterious.

7.2.1 Appendix: The fixation probability of weakly selected alleles

What is the probability a weakly beneficial or deleterious additive allele fixes in our population? We'll let $P(\Delta p)$ be the probability that our allele frequency shifts by Δp in the next generation. Using this, we can write our probability $p_F(p)$ in terms of the probability of achieving fixation averaged over the frequency in the next generation

$$p_F(p) = \int p_F(p + \Delta p)P(\Delta p)d(\Delta p) \quad (7.15)$$

This is very similar to the technique that we used when deriving our probability of escaping loss in a very large population above.

So we need an expression for $p_F(p + \Delta p)$. To obtain this, we'll do a Taylor series expansion of $p_F(p)$, assuming that Δp is small:

$$p_F(p + \Delta p) \approx p_F(p) + \Delta p \frac{dp_F(p)}{dp} + (\Delta p)^2 \frac{d^2 p_F(p)}{dp^2}(p) \quad (7.16)$$



Figure 7.12: Common Cuttlefish (*Sepia officinalis*). Cefalopodi viventi nel Golfo di Napoli (1896). Jatta G. Image from the Biodiversity Heritage Library. Contributed by Smithsonian Libraries. Licensed under CC BY-2.0.

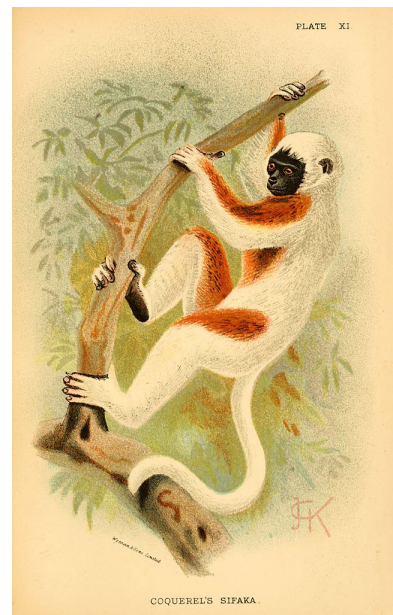


Figure 7.13: Coquerel's Sifaka (*Propithecus coquereli*). A hand-book to the primates (1894). Forbes, H. O. Image from the Biodiversity Heritage Library. Contributed by Smithsonian Libraries. Licensed under CC BY-2.0.

ignoring higher order terms.

⁴⁹⁴⁸ Taking the expectation over Δp on both sides, as in eqn. 7.15, we obtain

$$p_F(p) = p_F(p) + \mathbb{E}(\Delta p) \frac{dp_F(p)}{dp} + \mathbb{E}((\Delta p)^2) \frac{d^2 p_F(p)}{dp^2} \quad (7.17)$$

⁴⁹⁵⁰ Well, $\mathbb{E}(\Delta p) = \frac{s}{2}p(1-p)$ and $Var(\Delta p) = \mathbb{E}((\Delta p)^2) - \mathbb{E}^2(\Delta p)$, so if $s \ll 1$ then $\mathbb{E}^2(\Delta p) \approx 0$, and $\mathbb{E}(\Delta p)^2 = \frac{p(1-p)}{2N}$. Substituting in these
⁴⁹⁵² values and subtracting p from both sides of our equation, this leaves us with

$$0 = \frac{s}{2}p(1-p) \frac{dp_F(p)}{dp} + \frac{p(1-p)}{2N} \frac{d^2 p_F(p)}{dp^2} \quad (7.18)$$

⁴⁹⁵⁴ and we can specify the boundary conditions to be $p_F(1) = 1$ and $p_F(0) = 0$. Solving this differential equation is a somewhat involved
⁴⁹⁵⁶ process, but in doing so we find that

$$p_F(p) = \frac{1 - e^{-2Ns p}}{1 - e^{-2Ns}} \quad (7.19)$$

This proof can be extended to alleles with arbitrary dominance, however, this does not lead to a analytically tractable expression so we do not pursue this here.
⁴⁹⁵⁸

The Effects of Linked Selection.

4962 GENETIC DRIFT IS NOT THE ONLY SOURCE OF RANDOMNESS
in the dynamics of alleles. Alleles also experience random fluctua-
4964 tions in frequency due to the fact that they present on a set of random
genetic backgrounds with different fitnesses. For example, when a
4966 beneficial allele arises via a single mutation, it arises on a particular
genetic background, i.e. a particular haplotype (Figure 8.1A). Imagine
4968 this mutation arising in a region with no recombination, or in an or-
ganism where genetic exchange is rare. If our beneficial allele becomes
4970 established in the population, i.e. escapes loss by genetic drift in those
first few generations, it will start to increase in frequency rapidly. As
4972 it rises in frequency, so will the alleles that happened to be present
on the haplotype that the mutation arose on (if those other alleles are
4974 neutral or at least not too deleterious). These other alleles are get-
ting to 'hitchhiking' along. The alleles that are not on that particular
4976 background are swept out of the population, so the net effect of this
selective sweep is to remove genetic diversity from the population. Di-
4978 versity will eventually recover, as new mutations arise and some slowly
drift up in frequency. But in the short-term, selective sweeps remove
4980 genetic variation from populations.

4982 WILLIAMS and PENNINGS (2019) have visualized selective
sweeps in HIV. In Figure 8.1B) we see a set of HIV haplotypes sam-
pled from a patient before and after of a selective sweep of a drug-
4984 resistant mutation. The patient is taking a retrotransposase inhibitor
(Efavirenz), but sadly within 161 days a drug-resistant mutation that
4986 changes the HIV retrotransposase protein has arisen and spread. Note
how a particular haplotype is now fixed in the sample, and little ge-
4988 netic diversity remains, due to the hitchhiking effect of the strong
selective sweep of this allele.

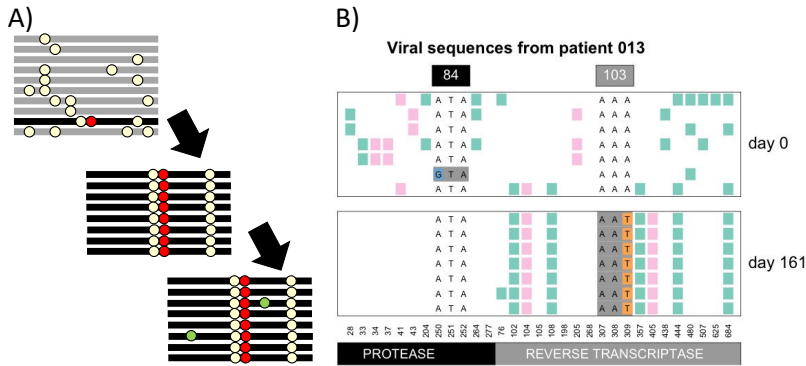


Figure 8.1: **A)** In the top panel, a selected mutation (red dot) arises on a particular haplotype in the population. It sweeps to fixation, carrying with it the haplotype on which it arose, middle panel, erasing the standing genetic diversity in the region. The bottom panel is some time after the selective sweep when some new neutral alleles (green dots) have started to drift up in frequency. **B)** Top panel: HIV sequences from a patient at the start of drug treatment in the protease and retrotransposase coding regions. Bottom panel: A sample 161 days later, after a drug resistant mutation has spread, the $A \rightarrow T$ in the 103rd codon of retrotransposase. Each row is a haplotype, with the alleles present shown as coloured blocks. Figure B from WILLIAMS and PENNINGS (2019), licensed under CC BY 4.0.

4990 To better understand hitchhiking, first let's imagine examining variation at a locus fully linked to our selected locus, just after our sweep
 4992 reached fixation. Neutral alleles sampled at this locus must trace their ancestral lineages back to the neutral allele on whose background the
 4994 selected allele initially arose (Figure 8.6). This is because that background neutral allele, which existed τ generations ago, is the ancestor
 4996 of the entire population at this fully linked locus. Our individuals
 4998 who carry the beneficial allele are, from the perspective of these alleles, experiencing a rapidly expanding population. Therefore, a pair
 5000 of neutral alleles sampled at our linked neutral locus will be forced to coalesce $\approx \tau$ generations ago. A newly derived allele with an additive
 5002 selection coefficient s will take a time $\tau = 4 \log(2N)/s$ generations
 5004 to reach fixation within our population (see eqn. (6.39)). This is a very short-time scale compared to the average neutral coalescent time
 5006 of $2N$ generations for a pair of alleles. Thus we expect little variation, as few mutations will have arisen on these very short branches, and those that have done will likely be singletons in our sample.

Now let's think about a sweep in a recombining region. Again the
 5008 selected mutation arises on a particular haplotype, and it and its
 5100 haplotype starts to increase in frequency in the population. However,
 5102 now recombination events can occur between haplotypes carrying and
 5104 not carrying the selected allele, in individuals who are heterozygote
 5106 for the selected allele. These recombination events allow alleles that
 5108 were not present on the original selected haplotype to avoid being
 5110 swept out of the population, and also decouple the selected allele
 5112 somewhat from hitchhiking alleles, preventing many of them from
 5114 hitchhiking all the way to fixation. Far out from the selected site,
 5116 the recombination rate is high enough that alleles that were present
 5118 on the original background barely get to hitchhike along at all, as
 recombination breaks up their association with the selected allele very

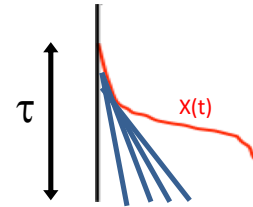


Figure 8.2: The coalescent of 4 lineages, marked in blue, at a locus completed linked to our selected allele. The frequency trajectory of the selected allele $X(t)$ is shown in red.

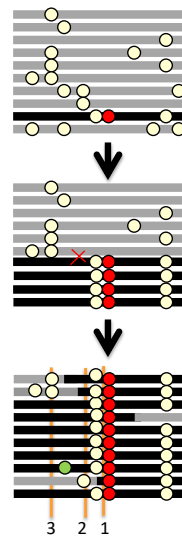


Figure 8.3: A cartoon depiction of a sweep of a red beneficial allele over three time points. The haplotype that the beneficial arose on by mutation is shown in black. The three vertical orange lines mark the loci shown in Figure 8.4. Neutral alleles segregating prior to the sweep appear as white circles, new mutations after the sweep as green circles.

5020 rapidly.

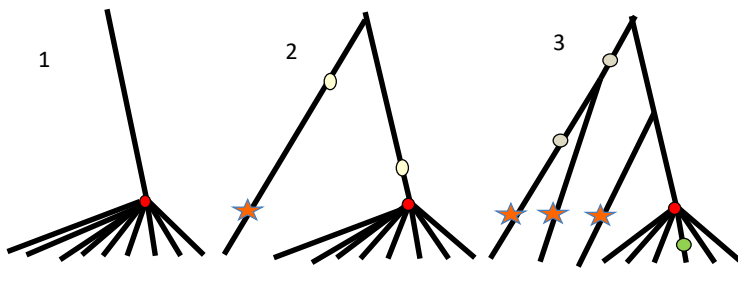


Figure 8.4: Coalescent genealogies at three loci different distances along the genome from a selective sweep. The locations of these three loci along the genome are marked in Figure 8.3. The selected mutation is shown in red. Lineages descended from recombination events during the sweep are marked in stars. Neutral mutations close to each of the loci are shown on the genealogy.

What do the coalescent genealogies look like at loci various distances away from the selected site? Well, close to the selected site all our alleles in the present day trace back to a most recent common ancestral allele present on that selected haplotype, and so are all forced to coalesce around τ generations ago (locus 1). Slightly further out from the selected site (locus 2), we have lineages that don't trace their ancestry back to the original selected haplotype, but instead are descended from recombinant haplotypes that recombined onto the sweep (the haplotype 2 from the bottom). These lineages can coalesce neutrally with the other ancestral lineages over far deeper time scales and mutations on these deeper lineages correspond to the standing diversity present in our population prior to the sweep. As we move even further out from the selected site (locus 3), we encounter more and more lineages descended from recombinant haplotypes that coalesce neutrally much deeper in time than τ , allowing diversity to recover to background levels as we move away from the selected site.

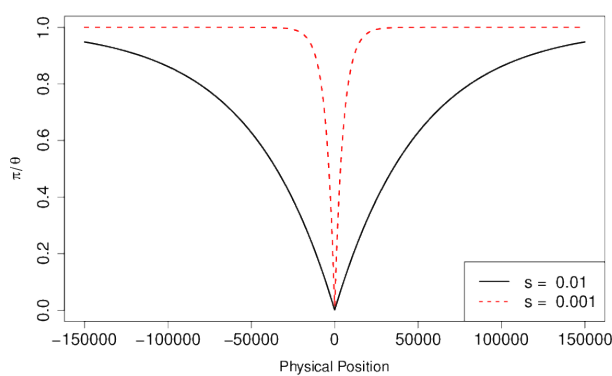


Figure 8.5: The expected reduction in diversity compared to its neutral expectation as a function of the distance away from a site where a selected allele has just gone to fixation. The sweeps associated with two different strengths of selection are shown, corresponding to a short timescale (τ) for the sweep and long one. The recombination rate is $r_{BP} = 1 \times 10^{-8}$. Code here.

To model the expected pattern of diversity surrounding a selected site, we can think about a pair of alleles sampled at a neutral locus a recombination distance r away from our selected site. Our pair of

5040 alleles will be forced to coalesce $\approx \tau$ generations if neither of them of
are descended from recombinant haplotypes.

5042 We know that in the present day our neutral lineage is linked to the
selected allele. The probability that our lineage, in some generation
5044 t back in time, is in a heterozygote is $1 - X(t)$, and the probability
that a recombination occurs in that individual is r . So the probability
5046 that our neutral lineage is descended from a recombinant haplotype t
generations back is

$$r(1 - X(t)) \quad (8.1)$$

5048 So the probability (p_{NR}) that our lineage is not descended from a re-
combinant haplotype from a recombination event in the τ generations
5050 it takes our selected allele to move through the population is

$$p_{NR} = \prod_{t=1}^{\tau} (1 - r(1 - X(t))) \quad (8.2)$$

5052 Assuming that r is small, then $(1 - r(1 - X(t))) \approx e^{-r(1-X(t))}$, such
that

$$p_{NR} = \prod_{t=1}^{\tau} (1 - r(1 - X(t))) \approx \exp\left(-r \sum_{t=1}^{\tau} 1 - X(t)\right) = \exp\left(-r\tau(1 - \hat{X})\right) \quad (8.3)$$

5054 where \hat{X} is the average frequency of the derived beneficial allele across
its trajectory as it sweeps up in frequency, $\hat{X} = \frac{1}{\tau} \sum_{t=1}^{\tau} X(t)$. As
5056 our allele is additive, its trajectory for frequencies < 0.5 is the mirror
image of its trajectory for frequencies > 0.5 , therefore its average
frequency $\hat{X} = 0.5$. This simplifies our expression to

$$p_{NR} = e^{-r\tau/2}. \quad (8.4)$$

5058 The probability that neither of our lineages is descended from a re-
combinant haplotype, and hence are forced to coalesce, is p_{NR}^2 (as-
5060 suming that they coalesce at a time close to τ so that they recombine
independently of each other for times $< \tau$).

5062 If one or other of our lineages is descended from a recombinant
haplotype, it will take them on average $\approx 2N$ generations to find a
5064 common ancestor, as we are back to our neutral coalescent probabil-
ities. Thus, the expected time till our pair of lineages find a common
5066 ancestor is

$$\mathbb{E}(T_2) = \tau \times p_{NR}^2 + (1 - p_{NR}^2)(\tau + 2N) \approx (1 - p_{NR}^2) 2N \quad (8.5)$$

5068 where this last approximation assumes that $\tau \ll 2N$. So the expected
pairwise diversity for neutral alleles at a recombination distance r
away from the selected sweep (π_r) is

$$\mathbb{E}(\pi_r) = 2\mu\mathbb{E}(T_2) \approx \pi_0 (1 - e^{-r\tau}) \quad (8.6)$$

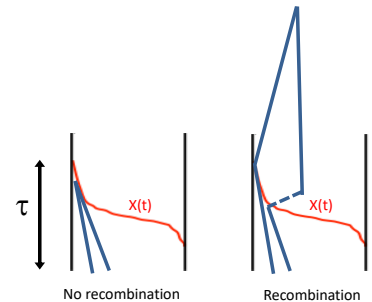
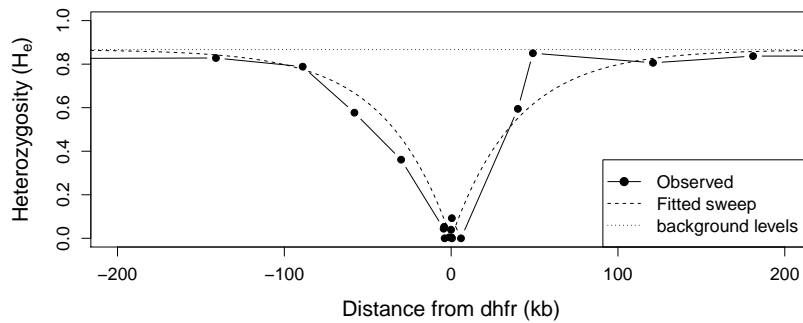


Figure 8.6:

5070 So diversity increases as we move away from the selected site, slowly
and exponentially plateauing to its neutral expectation π_0 .
5072 The malaria pathogen (*Plasmodium falciparum*) has evolved drug
resistance to anti-malaria drugs, often by changes at the dhfr gene.
5074 Figure 8.8 shows levels of genetic diversity (heterozygosity) at a set
of markers moving out from the dhfr gene in a set of drug resistant
5076 malaria sequences collected in Thailand (NASH *et al.*, 2005). We see
the characteristic dip in diversity around the gene, with zero diversity
5078 at a number of the loci very close to the gene, suggesting a strong
selective sweep. Fitting our simple model of a sweep to this data, we
5080 estimate that $\tau \approx 40$ generations, corresponding to the drug-resistance
allele fixing in very short time period.



5082 To get a sense of the physical scale over which diversity is reduced,
consider a region where recombination occurs at a rate r_{BP} per base
5084 pair per generation, and a locus ℓ base pairs away from the selected
site, such that $r = r_{BP}\ell$ (where $r_{BP}\ell \ll 1$ so we don't need to worry
5086 about more than one recombination event occurring per generation).
Typical recombination rates are on the order of $r_{BP} = 10^{-8}$. In Figure
5088 8.5 we show the reduction in diversity, given by eqn. (8.6), for two
different selection coefficients.

5090 For our expected diversity level to recover to 50% of its neutral
expectation $\mathbb{E}(\pi_r)/\theta = 0.5$, requires a physical distance ℓ^* such that
5092 $\log(0.5) = -r_{BP}\ell^*\tau$, and by re-arrangement,

$$\ell^* = \frac{-\log(0.5)}{r_{BP}\tau}. \quad (8.7)$$

As τ depends inversely on the selection s (eqn. (6.39)), the width
5094 of our trough of reduced diversity depends on s/r_{BP} . All else being
equal, we expect stronger sweeps or sweeps in regions of low recombi-
5096 nation to have a larger hitchhiking effect. For example, in a genomic
region with a recombination rate $r_{BP} = 10^{-8}\text{bp}^{-1}$ a selection coeffi-
5098 cient of $s = 0.1\%$ would reduce diversity over 10's of kb, while a sweep
of $s = 1\%$ would affect $\sim 100\text{kb}$.

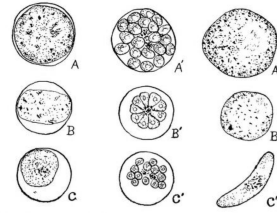


FIG. 47. Comparison of three species of malaria parasites $\times 2000$ (figures selected largely from Manson). A, A' and A'', *Plasmodium vivax*; B, B' and B'', *Plasmodium vivax*; C and C', *Plasmodium falciparum*. A, B and C, mature parasites in red corpuscles. A', B' and C', segmented parasites ready to leave corpuscles. A'', B'' and C'', mature gametocytes.

Figure 8.7: Three species of malaria parasites (*Plasmodium*) in red blood cells.

Animal parasites and human disease (1918). Chandler, A.C. Image from the Biodiversity Heritage Library. Contributed by Cornell University Library. Not in copyright.

Figure 8.8: Levels of heterozygosity at a set of microsatellite markers surrounding the dhfr gene in samples of drug-resistant malaria (*Plasmodium falciparum*) from Thailand. The dotted horizontal line gives the average level of heterozygosity found at these markers in a set of drug-resistant malaria; we take this background as our π_0 . The dashed line shows our fitted hitchhiking model from equation 8.6 with $\tau \approx 40$, fitted by non-linear least squares. The recombination rate in *P. falciparum* is $r_{BP} \approx 10^{-6}\text{bp}^{-1}$. Data from NASH *et al.* (2005). Code here.

5100 **Question 1.** VAN'T HOF *et al.* (2011) identified the genetic
 5102 basis of melanism in the peppered moth (*Biston betularia*). This al-
 5104 lele swept to fixation in northern parts of the UK; a classic case of
 5106 adaptation to industrial pollution (made famous by the work of KET-
 5108 TLEWELL, see MAJERUS (2009) and COOK *et al.* (2012)). The
 5110 genetic basis of melanism is a transposable element (TE) inserted
 5112 into a pigmentation gene. VAN'T HOF *et al.* found that diversity
 5114 is suppressed in a broad region around the TE. Specifically, on the
 5116 background of the TE, it takes roughly 200 kb in either direction for
 5118 diversity levels to recover to 50% of genome-wide levels.

5120 Random facts: In all moths and butterflies only males recombine;
 5122 chromosomes are transmitted without recombination in females. The
 5124 recombination rate in males is 2.9 cM/Mb. Peppered moths have an
 5126 effective population size of roughly a hundred thousand individuals.
 5128 Kettlewell used to eat moths when out collecting them in the field
 (personal communication, Art. Shapiro).

5130 **A)** Briefly explain how this pattern offers further evidence that the
 5132 melanic allele was favoured by selection.

5134 **B)** Using this information, and assuming the allele's effects on
 5136 fitness are additive, what is your estimate of the age of the allele?

5138 **C)** What is your estimate of the selection coefficient favouring this
 5140 melanic allele?

5142 *Other signals of selective sweeps* The primary signal of a recently
 5144 completed selective sweep is the characteristic reduction in diversity
 5146 surrounding the selected site. However, sweeps do leave other signals
 5148 and these have also often been used to identify loci undergoing selec-
 5150 tion. For example, neutral alleles further away from the selected site
 5152 may hitchhiking only part of the way to fixation if recombination oc-
 5154 curs during the sweep, which can lead to an excess of high-frequency
 5156 derived alleles at intermediate distances away from the selected site,
 5158 a pattern lasting for a short time after a sweep (FAY and WU, 2000;
 5160 PRZEWORSKI, 2002; KIM, 2006). Also, as neutral diversity levels
 5162 slowly recover through an influx of new mutations after a sweep, there
 5164 is a strong skew towards low frequency derived alleles, a pattern that
 5166 persists for many generations (BRAVERMAN *et al.*, 1995; PRZE-
 5168 WORSKI, 2002; KIM, 2006). The excess of rare alleles, compared to
 5170 a neutral model, can be captured by statistics such as Tajima's D
 5172 (which we encountered back in our discussion of the neutral site fre-
 5174 quency eqn 3.43). Thus one way to look for loci that have undergone
 5176 selective sweeps is to calculate Tajima's D from data in windows along
 5178 the genome and look for strong departures from the null distribution.

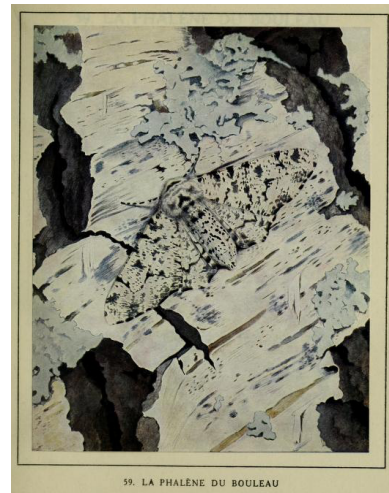


Figure 8.9: peppered moth (*Biston betularia*), non-melanic morph
Les papillons dans la nature (1934). Robert, P.-A. Image from the Biodiversity Heritage Library. Contributed by University of Illinois Urbana-Champaign. Not in copyright.

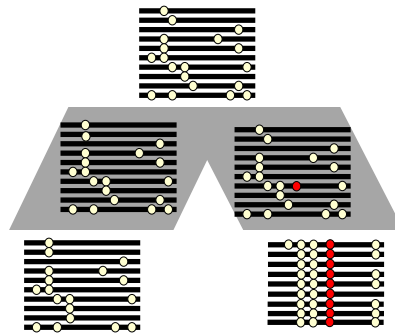


Figure 8.10: Two populations descended from a common ancestral population. A beneficial mutation has occurred in population and swept to fixation.

We can also use comparisons among multiple populations to look

5142 for evidence of sweeps occurring in one of the populations, for example
5143 to identify alleles involved in local adaptation (see 8.11). A selective
5144 sweep will decrease the within-population diversity (H_S) surrounding
5145 the selected site, without affecting the diversity between different
5146 populations. Thus local sweeps create peaks of F_{ST} between weakly
5147 differentiated populations.

5148 HOHENLOHE *et al.* (2010) studied genome-wide patterns of F_{ST}
5149 between marine and freshwater populations of threespine stickleback
5150 (*Gasterosteus aculeatus*). Between different marine populations, they
5151 found no strong peaks of F_{ST} ; however, between the marine and fresh-
5152 water comparisons they found a number of high F_{ST} peaks that were
5153 replicated over a number of freshwater-marine comparisons. They
5154 identified a number of novel regions responsible for the adaptation
5155 of sticklebacks to freshwater environments and also a number of loci
5156 previously identified in crosses between marine and freshwater pop-
5157ulations. For example, the first peak of Linkage Group IV includes
5158 Ectodysplasin A (Eda), a gene involved in the adaptive loss of armour
5159 plating in freshwater environments.

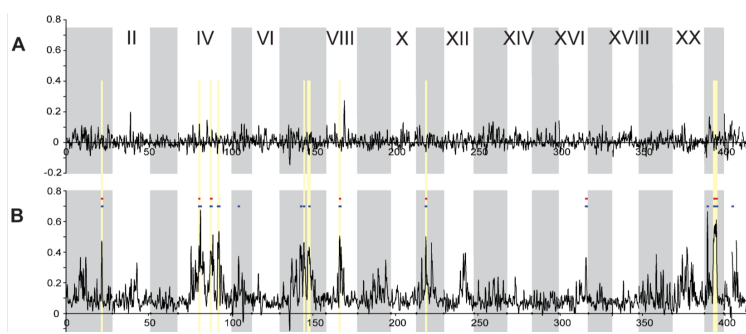


Figure 8.11: F_{ST} across the stickleback genome, with colored bars indicating significantly elevated ($p \leq 10^{-5}$, blue; $p \leq 10^{-7}$, red) and reduced ($p \leq 10^{-5}$, green) values. The alternating white and grey panels indicate different linkage groups. **A)** F_{ST} between two oceanic populations **B)** Average F_{ST} between a freshwater population and the two marine populations. Figure and caption text from HOHENLOHE *et al.* (2010), licensed under CC BY 4.0.

5160 *Soft Sweeps from multiple mutations and standing variation.* In our sweep model above, we assumed that selection favoured a beneficial
 5162 allele from the moment it entered the population as a single copy
 5164 mutation (left panel, Figure 8.12). However, when a novel selection
 5166 pressure switches on, multiple mutations at the same gene may start
 5168 to sweep, such that no one of these alleles sweeps to fixation (middle
 panel, Figure 8.12). These sweeps involving multiple mutations signifi-
 cantly soften the impact of selection on genomic diversity, and so are
 called 'soft sweeps'.

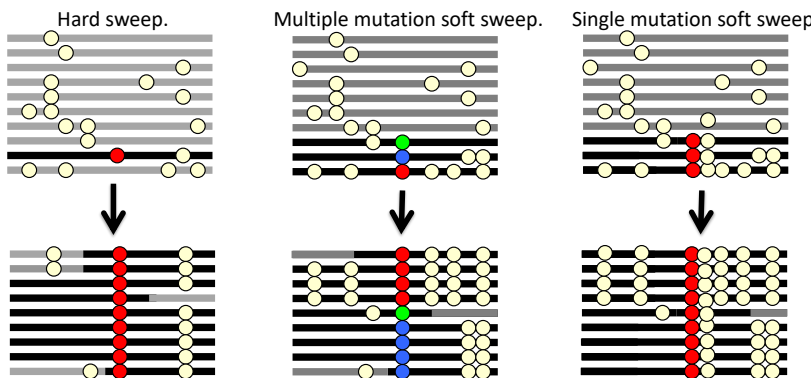


Figure 8.12: Three types of sweeps.

5170 Another way that the impact of a sweep can be softened is if our
 5172 allele was segregating in the population for some time before it became
 beneficial. That additional time means that our allele can have recom-
 5174 bined onto various haplotype backgrounds, such that when selection
 pressures switch, the selected allele sweeps up in frequency on multiple
 5176 different haplotypes (right panel, Figure 8.12). Detecting and differ-
 entiating these different types of sweeps is an active area of empirical
 research and theory in population genomics (see HERMISSON and
 PENNINGS (2017) for an overview of developments in this area).

5178 8.1 The genome-wide effects of linked selection.

To what extent are patterns of variation along the genome and among
 5180 species shaped by linked selection, such as selective sweeps? We can
 hope to identify individual cases of strong selective sweeps along the
 5182 genome, but how do they contribute to broader patterns of variation?

Two observations have puzzled population geneticists since the in-
 5184 ception of molecular population genetics. The first is the relatively
 high level of genetic variation observed in most obligately sexual
 5186 species. The neutral theory of molecular evolution was developed in
 part to explain these high levels of diversity. As we saw in Chapter
 5188 3, under a simple neutral model, with constant population size, we

should expect the amount of neutral genetic diversity to scale with the product of the population size and mutation rate. The second observation, however, is the relatively narrow range of polymorphism across species with vastly different census sizes (see Figure 2.2 and LEFFLER *et al.* (2012) for a recent review). As highlighted by LEWONTIN (1974) in his discussion of the paradox of variation, this observation seemingly contradicts the prediction of the neutral theory that genetic diversity should scale with the census population size. There are a number of explanations for the discrepancy between genetic diversity levels and census population sizes. The first is that the effective size of the population (N_e) is often much lower than the census size, due to high variance in reproductive success and frequent bottlenecks (as discussed in Chapter 3). The second major explanation, put forward by MAYNARD SMITH and HAIGH (1974), is that neutral levels of diversity are also systematically reduced by the effects of linked selection. In large populations, selective sweeps and other forms of linked selection may come to dominate over genetic drift as a source of stochasticity in allele frequencies, potentially establishing an upper limit to levels of diversity (KAPLAN *et al.*, 1989; GILLESPIE, 2000).

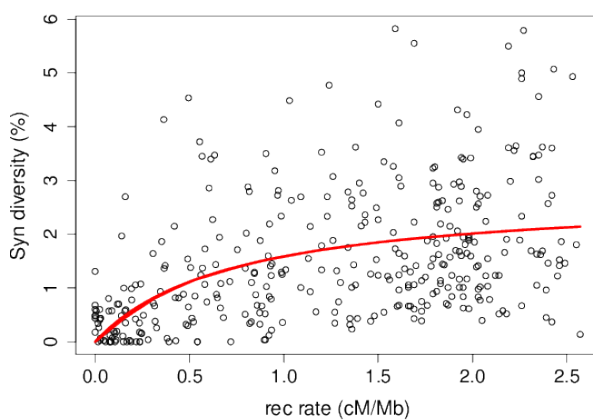


Figure 8.13: The relationship between (sex-averaged) recombination rate and synonymous site pairwise diversity (π) in *Drosophila melanogaster*. The curve is the predicted relationship between π and recombination rate, obtained by fitting the recurrent hitchhiking equation (8.13) to this data using non-linear least squares via the `nls()` function in R. Data from (SHAPIRO *et al.*, 2007), kindly provided by Peter Andolfatto, see SELLA *et al.* (2009) for details. Code here.

One strong line of evidence for the action of linked selection in reducing levels of polymorphism is the positive correlation between putatively neutral diversity and recombination seen in a number of species, as, all else being equal, linked selection should remove diversity more quickly in regions of low recombination (AGUADÉ *et al.*, 1989; BEGUN and AQUADRO, 1992; WIEHE and STEPHAN, 1993b; CUTTER and CHOI, 2010; CAI *et al.*, 2009). For example, *Drosophila melanogaster* diversity levels are much lower in genomic regions of low recombination (see Figure 8.13). This pattern can not

be explained by differences in mutation rate between low and high recombination regions as this pattern is not seen strongly in divergence data among species.

These patterns could reflect the action of selective sweeps happening recurrently along the genome. In the next section we'll present a model for how levels of genetic diversity should depend on recombination and the density of functional sites under a model of recurrent selective sweeps. However, other forms of linked selection can impact genetic diversity in similar ways. For example, linked genetic diversity is continuously lost from natural populations due to the removal of haplotypes that carry deleterious alleles (CHARLESWORTH *et al.*, 1995; HUDSON and KAPLAN, 1995b); this is called the 'background selection' model. Below we'll discuss the background selection model and its basic predictions.

More generally, a wide range of models of selection predict the removal of neutral diversity linked to selected sites. This is because the diversity-reducing effects of high variance in reproductive success are compounded over the generations when there is heritable variance in fitness (ROBERTSON, 1961; SANTIAGO and CABALLERO, 1995, 1998; BARTON, 2000). Many different modes of linked selection likely contribute to these genome-wide patterns of diversity; the present challenge is how to differentiate among these different modes.

8.1.1 A simple recurrent model of selective sweeps

To explain how a constant influx of sweeps could impact levels of diversity, here we will develop a model of recurrent selective sweeps.

Imagine we sample a pair of neutral alleles at a locus a genetic distance r away from a locus where sweeps are initiated within the population at some very low rate ν per generation. The waiting time between sweeps at our locus is exponentially distributed $\sim \text{Exp}(\nu)$. Each sweep rapidly transits through the population in τ generations, such that each sweep is finished long before the next sweep ($\tau \ll 1/\nu$).

As before, the chance that our neutral lineage fails to recombine off the sweep is p_{NR} , such that the probability that our pair of lineages are forced to coalesce by a sweep is $e^{-r\tau}$. Our lineages therefore have a very low probability

$$\nu e^{-r\tau} \tag{8.8}$$

of being forced to coalesce by a sweep per generation. If our lineages do not coalesce due to a sweep, they coalesce at a neutral rate of $1/2N$ per generation. Thus the average waiting time till a coalescent event between our neutral pair of lineages due to either a sweep or a neutral coalescent event is

$$\mathbb{E}(T_2) = \frac{1}{\nu e^{-r\tau} + 1/2N} \tag{8.9}$$

Now imagine that the sweeps don't occur at a fixed location with
 5258 respect to our locus of interest, but now occur uniformly at random
 across our genome. The sweeps are initiated at a very low rate of ν_{BP}
 5260 per basepair per generation. The rate of coalescence due to sweeps
 at a locus ℓ basepairs away from our neutral loci is $\nu_{BP}e^{-r_{BP}\ell\tau}$. If
 5262 our neutral locus is in the middle of a chromosome that stretches L
 basepairs in either direction, the total rate of sweeps per generation
 5264 that could force our pair of lineages to coalesce is

$$2 \int_0^L \nu_{BP} e^{-r_{BP}\ell\tau} d\ell = \frac{2\nu_{BP}}{r_{BP}\tau} (1 - e^{-r_{BP}\tau L}) \quad (8.10)$$

so that if L is very large ($r_{BP}\tau L \gg 1$), the rate of coalescence per
 5266 generation due to sweeps is $2\nu_{BP}/r_{BP}\tau$. The total rate of coalescence
 for a pair of lineages per generation is then

$$\frac{2\nu_{BP}}{r_{BP}\tau} + \frac{1}{2N} \quad (8.11)$$

5268 So our average time till a pair of lineages coalesce is

$$\mathbb{E}(T_2) = \frac{1}{\frac{2\nu_{BP}}{r_{BP}\tau} + 1/2N} = \frac{r_{BP}2N}{4N\nu_{BP}/\tau + r_{BP}} \quad (8.12)$$

such that our expected pairwise diversity ($\pi = 2\mu\mathbb{E}(T_2)$) in a region
 5270 with recombination rate r_{BP} that experiences sweeps at rate ν_{BP} is

$$\mathbb{E}(\pi) = \pi_0 \frac{r_{BP}}{\frac{4N\nu_{BP}}{\tau} + r_{BP}} \quad (8.13)$$

where π_0 is our expected diversity without any selective sweeps,
 5272 ($pi_0 = \theta = 4N\mu$). The expected diversity increases with r_{BP} , as
 higher recombination rates decrease the likelihood a neutral allele
 5274 hitchhikes along with a sweep and is thus forced to coalesce by the
 sweep. Expected diversity decreases with ν_{BP} , as a greater density
 5276 of functional sites experiencing sweeps increases the chance of being
 linked to a nearby sweep. As we move to high r_{BP} , assuming that ν_{BP}
 5278 doesn't increase with r_{BP} , our level of diversity should plateau to θ ,
 the level of genetic diversity of a neutral site completely unlinked to
 5280 any selected loci. If we assume that our genome experiences a constant
 rate of sweeps of a given strength, i.e. that $4N\nu_{BP}/\tau$ is a constant, we
 5282 can fit the variation in π across regions that vary in their recombi-
 nation rate (r_{BP}) to estimate a population's rate of recurrent sweeps
 5284 per basepair. An example of fitting this curve to data from *Drosophila*
melanogaster is shown in Figure 8.13; see WIEHE and STEPHAN
 5286 (1993a) for an early example of fitting a similar recurrent hitchhiking
 model to such data. The parameter giving us this best-fitting curve is
 5288 $4N\nu_{BP}/\tau \approx 7 \times 10^{-9}$. With an effect population size of a million and as-
 suming that the sweeps take a thousand generations to reach fixation,

we find this implies $\nu_{BP} \approx 10^{-12}$. Thus, a really low rate of moderately strong sweeps, roughly one every megabase every million generations, is all we need to explain the profound dip in diversity seen in regions of the genome with low recombination. However, sweeps from positively selected alleles are not the only cause of genome-wide signals of linked selection. Selection against deleterious alleles can also drive these patterns.

8.1.2 Background selection

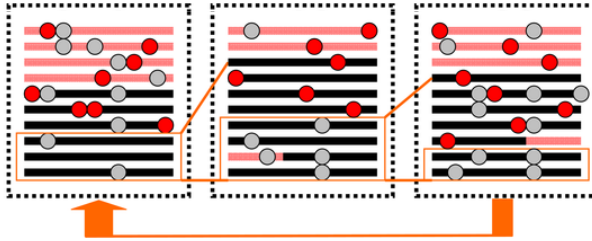
Populations experience a constant influx of deleterious mutations at functional loci while selection acts to purge them from the population, thus preventing deleterious substitutions and maintaining function at these loci. As we discussed in Chapter 6, this balance between mutation and selection results in a constant level of deleterious variation in the population. The constant selection against this deleterious variation has effects on diversity at linked sites. Each deleterious mutation arises at random on a haplotype in the population, and as selection purges this mutation, it removes with it any neutral alleles that were also on this haplotype. This constant removal of linked alleles from the population acts to reduce diversity in regions surrounding functional loci (HUDSON and KAPLAN, 1995a; NORDBORG *et al.*, 1996), an effect known as background selection (BGS).

What proportion of our haplotypes are free of deleterious mutations in any given generation, and so free to contribute to future generations? Well, under mutation-selection balance, a constrained locus with a mutation rate μ towards deleterious alleles that experience a selection coefficient sh against them in heterozygotes, will result in μ/sh chromosomes carrying the deleterious allele. Some of these haplotypes may be passed on to the next generation, but if they are fully linked to the deleterious locus they will all eventually be lost because they carry a deleterious mutation at a site under constraint. Thus, for a neutral polymorphism completely linked to a constrained locus, only $2N(1 - \mu/sh)$ alleles get to contribute to future generations. Therefore, the level of pairwise diversity in a constant population due to BGS at such a locus will be

$$\mathbb{E}[\pi] = 2\mu \times 2N(1 - \mu/sh) = \pi_0(1 - \mu/sh) \quad (8.14)$$

where $\pi_0 = 4N\mu$, the level of neutral pairwise diversity in the absence of linked selection.

The effects of background selection are more pronounced in regions of low recombination, where neutral alleles are less able to recombine off the background of deleterious alleles. Thus, under background selection, we also expect to see reduced diversity in regions of lower recombination.



For a neutral locus that is a recombination fraction r away from a
5332 locus subject to constraint, the level of diversity is

$$\mathbb{E}[\pi] = \pi_0 \left(1 - \frac{\mu sh}{2(r+sh)^2}\right) \quad (8.15)$$

As we move away from a locus experiencing purifying selection, we
5334 increase r , and diversity should recover. For example, moving away
from genic regions in the maize genome we see the average level of
5336 diversity recover. This occurs in both maize and teosinte, the wild
progenitor of maize. The dip in diversity around non-synonymous sites
5338 is stronger in teosinte, perhaps because the accelerated drift due to
the bottleneck in maize may have somewhat released constraint on
5340 sites where very weakly deleterious alleles segregated previously at
mutation-selection balance.

More generally, if a neutral locus is surrounded by L loci experiencing
5342 purifying selection at recombination distances r_1, \dots, r_L , then
compounding equation (8.16) across these loci, the expected reduced
5344 diversity is approximately

$$\mathbb{E}[\pi] = \pi_0 \prod_{i=1}^L \left(1 - \frac{\mu sh}{2(r_i+sh)^2}\right) \approx \exp\left(\sum_{i=1}^L \frac{\mu sh}{2(r_i+sh)^2}\right) \quad (8.16)$$

To model an average neutral locus in a genomic region with a given
5346 recombination rate, we can imagine that our neutral locus is situated
in the center of a large region with total recombination rate R and
5348 total deleterious mutation rate U , where $U = \mu L$. Then our expression
for diversity, equation (8.16), simplifies to

$$\mathbb{E}[\pi] \approx \pi_0 \exp(-U/(sh+R)) \approx \pi_0 \exp(-U/R). \quad (8.17)$$

In this last approximation, we assume that we're looking at a large
5352 region, with $R \gg sh$. Note that much like genetic load, equation
(6.53), this expression depends only on the total deleterious mutation
5354 rate. Any dependence on the selection coefficient drops out, as weakly
selected mutations segregate in the population at higher frequencies,
5356 but are also removed from the population more slowly, allowing more
of the genome to recombine off the deleterious background.

Figure 8.14: A cartoon depiction of a region for 10 haplotypes experiencing background selection. Neutral mutations are shown as gray circles, and deleterious mutations in red. Over time, chromosomes carrying deleterious mutations are removed from the population, such that most individuals are descended from a subset of chromosomes free of deleterious alleles (highlighted here by orange boxes). Mutation is constantly generating new deleterious alleles on the background of chromosomes previously free of deleterious alleles. Figure modified from SELLA *et al.* (2009), licensed under CC BY 4.0.

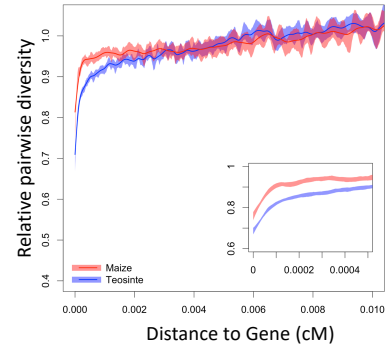


Figure 8.15: Relative diversity compared to the mean diversity in windows ≥ 0.01 cM as a function of the distance to the nearest gene. See (BEISSINGER *et al.*, 2016) for details. Figure licensed under CC BY 4.0 by Jeff Ross-Ibarra.

5358 For a first go at fitting this to genome-wide data, we could look
 at diversity in windows of length W bp (as in Figure 8.16). If we
 5360 assume that there is a constant rate of deleterious mutation per base
 pair, μ_{BP} , then $U = \mu_{BP}W$. Furthermore, if our genomic window
 5362 has a recombination rate r_{BP} per base-pair, our total genetic length
 is $R = r_{BP}W$. Making these substitutions in equation (8.17), our
 5364 window size cancels out to give

$$\mathbb{E}[\pi] \approx \pi_0 \exp(-\mu_{BP}/r_{bp}) \quad (8.18)$$

5366 Looking across windows that vary in their recombination rate, i.e.
 5368 r_{BP} , we can fit equation (8.18) to data to estimate μ_{BP} . An example
 of doing this to data from *D. melanogaster* is shown in Figure 8.16,
 5370 yielding an estimate of the deleterious mutation rate of $\mu_{BP} \approx 3.2 \times$
 10^{-9} . This is roughly on the same order as the mutation rate per
 5372 base pair in *D. melanogaster*, and so this deleterious mutation rate
 estimate is somewhat high as it would require most of the genome to
 5374 be constrained, but as a first approximation it's not terrible. Note
 how similar the fit is to a model of hitchhiking, suggesting that both
 5376 BGS and hitchhiking are capable of explaining the broad relationship
 between diversity and recombination seen in *D. melanogaster* and
 other species.

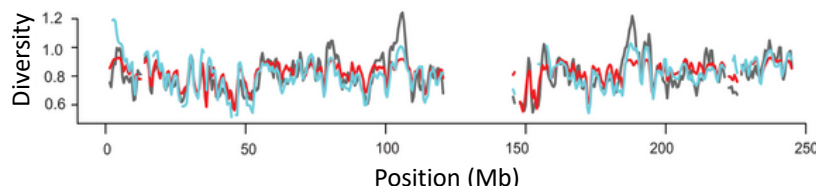


Figure 8.16: The relationship between recombination rate and synonymous site pairwise diversity (π) in *D. melanogaster*, as in Figure 8.13. The red curve is the predicted relationship between π and recombination rate, obtained by fitting the BGS equation (8.17) to this data using non-linear least squares via the `nls()` function in R. The blue line is the recurrent hitchhiking equation line from Figure 8.13. Code here.

5378 As our annotations of functional regions of the genome have im-
 proved, so have our methods to infer background selection. A more
 5380 rigorous version of this analysis today would incorporate variation in
 coding density among windows into the parameter μ_{BP} . With de-
 tailed genomic annotations showing coding regions and constrained
 5382 non-coding regions, we can also move beyond just analyzing broad-
 scale patterns. For example, MCVICKER *et al.* (2009) fit a model
 5384 of background selection to putatively neutral pairwise diversity along
 the human genome, using equation 8.16 to estimate the effect of BGS
 5386 at each locus, weighing the genetic distance to all of the surround-
 ing coding regions and constrained non-coding sites. This allowed
 5388 MCVICKER *et al.* (2009) to estimate mutation rates and average
 selection coefficients acting against deleterious alleles in these regions
 5390 of the genome. This best fitting model also allowed them to predict

Figure 8.17: Observed (black line) and predicted pairwise diversity across chromosome 1, from a background selection model that assumes a uniform mutation rate (red line) or a mutation rate that varies with local human/dog divergence (blue line). Figure from (MCVICKER *et al.*, 2009), licensed under CC BY 4.0.

diversity levels along the genome, a section of which is shown in figure 5392 8.17. Thus, broad-scale features of polymorphism along the genome are well described by background selection (or by linked selection more 5394 generally).

The deleterious mutation rates estimated by MC VICKER *et al.* 5396 (2009) from fitting a model of BGS were again too high, as in the *Drosophila* example above, suggesting the BGS alone is not sufficient 5398 to explain all of the effect of linked selection. But how then do we go about distinguishing the impact of BGS from hitchhiking?

5400 *Distinguishing the impact of hitchhiking from background selection in genome-wide data* A variety of approaches have been taken to 5402 start to separate the effects of hitchhiking from background selection. Much of the strongest evidence showing the effects of both comes from 5404 *Drosophila melanogaster* and we review some of that evidence here. Hitchhiking is expected to have systematic effects on the neutral site 5406 frequency spectrum, distorting it towards rare minor alleles, (reflecting the slow recovery of diversity following a sweep). Therefore, we should 5408 expect a distortion of summary statistics such as Tajima's D in regions of low recombination if hitchhiking is contributing to the reduction in 5410 diversity in these regions (BRAVERMAN *et al.*, 1995; PRZEWORSKI, 2002; KIM, 2006). In *D. melanogaster*, there is a greater skew towards 5412 rare alleles at putatively neutral sites in regions of low recombination (ANDOLFATTO and PRZEWORSKI, 2001; SHAPIRO *et al.*, 2007), 5414 see left panel of Figure 8.18. However, while this skew isn't expected under simple models of strong background selection, other models of 5416 background selection can lead to such patterns.

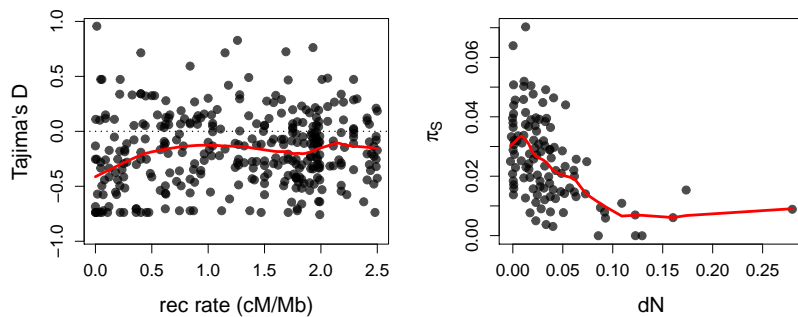


Figure 8.18: **Left)** Average Tajima's D in genomic windows plotted against their recombination rate in *D. melanogaster*. Data from SHAPIRO *et al.* (2007). **Right)** Synonymous pairwise diversity in genomic windows as a function of the density of non-synonymous substitutions in the window. Data from ANDOLFATTO (2007). Code here.

Another prediction of the hitchhiking model, where an allele sweeps 5418 to fixation, is that there should be a functional substitution associated with each sweep. Or, to flip that around, we might expect to 5420 see a greater impact of hitchhiking where there are more functional

substitutions. For example, regions surrounding non-synonymous substitutions should have lower levels of diversity, if a high fraction of non-synonymous substitutions are adaptive. Again, this pattern is seen in *D. melanogaster* (ANDOLFATTO, 2007; MACPHERSON *et al.*, 2007; SATTATH *et al.*, 2011b), right side of Figure 8.18.

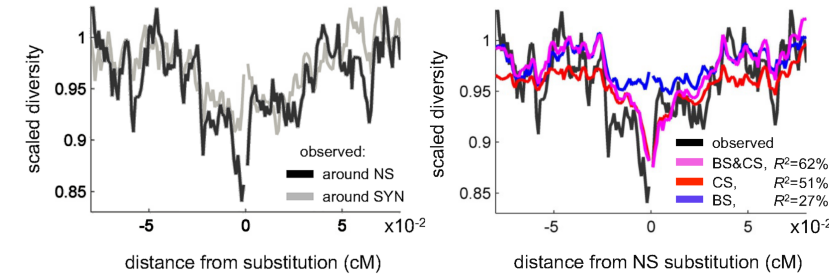


Figure 8.19: **Left)** Scaled synonymous pairwise diversity levels around non-synonymous (NS) and synonymous (SYN) substitutions in *D. melanogaster*. **Right)** Predicted scaled diversity levels around non-synonymous substitutions based on models including background selection (BS), classic sweeps (CS) and both (BS & CS). Figure from ELYASHIV *et al.* (2016), licensed under CC BY 4.0.

Pushing this idea further, we can look at the dip in diversity surrounding a non-synonymous substitution averaged across all the substitutions in the genome. ELYASHIV *et al.* (2016) found a stronger dip in diversity around non-synonymous substitutions than synonymous substitutions (see also SATTATH *et al.*, 2011a). Extending the model of MCVICKER *et al.* (2009) to fit a model of background selection and hitchhiking to putative neutral diversity along the genome, they found that the dip in diversity around synonymous substitutions comes mostly from BGS. But to fully explain the dip in diversity around non-synonymous substitutions, a reasonable proportion of these non-synonymous substitutions have to have been accompanied by a classic (hard) sweep. The majority of these sweeps are estimated to be due to very weak selection, with selection coefficients $< 10^{-4}$. Furthermore, ELYASHIV *et al.* (2016) estimated a 77 - 89% reduction in neutral diversity due to selection on linked sites, and concluded that no genomic window was entirely free of the effects of selection. Thus linked selection has a profound effect in some species such as *Drosophila melanogaster*.

Interaction of multiple selected loci.

- 5446 Consider two biallelic loci segregating for A/a and B/b . There are four
 5447 haplotypes, AB , Ab , aB , ab , which for simplicity we label 1-4. The
 5448 frequency of our four haplotypes are x_1 , x_2 , x_3 , and x_4 . Each indi-
 5449 vidual has a genotype consisting of two haplotypes; we label w_{ij} the
 5450 fitness of an individual with the genotype made up of haplotype i and
 5451 j (we assume that $w_{ij} = w_{ji}$, i.e. there are no parent of origin effects).
 5452 Assuming that these fitnesses reflect differences due to viability selec-
 5453 tion, and that individuals mate at random, we can write the following
 5454 table of our genotype proportions after selection:

	AB	Ab	aB	ab
AB	$w_{11}x_1^2$	$w_{12}2x_1x_2$	$w_{13}2x_1x_3$	$w_{14}2x_1x_4$
Ab	•	$w_{22}x_2^2$	$w_{23}2x_2x_3$	$w_{24}2x_2x_4$
aB	•	•	$w_{33}x_3^2$	$w_{34}2x_3x_4$
ab	•	•	•	$w_{44}x_4^2$

- 5455 This follows from assuming that our haplotypes are brought together
 5456 at random (HWE), then discounted by their fitnesses. Our mean
 5457 fitness \bar{w} is the sum of all the entries in the table, so dividing by \bar{w}
 5458 normalizes the complete table to sum to one. The frequency of the AB
 5459 haplotype (1) in the next generation of gametes is

$$x'_1 = \frac{(w_{11}x_1^2 + \frac{1}{2}w_{12}2x_1x_2 + \frac{1}{2}w_{13}2x_1x_3 + \frac{1}{2}(1-r)w_{14}2x_1x_4 + \frac{1}{2}rw_{23}2x_2x_3)}{\bar{w}} \quad (9.1)$$

- 5460 This is a bit of a mouthful, but each of the terms is easy to under-
 5461 stand. Each of the HWE genotype frequencies (e.g. $2x_1x_2$) is weighted
 5462 by its fitness relative to the mean fitness (w_{ij}/\bar{w}), and by its proba-
 5463 bility of transmitting the AB haplotype to the next generation. For
 5464 example, AB/Ab individuals (1/2) transmit the AB haplotype only
 5465 half the time. The final two terms include the recombination fraction
 5466 (r). The first term involving recombination refers to the AB/ab geno-
 5467 type (1/4), who with probability $(1-r)/2$ transmits a non-recombinant
 5468 AB haplotype to the gamete. Similarly, the second term refers to the

5470 Ab/aB genotype; a proportion $r/2$ of its gametes carry the recombinant AB haplotype.

5472 In the single locus case, we defined the marginal fitness of an allele. Here it will help us to define the marginal fitness of the i^{th} haplotype:

$$\bar{w}_i = \sum_{j=1}^4 w_{ij} x_j \quad (9.2)$$

5474 This is the fitness of the i^{th} haplotype averaged over all of the *diploid* genotypes it could occur in, weighted by their probability under random mating. Using this notation, and with some rearrangement of equation (9.1), we obtain

$$x'_1 = \frac{x_1 \bar{w}_1 - w_{14} r D}{\bar{w}} \quad (9.3)$$

5478 Here we have assumed that $w_{23} = w_{14}$, i.e. that the fitness of AB/ab individuals is the same as Ab/aB individuals (i.e. that fitness depends only on the alleles carried by an individual, and not on which chromosome they are carried; this assumption is sometimes called no 5480 *cis*-epistasis).

5482 We can then write the change in the frequency of our 1 haplotype as

$$\Delta x_1 = \frac{x_1 (\bar{w}_1 - \bar{w}) - r w_{14} D}{\bar{w}} \quad (9.4)$$

5484 Generalizing this result, we write the change in *any haplotype i from* our set of four haplotypes as

$$\Delta x_i = \frac{x_i (\bar{w}_i - \bar{w}) \pm r w_{14} D}{\bar{w}} \quad (9.5)$$

5486 where the coupling haplotypes 1 and 4 use $+D$ and repulsion haplotypes 2 and 3 use $-D$. Note that the sum of these four Δx_i is zero, as our haplotype frequencies sum to one.

5488 So the change in the frequency of a haplotype (e.g. AB, haplotype 1) is determined by the interplay of two factors: First, the extent 5490 to which the marginal fitness of our haplotype is higher (or lower) than the mean fitness of the population (the magnitude and sign of 5492 $(\bar{w}_1 - \bar{w})/\bar{w}$). Second, whether there is a deficit or any excess of our 5494 haplotype compared to linkage equilibrium (the magnitude and sign of 5496 D), modified by the strength of recombination. This tension between 5498 selection promoting particular haplotypic combinations, and recombination breaking up overly common haplotypes is the key to a lot of interesting dynamics and evolutionary processes.

5500 9.1 Types of interaction between selection and recombination

To illustrate these ideas we make use of Muller diagrams (MULLER, 5502 1932), where we visualize the allele dynamics in terms of a plot of the stack frequencies over time.

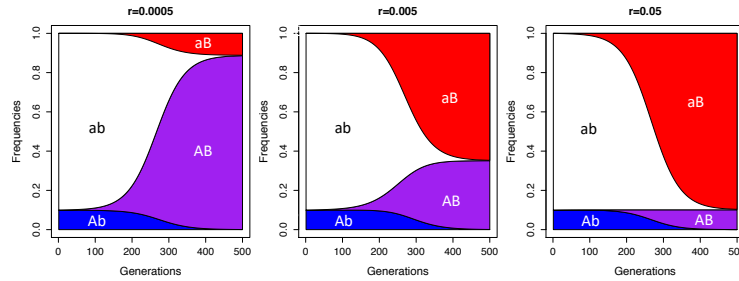
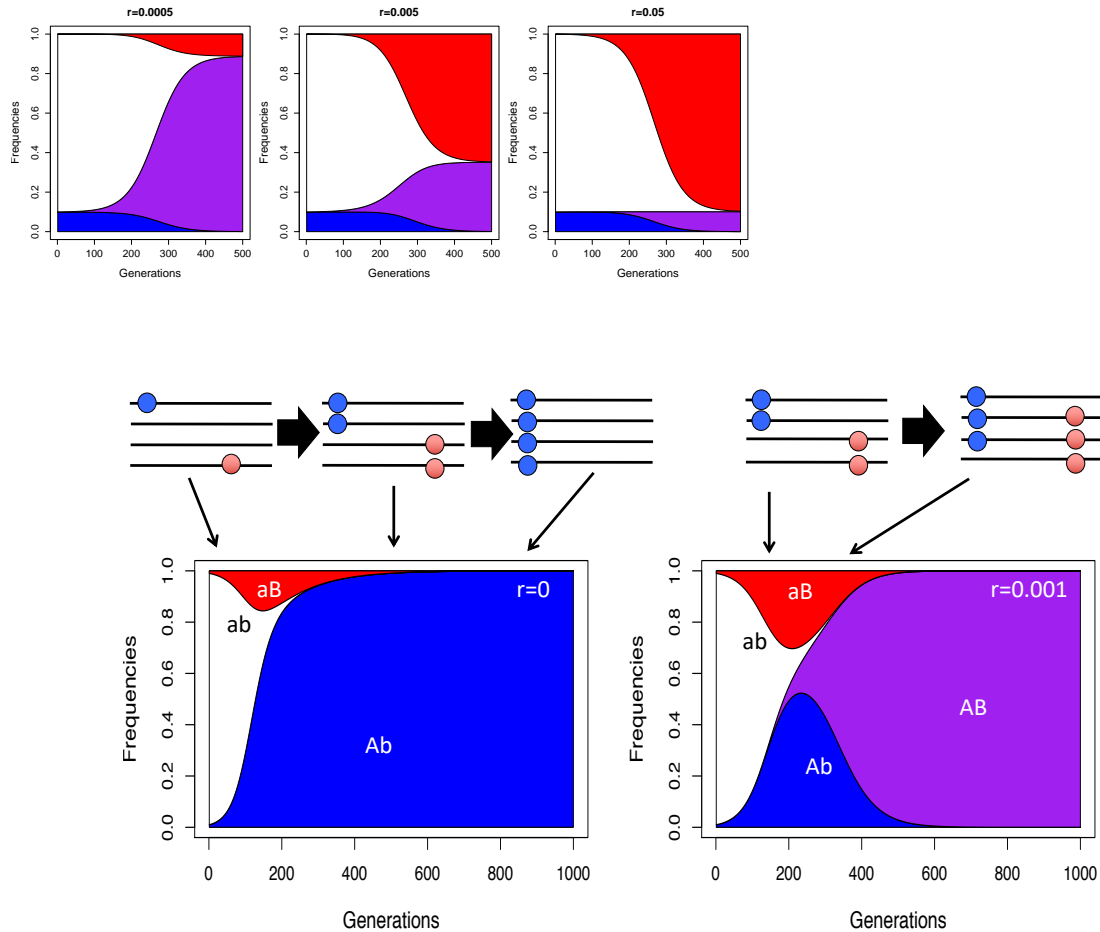


Figure 9.1: A beneficial mutation B arises on the background of a neutral allele whose initial frequency is $p_A = 10\%$. The beneficial allele has a strong, additive selection coefficient of $hs = 0.05$.

5504 *The hitchhiking of deleterious alleles* Let's start by revisiting our
 5506 neutral hitchhiking in this two locus setting in the previous chapter we
 5508 saw that neutral alleles can hitchhike along with our selected allele if
 5510 they are tightly linked enough. Figure 9.1 shows the frequency trajec-
 5512 tories of the various haplotypes for neutral allele (A) that is present at
 5514 10% frequency in the population when our beneficial allele (B) arises
 on its background. When the recombination rate (r) is low between
 the loci, A gets to hitchhike to high frequency, but for higher recombi-
 nation rates it only gets dragged to intermediate frequencies. For the
 highest recombination rate shown ($r \approx s$) the neutral allele's dynamics
 ($p_{Ab} + p_{AB}$) are barely changed at all, as it recombines on and off the
 sweeping allele frequently and so barely perceives the sweep.

5516 *The hitchhiking of deleterious alleles* Deleterious alleles can also
 5518 hitchhike along with beneficial mutations if they are not too deleterious
 5520 compared to the benefits offered by the selected allele. Again our allele
 5522 A is at 10% frequency in the population in Figure ??, but this time it
 5524 is deleterious and so initially decreasing in frequency across the genera-
 5526 tions when the beneficial mutation (B) arises on its background. If
 5528 the loci are tightly linked, and A were too deleterious, B would never
 5530 get to take off in the population. However, if the benefits of B out-
 5532 weighs the cost of A , even in the case of no recombination between our
 5534 loci, allele A gets to hitchhike to fixation and merely slows down B 's
 rate of increase and their combined fitness is reduced. With moderate
 amounts of recombination between the loci, our deleterious starts to
 hitchhike but before it can get to fixation the beneficial allele man-
 ages to recombine off its background. This recombinant aB haplotype,
 which has higher fittest as it lacks the deleterious allele, now sweeps
 through the population displacing the AB haplotype. For higher re-
 combination events we have to wait less long for a recombination to
 breakup the hitchhiking deleterious allele, so the adaptive allele easily
 escapes its background. For the purposes of illustration here we've
 used a relatively common deleterious allele, but in reality these alleles
 will likely be often be rare in the population and at mutation selection

balance. If they are rare it is likely that a beneficial mutation arises
5538 on a specific deleterious allele's background, but as we have seen there
5540 are likely going to be many rare deleterious alleles in the population so
it is likely that a beneficial mutations may often have to contend with
deleterious hitchhikers.



5542 *Clonal interference between favourable alleles.* When rates of sex and
recombination are zero, or very low, positively selected alleles can pre-
5544 vent each other reach fixation and so the rate of adaptation can be
slowed. In the absence of sex and recombination, when two positively
5546 selected alleles arise on different genetic backgrounds in the popula-
tion they cannot both fix (left side of Figure 9.2). They can initially
5548 increase in frequency, but necessarily compete with each other when
they become common. This is called selective interference, or sometime
5550 clonal interference. If one of the alleles has a much larger selection
coefficient it will fix, forcing the other allele from the population, but

Figure 9.2: Interference between two positively selected alleles. **Left)** the red and blue (A and B) beneficial alleles arise on different haplotypes. They rise in frequency, but in the absence of recombination only one can fix. This is shown in a Muller diagram, where p_{AB} is initially set to zero. **Right)** In the presence of recombination the population can generate the recombinant (AB) haplotype, which can subsequently fix.

when they are relatively equally matched it may take some time for this situation to resolve itself resulting in a traffic jam in the population. Thus in an asexual adaptive alleles necessarily have to fix sequentially. However, with even a small amount of recombination beneficial alleles can recombine on to each others background, allowing them to fix in parallel (right side of Figure 9.2).

Given the rapid evolution of HIV we can see interference taking place over very short time periods indeed. HIV uses its reverse transcriptase (RT) gene to write itself from an RNA virus into its host's DNA, allowing HIV to hijack the hosts regulatory machinery, a critical part of its life cycle. One of the early HIV drugs was Efavirenz, which inhibits HIV's RT protein. Sadly, mutations are common in the RT HIV gene, and these mutations, in the presence of the drug, confer a profound fitness advantage, allowing them to spread through the HIV population in patients undergoing anti-HIV treatment. In Figure 9.3 we see that by day 224 after the start of drug treatment two different drug-resistance amino-acid changes beginning to spread within a patient (also shown as a Muller diagram in Figure 9.4). Because these alleles occur on different genetic backgrounds, with little chance for genetic exchange between them, they interfere in each other progress as they compete to fix within the population. Eventually the amino acid change at site 188 wins out.

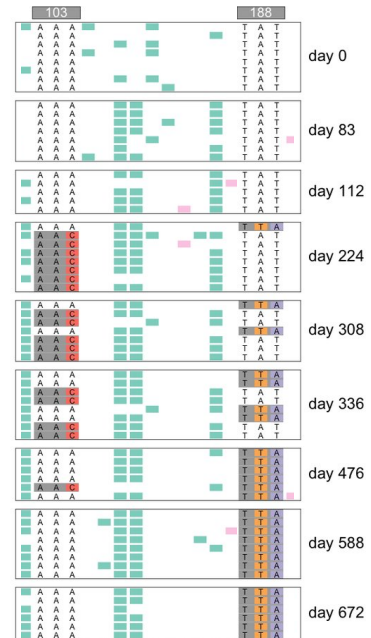
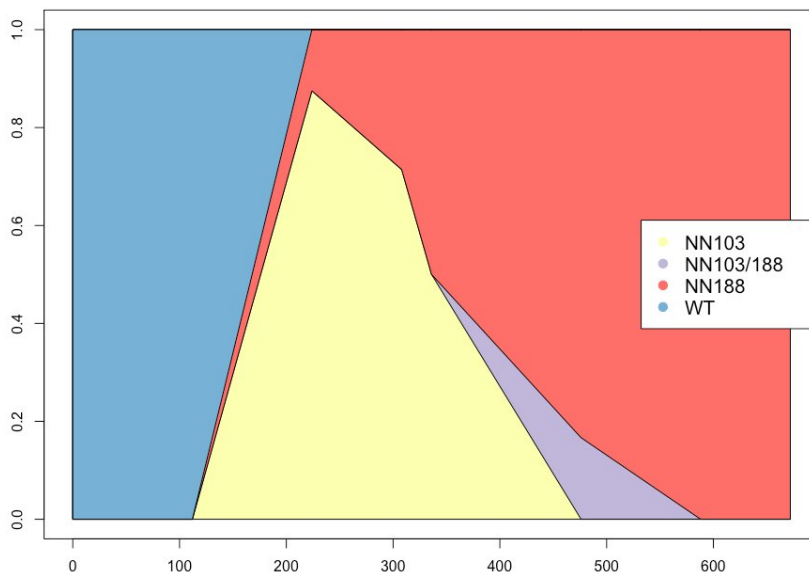


Figure 9.3: HIV sequences from a patient over the course of drug treatment in the retrotransposase coding region. Figure cropped from WILLIAMS and PENNINGS (2019), licensed under CC BY 4.0.
Figure 9.4: Muller plot of the drug resistance interference dynamics from Figure 9.3. Figure from WILLIAMS and PENNINGS (2019), licensed under CC BY 4.0.

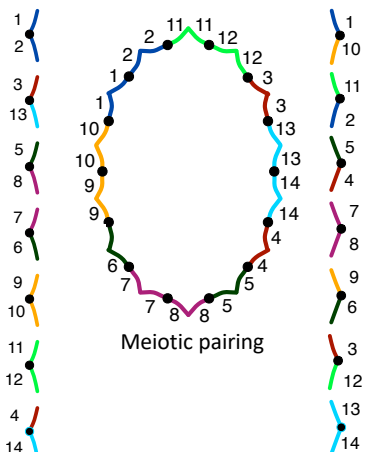
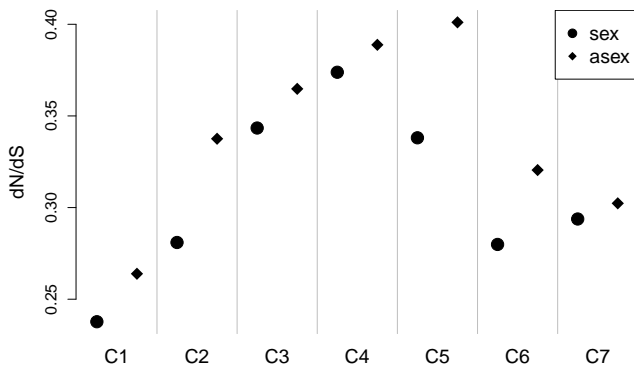


Figure 9.5: A schematic diagram of the karyotype of an evening primrose. The two columns show a heterozygote individual's diploid chromosomal complement. Each chromosome is heterozygote for two different translocations. For example both the top-most chromosomes has one arm from chromosome 1, but the other arm is heterozygote for a large translocation from the ancestral chromosome 2 and 10. Due to these translocations the meiotic pairing form a complete ring of chromosomes, which prevent crossing over and independent segregation. Thanks to Ian Hallister for this diagram.

An example of the costs of asexuality. In the Evening primrose genus (*Oenothera*), there are a number of young, independently-derived,

5576 asexual species. In each species this asexuality is due to a complicated
 5578 series of reciprocal translocations which prevent recombination and
 5580 segregation and ensure that every plant is permanently-heterozygote
 5582 for these rearrangements due to lethality. This system is quite compli-
 5584 cated, and super cool. We don't need to worry about the details but
 importantly each species is functionally asexual. HOLLISTER *et al.*
 (2014) sampled transcriptome data from across the Evening primrose
 clade, and took advantage of 7 independent, asexual-sexual sister pairs
 of species to examine the impact of the evolution of asexuality for
 molecular evolution.



5586 The d_N/d_S for the sexual and asexual species for each of the seven
 5587 pairs (C1-C7) is shown in Figure 9.6. In every pair d_N/d_S is higher in
 5588 the asexual species. The genomes of the asexual species are evolving in
 a less constrained fashion, likely due to weakly deleterious mutations
 5590 accumulating due to hitchhiking with beneficial alleles and the slow
 crank of Muller's ratchet.

5592 *The maintainance of combinations of alleles in the face of recom-
 5593 bination.* In some cases balancing selection may be attempting to
 5594 maintain multiple combinations of alleles in the population that work
 well together. However, recombination may be constantly ripping
 5596 those alleles away from each other making it difficult to maintain these
 alleles. This can select for the suppression of recombination. Some of
 5598 the most dramatic demonstrations of this tension involve the evolution
 of so-called super genes. We'll first consider the evolution of a mimicry
 5600 supergene in *Heliconius numata* as an example of this.

Some of the most spectacular examples of Müllerian mimicry in
 5602 the world are found in *Heliconius* butterflies. These butterflies are
 unpalatable to predators, and different species mimic each other so

Figure 9.6: d_N/d_S calculated on sexual (circles) and asexual (diamonds)



Figure 9.7: Showy evening primrose (*Oenothera speciosa*), the sexual species in the clade C2 from Figure 9.6.

Favourite flowers of garden and greenhouse (1896). Step, E. Image from the Biodiversity Heritage Library. Contributed by Missouri Botanical Garden. Licensed under CC BY-2.0.

5604 benefiting from not being eaten by predators, which rapidly learn to
 avoid all these species). In many of these species multiple mimicry
 5606 morphs are found as we move across geographic space. In *Heliconius*
 5608 *numata* a number of different morphs mimic morphs from a distantly
 related *Melinaea* species.

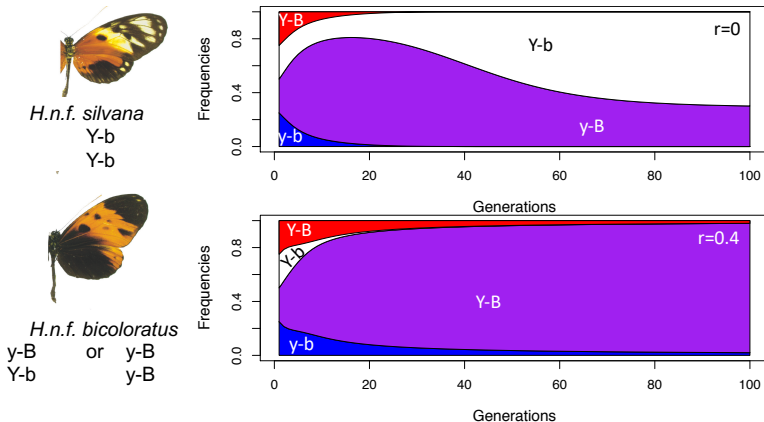


Figure 9.8: Five sympatric forms of *H. numata* from northern Peru, and their distantly related comimetic *Melinaea* species. First row: *M. menophilus* ssp. nov., *M. ludovica ludovica*, *M. marsaeus rileyi*, *M. marsaeus mothone*, and *M. marsaeus phasiana*. Second row, *H. n. f. tarapotensis*, *H. n. f. silvana*, *H. n.f. aurora*, *H. n.f. bicoloratus*, and *H. n. f. arcuella*. Figure and caption from JORON et al. (2006) cropped, licensed under CC BY 4.0.

To keep things relatively simple lets focus on two differences between *silvana* and *bicoloratus*, the yellow stripe on the top wing of *silvana* and the black bottom wing of *bicoloratus*. Lets imagine that 5610 these two differences are due to a simple two locus system. The first 5612 locus segregates for Y/y, where the Y allele encodes for a top-wing 5614 yellow band, and y encodes for the absence of the yellow band. The 5616 second locus segregates for B/b where B encodes for the bottom-wing 5618 being black, and b for the absence of black on the bottom wing. If Y 5620 is recessive and B is dominant, then the *silvana* phenotype corresponds 5622 to a YY bb genotype. Due to the dominance of the y and B alleles the 5624 *bicoloratus* phenotype can be achieved by various genotypes (Yy Bb, 5626 yy BB, Yy BB, yy Bb). Both of these phenotypes offer an advantage 5628 as they mimic a *M. menophilus* model. But there are also genotypes 5630 that don't do as well; YY BB individuals have a yellow band and a 5632 black bottom and so don't do a great job mimicing anything and so will be eaten. Thinking about the four possible haplotypes, y-B has 5634 high marginal fitness as due to its combo of dominant alleles it'll always produce a *bicoloratus* phenotype. Likewise the Y-b haplotype has high marginal fitness, as it does well in the homozygous state (*silvana* phenotype), and when it is paired with the y-B allele. However, the Y-B and y-b haplotypes fair less well as they carry two alleles that 5636 don't work well with each other and so are often individuals who suffer 5638 high rates of predation.

If no recombination occurs between these loci ($r = 0$, Figure 9.9), 5632 then the Y-B and y-b are selected out of the population, and the y-B 5634 and Y-b can be stably maintained. However, when there's too 5636

Figure 9.9:



much recombination between our loci (e.g. $r = 0.4$, Figure 9.9) the
 5636 high-fitness haplotypes keep getting ripped apart by recombination
 and the Y-b is lost from the population as it's recessive advantage is
 5638 lost as it's too often being broken up by recombination in heterozy-
 gotes.

5640 *Supergenes to the rescue!* So our polymorphisms can only be main-
 tained if they are tightly linked, i.e. if these alleles arose at loci that are
 5642 genetically close to each other. But how is it possible that these alleles
 arose close to each other? Well the trick is that they don't necessarily
 5644 have to arise very close to each other. If such a system is polymor-
 phic but being regularly broken up by recombination, a chromosomal
 5646 inversion—the flipping around of a whole section of chromosome—can
 arise and will suppress recombination. Imagine that our two loci are
 5648 far apart genetically, and a chromosomal inversion arises on the Y-b
 background forming the b-Y haplotype. This inverted haplotype will
 5650 not recombine with the y-B haplotype when it is present in a het-
 erozygote, thus it is not broken down by recombination. This inverted
 5652 haplotype, which enjoys the fitness benefits of the Y-b, can therefore
 replace the Y-b haplotype in the population. The two other low fitness
 5654 haplotypes will disappear as they are no longer being generated by re-
 combination, leaving just the y-B and b-Y. The polymorphism system
 5656 now behaves like alleles at a single locus, a super gene (e.g. like $r = 0$
 in Figure 9.9).

“coadapted combinations
 of several or many genes
 locked in inverted sections of
 chromosomes and therefore
 inherited as single units.”
 DOBZHANSKY (1970) on
 supergenes.

Now the *H. numata* system is vastly more complicated than our toy two locus system, presumably involving many changes and refinements, but the same principle holds (JORON *et al.*, 2011). The differences between the different *H. numata* mimetic morphs is found on a single chromosome, and the inheritance behaves as if controlled by a single locus (albeit with many alleles). The *H. n. f. silvana* individuals carry a recessive haplotype of alleles that which is known to be locked together by a ~ 400kb inversion, that is a different chromosomal orientation from the *bicoloratus* allele (haplotype) which acts as a dominant allele. Other alleles at this same chromosomal region provide the genetic basis of the other morphs, and sometimes correspond to further inversions with a range of dominance relationships.

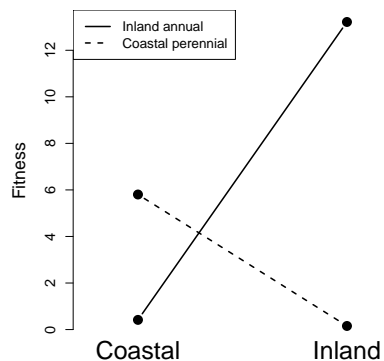


Figure 9.10: **Left)** A coastal perennial and an Inland annuals *Mimulus guttatus* LOWRY and WILLIS (2010), image from LOWRY and WILLIS (2010) licensed under CC BY 4.0. **Right)** A reciprocal transplant experiment showing that coastal perennial and an Inland annuals are locally adapted to their respective habitats. Data from LOWRY and WILLIS (2010), Code here..

Local Adaptation, Speciation, and Inversions. Inversions have long been thought to play an important role in local adaptation and speciation. One example of an inversion underlying local adaptation occurs in *Mimulus guttatus*, in Western North America, where there are annual and perennial ecomorphs. The perennial form grows in many places along the Pacific coast, and in other places with year around moisture; it invests a lot of resources in achieving large size and laying down resources for the next year, and as a result flowers late. The annual form grows inland, e.g. the California central valley, where it has to invest all its effort in flowering rapidly before the long, hot, dry summer. Neither ecomorph does well in the other's environment. The perennials get crisped before they have a chance to flower, while the annuals suffer from high rates of herbivory and cannot tolerate the salt spray. LOWRY and WILLIS (2010) found that large inversion controloed a lot of of the phenotypic variation in flowering time and a range of other morphological differences between these two morphs. They also showed that the inversion controled a reasonable proportion of the differences in fitness in the field, consistent with it underlying

5688 the fitness tradeoffs involved in local adaptation.

Why would an inversion be involved in locking together local
 adapted alleles? The basic idea, like above, is an inversion can be
 selected for we have two (or more) loci segregating for locally adapted
 alleles. Locally advantageous haplotypes are in danger of being broken
 up by recombination with maladapted haplotypes, which are con-
 stantly being introduced into each population by migration from the
 other. If an inversion arises that locks these alleles together in one
 population, it can be selected for as does not suffer the ill effects from
 recombination with migrating maladaptive haplotype.

5698 9.1.1 Sex Chromosomes and the dynamics of selection and recom- bination.

The production of different sized gametes (anisogamy) has arisen a
 number of times in multi-cellular life, with male and female gametes
 are defined by their relative sizes. The smaller, and often more mobile,
 gametes are defined male gametes (e.g. sperm), while the larger, well
 provisioned, and often less mobile are defined as female gametes (e.g.
 egg cell). The evolution of anisogamy is thought to be due to disrupt-
 tive selection due to a tradeoff pulling in opposite directions towards
 mobile gametes able to move further and in the opposite direction
 towards better provisioned gametes better able to build larger zygotes.
 In many organisms individuals can produce both male and female ga-
 metes, while some species have evolved separate sexes, likely in part as
 an inbreeding avoidance mechanism. There is huge diversity in sex de-
 termination mechanisms across the eukaryotic tree (Figure 9.13. This
 is all to say, that biology is wonderfully complicated.

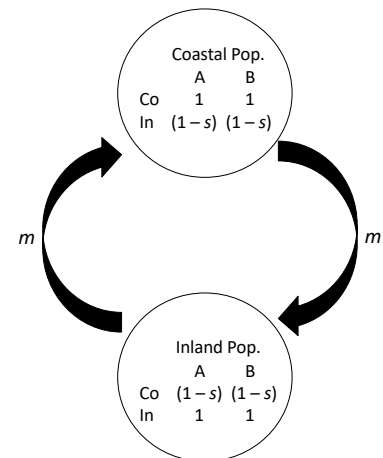


Figure 9.11: A two locus, two population migration-selection balance system. Two loci A and B segregate for an Inland and Coastal adapted alleles.

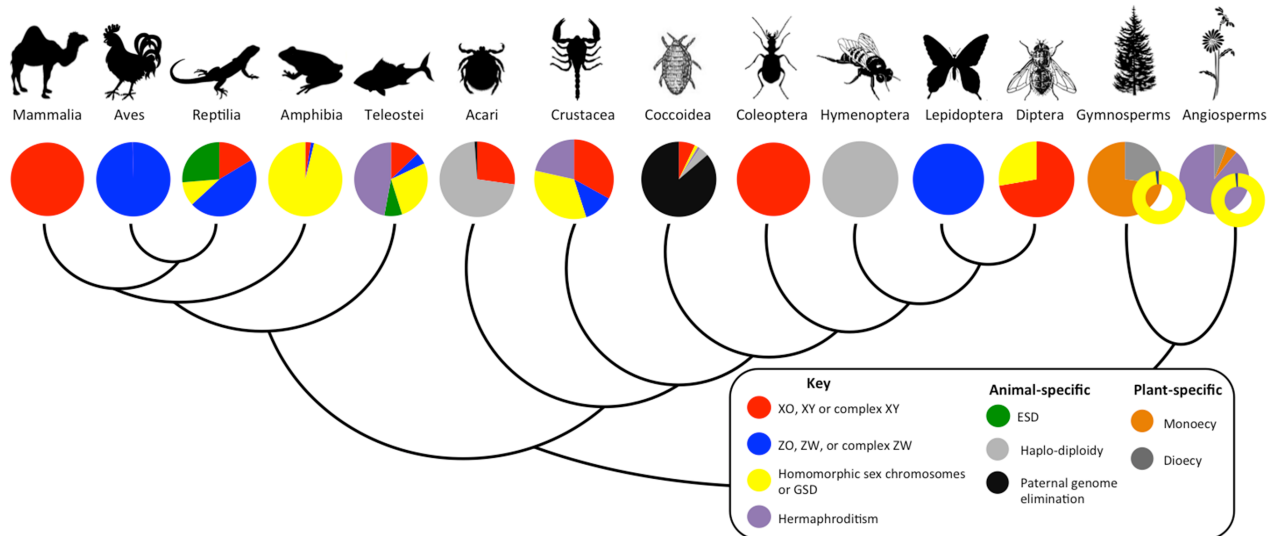
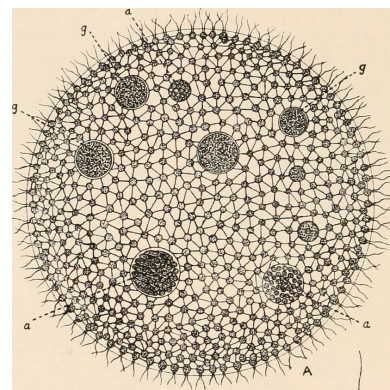


Figure 9.13: Diversity of sex deter-
 mination systems for representative
 plant and animal clades. Figure
 and caption from BACHTROG *et al.*
 (2014), licensed under CC BY 4.0.

In mammals, and many other systems with genetic sex determination, the genes responsible for sex determination lie on a pair of heteromorphic sex chromosomes, i.e. pair of chromosomes that are quite different in size. In mammals it is the male determining Y chromosome that has a very small gene content compared to the X chromosome (Figure 9.14). But in other groups such as birds, and some snakes, females carry a gene poor W with males being the homogametic sex, carrying two Zs. If you are still reading send Graham a picture of Nettie Stevens, she discovered sex chromosomes in 1905 (STEVENS, 1905). These examples of heteromorphic sex chromosomes, and many others like them, are thought to have arisen from an ancestral pair of autosomes? What then explains their evolution?

A broad explanation for the evolution of sex chromosome goes as follows:

In lake Malawi there are many very closely related cichlids species. In many of these species the males are brightly coloured to attract females, while the females are often brown to help them avoid predators. In some of these species there is an alternative orange morph, called the marmalade cat morph, which are cryptic against the rocky bottom of the lake. This morph is due to a dominant (?) mutation called OB at the pax7 (?), and the allele appears to be shared across many of these species. This OB allele works well in females, however, in the males the OB allele disrupts their bright colouration. Thus the OB polymorphism is sexually antagonistic, i.e. it works well in females and poorly in males.

Males carrying the male-deleterious OB allele are rarely found, despite the allele being common in females. Why is that? Well because the OB allele is tightly linked to a newly emerged female-determining allele (W), with males carrying two copies of the Z allele. Males usually are homozygous for the ob-Z haplotype, while females can be either orange (OB-W/ob-Z) or brown (ob-W/ob-Z). Recombination between these two loci seems to be very rare, and so the sexually antagonistic allele OB appears to be mainly female specific. An inversion on the Z background would lock together the

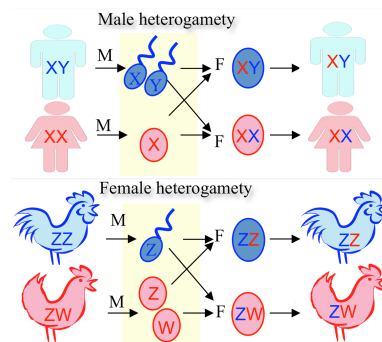


Figure 9.14: Figure from BACHTRÖG *et al.* (2014), licensed under CC BY 4.0cropped from original.



Figure 9.15:

Image credits: Blue mbuna Male *L. fuelleborni* by Chmee2; OB Male *L. fuelleborni* by Dorenko; Brown ob *Tropheops* female by Alexandra Tyers; Female *L. fuelleborni* orange morph, by Mikko Stenberg

5748 *Bibliography*

- 5750 AGUADÉ, M., N. MIYASHITA, and C. H. LANGLEY, 1989 Reduced variation in the yellow-achaete-scute region in natural populations of *Drosophila melanogaster*. *Genetics* **122**: 607–615.
- 5752 AGUILLO, S. M., J. W. FITZPATRICK, R. BOWMAN, S. J. SCHOECH, A. G. CLARK, G. COOP, and N. CHEN, 2017, 08) Deconstructing isolation-by-distance: The genomic consequences of limited dispersal. *PLOS Genetics* **13**(8): 1–27.
- 5756 AKÇAY, E. and J. VAN CLEVE, 2016 There is no fitness but fitness, and the lineage is its bearer. *Phil. Trans. R. Soc. B* **371**(1687): 20150085.
- 5760 ALCAIDE, M., E. S. SCORDATO, T. D. PRICE, and D. E. IRWIN, 2014 Genomic divergence in a ring species complex. *Nature* **511**(7507): 83.
- 5762 ALEXANDER, D. H., J. NOVEMBRE, and K. LANGE, 2009 Fast model-based estimation of ancestry in unrelated individuals. *Genome research* **19**(9): 1655–1664.
- 5766 ALGEE-HEWITT, B. F., M. D. EDGE, J. KIM, J. Z. LI, and N. A. ROSENBERG, 2016 Individual identifiability predicts population identifiability in forensic microsatellite markers. *Current Biology* **26**(7): 935–942.
- 5770 ALLENDORF, F. W. and J. J. HARD, 2009 Human-induced evolution caused by unnatural selection through harvest of wild animals. *Proceedings of the National Academy of Sciences* **106**(Supplement 1): 9987–9994.
- 5774 ALVAREZ, G., F. C. CEBALLOS, and C. QUINTEIRO, 2009 The role of inbreeding in the extinction of a European royal dynasty. *PLoS One* **4**(4): e5174.

- 5776 ANDOLFATTO, P., 2007 Hitchhiking effects of recurrent beneficial
amino acid substitutions in the *Drosophila melanogaster* genome.
5778 *Genome Res.* **17**: 1755–1762.
- 5780 ANDOLFATTO, P. and M. PRZEWORSKI, 2001 Regions of lower
crossing over harbor more rare variants in African populations of
Drosophila melanogaster. *Genetics* **158**: 657–665.
- 5782 AYLLON, F., E. KJÆRNER-SEMB, T. FURMANEK, V. WEN-
NEVIK, M. F. SOLBERG, G. DAHLE, G. L. TARANGER,
5784 K. A. GLOVER, M. S. ALMÉN, C. J. RUBIN, and OTHERS,
2015 The vgl3 locus controls age at maturity in wild and domesti-
5786 cated Atlantic salmon (*Salmo salar* L.) males. *PLoS genetics* **11**(11):
e1005628.
- 5788 BACHTROG, D., J. E. MANK, C. L. PEICHEL, M. KIRK-
PATRICK, S. P. OTTO, T.-L. ASHMAN, M. W. HAHN,
5790 J. KITANO, I. MAYROSE, R. MING, and OTHERS, 2014 Sex
determination: why so many ways of doing it? *PLoS biology* **12**(7):
5792 e1001899.
- 5794 BARRETT, R. D. H., S. M. ROGERS, and D. SCHLUTER,
2008 Natural Selection on a Major Armor Gene in Threespine
Stickleback. *Science* **322**(5899): 255–257.
- 5796 BARSON, N. J., T. AYKANAT, K. HINDAR, M. BARANSKI,
G. H. BOLSTAD, P. FISKE, C. JACQ, A. J. JENSEN, S. E.
5798 JOHNSTON, S. KARLSSON, and OTHERS, 2015 Sex-dependent
dominance at a single locus maintains variation in age at maturity
5800 in salmon. *Nature* **528**(7582): 405.
- 5802 BARTON, N. and G. HEWITT, 1981 A chromosomal cline in the
grasshopper *Podisma pedestris*. *Evolution*: 1008–1018.
- 5804 BARTON, N. H., 2000 Genetic hitchhiking. *Philos. Trans. R. Soc.
Lond., B, Biol. Sci.* **355**: 1553–1562.
- 5806 BAZYKIN, A., 1969 Hypothetical mechanism of speciation. *Evolu-
tion* **23**(4): 685–687.
- 5808 BECQUET, C., N. PATTERSON, A. C. STONE, M. PRZE-
WORSKI, and D. REICH, 2007 Genetic structure of chimpanzee
populations. *PLoS genetics* **3**(4): e66.
- 5810 BEGUN, D. J. and C. F. AQUADRO, 1992 Levels of naturally
occurring DNA polymorphism correlate with recombination rates in
5812 *D. melanogaster*. *Nature* **356**: 519–520.

- BEISSINGER, T. M., L. WANG, K. CROSBY, A. DURVA-
5814 SULA, M. B. HUFFORD, and J. ROSS-IBARRA, 2016 Recent
demography drives changes in linked selection across the maize
5816 genome. *Nature plants* **2**(7): 16084.
- BELL, M. A., M. P. TRAVIS, and D. M. BLOUW, 2006 Infer-
5818 ring natural selection in a fossil threespine stickleback. *Paleobiology* **32**(4): 562–577.
- 5820 BOX, G. E., 1979 Robustness in the strategy of scientific model
building. In *Robustness in statistics*, pp. 201–236. Elsevier.
- 5822 BRADBURD, G. S., P. L. RALPH, and G. M. COOP, 2016
A spatial framework for understanding population structure and
5824 admixture. *PLoS genetics* **12**(1): e1005703.
- 5826 BRANDVAIN, Y., A. M. KENNEY, L. FLAGEL, G. COOP, and
A. L. SWEIGART, 2014 Speciation and introgression between
Mimulus nasutus and Mimulus guttatus. *PLoS Genetics* **10**(6):
5828 e1004410.
- 5830 BRAVERMAN, J. M., R. R. HUDSON, N. L. KAPLAN, C. H.
ANGLEY, and W. STEPHAN, 1995 The hitchhiking effect on
the site frequency spectrum of DNA polymorphisms. *Genetics* **140**:
5832 783–796.
- 5834 BRODIE III, E. D., 1992 Correlational selection for color pattern
and antipredator behavior in the garter snake *Thamnophis ordi-*
noides. *Evolution* **46**(5): 1284–1298.
- 5836 CAI, J. J., J. M. MACPHERSON, G. SELLA, and D. A.
PETROV, 2009 Pervasive hitchhiking at coding and regulatory
5838 sites in humans. *PLoS Genet.* **5**: e1000336.
- CASSA, C. A., D. WEGHORN, D. J. BALICK, D. M. JOR-
5840 DAN, D. NUSINOW, K. E. SAMOCHA, A. O'DONNELL-
LURIA, D. G. MACARTHUR, M. J. DALY, D. R. BEIER,
5842 and OTHERS, 2017 Estimating the selective effects of heterozy-
gous protein-truncating variants from human exome data. *Nature*
5844 *genetics* **49**(5): 806.
- CHARLESWORTH, B., 2009 Effective population size and pat-
5846 terns of molecular evolution and variation. *Nature Reviews Ge-*
netics **10**(3): 195.
- 5848 CHARLESWORTH, D., B. CHARLESWORTH, and M. T. MOR-
GAN, 1995 The pattern of neutral molecular variation under the
5850 background selection model. *Genetics* **141**: 1619–1632.

- CHEN, N., E. J. COSGROVE, R. BOWMAN, J. W. FITZ-
 5852 PATRICK, and A. G. CLARK, 2016 Genomic Consequences of
 Population Decline in the Endangered Florida Scrub-Jay. *Current
 5854 Biology* **26**(21): 2974 – 2979.
- COOK, L. M., B. S. GRANT, I. J. SACCHERI, and J. MAL-
 5856 LET, 2012 Selective bird predation on the peppered moth: the last
 experiment of Michael Majerus. *Biology Letters* **8**(4): 609–612.
- COTTERMAN, C. W., 1940 A calculus for statistico-genetics. Ph.
 D. thesis, The Ohio State University.
- COUSMINER, D. L., D. J. BERRY, N. J. TIMPSON, W. ANG,
 E. THIERING, E. M. BYRNE, H. R. TAAL, V. HUIKARI,
 5860 J. P. BRADFIELD, M. KERKHOF, and OTHERS, 2013
 5862 Genome-wide association and longitudinal analyses reveal genetic
 5864 loci linking pubertal height growth, pubertal timing and childhood
 adiposity. *Human molecular genetics* **22**(13): 2735–2747.
- CUTTER, A. D. and J. Y. CHOI, 2010 Natural selection shapes
 nucleotide polymorphism across the genome of the nematode
 5866 *Caenorhabditis briggsae*. *Genome Res.* **20**: 1103–1111.
- DARWIN, C., 1859 *On the Origin of Species by Means of Natural
 Selection*. London: Murray. or the Preservation of Favored Races in
 5870 the Struggle for Life.
- DARWIN, C., 1876 The effect of cross and self fertilization in the
 vegetable kingdom: Murray. London, UK.
- DARWIN, C., 1888 *The descent of man and selection in relation to
 sex*, Volume 1. Murray.
- DEMPSTER, E., 1955 Maintenance of genetic heterogeneity. *Cold
 Spring Harb Symp Quant Biol* **20**: 25–32.
- DICKERSON, R. E., 1971 The structure of cytochrome c and the
 rates of molecular evolution. *Journal of Molecular Evolution* **1**(1):
 5878 26–45.
- DOBZHANSKY, T., 1943 Genetics of natural populations IX. Tem-
 5882 poral changes in the composition of populations of *Drosophila pseu-*
doobscura. *Genetics* **28**(2): 162.
- DOBZHANSKY, T., 1951 *Genetics and the Origin of Species* (3rd
 Ed. ed.), pp. 16.
- DOBZHANSKY, T., 1970 *Genetics of the evolutionary process*, Vol-
 5886 ume 139. Columbia University Press.

- 5888 ELTON, C., 1942 *Voles, mice and lemmings. Problems in population dynamics.* Oxford: Clarendon Press.
- 5890 ELYASHIV, E., S. SATTATH, T. T. HU, A. STRUTSOVSKY,
G. MCVICKER, P. ANDOLFATTO, G. COOP, and G. SELLA,
5892 2016 A genomic map of the effects of linked selection in *Drosophila*.
PLoS genetics 12(8): e1006130.
- 5894 EWENS, W. J., 2010 What is the gene trying to do? *British Journal for the Philosophy of Science* 62(1): 155–176.
- 5896 EWENS, W. J., 2016 Motoo Kimura and James Crow on the Infinitely Many Alleles Model. *Genetics* 202(4): 1243–1245.
- 5898 FAY, J. C. and C. I. WU, 2000 Hitchhiking under positive Darwinian selection. *Genetics* 155: 1405–1413.
- 5900 FEDER, A. F., C. KLINE, P. POLACINO, M. COTTRELL,
A. D. KASHUBA, B. F. KEELE, S.-L. HU, D. A. PETROV,
5902 P. S. PENNINGS, and Z. AMBROSE, 2017 A spatio-temporal assessment of simian/human immunodeficiency virus (SHIV) evolution reveals a highly dynamic process within the host. *PLoS pathogens* 13(5): e1006358.
- 5904 FISHER, R. A., 1915 The evolution of sexual preference. *The Eugenics Review* 7(3): 184.
- 5906 FISHER, R. A., 1923 XXI.—on the dominance ratio. *Proceedings of the royal society of Edinburgh* 42: 321–341.
- 5908 FISHER, R. A., 1930 *The genetical theory of natural selection: a complete variorum edition.* Oxford University Press.
- 5910 FRANCIOLI, L. C., A. MENELAOU, S. L. PULIT,
F. VAN DIJK, P. F. PALAMARA, C. C. ELBERS, P. B.
5912 NEERINCX, K. YE, V. GURYEV, W. P. KLOOSTERMAN,
5914 and OTHERS, 2014 Whole-genome sequence variation, population structure and demographic history of the Dutch population. *Nature genetics* 46(8): 818.
- 5916 FRENTIU, F. D., G. D. BERNARD, C. I. CUEVAS, M. P.
SISON-MANGUS, K. L. PRUDIC, and A. D. BRISCOE, 2007
5918 Adaptive evolution of color vision as seen through the eyes of butterflies. *Proceedings of the National Academy of Sciences* 104(suppl 1): 8634–8640.
- 5920 GALEN, C., 1996 Rates of floral evolution: adaptation to bumblebee pollination in an alpine wildflower, *Polemonium viscosum*. *Evolution* 50(1): 120–125.
- 5922

- 5926 GALTIER, N., 2016 Adaptive protein evolution in animals and the
effective population size hypothesis. *PLoS genetics* **12**(1): e1005774.
- 5928 GIGORD, L. D., M. R. MACNAIR, and A. SMITHSON, 2001
Negative frequency-dependent selection maintains a dramatic
5930 flower color polymorphism in the rewardless orchid *Dactylorhiza*
sambucina (L.) Soo. *Proceedings of the National Academy of Sci-*
5932 *ences* **98**(11): 6253–6255.
- GILLESPIE, J. H., 2000 Genetic drift in an infinite population. The
5934 pseudohitchhiking model. *Genetics* **155**: 909–919.
- HALDANE, J., 1942 The selective elimination of silver foxes in east-
5936 ern Canada. *Journal of Genetics* **44**(2-3): 296–304.
- HALDANE, J. and S. JAYAKAR, 1963 Polymorphism due to selec-
5938 tion of varying direction. *Journal of Genetics* **58**(2): 237–242.
- HALDANE, J. B. S., 1927 A mathematical theory of natural and
5940 artificial selection, part V: selection and mutation. In *Mathematical*
Proceedings of the Cambridge Philosophical Society, Volume 23, pp.
5942 838–844. Cambridge University Press.
- HALDANE, J. B. S., 1937 The Effect of Variation of Fitness. *The*
5944 *American Naturalist* **71**(735): 337–349.
- HAMILTON, W. D., 1964a The genetical evolution of social be-
5946 haviour. II. *Journal of theoretical biology* **7**(1): 17–52.
- HAMILTON, W. D., 1964b The genetical evolution of social be-
5948 haviour. II. *Journal of theoretical biology* **7**(1): 17–52.
- HERMISSON, J. and P. S. PENNINGS, 2017 Soft sweeps and
5950 beyond: understanding the patterns and probabilities of selection
footprints under rapid adaptation. *Methods in Ecology and Evolu-*
5952 *tion* **8**(6): 700–716.
- HEY, J. and R. M. KLIMAN, 2002 Interactions between nat-
5954 ural selection, recombination and gene density in the genes of
Drosophila. *Genetics* **160**(2): 595–608.
- HOEKSTRA, H. E., K. E. DRUMM, and M. W. NACHMAN,
5956 2004 Ecological genetics of adaptive color polymorphism in pocket
mice: geographic variation in selected and neutral genes. *Evolu-*
5958 *tion* **58**(6): 1329–1341.
- HOHENLOHE, P. A., S. BASSHAM, P. D. ETTER,
5960 N. STIFFLER, E. A. JOHNSON, and W. A. CRESKO, 2010
Population genomics of parallel adaptation in threespine stickleback
5962 using sequenced RAD tags. *PLoS genetics* **6**(2): e1000862.

- 5964 HOLLISTER, J. D., S. GREINER, W. WANG, J. WANG,
Y. ZHANG, G. K.-S. WONG, S. I. WRIGHT, and M. T.
5966 JOHNSON, 2014 Recurrent loss of sex is associated with accumula-
tion of deleterious mutations in Oenothera. Molecular biology and
5968 evolution **32**(4): 896–905.
- HOPKINS, J., G. BAUDRY, U. CANDOLIN, and A. KAITALA,
5970 2015 I'm sexy and I glow it: female ornamentation in a nocturnal
capital breeder. Biology letters **11**(10): 20150599.
- 5972 HOUDE, A. E., 1994 Effect of artificial selection on male colour
patterns on mating preference of female guppies. Proc. R. Soc.
5974 Lond. B **256**(1346): 125–130.
- HOWES, R. E., M. DEWI, F. B. PIEL, W. M. MONTEIRO,
5976 K. E. BATTLE, J. P. MESSINA, A. SAKUNTABHAI, A. W.
SATYAGRAHA, T. N. WILLIAMS, J. K. BAIRD, and S. I.
5978 HAY, 2013 Spatial distribution of G6PD deficiency variants across
malaria-endemic regions. Malar. J. **12**: 418.
- 5980 HOWES, R. E., F. B. PIEL, A. P. PATIL, O. A. NYANGIRI,
P. W. GETHING, M. DEWI, M. M. HOGG, K. E. BAT-
5982 TLE, C. D. PADILLA, J. K. BAIRD, and S. I. HAY, 2012
G6PD deficiency prevalence and estimates of affected populations in
5984 malaria endemic countries: a geostatistical model-based map. PLoS
Medicine **9**(11): e1001339.
- 5986 HUDSON, R. R., 2015, 07)A New Proof of the Expected Frequency
Spectrum under the Standard Neutral Model. PLOS ONE **10**(7):
5988 1–5.
- HUDSON, R. R. and N. L. KAPLAN, 1995a Deleterious back-
5990 ground selection with recombination. Genetics **141**: 1605–1617.
- HUDSON, R. R. and N. L. KAPLAN, 1995b The coalescent pro-
5992 cess and background selection. Philos. Trans. R. Soc. Lond., B, Biol.
Sci. **349**: 19–23.
- 5994 HUDSON, R. R., M. KREITMAN, and M. AGUADÉ, 1987 A test
of neutral molecular evolution based on nucleotide data. Genet-
5996 ics **116**(1): 153–159.
- HUNT, G., M. A. BELL, and M. P. TRAVIS, 2008 Evolution
5998 toward a new adaptive optimum: phenotypic evolution in a fossil
stickleback lineage. Evolution **62**(3): 700–710.
- 6000 JAIN, S. and A. D. BRADSHAW, 1966 Evolutionary divergence
among adjacent plant populations I. The evidence and its theoreti-
6002 cal analysis. Heredity **21**(3): 407.

- JANICKE, T., I. K. HÄDERER, M. J. LAJEUNESSE, and N. ANTHES, 2016 Darwinian sex roles confirmed across the animal kingdom. *Science advances* 2(2): e1500983.
- JENNINGS, W. B. and S. V. EDWARDS, 2005 Speciation history of Australian grass finches (*Poephila*) inferred from thirty gene trees. *Evolution* 59(9): 2033–2047.
- JOHANNSEN, W., 1911 The Genotype Conception of Heredity. *The American Naturalist* 45(531): 129–159.
- JOHNSTON, S. E., J. GRATTON, C. BERENOS, J. G. PILKINGTON, T. H. CLUTTON-BROCK, J. M. PEMBERTON, and J. SLATE, 2013 Life history trade-offs at a single locus maintain sexually selected genetic variation. *Nature* 502(7469): 93.
- JORON, M., L. FREZAL, R. T. JONES, N. L. CHAMBERLAIN, S. F. LEE, C. R. HAAG, A. WHIBLEY, M. BECUWE, S. W. BAXTER, L. FERGUSON, and OTHERS, 2011 Chromosomal rearrangements maintain a polymorphic supergene controlling butterfly mimicry. *Nature* 477(7363): 203.
- JORON, M., R. PAPA, M. BELTRÁN, N. CHAMBERLAIN, J. MAVÁREZ, S. BAXTER, M. ABANTO, E. BERMINGHAM, S. J. HUMPHRAY, J. ROGERS, and OTHERS, 2006 A conserved supergene locus controls colour pattern diversity in *Heliocinus* butterflies. *PLoS biology* 4(10): e303.
- JUKEMA, J. and T. PIERSMA, 2006 Permanent female mimics in a lekking shorebird. *Biology letters* 2(2): 161–164.
- KAPLAN, N. L., R. R. HUDSON, and C. H. LANGLEY, 1989 The hitchhiking effect revisited. *Genetics* 123: 887–899.
- KARN, M. N. and L. PENROSE, 1951 Birth weight and gestation time in relation to maternal age, parity and infant survival. *Annals of eugenics* 16(1): 147–164.
- KETTLEWELL, H. B. D., 1955 Selection experiments on industrial melanism in the Lepidoptera. *Heredity* 9(3): 323.
- KIM, Y., 2006 Allele frequency distribution under recurrent selective sweeps. *Genetics* 172: 1967–1978.
- KIMURA, M., 1968 Evolutionary rate at the molecular level. *Nature* 217(5129): 624–626.
- KIMURA, M., 1983 *The neutral theory of molecular evolution*. Cambridge University Press.

- 6040 KIMURA, M. and J. F. CROW, 1964 The number of alleles that
can be maintained in a finite population. *Genetics* **49**(4): 725.
- 6042 KIMURA, M. and T. OHTA, 1974 On some principles governing
molecular evolution. *Proceedings of the National Academy of
Sciences* **71**(7): 2848–2852.
- 6046 KING, J. L. and T. H. JUKES, 1969 Non-darwinian evolution.
Science **164**(3881): 788–798.
- 6048 KORNEGAY, J. R., J. W. SCHILLING, and A. C. WILSON,
1994 Molecular adaptation of a leaf-eating bird: stomach lysozyme
of the hoatzin. *Molecular Biology and Evolution* **11**(6): 921–928.
- 6050 KRAKAUER, A. H., 2005 Kin selection and cooperative courtship in
wild turkeys. *Nature* **434**(7029): 69.
- 6052 KRUUK, L. E., J. SLATE, J. M. PEMBERTON, S. BROTH-
ERSTONE, F. GUINNESS, and T. CLUTTON-BROCK, 2002
Antler size in red deer: heritability and selection but no evolution.
Evolution **56**(8): 1683–1695.
- 6056 KÜPPER, C., M. STOCKS, J. E. RISSE, N. DOS REMEDIOS,
L. L. FARRELL, S. B. MCRAE, T. C. MORGAN, N. KAR-
LIONOVA, P. PINCHUK, Y. I. VERKUIL, and OTHERS, 2016
A supergene determines highly divergent male reproductive morphs
in the ruff. *Nature Genetics* **48**(1): 79.
- 6062 KWIATKOWSKI, D. P., 2005, August)How malaria has affected
the human genome and what human genetics can teach us about
malaria. *Am. J. Hum. Genet.* **77**(2): 171–192.
- 6064 LAMICHHANEY, S., G. FAN, F. WIDEMO, U. GUNNARS-
SON, D. S. THALMANN, M. P. HOEPPNER, S. KERJE,
U. GUSTAFSON, C. SHI, H. ZHANG, and OTHERS, 2016
Structural genomic changes underlie alternative reproductive strate-
gies in the ruff (*Philomachus pugnax*). *Nature Genetics* **48**(1): 84.
- 6070 LANDE, R., 1976 Natural selection and random genetic drift in
phenotypic evolution. *Evolution* **30**(2): 314–334.
- 6072 LANDE, R., 1979 Quantitative genetic analysis of multivariate evo-
lution, applied to brain: body size allometry. *Evolution* **33**(1Part2):
402–416.
- 6074 LAURIE, C. C., D. A. NICKERSON, A. D. ANDERSON, B. S.
WEIR, R. J. LIVINGSTON, M. D. DEAN, K. L. SMITH,
E. E. SCHADT, and M. W. NACHMAN, 2007, 08)Linkage Dise-
quilibrium in Wild Mice. *PLOS Genetics* **3**(8): 1–9.

- 6078 LAWSON, D. J., L. VAN DORP, and D. FALUSH, 2018 A tutorial
 6080 on how not to over-interpret STRUCTURE and ADMIXTURE bar plots. *Nature communications* 9(1): 3258.
- 6082 LEFÉBURE, T., C. MORVAN, F. MALARD, C. FRANÇOIS,
 6084 L. KONECNY-DUPRÉ, L. GUÉGUEN, M. WEISS-GAYET,
 A. SEGUIN-ORLANDO, L. ERMINI, C. DER SARKISSIAN,
 and OTHERS, 2017 Less effective selection leads to larger genomes. *Genome research*: gr-212589.
- 6086 LEFFLER, E. M., K. BULLAUGHEY, D. R. MATUTE, W. K.
 MEYER, L. SEGUREL, A. VENKAT, P. ANDOLFATTO, and
 6088 M. PRZEWORSKI, 2012 Revisiting an old riddle: what determines genetic diversity levels within species? *PLoS biology* 10(9):
 6090 e1001388.
- 6092 LEK, M., K. J. KARCZEWSKI, E. V. MINIKEL, K. E.
 SAMOCHA, E. BANKS, T. FENNELL, A. H. O'DONNELL-
 6094 LURIA, J. S. WARE, A. J. HILL, B. B. CUMMINGS, and
 OTHERS, 2016 Analysis of protein-coding genetic variation in
 60,706 humans. *Nature* 536(7616): 285.
- 6096 LENORMAND, T., D. BOURGUET, T. GUILLEMAUD, and
 M. RAYMOND, 1999 Tracking the evolution of insecticide resistance in the mosquito *Culex pipiens*. *Nature* 400(6747): 861.
- 6100 LEWONTIN, R. C., 1970 The units of selection. *Annual review of ecology and systematics* 1(1): 1–18.
- 6102 LEWONTIN, R. C., 1974 *The Genetic Basis of Evolutionary Change*. Columbia University Press, New York.
- 6104 LEWONTIN, R. C., 1994, 05)[DNA Fingerprinting: A Review of the Controversy]: Comment: The Use of DNA Profiles in Forensic Contexts. *Statist. Sci.* 9(2): 259–262.
- 6106 LEWONTIN, R. C., 2001 *Thinking about evolution: historical, philosophical, and political perspectives*, Chapter Natural History and
 6108 Formalism in Evolutionary Genetics, pp. 7–20. Cambridge University Press.
- 6110 LI, J. Z., D. M. ABSHER, H. TANG, A. M. SOUTHWICK,
 A. M. CASTO, S. RAMACHANDRAN, H. M. CANN, G. S.
 6112 BARSH, M. FELDMAN, L. L. CAVALLI-SFORZA, and OTHERS, 2008 Worldwide human relationships inferred from genome-wide patterns of variation. *science* 319(5866): 1100–1104.
- 6114 LISTER, A., 1989 Rapid dwarfing of red deer on Jersey in the last interglacial. *Nature* 342(6249): 539.

- LOCKE, D. P., L. W. HILLIER, W. C. WARREN, K. C.
6118 WORLEY, L. V. NAZARETH, D. M. MUZNY, S.-P. YANG,
Z. WANG, A. T. CHINWALLA, P. MINX, and OTHERS, 2011
6120 Comparative and demographic analysis of orang-utan genomes.
Nature 469(7331): 529.
- LOSOS, J. B., S. J. ARNOLD, G. BEJERANO, E. BRODIE III,
D. HIBBETT, H. E. HOEKSTRA, D. P. MINDELL, A. MON-
6124 TEIRO, C. MORITZ, H. A. ORR, and OTHERS, 2013 Evolutionary biology for the 21st century. PLoS Biology 11(1): e1001466.
- LOUICHAROEN, C., E. PATIN, R. PAUL, I. NUCHPRAY-
6126 OON, B. WITOONPANICH, C. PEERAPITTAYAMONGKOL,
I. CASADEMONT, T. SURA, N. M. LAIRD, P. SINGHASI-
6128 VANON, L. QUINTANA-MURCI, and A. SAKUNTABHAI, 2009,
6130 December)Positively selected G6PD-Mahidol mutation reduces *Plas-
modium vivax* density in Southeast Asians. Science 326(5959):
6132 1546–1549.
- LOWRY, D. B. and J. H. WILLIS, 2010 A widespread chromo-
6134 somal inversion polymorphism contributes to a major life-history
transition, local adaptation, and reproductive isolation. PLoS biol-
6136 ogy 8(9): e1000500.
- MACARTHUR, D. G., S. BALASUBRAMANIAN, A. FRANK-
6138 ISH, N. HUANG, J. MORRIS, K. WALTER, L. JOSTINS,
L. HABEGGER, J. K. PICKRELL, S. B. MONTGOMERY, and
6140 OTHERS, 2012 A systematic survey of loss-of-function variants in
human protein-coding genes. Science 335(6070): 823–828.
- MACPHERSON, J. M., G. SELLA, J. C. DAVIS, and D. A.
PETROV, 2007 Genomewide spatial correspondence between non-
6144 synonymous divergence and neutral polymorphism reveals extensive
adaptation in *Drosophila*. Genetics 177: 2083–2099.
- MAJERUS, M. E., 2009 Industrial melanism in the peppered moth,
Biston betularia: an excellent teaching example of Darwinian evolu-
6146 tion in action. Evolution: Education and Outreach 2(1): 63.
- MALÉCOT, G., 1948 Les mathématiques de l'hérédité.
- 6150 MALÉCOT, G., 1969 The Mathematics of Heredity (Revised, edited
and translated by Yermanos, DM).
- MARCINIAK, S. and G. H. PERRY, 2017 Harnessing ancient
6152 genomes to study the history of human adaptation. Nature Reviews
6154 Genetics 18(11): 659.

- MAYNARD SMITH, J., 1964 Group selection and kin selection.
6156 Nature 201(4924): 1145.
- MAYNARD SMITH, J. and J. HAIGH, 1974 The hitch-hiking
6158 effect of a favourable gene. Genet. Res. 23: 23–35.
- MCDONALD, J. H. and M. KREITMAN, 1991 Adaptive protein
6160 evolution at the Adh locus in Drosophila. Nature 351(6328): 652.
- MCVICKER, G., D. GORDON, C. DAVIS, and P. GREEN, 2009
6162 Widespread genomic signatures of natural selection in hominid
evolution. PLoS Genet. 5: e1000471.
- 6164 MENOZZI, P., A. PIAZZA, and L. CAVALLI-SFORZA, 1978
Synthetic maps of human gene frequencies in Europeans. Sci-
6166 ence 201(4358): 786–792.
- MEREDITH, R. W., J. GATESY, W. J. MURPHY, O. A. RY-
6168 DER, and M. S. SPRINGER, 2009, 09)Molecular Decay of the
Tooth Gene Enamelin (ENAM) Mirrors the Loss of Enamel in the
6170 Fossil Record of Placental Mammals. PLOS Genetics 5(9): 1–12.
- MESSIER, W. and C.-B. STEWART, 1997 Episodic adaptive
6172 evolution of primate lysozymes. Nature 385(6612): 151.
- MULLER, H. J., 1932 Some genetic aspects of sex. The American
6174 Naturalist 66(703): 118–138.
- NACHMAN, M. W., H. E. HOEKSTRA, and S. L.
6176 D'AGOSTINO, 2003 The genetic basis of adaptive melanism
in pocket mice. Proceedings of the National Academy of Sci-
6178 ences 100(9): 5268–5273.
- NASH, D., S. NAIR, M. MAYXAY, P. N. NEWTON, J.-P.
6180 GUTHMANN, F. NOSTEN, and T. J. ANDERSON, 2005 Selec-
tion strength and hitchhiking around two anti-malarial resistance
6182 genes. Proceedings of the Royal Society of London B: Biological
Sciences 272(1568): 1153–1161.
- NELSON, M. R., D. WEGMANN, M. G. EHM, D. KESSNER,
6184 P. S. JEAN, C. VERZILLI, J. SHEN, Z. TANG, S.-A. BA-
6186 CANU, D. FRASER, and OTHERS, 2012 An abundance of rare
functional variants in 202 drug target genes sequenced in 14,002
6188 people. Science: 1217876.
- NORBORG, M., B. CHARLESWORTH, and
6190 D. CHARLESWORTH, 1996 The effect of recombination on back-
ground selection. Genet. Res. 67: 159–174.

- 6192 NOVEMBRE, J. and M. STEPHENS, 2008 Interpreting principal
component analyses of spatial population genetic variation. *Nature*
6194 *genetics* **40**(5): 646.
- 6196 OHTA, T., 1972 Population size and rate of evolution. *Journal of*
Molecular Evolution **1**(4): 305–314.
- 6198 OHTA, T., 1973 Slightly deleterious mutant substitutions in evolu-
tion. *Nature* **246**(5428): 96.
- 6200 OHTA, T., 1987 Very slightly deleterious mutations and the molecu-
lar clock. *Journal of Molecular Evolution* **26**(1-2): 1–6.
- 6202 OHTA, T. and J. H. GILLESPIE, 1996 Development of neutral
and nearly neutral theories. *Theoretical population biology* **49**(2):
128–142.
- 6204 OWEN, D. and D. CHANTER, 1972 Polymorphic mimicry in a
population of the African butterfly, *Pseudacraea eurytus* (L.) (Lep.
6206 Nymphalidae). *Insect Systematics & Evolution* **3**(4): 258–266.
- 6208 PAABY, A. B., A. O. BERGLAND, E. L. BEHRMAN, and
P. S. SCHMIDT, 2014 A highly pleiotropic amino acid polymor-
phism in the *Drosophila* insulin receptor contributes to life-history
6210 adaptation. *Evolution* **68**(12): 3395–3409.
- 6212 PATTERTON, N., A. L. PRICE, and D. REICH, 2006 Population
structure and eigenanalysis. *PLoS genetics* **2**(12): e190.
- 6214 PICKRELL, J. K., T. BERISA, J. Z. LIU, L. SÉGUREL, J. Y.
TUNG, and D. A. HINDS, 2016 Detection and interpretation of
shared genetic influences on 42 human traits. *Nature genetics* **48**(7):
6216 709.
- 6218 POTTI, J. and D. CANAL, 2011 Heritability and genetic corre-
lation between the sexes in a songbird sexual ornament. *Hered-
ity* **106**(6): 945.
- 6220 PRITCHARD, J. K., M. STEPHENS, and P. DONNELLY, 2000
Inference of population structure using multilocus genotype data.
6222 *Genetics* **155**(2): 945–959.
- 6224 PROVINE, W. B., 2001 *The origins of theoretical population genet-
ics: with a new afterword*. University of Chicago Press.
- 6226 PRZEWORSKI, M., 2002 The signature of positive selection at ran-
domly chosen loci. *Genetics* **160**: 1179–1189.

- PTAK, S. E., A. D. ROEDER, M. STEPHENS, Y. GILAD,
 6228 S. PÄÄBO, and M. PRZEWORSKI, 2004 Absence of the TAP2
 human recombination hotspot in chimpanzees. *PLoS biology* 2(6):
 6230 e155.
- QUELLER, D. C., 1992 Quantitative genetics, inclusive fitness, and
 6232 group selection. *The American Naturalist* 139(3): 540–558.
- R, 2018 R: A Language and Environment for Statistical Computing.
- 6234 RALPH, P. L. and G. COOP, 2015 The role of standing varia-
 tion in geographic convergent adaptation. *The American Natural-
 ist* 186(S1): S5–S23.
- RANDS, C. M., S. MEADER, C. P. PONTING, and
 6238 G. LUNTER, 2014 8.2% of the human genome is constrained:
 variation in rates of turnover across functional element classes in the
 6240 human lineage. *PLoS genetics* 10(7): e1004525.
- RICHARDS, C. M., 2000 Inbreeding depression and genetic rescue
 6242 in a plant metapopulation. *The American Naturalist* 155(3): 383–
 394.
- 6244 RITLAND, K., C. NEWTON, and H. MARSHALL, 2001 Inher-
 itance and population structure of the white-phased “Kermode”
 6246 black bear. *Current Biology* 11(18): 1468 – 1472.
- ROBERTSON, A., 1961 Inbreeding in artificial selection programmes.
 6248 *Genet. Res.* 2: 189—194.
- ROBINSON, J. A., D. ORTEGA-DEL VECCHYO, Z. FAN,
 6250 B. Y. KIM, C. D. MARSDEN, K. E. LOHMUELLER, R. K.
 WAYNE, and OTHERS, 2016 Genomic flatlining in the endangered
 6252 island fox. *Current Biology* 26(9): 1183–1189.
- ROBINSON, L. M., J. R. BOLAND, and J. M. BRAVERMAN,
 6254 2016 Revisiting a Classic Study of the Molecular Clock. *Journal of
 molecular evolution* 82(2-3): 110–116.
- ROSENBERG, N. A., J. K. PRITCHARD, J. L. WEBER,
 6256 H. M. CANN, K. K. KIDD, L. A. ZHIVOTOVSKY, and
 6258 M. W. FELDMAN, 2002 Genetic structure of human populations.
science 298(5602): 2381–2385.
- RUWENDE, C., S. C. KHOO, R. W. SNOW, S. N. YATES,
 6260 D. KWIATKOWSKI, S. GUPTA, P. WARN, C. E. ALLSOPP,
 6262 S. C. GILBERT, and N. PESCHU, 1995, July)Natural selection of
 hemi- and heterozygotes for G6PD deficiency in Africa by resistance
 6264 to severe malaria. *Nature* 376(6537): 246–249.

- SAMS, A. J. and A. R. BOYKO, 2018a Fine-scale resolution and analysis of runs of homozygosity in domestic dogs. bioRxiv.
6266
- SAMS, A. J. and A. R. BOYKO, 2018b Fine-Scale Resolution of Runs of Homozygosity Reveal Patterns of Inbreeding and Substantial Overlap with Recessive Disease Genotypes in Domestic Dogs.
6268
- G3: Genes, Genomes, Genetics: g3–200836.
6270
- SANKARARAMAN, S., N. PATTERSON, H. LI, S. PÄÄBO, and D. REICH, 2012, 10)The Date of Interbreeding between Neandertals and Modern Humans. PLOS Genetics 8(10): 1–9.
6272
- SANTIAGO, E. and A. CABALLERO, 1995 Effective size of populations under selection. Genetics 139: 1013–1030.
6274
- SANTIAGO, E. and A. CABALLERO, 1998 Effective size and polymorphism of linked neutral loci in populations under directional selection. Genetics 149: 2105–2117.
6276
- SATTATH, S., E. ELYASHIV, O. KOLODNY, Y. RINOTT, and G. SELLA, 2011a Pervasive adaptive protein evolution apparent in diversity patterns around amino acid substitutions in *Drosophila simulans*. PLoS genetics 7(2): e1001302.
6280
- SATTATH, S., E. ELYASHIV, O. KOLODNY, Y. RINOTT, and G. SELLA, 2011b Pervasive adaptive protein evolution apparent in diversity patterns around amino acid substitutions in *Drosophila simulans*. PLoS Genet. 7: e1001302.
6284
- SCHEMSKE, D. W. and P. BIERZYCHUDEK, 2001 Perspective: evolution of flower color in the desert annual Linanthus parryae: Wright revisited. Evolution 55(7): 1269–1282.
6288
- SELLA, G., D. A. PETROV, M. PRZEWORSKI, and P. ANDOLFATTO, 2009 Pervasive natural selection in the *Drosophila* genome? PLoS genetics 5(6): e1000495.
6290
- SHAPIRO, J. A., W. HUANG, C. ZHANG, M. J. HUBISZ, J. LU, D. A. TURISSINI, S. FANG, H. Y. WANG, R. R. HUDSON, R. NIELSEN, Z. CHEN, and C. I. WU, 2007 Adaptive genic evolution in the *Drosophila* genomes. Proc. Natl. Acad. Sci. U.S.A. 104: 2271–2276.
6294
- SMITH, T. B., 1993 Disruptive selection and the genetic basis of bill size polymorphism in the African finch Pyrenestes. Nature 363(6430): 618.
6298
- SMITHSON, A. and M. R. MACNAIR, 1997 Negative frequency-dependent selection by pollinators on artificial flowers without rewards. Evolution 51(3): 715–723.
6302

- 6304 STEVENS, N. M., 1905 *Studies in Spermatogenesis: With especial
reference to the "accessory chromosome"*, Volume 36. Carnegie
6306 Institution of Washington.
- 6308 STURTEVANT, A. H., 1915 The behavior of the chromosomes as
studied through linkage. *Zeitschrift für induktive Abstammungs- und
Vererbungslehre* 13(1): 234–287.
- 6310 TAJIMA, F., 1989 Statistical method for testing the neutral muta-
tion hypothesis by DNA polymorphism. *Genetics* 123(3): 585–595.
- 6312 TISHKOFF, S. A., R. VARKONYI, N. CAHINHINAN,
S. ABBES, G. ARGYROPOULOS, G. DESTRO-BISOL,
6314 A. DROUSIOTOU, B. DANGERFIELD, G. LEFRANC,
J. LOISELET, A. PIRO, M. STONEKING, A. TAGARELLI,
6316 G. TAGARELLI, E. H. TOUMA, S. M. WILLIAMS, and
A. G. CLARK, 2001 Haplotype Diversity and Linkage Disequi-
6318 librium at Human G6PD: Recent Origin of Alleles That Confer
Malarial Resistance. *Science* 293(5529): 455–462.
- 6320 TOEWS, D. P., S. A. TAYLOR, R. VALLENDER, A. BRELS-
FORD, B. G. BUTCHER, P. W. MESSEY, and I. J.
6322 LOVETTE, 2016 Plumage Genes and Little Else Distinguish the
Genomes of Hybridizing Warblers. *Current Biology* 26(17): 2313 –
6324 2318.
- 6326 TURELLI, M., D. W. SCHEMSKE, and P. BIERZYCHUDEK,
2001 Stable two-allele polymorphisms maintained by fluctuating
fitnesses and seed banks: protecting the blues in Linanthus parryae.
6328 *Evolution* 55(7): 1283–1298.
- 6330 ULIZZI, L. and L. TERRENATO, 1992 Natural selection associated
with birth weight. VI. Towards the end of the stabilizing compo-
6332 nent. *Annals of human genetics* 56(2): 113–118.
- 6334 VAN'T HOF, A. E., N. EDMONDS, M. DALÍKOVÁ, F. MAREC,
and I. J. SACCHERI, 2011 Industrial melanism in British pep-
6336 pered moths has a singular and recent mutational origin. *Sci-
ence* 332(6032): 958–960.
- 6338 VOIGHT, B. F., A. M. ADAMS, L. A. FRISSE, Y. QIAN,
R. R. HUDSON, and A. DI RIENZO, 2005 Interrogating mul-
6340 tiple aspects of variation in a full resequencing data set to infer hu-
man population size changes. *Proceedings of the National Academy
of Sciences* 102(51): 18508–18513.
- 6342 VONHOLDT, B. M., J. P. POLLINGER, D. A. EARL,
J. C. KNOWLES, A. R. BOYKO, H. PARKER, E. GEF-

- FEN, M. PILOT, W. JEDRZEJEWSKI, B. JEDRZEJEW-
6344 SKA, V. SIDOROVICH, C. GRECO, E. RANDI, M. MU-
SIANI, R. KAYS, C. D. BUSTAMANTE, E. A. OSTRANDER,
6346 J. NOVEMBRE, and R. K. WAYNE, 2011 A genome-wide per-
spective on the evolutionary history of enigmatic wolf-like canids.
6348 Genome Research.
- WANG, J., J. DING, B. TAN, K. M. ROBINSON, I. H.
6350 MICHELSON, A. JOHANSSON, B. NYSTEDT, D. G.
SCOFIELD, O. NILSSON, S. JANSSON, and OTHERS, 2018
6352 A major locus controls local adaptation and adaptive life history
variation in a perennial plant. *Genome biology* 19(1): 72.
- 6354 WATTERSON, G., 1975 On the number of segregating sites in ge-
netical models without recombination. *Theoretical population
biology* 7(2): 256–276.
- WEIS, A. E. and W. L. GORMAN, 1990 Measuring selection
6358 on reaction norms: an exploration of the *Eurosta-Solidago* system.
Evolution 44(4): 820–831.
- 6360 WHEELER, W. M., 1907 Pink Insect Mutants. *The American
Naturalist* 41(492): 773–780.
- 6362 WIDEMO, F., 1998 Alternative reproductive strategies in the ruff,
Philomachus pugnax: a mixed ESS? *Animal Behaviour* 56(2): 329–
6364 336.
- 6366 WIEHE, T. and W. STEPHAN, 1993a Analysis of a genetic hitch-
hiking model, and its application to DNA polymorphism data from
Drosophila melanogaster. *Molecular Biology and Evolution* 10(4):
6368 842–854.
- 6370 WIEHE, T. H. and W. STEPHAN, 1993b Analysis of a genetic
hitchhiking model, and its application to DNA polymorphism data
from *Drosophila melanogaster*. *Mol. Biol. Evol.* 10: 842–854.
- 6372 WILKINSON, G. S., 1993 Artificial sexual selection alters allometry
in the stalk-eyed fly *Cyrtodiopsis dalmanni* (Diptera: Diopsidae).
6374 Genetics Research 62(3): 213–222.
- 6376 WILLIAMS, G. C., 1966 *Adaptation and Natural Selection*. Prince-
ton.
- 6378 WILLIAMS, K.-A. and P. S. PENNINGS, 2019 Drug resistance
evolution in HIV in the late 1990s: hard sweeps, soft sweeps, clonal
interference and the accumulation of drug resistance mutations.
6380 bioRxiv.

- WISELY, S. M., S. W. BUSKIRK, M. A. FLEMING, D. B.
6382 McDONALD, and E. A. OSTRANDER, 2002 Genetic Diversity
and Fitness in Black-Footed Ferrets Before and During a Bottle-
6384 neck. *Journal of Heredity* 93(4): 231–237.
- WRIGHT, K. M., U. HELLSTEN, C. XU, A. L. JEONG,
6386 A. SREEDASYAM, J. A. CHAPMAN, J. SCHMUTZ, G. COOP,
D. S. ROKHSAR, and J. H. WILLIS, 2015 Adaptation to
6388 heavy-metal contaminated environments proceeds via selection
on pre-existing genetic variation. *bioRxiv*: 029900.
- 6390 WRIGHT, S., 1943 Isolation by Distance. *Genetics* 28(2): 114–138.
- WRIGHT, S., 1949 The Genetical Structure of Populations. *Annals
6392 of Eugenics* 15(1): 323–354.
- WRIGHT, S. and T. DOBZHANSKY, 1946 Genetics of natural
6394 populations. XII. Experimental reproduction of some of the changes
caused by natural selection in certain populations of *Drosophila
6396 pseudoobscura*. *Genetics* 31(2): 125.
- WRIGHT, S. I., I. V. BI, S. G. SCHROEDER, M. YAMASAKI,
6398 J. F. DOEBLEY, M. D. McMULLEN, and B. S. GAUT,
2005 The Effects of Artificial Selection on the Maize Genome.
6400 *Science* 308(5726): 1310–1314.
- YANG, Z., 1998 Likelihood ratio tests for detecting positive selection
6402 and application to primate lysozyme evolution. *Molecular Biology
and Evolution* 15(5): 568–573.
- 6404 ZUCKERKANDL, E. and L. PAULING, 1965 Evolutionary diver-
gence and convergence in proteins. In *Evolving genes and proteins*,
6406 pp. 97–166. Elsevier.